Geochemical investigations of salt marsh pore waters and sediments at Langeoog island in course of a simulated transgression

Untersuchungen zur Porenwasser- und Sedimentgeochemie in den Salzwiesen von Langeoog im Zuge einer simulierten Transgression

Von der Fakultät für Mathematik und Naturwissenschaften der Carl von Ossietzky Universität Oldenburg zur Erlangung des Grades und Titels einer

Doktorin der Naturwissenschaften   Dr. rer. nat.

angenommene Dissertation

von Frau Kerstin Kolditz

geboren am 09.09.1974   in Jena

Abstract

Salt marshes form part of the intertidal landscape of the southern North Sea. The salt marshes of the East Frisian barrier island Langeoog, NW Germany belong to the barrier-connected salt marsh type and were protected by a summer dike, which was removed in 2004. In course of this de-embankment an approximately 2.2 km² large salt marsh area is now exposed to the regular tidal inundations. Thus, a transgressive situation was created caused by the simulated sea level rise.

This study deals with the implications of this simulated sea level rise on the de-embanked salt marshes. Pore water as well as sediment geochemistry analyses down to 5 m sediment depth were carried out along a transect including sites of saline water influenced grassland, high salt marsh, low salt marsh, and transition zone from low salt marsh to tidal flat.

The barrier island development is documented by differences in the sediment geochemistry, abundance of heavy minerals, and varying diatom communities of the single lithologiacl units. Correlations between FeO and TiO_2 along with SEM-EDX analyses evidence the presence of ilmenite as the dominating heavy mineral accompanied by zircon and garnets. Ternary plots are used for the visualisation of the relationship between sediment geochemistry (represented by the major oxides SiO_2, Al_2O_3, TiO_2, and the trace metal Zr) and the depositional energy. Results of the diatom analyses are used as an independent indicator for the reconstruction of the barrier island development and also reflect the varying energetic conditions. The studied Holocene sediment sequence consists of four lithological units. It starts on its basis with low energetic mixed flat deposits of marine origin followed by sand flat deposits of higher energetic and marine depositional conditions. The highest depositional energy was found for the relocated beach sands which were accumulated after several dune breaching events. Marsh soil deposits of low energetic and marine-terrestrial depositional conditions form the top of the sequence.

The marine sediments now accumulated under transgressive conditions were also characterised. These sediments were sampled by the means of sediment settling traps. They are dominated by the silt fraction (88-89%), followed by the clay fraction (10-12%), and the sand fraction (0.5-1%). Seasonal variations in grain size distribution are observed. The clay fraction increases in summer and decreases in winter whereas the coarse silt fraction show the opposite

pattern. The sedimentation rates of 3.8 to 7.2 mm/yr indicate vertical salt marsh growth when compared to the relative sea level rise of 1.0-3.0 mm/yr. Geochemical analyses indicate that the suspended particulate matter of the adjacent Wadden Sea forms a major source for the salt marsh accumulation. The geochemistry of bulk parameters (POC, TIC) and major elements (Ti, Al, Fe, Ca) are very similar.

The comparison to Holocene coastal deposits of similar genesis offers a mixed geochemical signature. Both, the geochemistry of Holocene tidal flat and Holocene brackish deposits are reflected in the geochemistry of the sediments from the settling traps. Thus, an early stage of sea level rise is documented at Langeoog Island.

Along the transect pore water analyses are also carried out on order to investigate the implications of the de-embankment on pore water geochemistry. The pore waters were sampled with in situ pore water samplers down to 5 m sediment depth and analysed for iron, manganese, ammonia, phosphate, dissolved organic carbon, and sulphate. Pore water analyses are complemented by on site measurements of pH and salinity. Additionally, sediment samples were analysed for bulk parameters (TC, TIC, TOC, TS), selected major elements (Si, Al, Fe, Mn), and reactive iron and manganese. The sediments along the study transect form an important iron source for the pore waters indicated by high percentage of reactive iron in the sediments and the high concentration of dissolved iron in the pore water. Ultra-filtration experiments showed that the iron in the pore waters is dominated by organically complexed iron. The iron complexation is most likely controlled by humic substances and in the rhizosphere accompanied by siderophores. The pore water may serve as significant source of dissolved iron which may account for elevated pyrite contents frequently observed in Holocene coastal peats.

The restored regular tidal flooding resulted in considerable increase in pore water iron, manganese, phosphate, and ammonia concentrations. This was observed after a storm surge event which leads to the inundation of a normally protected site.

This combined pore water and solid phase geochemical study extends the understanding of processes associated with inundations of formerly flood-protected coastal areas. It not only may serve as a basis of future sea level scenarios, but also helps re-interpreting geochemical signatures in Holocene coastal sedimentary sequences.

Kurzfassung

Salzwiesen sind Teil der intertidalen Landschaft der südlichen Nordsee. Die Salzwiesen der ostfriesischen Barriereinsel Langeoog (NW Deutschland) waren bis 2004 durch einen Sommerdeich geschützt. Im Zuge einer Rückdeichung wurden ca. 2,2 km² Salzwiesenfläche wieder dem regulären tidalen Überflutungsrhythmus ausgesetzt. Somit entstand eine transgressive Situation in diesem Gebiet, welche durch einen simulierten Meeressiegelanstieg hervorgerufen wurde.

In dieser Studie werden die Auswirkungen dieses simulierten Meeresspiegelanstieges auf das rückgedeichte Salzwiesengebiet untersucht. Sowohl Porenwasseruntersuchungen als auch geochemische Analysen des Sediments bis in eine Tiefe von 5 m wurden entlang eines N-S gerichteten Transektes durchgeführt. Dieser Transekt beinhaltet verschiedene Salzwiesenzonen, beginnend im Norden mit salzwasserbeeinflusstem Grünland über obere Salzwiese und untere Salzwiese bis zum Übergang der unteren Salzwiese in die Pionierzone im Süden.

Die Entwicklung der Barriereinsel Langeoog während des Holozäns wird durch Unterschiede in der Geochemie der Sedimente, das Auftreten verschiedener Schwerminerale sowie den Variationen in den Diatomeengesellschaften belegt. Neben SEM-EDX-Analysen beweisen Korrelationen zwischen FeO und TiO2, daß Ilmenit das vorherrschende Schwermineral in den untersuchten Sedimenten ist. Begleitminerale sind Zirkon und Granate. Anhand von Dreiecksplots kann der Zusammenhang zwischen der Geochemie und der Ablagerungsenergie der untersuchten Sedimente gezeigt werden. Die Ergebnisse der Diatomeenuntersuchungen dienen als unabhängiger Indikator für die Rekonstruktion der Entwicklung Langeoogs und spiegeln die verschiedenen Ablagerungsenergien der einzelnen Sedimentpakete wider. Die untersuchten holozänen Sedimente Langeoogs lassen sich in vier lithologische Einheiten unterscheiden. Die Sequenz beginnt an der Basis mit marinen Mischwattablagerungen niedrig energetischen Ursprungs. Darauf folgen marine Sandwattablagerungen, welche unter höher energetischen Bedingungen abgelagert wurden. Die dritte Einheit bilden die umgelagerten Strandsande. Diese wurden während einiger Dünendurchbrüche im Norden der Insel in das Untersuchungsgebiet eingeschwemmt und weisen die höchste Ablagerungsenergie auf. Marschböden bilden die letzte lithologische Einheit

am Top der untersuchten Sequenz. Sie wurden unter niedrig energetischen und marine-terrestrischen Bedingungen abgelagert.

Die marinen Sedimente, die aktuell nach der Rückdeichung ins Untersuchungsgebiet eingetragen werden, wurden ebenfalls untersucht. Diese Sedimente wurden mit Hilfe von Sedimentfallen beprobt. Die dominierende Korngröße des eingetragenen Materials ist Silt (88-89%), gefolgt von Ton (10-12%) und Sand (0,5-1%). Die Korngrößenzusammensetzung unterliegt saisonalen Schwankungen. Die Tonfraktion steigt im Sommer und nimmt im Winter ab. Die Grobsiltfraktion sinkt dagegen im Sommer und nimmt im Winter ab. Die kalkulierten Sedimentationsraten von 3,8 bis 7,2 mm/a weisen im Vergleich zum relativen Meeresspiegelanstieg von 1,0 bis 3,0 mm/a auf ein vertikales Wachstum der Salzwiesen hin. Die geochemischen Daten belegen, dass die Schwebstoffe des angrenzenden Wattenmeeres die Hauptquelle des eingetragenen Materials darstellen. Es bestehen große Ähnlichkeiten bezüglich der POC-, TIC-Gehalte und der Hauptelemente Ti, Al, Fe und Ca.

Der Vergleich zu Holozänen Küstensedimenten unterschiedlicher Genese zeigt eine gemischte geochemische Signatur. Sowohl die Geochemie Holozäner Wattsedimente als auch die brackischer Sedimente spiegelt sich im Material der Sedimentfallen wider. Daraus lässt sich schlussfolgern, dass sich die rückgedeichte Salzwiesenfläche auf Langeoog in einem frühen Stadium eines Meeresspiegelanstiegs befindet.

Des Weiteren wurden die Auswirkungen der Rückdeichung und des damit verbundenen simulierten Meeresspiegelanstieges auf das Porenwasser der Salzwiesen untersucht. Das Porenwasser wurde entlang des oben genannten Transektes mittels in-situ Probenehmern über einen Zeitraum von 13 Monaten beprobt. Die Proben wurden auf Spurenmetalle (Fe, Mn), Nährstoffe (NH_4^+, PO_4^{3-}), gelösten organischen Kohlenstoff und Sulfat analysiert. Während der Probenahme wurden vor Ort pH-Wert und Salzgehalt bestimmt. Zusätzlich wurden Ultrafiltrationsexperimente mit 5 kDa MWCO durchgeführt. Das Sediment wurde mittels Rammkernsondierung beprobt. Die Sedimentproben wurden auf ihre Gehalte an TC, TIC, TOC, TS sowie Si, Al, Fe und Mn analysiert. Des Weiteren wurden reaktives Eisen und Mangan bestimmt.

Die Sedimente sind durch einen sehr hohen Quarzanteil, sehr niedrige Kohlenstoff- und Schwefelgehalte charakterisiert. Der hohe Anteil reaktiven Eisens (bis zu 40%) kennzeichnet die Salzwiesensedimente als wichtige Eisenquelle für das Porenwasser. Das Porenwasser

weist hohe Konzentrationen an gelöstem Eisen (bis zu 583 µM) auf. Diese resultieren höchstwahrscheinlich aus der Reduktion und Lösung oxidischer Eisenminerale durch organische Liganden oder organische Fe(II)-Komplexe. Die Komplexierung des Eisens durch Huminstoffe und Siderophore in Kombination mit dem neutralen pH-Wert des Porenwassers hält das Eisen in Lösung. Aus diesem Grund können die untersuchten Salzwiesen als ein wichtiges Eisenreservoir angesehen werden, das, entsprechende Bildungsbedingungen vorausgesetzt, erhöhte Pyritgehalte in Holozänen Küstentorfen erklären könnte.

Die Wiederherstellung des Tideneinflusses im Untersuchungsgebiet durch die Rückdeichung verursachte einen erheblichen Anstieg der Konzentrationen von Eisen, Mangan, Phosphat und Ammonium im Porenwasser. Dieser Effekt wurde hier nach einem Sturmflutereignis beobachtet. Diese Ergebnisse belegen, dass Rückdeichungsmaßnamen mit großer Sorgfalt insbesondere im Hinblick auf die Freisetzung von Nährstoffen und deren Auswirkungen auf die Qualität des Porenwassers durchgeführt werden sollten.

Diese kombinierte Porenwasser- und Sedimentstudie erweitert das Verständnis der Prozesse, die während eines Meeresspiegelanstieges auftreten können. Sie dient nicht nur als Informationsbasis für zukünftige Meeresspiegelanstiegsszenarien sondern unterstützt ebenfalls die Interpretation geochemischer Signaturen in Holozänen Küstensedimentsequenzen.

Table of contents

Figure legends

Table legends

1. Introduction

Salt marshes are widely distributed intertidal landscapes forming the transition between the terrestrial and marine realm. The salt marsh areas along the Wadden Sea coast of the Netherlands, Germany, and Denmark extend to approximately 360 km² (Stock, 2003). The major part of these salt marshes belongs to the clay-rich floodplains along the mainland coast of the Wadden Sea which were predominately formed as the result of land reclamations. Salt marshes can also be found on barrier islands of the southern North Sea. The area of the salt marshes in the Wadden Sea of Lower Saxony (NW Germany) amounts to 26.4 km^2 on the East Frisian barrier islands, 54.6 km^2 in the mainland coastal zone, and 19 km^2 within summer polders (Stock, 2003).

Generally, salt marshes are muddy to sandy coastal and estuarine grasslands mainly covered by halophytic vegetation which are periodically flooded by seawater (Allen, 2000; Beeftink and Rozema, 1988). Salt marshes at the coastline of the southern North Sea belong to the foreland and barrier-connected salt marsh types (Beeftink and Rozema, 1988). The salt marshes of the Frisian Islands belong to the open-coastal back-barrier salt marsh type. This type is defined as a sandy-muddy system on the sheltered landwards side of coastal barrier islands and spits (Allen, 2000). Sandy salt marshes are developed especially on the barrier islands (Stock, 2003).

In Europe salt marshes are endangered habitats and protected areas (Stock, 2003). Since June 2009, the protected area of the Dutch Wadden Sea and the German Wadden Sea National Parks of Lower Saxony and Schleswig-Holstein are declared to world natural heritage by the UNESCO. However, natural salt marshes are rare along the coast of the Wadden Sea as a consequence of extended dike building and land reclamation since the Middle-ages (Flemming and Nyandwi, 1994). Thus, salt marshes were mostly embanked in the past because of agriculture and cattle grazing on so-called summer polders. The present salt marsh protection intends the development of natural salt marshes, which should be achieved by the termination of agricultural utilization and de-embankments of previously reclaimed areas (Ahlhorn and Kunz, 2002; Stock, 2003).

1.1. Holocene coastal development of NW Germany

The Holocene coastal sediments of NW-Germany result from the sea-level rise after the last glacial maximum, 18,000 years before present (BP). At that time, the sea level was 110-130 m lower than today (Cameron et al., 1987, Long et al., 1988). The subsequent sea-level rise was 90-95% climatically controlled (Sindowski and Streif, 1974). From 10,000 to 8,100 years BP the deeper areas of the North Sea were characterized by brackish conditions (Eisma et al., 1981). Reliable data about the late glacial and early Holocene sea-level rise in the study area are not available because of the shallow water depth (mostly less than 45 m) in the German Bight (Streif, 1990). Between 8,600-7,100 years BP the sea level was rising at a rate of about 2 m per 100 years and reached a depth of 15 m below the present level (Ludwig and Figge, 1979). This steep rise probably lasted until 6,500 years BP (Menke, 1976) followed by a distinct slow down with phases of stagnation and even regression of the sea level.

The depositional history of the barrier islands and the adjacent tidal flat systems of the southern North Sea coast is directly related to climatic changes during the Holocene sea-level rise. The last transgressive cycle started in the Weichselian Late-Glacial and still continues today as it is proven with tidal gauge measurements along the northwest German coastline (Töppe, 1994). The salt marsh sediments form part of the Holocene accumulation wedge (Fig. 1.1). Its development started about 7,500 BP caused by the Holocene sea level rise (Hoselmann and Streif, 2004; Streif, 1990, 2004). The coastline shifted continuously in a south-western direction due to continued sea-level rise (Hanisch, 1980, Streif, 2004). However, from about 7,300 BP the transgression was interrupted by several fluctuations and even regressive phases (Fig. 1.2). This is clearly reflected by the formation of peat layers found within clastic sediments of predominantly marine origin (Fig. 1.1; Dellwig et al., 1998, 1999; Freund und Streif, 1999; Streif, 1990, 2004). The sediments of the Holocene wedge are chiefly derived from the sediments of the seafloor (Veenstra, 1982), i.e., eroded Pleistocene deposits and Holocene marine sediments from the North Sea (Hoselmann and Streif, 2004). The latter authors reported that 90% are delivered from marine sources and only 10% are of fluvial origin.
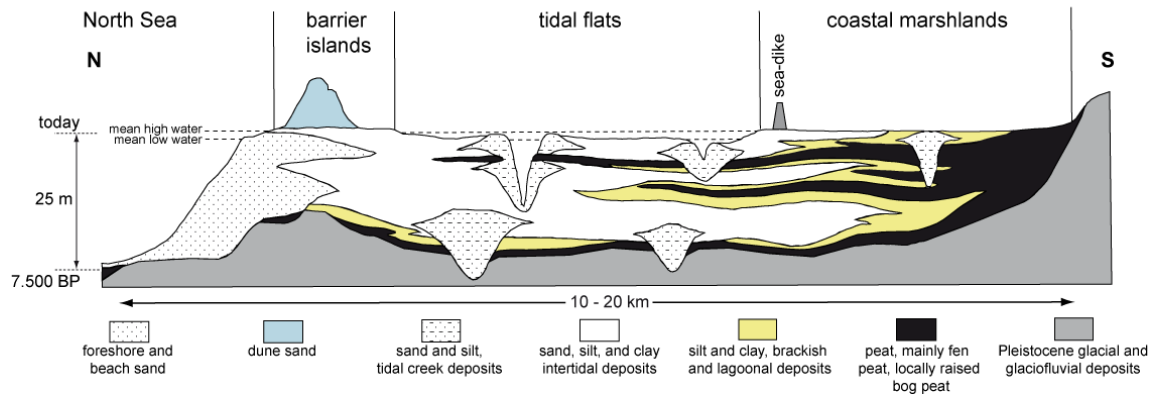
Fig. 1.1: Schematic cross section through the coastal Holocene accumulation wedge (Streif, 2004)

The time period since 1,000 years BP is strongly influenced by anthropogenic activities (dike building and draining), which hampered the natural sedimentation. However, some samples from the East Frisian Islands show that between 900 and 600 years BP the present mean sea level was achieved (Streif, 1986). The coastal deposits contain a large number of different sediment facies which range from lagoonal to tidal flat sediments depending on exposition to the open sea. According to Eisma and Kalf (1987) the Wadden Sea is one of the few areas of the North Sea in which accumulation and deposition of suspended particulate matter occurs. Eisma (1981) reported that the tidal flats of the Wadden Sea and the Wash embayment in eastern England account for 12-18% of the total amount of suspended matter deposited in the North Sea area.
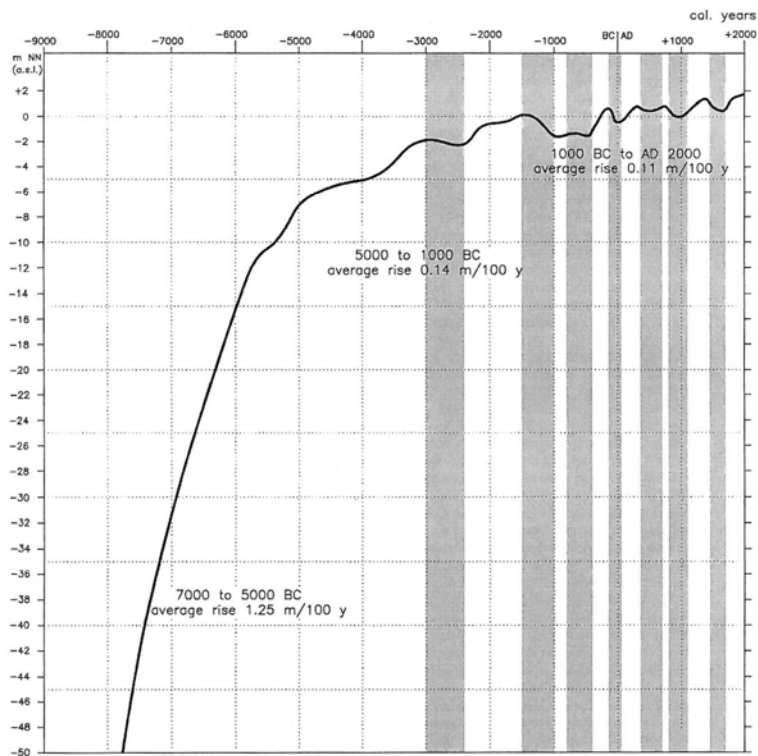
Fig. 1.2: Simplified sea level curve for the southern North Sea (Behre, 2007); the time scale is in calibrated/calendar years; grey shaded fields = regressions, white fields = transgressions

1.2. Iron cycling in salt marsh sediments

Salt marshes are highly productive areas. A large portion of their productivity occurs subsurface in the form of roots and rhizomes (Schuhbauer and Hopkinson, 1984; Valiela et al., 1976). The salt marsh vegetation, e.g. *Spartina alterniflora*, oxidises the sediments (Howes et al., 1981), which results in organic matter degradation via aerobic respiration (e.g. Howes et al., 1984). Several recent studies suggested that ferric iron reduction may account for a significant fraction of organic matter re-mineralization in salt marsh sediments (e.g. Bull and Taillefert, 2001; Carey and Taillefert, 2005, Kostka et al., 2002; Luther et al., 1992, Taillefert et al., 2007) resulting in an intensification of the iron cycle. Iron cycling in salt marshes is controlled by sulphate reduction and sediment oxidation (Giblin, 1988; Giblin and Howarth, 1984; Hines et al. 1989; Kostka and Luther, 1995; Luther and Church, 1988). Near surface anoxic conditions are common for salt marshes (Hines et al., 1989; Howarth and Giblin, 1983, Howarth and Teal, 1979) because of high rates of organic carbon oxidation in the uppermost centimetres of the sediment (Koretsky et al., 2005). This is fuelled by the high productivity of these areas and generally attributed to microbial sulphate reduction (Canfield, 1989; Howarth and Teal, 1979, Kostka et al., 2002). During early diagenesis sulphate reduction and the release of hydrogen sulphide as a by-product could lead to the formation of iron monosulphides and pyrite in the

presence of dissolved Fe^{2+} (e.g. Giblin, 1988; Hines et al., 1989; Howarth and Teal, 1979; Lord and Church, 1983; Otero and Macias, 2002).

The presence of iron oxides inhibits sulphate reduction since organic matter oxidation with iron oxides provides more energy for microorganisms than using sulphate as an electron acceptor (Bull and Taillefert, 2001; Kostka et al., 2002, Taillefert et al., 2007). The presence of both macrophytic roots/rhizomes and fungi/bacteria and their interaction with the sediment as well as the presence of humic substances in pore waters as well play an important role in salt marsh iron cycling (Buyer and Sikora, 1990; Carrasco et al., 2007; Crowley et al., 1991; Lindsay, 1991; Luther et al., 1992; Winkelmann, 2007). Luther et al. (1992) describe an iron cycle in salt marsh sediments, which is based on iron complexation by organic ligands (Fig. 1.3).
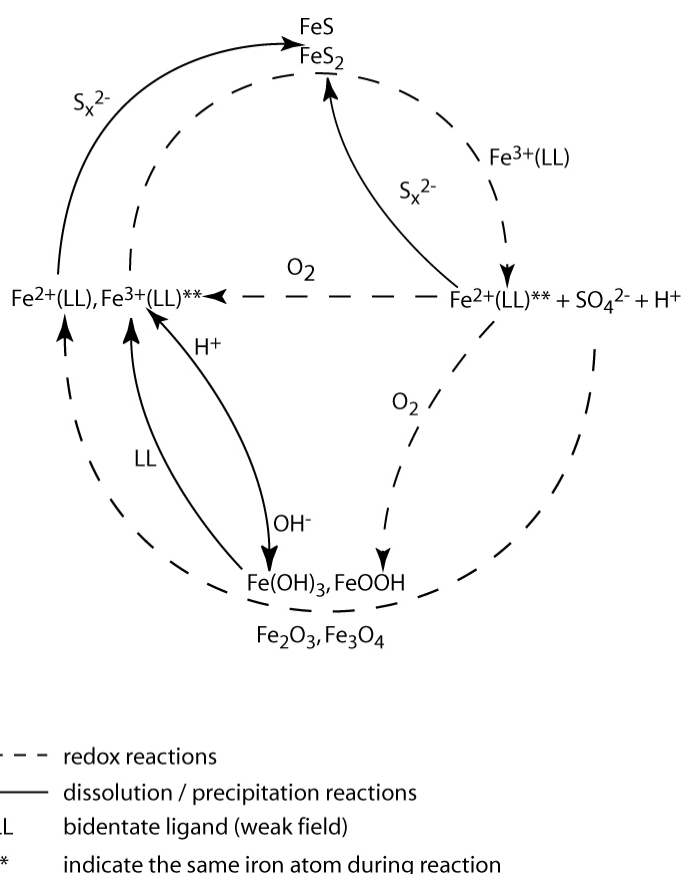
Fig. 1.3: Iron cycle in salt marsh sediments after Luther et al. (1992)

This cycle of iron solubilisation continues as long as bacteria and/or plants produce organic ligands. The cycle stops when sulphate reduction rates are high and organic ligand production is low. The main reactions of the iron cycle are:

- Solubilisation of Fe(III) by organic ligands

- Reduction of soluble Fe(III) to Fe(II) by these ligands, soluble reduced sulphur or solid phase reduced sulphur

- Oxidation of the resulting Fe(II) (complexed to organic ligands) by Fe(III) minerals

- Formation of iron sulphide minerals when dissolved sulphide is in excess.

The Fe(III) minerals dissolution can occur in non-reductive (Eq. 1-2) and reductive pathways (Eq. 3-5), which is drawn in the lower part of the iron cycle scheme (Fig. 1.3):

(1) $\quad FeOOH + 3H^+ \quad\quad\quad \rightarrow Fe^{3+} + 2H_2O$

(2) $\quad FeOOH + C_6H_4(OH)_2 \quad \rightarrow \{Fe^{3+}[C_6H_4(O)_2]\}^+ + OH^- + H_2O$

(3) $\quad 2FeOOH + H_2S \quad\quad\quad \rightarrow 2Fe^{2+} + S° + 4OH^-$

(4) $\quad 2FeOOH + C_6H_4(OH)_2 \rightarrow 2Fe^{2+} + 4OH^- + C_6H_4(O)_2$

(5) $\quad FeOOH + H^+ + **Fe^{2+}(LL) \quad \overset{LL}{\rightarrow} **Fe^{3+}(LL) + Fe^{2+}(LL) + 2OH^-$
    ** same iron atom during reaction
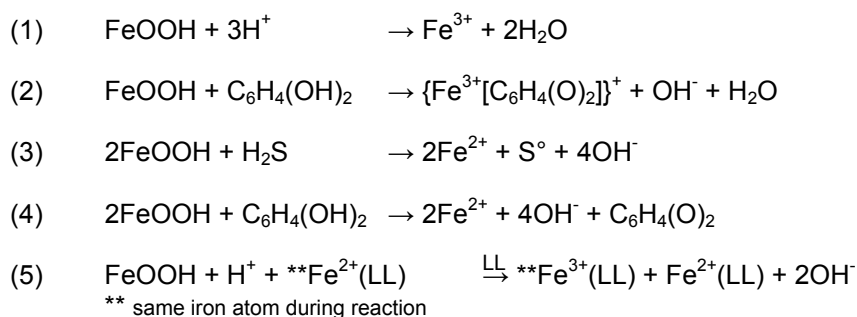
Equation (1), (2), and (5) permit the formation of aqueous Fe(III) complexes. Equation (3) and (4) show the reduction of Fe(III) minerals by H_2S and organic compounds. The Fe(III) complexes oxidise solid sulphide minerals when H_2S is absent. These reactions produce no soluble Fe(III). Equation (5) demonstrates the reduction of Fe(III) minerals by Fe(II), which is complexed by organic compounds (LL). Ferric iron reduction is promoted by siderophores, exuded by plant roots, fungi and bacteria (Amon and Benner, 1996; Buyer and Sikora, 1990; Crowley et al., 1991; Hersman et al., 1995; Kraemer, 2004; Neilands, 1981) as well as by humic substances (Cesco et al., 2000; Francois, 1990; Van Dijk, 1971).

The upper part of the iron cycle scheme (Fig. 1.3) shows the iron sulphide oxidation and formation reactions (Eq. 6-8):

(6) $\quad FeS_2 + 14Fe^{3+} + 8H_2O \rightarrow 15Fe^{2+} + 2SO_4^{2-} + 16H^+$

(7) $\quad Fe^{2+} + HS^- \quad\quad\quad\quad\quad \rightarrow FeS + H^+$

(8) $\quad FeS + S_x^{2-} \quad\quad\quad\quad\quad \rightarrow FeS_2 + S^{2-}_{(x-1)}$
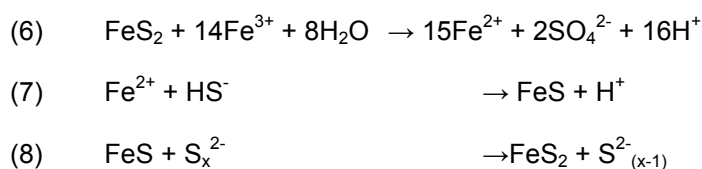
The reactions which represent the iron cycle indicate that the iron mineral system has a substantial acid-base-buffering capacity. While the upper part of the iron cycle produces an acid (Eq. 6-8) the lower part provides a base (Eq. 1-5). Luther et al. (1992) concluded that Fe(III)

solubilised by the processes described above is the likely primary oxidant for reduced sulphur in salt marsh sediments. They further postulated that the reactivity of Fe(III) minerals will increase in salt marshes when primary productivity and ligand production is high.

1.3. Objectives of the study

This study forms part of the interdisciplinary research project: "Simulated transgression in the course of the de-embankment of the summer polder area of Langeoog Island: Succession and dynamic in the littoral facies region" initiated by the Institute of Chemistry and Biology of the Marine Environment (ICBM) and the Terramare Research Centre (since 2008 part of the ICBM). In 2004 a de-embankment at the East Frisian barrier island Langeoog was carried out to compensate for the loss of natural areas in course of the construction of the gas pipes Europipe I and II within the Wadden Sea National Park of Lower Saxony. The de-embanked salt marsh area of approximately 2.2 km² at Langeoog Island is now exposed to the regular tidal flooding. The dike crest height of the removed summer dike ranged between +2.0 m NN and +2.25 m NN and enabled seawater flooding only during storm surges (Ahlhorn and Kunz, 2002).

This de-embankment at Langeoog Island offered the unique opportunity to investigate short- and long-term processes during a simulated sea level rise in a natural environment. The restored tidal inundations are expected to cause changes in the geochemistry of pore waters and sediments as well as changes in the plant communities and vegetation cover, respectively. Implications on sedimentation processes and morphology are also supposed. Furthermore, the project provides an important data basis for future de-embankments and effects of marine inundations due to the global sea level rise.

Chapter 2 presents the geochemical, heavy mineralogical, and diatom investigations of the salt marsh and tidal flat sediments from Langeoog Island. This study deals with the sediment geochemistry as tracer for the heavy mineral composition of the sediments. The sediment geochemistry and the diatom analyses are used for the characterisation of different depositional energy conditions and the reconstruction of the sedimentary history.

Chapter 3 examines the sedimentation processes after the de-embankment. The main objectives of this chapter are the geochemical characterisation of the deposited material, the determination of the major sources, and the comparison of deposited material and Holocene coastal sediments in order to improve our knowledge about sedimentation processes under

transgressive conditions, finally, leading to a balance of the imported material and compounds to the de-embanked area. Furthermore, the seasonal behaviour of the redox-sensitive trace metals Mo and Mn was investigated as both metals reveal significant changes in their seasonal patterns in the open water column (appendix A 1; Dellwig et al, 2007a,b) which are likely also reflected in the material deposited in the salt marshes.

Chapter 4 presents the implications of the de-embankment on the salt marsh pore water geochemistry. Pore waters were sampled with in-situ pore water samplers down to 5 m sediment depth (appendix A 2; Beck et al., 2007) and were analysed for redox-sensitive metals (Fe, Mn), nutrients (NH_4^+, PO_4^{3-}), dissolved organic carbon, and sulphate. Sediment analyses complement the study in order to determine pathways of metal redox-cycling. The role of salt marshes as a possible iron source for pyrite formation is also discussed.

1.4. Outline of the author's contribution

The thesis comprises three manuscripts, which are presented in chapters 2 to 4. The author's contribution to each manuscript is described below. Three further manuscripts are presented in the appendix.

Chapter 2

"Geochemistry of Holocene salt marsh and tidal flat sediments on a barrier island in the southern North Sea (Langeoog, NW Germany)"

This study focuses on sediment geochemistry and diatom analyses as tools for characterisation of the different depositional energy conditions and the reconstruction of the sedimentary history. The concept of the study was developed by the author and co-authors. The presented sediment and diatom data based on hammer and vibro cores. The latter ones were accomplished by the co-authors Olaf Dellwig and Holger Freund as well as Helmo Nikolai and Maik Grunwald. The hammer cores were done by the author, the co-authors Jan Barkowski and Holger Freund supported by Malte Groh. The author herself described the sediments of the hammer cores and the co-author Holger Freund did the same for the vibro cores. Sediment samples were analysed for geochemical data by the author herself supported by Carola Lehners, Martina Wagner, Eleonore Gründken, René Ungermann, and Sebastian Eckert. Diatom analyses were provided by the co-author Jan Barkowski. The co-authors Olaf Dellwig,

Thomas Leipe and Rainer Bahlo carried out the SEM-EDX analyses. The interpretation of the results was done by the author herself except for chapter 2.4.4 SEM-EDX, supported by the suggestions of the co-authors. Writing and editorial handling of the publication was done by the author herself in cooperation with the co-authors Olaf Dellwig, Hans-Jürgen Brumsack, and Holger Freund. This manuscript was submitted to *Sedimentology* and is now in review.

Chapter 3

"Salt marsh sedimentation during simulated sea-level rise and its relation to Holocene coastal development of NW Germany"

The sedimentation processes after the de-embankment are examined in this study including a geochemical characterisation of the deposited material, an identification of the major sources, a comparison of deposited material with Holocene coastal sediments, and the investigation of the seasonal behaviour of the redox-sensitive trace metals Mn and Mo. Furthermore, the material and compounds imported to the de-embanked area are balanced.

By using sediment settling traps developed by the co-authors Jan Barkowski and Holger Freund the geochemical composition and the sediment amount of the deposited material was determined. The Sediment settling traps were sampled by the co-author Jan Barkowski, who also provided the data of sediment amount, grain size analyses and sedimentation rates assisted by Sandra Andratschke, Julia Pohl, and Gudrun Stolte. Geochemical analyses of the sediment settling trap material were carried out by the co-author Olaf Dellwig supported by Carola Lehners, Martina Wagner and Eleonore Gründken. He also contributed the data of the Holocene deposits and the suspended particulate matter. The surface pressure measurements were provided by the author herself. The concept of the study was developed by the author and Olaf Dellwig. Writing and editorial handling was done by the author herself supported by the suggestions from Olaf Dellwig and Hans-Jürgen Brumsack.

Chapter 4

"Effects of De-Embankment on Pore Water Geochemistry of Salt Marsh Sediments"

This study deals with the implications of a de-embankment on the salt marsh pore water geochemistry. The today's role of the salt marshes as a possible iron source for pyrite formation is discussed as well as the implications for Holocene pyrite formation. Pore waters were

sampled with the in-situ technique described in appendix A 2. The author herself conducted all pore water sampling campaigns and performed the pore water sampling and field measurements assisted by Malte Groh. Sediment samples were taken from hammer cores accomplished by the author herself, the co-authors Jan Barkowski and Holger Freund as well as Malte Groh. Pore waters were analysed by the author herself except for nutrients, which were determined by Carola Lehners, Eleonore Gründken, and Martina Wagner. Sediment samples were analysed for geochemical data by the author herself supported by Carola Lehners, Martina Wagner, Eleonore Gründken, René Ungermann, and Sebastian Eckert. The concept of the manuscript and the interpretation of the results were developed by the author herself in cooperation with the co-authors. Writing and editorial handling of the publication was done by the author herself except for chapter 4.5.2, which was written by the co-author Olaf Dellwig. Writing was supported by suggestions of Olaf Dellwig and Hans-Jürgen Brumsack. This chapter is published in *Journal of Coastal Research* **25**, 1222-1235.

2. Geochemistry of Holocene salt marsh and tidal flat sediments on a barrier island in the southern North Sea (Langeoog, NW Germany)

Kerstin Kolditz, Olaf Dellwig, Jan Barkowski, Rainer Bahlo, Thomas Leipe, Holger Freund and Hans-Jürgen Brumsack

Abstract

This study combines the results of geochemical and diatom investigations of Holocene sediments from the East Frisian barrier island of Langeoog. It improves the knowledge of the sedimentological and geochemical development of these deposits under the influence of a rising sea-level. The investigated sediments belong to the seaward side of the Holocene accumulation wedge. Four lithological units are distinguishable: marsh soil, relocated beach sands, sand flat, and mixed flat deposits. The study focuses especially on the geochemistry and distribution of heavy mineral-associated elements in the sedimentary record. Correlations between FeO and TiO_2 content indicate the presence of the heavy mineral ilmenite and are a useful tool for characterising depositional energy conditions. A dominating abundance of ilmenite followed by zircon, garnets and some other heavy minerals has been evidenced by SEM-EDX measurements. An increase in depositional energy is found for the lithological units in the following order: marsh soil, mixed flat, sand flat, and relocated beach sand. Ternary plots visualising the relationship between sediment geochemistry and prevailing energy conditions confirm the trends in depositional energy for the investigated marine-terrestrial sediments and are presumably applicable to other siliciclastic sedimentary systems. Beside the geochemical results diatom analyses used as an additional independent indicator for reconstruction of the sedimentary history. The composition of the diatom community also reflects the varying energetic conditions during sediment deposition.

2.1 Introduction

The depositional history of the barrier islands and adjacent tidal flat system of the southern North Sea coast is directly related to climatic changes during the Holocene sea-level rise. The last transgressive cycle started in the Weichselian Late-Glacial and still continues today as it is proven with tidal gauge measurements along the northwest German coastline (Töppe, 1994). During the Late Glacial Maximum the sea level of the North Sea was about 110 to 120 m lower than today and most parts of the North Sea basin were dry (Behre, 2004). Beginning in the Weichselian Late-glacial and especially during the early Holocene, climatic amelioration triggered a rapid and almost constant sea-level rise of about 1.25 m per century, which was predominantly controlled eustatically (Behre, 2003, 2007).
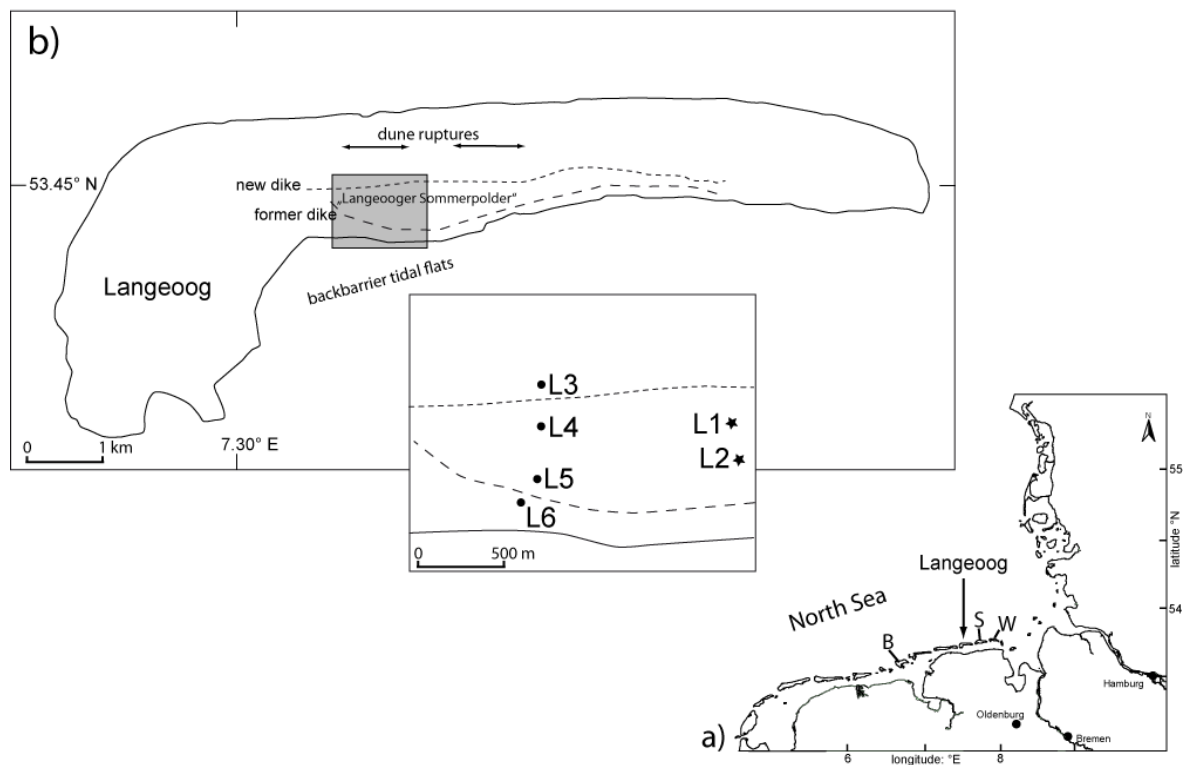
Fig. 2.1: a) Study area on the Southern North Sea coast: East Frisian barrier island of Langeoog, NW Germany, B=Borkum, S=Spiekeroog, W=Wangerooge; b) detailed view on study area on Langeoog island; study sites L1 to L6 marked on inset, ● hammer corings, ★ vibro cores

The development of the present-day coastal landscape started at about 7,500 BP when the sea-level reached a position of about 23-25 m below its present elevation. The coastline shifted continuously in a south-western direction due to continued sea-level rise (Hanisch, 1980; Streif, 2004). However, from about 7,300 BP onwards the continuous transgression was interrupted by several fluctuations and even regressive phases. This is clearly reflected by the

formation of peat layers found within the marine sediments of the Holocene wedge (Dellwig et al., 1998, 1999; Freund and Streif, 1999; Streif, 1990, 2004). The sediments of the Holocene wedge are chiefly derived from the sediments of the seafloor (Veenstra, 1982), i.e. eroded Pleistocene deposits and Holocene marine sediments from the North Sea (Hoselmann and Streif, 2004). The latter authors reported that 90% are delivered from marine sources and only 10% are of fluvial origin.

The barrier islands are the most prominent offshore feature of the German coastal landscape (Fig. 2.1a) where they protect the mainland from the direct influence of waves and storm surges. Size, shape, structure, and stability of these islands are directly related to marine morphodynamic processes, particularly sand supply, tidal range and wave energy. The loss of sediments, due to erosion of the seaward side of the barrier islands, limits the understanding of tidal ranges and coastal configurations prior to 2,000 BP. Several geological and palaeoecological studies of salt marshes and tidal flats have significantly increased the knowledge of the formation of barrier islands along the coast of Lower Saxony since 2,000 BP (e.g. Freund, 2003, Freund et al., 2003; Streif, 1986). Taking into consideration that the morphodynamic framework was roughly the same as today (Hanisch, 1980), a comparable coastline existed several kilometres northward and several metres below today's position. This is for instance documented by the occurrence of brackish-lagoonal sediments (roots and stems of *Phragmites communis* with ages of 7,960 ±205 BP; 7,980 ±60 BP; 7,540 ±80 BP) about 6 km northwards of the island of Wangerooge at a depth of –24 m NN (NN = German zero datum) at the base of the Holocene (Hanisch, 1980). During the late Holocene, sea level rose mainly eustatically controlled along the northwest German North Sea coast on average 0.14 m per century between 5,000 BP and 1,000 BP and 0.11 m per century from 1,000 BP until today, resulting in the southward shift of the coastline towards a higher position (Behre, 2003, 2007). It is widely recognised that due to the aforementioned morphodynamic features and the continuation of sea-level rise, the East Frisian barrier island chain still forms part of a highly dynamic system. Along with a distinct N-S migration, the islands are subject to W-E migration as a result of sand transport parallel to the coast. Several authors reported that dunes and most probably the shoreline of the islands must have moved approximately 500 m southwards during the last 2,000 years (Barckhausen, 1969; Hanisch, 1980; Streif, 1986). During this process, older sediments such as dune slack deposits, salt marsh horizons or tidal flat layers were

covered by the prograding dune sand and thus were preserved (Freund et al., 2003; Freund and Streif, 1999). Such preserved layers can be used as geological markers, e.g., for the reconstruction of sea-level rise or the geomorphological and geological development of a barrier island. Sedimentary records of clastic material reflect transgressive phases whereas organic-rich layers could only develop during stagnant or regressive phases. Diatom and pollen data as well as botanical remains provide valuable information concerning palaeosalinity, marine hydrodynamics, and vegetation cover.

On Langeoog island parts of the salt marshes were ditched for drainage and in 1934/35 the so-called "Langooger Sommerpolder" was protected by a summer dike to allow cattle grazing (Fig. 2.1b). This means that a total of 218 ha were excluded of regular inundation since that time, clearly shown in a shift of pioneer and lower salt marsh vegetation patterns into a brackish and high salt marsh vegetation and a lack of sediment input (appendix A 3, Barkowski et al., 2009). In 2004 a de-embankment was carried out in this area to compensate for the loss of natural habitats caused by the construction of the gas pipes Europipe I and II within the Wadden Sea National Park of Lower Saxony (Kolditz et al., 2009a). Altogether the former "Langeooger Sommerpolder" was exposed to the normal tidal regime since 2004, which is similar to an artificial sea-level rise resulting in effects of e.g. vegetation succession and sedimentology. We present the results of geochemical, heavy mineralogical, and diatom investigations to provide a better understanding of the sedimentological and geochemical development of these deposits under the influence of rising sea level. This study focuses on the geochemistry of the predominately sandy sediments of Langeoog island and especially on the distribution of heavy mineral-associated elements in the sedimentary record. We tested the hypothesis, 1) whether sediment geochemistry is an appropriate proxy perceiving heavy minerals and 2) whether heavy mineral-associated elements are useful indicators for interpreting depositional energy conditions. Diatom analyses and sediment SEM-EDX measurements serve as independent tools for verifying our hypothesis. Our investigations extend the knowledge of previous heavy mineral studies of Holocene coastal sediments (e.g. Dellwig et al., 2000; Hild, 1997; Ludwig and Figge, 1979; Schüttenhelm and Laban, 2005; Veenstra, 1982).

2.2 Environmental setting and marker strata on Langeoog island

The investigation area is situated on the landwards side of Langeoog island and is directly connected with the backbarrier tidal flat system between Langeoog island and the mainland (Fig. 2.1b). Semi-diurnal tides and a tidal range of 2.7 m characterise the hydrodynamic regime in this area. The mean high water reaches a height of 1.4 m NN on Langeoog island. The Holocene sediments in the region of the barrier islands consist of a marine-littoral sequence of 15 to 35 m thickness. Locally this sequence is overlain by aeolian dunes reaching up to 25 m NN (Streif, 2004).

The geological and palaeogeographical development of Langeoog island since 2,800 BP is described comprehensively by Barckhausen (1969) who introduced three marker strata. However, only one marker stratum (*Hydrobia*-layer, see below) is considered to be representative for the entire former island of Langeoog.

The oldest stratum is the *Hydrobia*-layer, named after the accumulation of laver spire snail or mud snail shells (*Hydrobia ulvae* Pennant 1777) characterising a transition zone between the upper intertidal and a northward lying supratidal sand bar. It consists of silt and clay grade sediment and large numbers of *Hydrobia* shells. This marker stratum indicates the southern edge of the very initial and probably still dune free former part of an island. The *Hydrobia* layer shows a large spatial distribution of several square kilometres in depths between –0.60 and -0.20 m NN and a slightly southwards slope (Barckhausen, 1969). The northern edge of the *Hydrobia*-layer lies under the present-day dunes and extends across several kilometres at a W-E direction. The *Hydrobia*-layer has a sharp and clear boundary towards the light grey sands of the former sand bar at its northern boundary whereas it has a nonpoint southern expansion towards the former tidal flat area. Due to the absence of radiocarbon ages Barckhausen (1969) could not give a physical age of the *Hydrobia* layer. However, studies by Freund and Streif (1999) dated *Hydrobia ulvae* at the westerly barrier island Borkum (Fig. 2.1a) from a comparable depth (-0.30 m NN to -0.23 m NN) at an age of 2,090 ± 115 BP confirmed by dated mussels (*Cardium edule*, 2,120 ± 115 BP). The *Hydrobia*-layer on the Island of Borkum is embedded in tidal flat sands. The *Hydrobia* layer of Langeoog island is overlain by blue-grey sandy tidal flat deposits of 0.3 to 0.9 m thickness showing that the island keeps growing up according to relative sea-level rise (Barckhausen, 1969).

The next marker strata is a superimposed salt marsh-horizon, named "Kleibank" (= clayey layer) by Barckhausen (1969). This layer consists of brackish silt and clay material rich in autochthonous and also allochthonous plant material. It has a limited spatial extent in the western and eastern part of Langeoog island and is lacking in the central part probably due to erosion effects and disadvantageous conditions of development, respectively. Thus, salt marsh-layers could only develop under the protection of a closed dune ridge whereas the ridge of the former island of Langeoog was most likely less developed in the central part during the formation of the "Kleibank" horizon. Therefore, washover-fans likely prevented the formation of salt marshes in this area. Additionally, it appears reasonable to separate the old salt-marsh areas of the island of Langeoog in the western and eastern part. Even in younger times (e.g. 1717 AD, Obstfeld, 2001) the island of Langoog was again divided in two parts, and the severe breaches ridge again took place in the central part of Langeoog where the "Kleibank" was not developed. The surface of this deposit lies between +0.55 to +1.00 m NN reaching an average thickness of up to 20 cm. However, the clayey layer does not occur in the study area of this work due to erosion events in the centre of Langeoog island. This is also true for the Lower and Upper peat bank, the most recent marker strata on Langeoog island. Their spatial distribution is restricted to the NW part of the island (Barckhausen, 1969). The Kleibank layers and the Lower and Upper peat bank are divided by eolian sediments.

2.3 Material and methods

2.3.1 Sample material

Sample material for all analyses originates from a transect of four hammer cores on Langeoog island in April 2007 (Figs. 2.1b and 2.2). The sites were chosen in order to reflect the different facies observed at the study site. Thus, the cores originate from salt-influenced grassland (L3), higher and lower salt marsh (L4, L6), and the transition zone lower salt marsh/tidal flat (L5). The hammer cores have total lengths of 3.99 m (L3), 4.24 m (L4), 4.47 m (L5), and 4.35 m (L6). Sediment samples (n=138) were taken at 10 cm intervals, stored in low density polyethylene (LDPE) bottles, and immediately frozen after return to the laboratory.

This transect is completed by sediments from boreholes L1 (total length = 2.36 m) and L2 (total length = 3.90 m) which were recovered in the Langeoog Sommerpolder area in March 2004 (Fig. 2.1b) by using vibrocore equipment with 5 m long aluminium tubes of 10 cm diameter

during a first exploration of the study site. Unfortunately, the marsh soil and the main part of the relocated beach sand are missing in core L2 and mixed flat sediment is absent in core L1 due to technical reasons. As these cores overlap in a depth range from +0.50 m NN to -0.16 m NN merging both, core L1 and core L2, creates a synthetic profile which includes all lithological units found in the hammer cores and simplifies the visualisation and interpretation of the diatom composition of the investigated sediments. Furthermore, the *Hydrobia*-layer at an elevation of -0.73 m NN as well as the occurrence of the four major lithological units allows comparison with the transect from site L3 to L6. After recovering cores L1 and L2, the tubes were directly cut in the field into 1m long sections. These sections were stored at 4°C before subsampling. Subsamples (n=60) were taken at 5-10 cm intervals, stored in PVC-bottles and frozen.

2.3.2 Geochemical analyses

Both, the sediment samples from hammer corings and the sediment samples from vibrocoring were treated in the same way. After freeze-drying, samples (n=198) were ground and homogenised in an agate mortar. Geochemical analyses of major elements (Si, Al, Ti, Fe, Ca) and trace metals (Mn, Sr, Zr) were carried out by X-ray fluorescence (Philips PW 2400) on fused glass discs (1:1 mixture of di-lithiumtetraborate/lithiumtetraborate). Total carbon (TC) and total sulphur (TS) were determined by a C/S elemental analyser (Eltra CS 500) (Prakash Babu et al., 1999). Accuracy and precision for sediment measurements were checked by parallel analysis of in-house standards (TW-TUC shale type material, Loess aeolian material, UT-S upper crust type material; Table 2.1).

Tab. 2.1: Precision and accuracy of sediment analyses

Analyte	Method	Precision %	Accuracy %
TS	IR Analyser	5.1	3.0
TC		0.7	-0.2
Si	XRF	0.7	-1.6
Al		0.8	-2.7
Ti		0.6	-0.5
Fe		0.6	-1.3
Ca		0.6	-3.6
Mn		0.9	-5.3
Zr		1.5	3.0
Sr		0.7	-4.9

2.3.3 Diatom analyses

Diatom analyses were carried out on sediment samples from boreholes L1 and L2 at 5-20 cm intervals. The samples (n=49) were prepared after the methodology of Schrader (1973). In order to decompose organic and inorganic compounds 0.5 g homogenous sediment were heated for 20 minutes at 150 °C in a 1:1 solution of hydrogen peroxide (30%) and concentrated acetic acid. This solution was then repeatedly rinsed and centrifuged with distilled water to remove the hydrogen peroxide, acetic acid, and decomposition products of organic and inorganic constituents (Vos and De Wolf, 1994). Samples were dispersed in 1% potassium hydrogen phosphate solution and again centrifuged in distilled water.

Diatom classification and counting were carried out with a Leitz light microscope (oil immersion, 1,000-fold magnification). Diatom classification was performed after Hartley (1996), Krammer and Lange-Bertalot (1997a, b, 2000), and Pankow (1990). The ecological diatom classification is based on Hartley (1996) and Zong (1997) with consideration of the halobous system by Simonsen (1962).

2.3.4 SEM-EDX analysis

Scanning electron microscopy (SEM) and energy dispersive X-ray micro-analyses (EDX) were performed on a FEI Quanta 400 microscope connected with an EDAX-Genesis system. Sediment material of the 63-100 µm fraction (obtained by sieving) was glued on Al stubs. The surface of the samples was covered by pure carbon (vacuum sputtered) to assure electric conductivity. Measurement parameters of the microscope system during analyses were: high vacuum; 15 kV electron beam; working distance: 10 mm; SE and BSE detector; variable enlargement. The X-ray microanalyses were done by spot analyses on selected particles taking EDX-spectra (EDAX-Econ 4 detector), identification and quantification of the elements after ZAF-correction. The problem of peak overlapping, especially for the Mn Kβ and Fe Kα lines at 6.4 to 6.5 keV was solved by holographic peak deconvolution (HPD) which takes the calculated ratio to the Mn Kα and Fe Kβ lines into account. Additionally, interference between P K and Zr Lα lines was checked by using an electron beam of 30 kV leading to excitation of Zr Kα and Zr Kβ without further P lines.

Both manual single particle analyses and automated particle analyses were carried out. The latter method is based on image processing, particle recognition and element analyses of

the particles on a series of different fields of the sample. The obtained data set was processed for mineral (or particle group) identification and quantification (counting). Minerals and particle groups can be defined by border values of the proven elements and calculated element concentrations or ratios.

2.4 Results

2.4.1 Sedimentary facies

The cross-section (Fig. 2.2) from salt-influenced grassland (L3) in the North to lower salt marsh (L6) in the South shows four major lithological units in the study area, these will be described in further detail below. Additionally, the transect is complemented by the synthetic profile of the combined cores L1 + L2 (Fig. 2.2). The *Hydrobia*-layer is seen in all cores at an elevation ranging from +0.17m to -0.95 m NN (NN = German zero datum; Fig. 2.2).

Marsh soil: The uppermost marsh soil deposits (Fig. 2.2) consist of brownish to greyish silt and clay, with locally occurring layers of fine to medium sand in cores L3 and L1+2. These deposits contain rootlets and chaff of plants belonging to the recent vegetation cover at each core site (Barkowski et al., 2009). According to observations in the field (10 vol% HCl) the southernmost site L6 is calcareous, whereas the other sites are non-calcareous. This finding is in accordance with the average Ca/Al ratios (0.18) and Ca/Sr (77) of the marsh soils which are identical to the average shale (Wedepohl, 1971). Only site L6 reveals higher values (Ca/Al = 0.26, Ca/Sr = 133) due to elevated contribution of mussel fragments. Thus, almost carbonate free detrital material is characterized by Ca/Sr ratios of about 70 while mussels reach value higher than 200 (Dellwig et al., 1999). The thickness varies between 0.17 m (L6) and 0.33 m (L1+2).
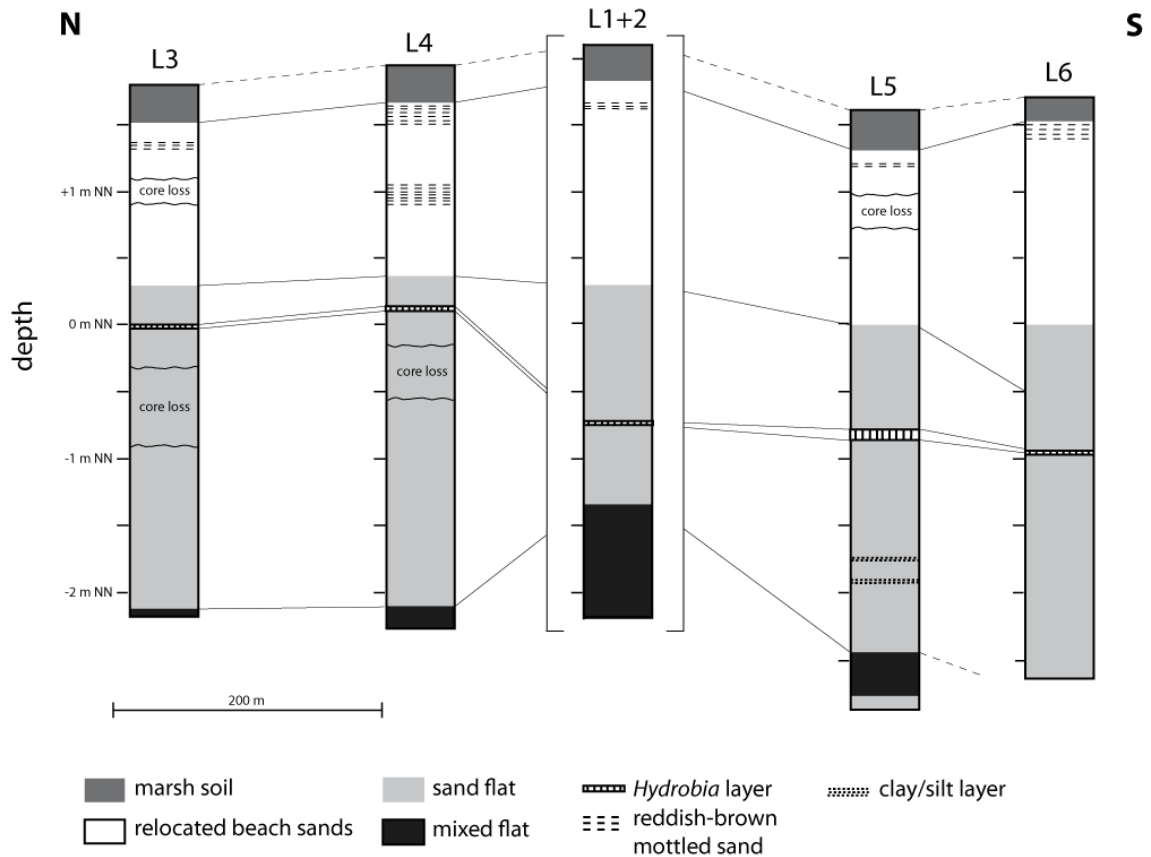
Fig. 2.2: Schematic geological cross section from hammer cores L3-L6 (N-S direction) complemented by vibro cores L1+L2, distances between sites true to scale; altitude normalized to NN = German zero datum for better comparison

Relocated beach sands: The underlying relocated beach sands (Fig. 2.2) are characterised by medium sand at L3, fine to medium sand at L4 and fine sand at L6 and L5, thus a decreasing trend in grain size from N to S is observed. The colour changes from beige and yellowish in the upper parts to grey and dark grey in the lower parts. Mottled areas of reddish-brown and brown colour are found in the upper part as well. The relocated beach sands are non-calcareous, only the base of core L4 is weakly calcareous. While the base shows slightly elevated Ca/Al and Ca/Sr ratios of 0.38 and 87 the values of the remaining deposits (Ca/Al = 0.27, Ca/Sr= 78) again coincide with the field observation. The relocated beach sands reach a maximum thickness of 1.54 m (L6).

Sand flat: The sand flat deposits (Fig. 2.2) consist of grey to dark grey fine sand. Two small layers of grey clay and silt with a thickness of 0.04 m are found at L5 (-1.75 m NN and -1.92 m NN depth) which are reflected by slightly increasing contents of Al_2O_3 (Fig. 2.4). In contrast to the relocated beach sands significant nest-like accumulations of fragmented echinoderms mixed with shell fragments of molluscs occur in addition to the above mentioned

Hydrobia-layer. Such molluscs fragments are also reflected in elevated Ca/Al (0.6) and Ca/Sr (117) ratios. The sand flat deposits reach a thickness between 1.63 m (L1+2) and 2.60 m (L6).

Mixed flat: Mixed flat deposits (Fig. 2.2) are cored at sites L5, L4, L3, and L1+2. They occur as alternations of fine sand and silt/clay or silt/clay lenses within fine sand. Generally they are characterised as grey coloured calcareous to highly calcareous deposits. These deposits show on average the highest Ca/Al ratios (0.77) with Ca/Sr ratios (174) clearly indicating remnants of marine calcareous organisms. Depending on drilling depth and thickness of overlaying strata they reveal a minimum thickness between 0.06 m (L3) and 0.86 m (L1+2). Due to the small thickness of these deposits at L3-L6 intersection with the overlaying sand flat deposits are possible. It can not be excluded that only the transition from sand flat to mixed flat deposits was cored.

2.4.2 Diatoms

Diatom analyses were carried out in sediments from the cores L1 and L2 (Figs. 2.1b and 2.2). The marsh soil deposits contain mesohalobous diatoms including *Diploneis interrupta* which shows the highest relative abundance of 41% (Fig. 2.3). This strongly silicified species is classified as a benthic marine/brackish aerophilous (adapted to irregular flooding) diatom (Vos and De Wolf, 1993). Less stable diatoms as the mesohalobous benthic epipelic species *Scolioneis tumida* or *Navicula peregrina* also appear, however showing lower abundance especially for the latter species (19%, 1%). They are related to fine-grained sediments, i.e. silt and clay (Vos and de Wolf, 1993). Marine planktonic diatoms (e.g. *Paralia sulcata*, *Delphineis surirella*) are abundant reaching a relative abundance of 31% and 18%, respectively. The number of diatom fragments in the marsh soil deposits is variable ranging from 261 to 800 and the number of total diatom valves (TDV) reaches a maximum value of 349 (Fig. 2.3).
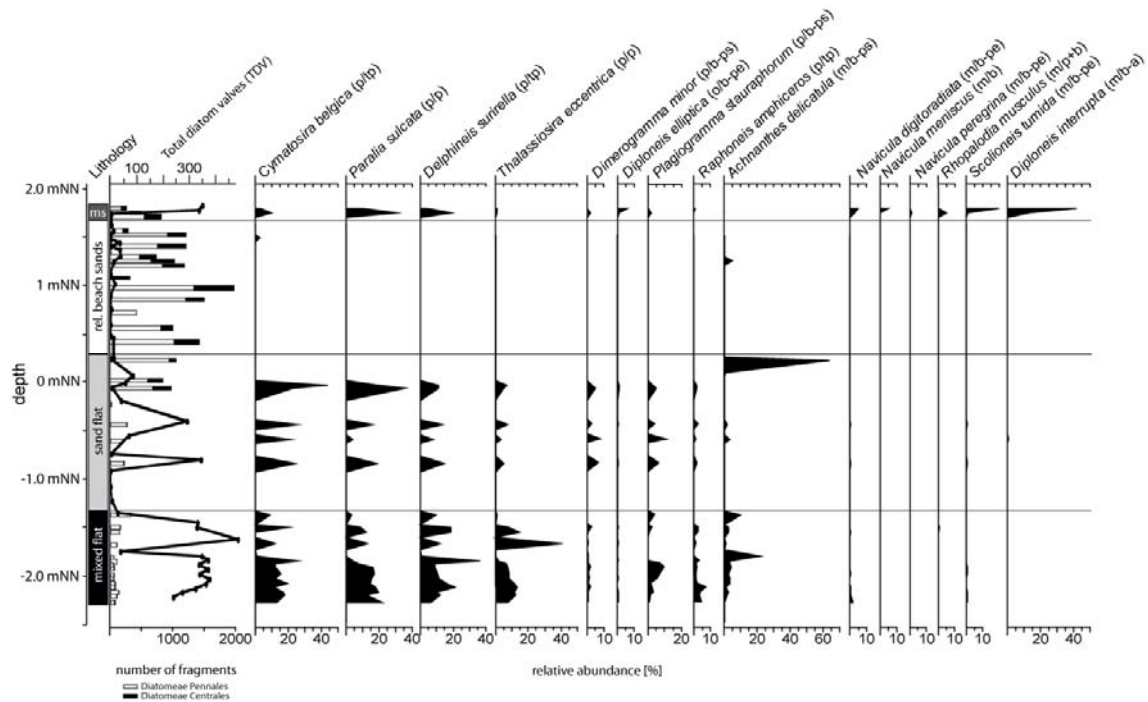
Fig. 2.3: Synthetic diatom profile of L1 and L2; Abbreviations in brackets behind diatom species: halobous group: p=polyhalobous, m=mesohalobous, o=oligohalobous / Life form: p=planktonic, tp=tychoplanktonic, b=benthic, -pe=epipelic, -ps=epipsammic, -a=aerophilous; lithology: ms=marsh soil; left side shows the lithology of L1 and L2, the total number of diatom valves (TDV = solid black line), and the number of diatom fragments (horizontal bares)

In contrast, the relocated beach sands are free of completely preserved diatom valves. The maximum number of fragmented diatoms, however, sharply increases from 485 to 2,000 when compared with the marsh soil deposits (Fig. 2.3).

The sand flat deposits contain especially strongly silicified species, e.g. *Paralia sulcata* and *Cymatosira belgica*, whereas the abundance of less conservable species decreases (Fig. 2.3).

The mixed flat deposits at the base of the synthetic profile are characterised by marine planktonic (sensu stricto) diatoms including *Paralia sulcata* (max. 24%) and *Thalassiosira eccentric* (max. 43%). Marine tychoplanktonic diatoms (frequently occuring in the water column, but also related to, e.g., benthic habitats) like *Cymatosira belgica* (Vos and de Wolf, 1993) are also abundant reaching maximum abundance of 29%. These diatoms are well-silicified which has resulted in high diatom valve preservation. In addition, the weakly silicified (less conservable) marine tychoplanktonic diatom *Raphoneis amphiceros* is also abundant (Fig. 2.3) in the mixed flat deposits due to less depositional energy. The benthic diatom *Achnanthes delicatula* appears in sandier parts of the mixed flat deposits. This species belongs to the marine/brackish epipsammnic (firmly attached to sand grains) diatoms (Vos and De Wolf,

1993). The number of diatom fragments is low whereas TDV reaches high numbers, e.g. 483 at -1.60 m NN depth.

2.4.3 Geochemical bulk composition of lithological units

The analytical results of the investigated sediments, i.e. contents of SiO_2, Al_2O_3, TiO_2, Fe_2O_3, CaO, TS, TC, Mn, Sr, and Zr are summarized in Table 2.2 for marsh soil, relocated beach sands, sand flat, and mixed flat deposits. Spatial information on geochemical sediment composition is given in Figure 2.4 by selected parameters for each site.

Marsh soil: The marsh soil deposits are characterised by enrichments in SiO_2 (quartz) and comparatively low Al_2O_3 (clay) contents (Fig. 2.4, Tab. 2.2) compared to other marsh soils from the Hamble estuary, UK (SiO_2 49.5-59.7%, Al_2O_3 12.7-14.5 %; Cundy and Croudace, 1995). A decrease in SiO_2 and corresponding increase in Al_2O_3 content (Fig. 2.4) is observed from the northernmost site L3 to site L5. At site L6 the SiO_2 content increases while the Al_2O_3 content decreases. The individual depth profiles of TiO_2 and Zr content show the same trend. For this reason only the Zr profiles are shown (Fig. 2.4). Both, TiO_2 and Zr contents, which are commonly associated with the heavy mineral fraction, show less varying trends from L3 to L6 (Fig. 2.4) which is also true forZr/Al ratios. The average Fe_2O_3 content of the marsh soil (2.3%; see Tab. 2.2) is comparable to values (2.2-6.5%) reported for salt marsh sediments of the tidal flat sedimentary regime of the Wash area, England (Macleod, 1973; Suttill et al., 1982). The Fe_2O_3 contents increase from L3 to L5 (Fig. 2.4) but then the marsh soil at site L6 reveals lower Fe_2O_3 content than site L5. The average Fe/Al ratio (Tab. 2.2) within the marsh soil deposits is comparable to average shale (Wedepohl, 1971). However, the Fe/Al ratios of the marsh soil deposits within the study transect increase from L3 to L6 (Fig. 2.4). The marsh soil deposits show an increase in Mn content from L3 to L6 (Fig. 2.4) which is also seen in the Mn/Al ratio (Fig. 2.4). The TS contents (average 0.1 %, Tab. 2.2) in the marsh soil deposits are very low when compared with salt marsh sediments, e.g. diked and seasonally flooded salt marshes at North Sunken Meadow, USA (Portnoy and Giblin, 1997) with TS contents up to 3.5%. The TC content of 2.7% predominately reflects organic carbon (Kolditz et al., 2009a) since total inorganic carbon contents are close to zero.

Relocated beach sands: High SiO_2 (quartz) contents are observed in the relocated beach sands, while the low average Al_2O_3 content reflects the low abundance of clay (Fig. 2.4,

Tab. 2.2). Within the study transect no significant spatial variation for these components are seen. The relocated beach sands reveal the highest Zr contents (L3 max. 4,907 µg/g, Fig. 2.4) as well as the highest TiO_2 contents (Tab. 2.2) compared to the other lithological units. The profiles of Zr content and Zr/Al ratio show a significant double peak. These peaks decrease from L3 to L6. The Fe_2O_3 contents and Fe/Al ratios demonstrate a decreasing trend from L3 to L6 and with increasing depth (Fig. 2.4). The Fe/Al ratios reveal pronounced Fe-enrichments, which cannot be explained by distinct changes in lithology, e.g. decreases in clay content (lower Al_2O_3 content). The observed Fe-enrichments correspond with higher Zr/Al ratios and higher Zr and TiO_2 contents (Fig. 2.4). The Fe_2O_3 and Fe/Al profiles also show the same double peak as for the Zr and Zr/Al profiles. Mn contents decrease from L3 to L6 with a slight increase at site L5 as do Mn/Al ratios (Fig. 2.4). The Mn/Al ratios indicate distinct Mn-enrichments similar to those found for Fe. The Mn-enrichments also coincide with the double peak of Zr/Al ratios and Zr contents (Fig. 2.4) as well as higher TiO_2 contents. The relocated beach sands are characterised by the lowest TS (0.02%) and TC (0.09%) contents (Kolditz et al., 2009a).

Sand flat: The sand flat deposits and the relocated beach sands have similar SiO_2 (quartz) and Al_2O_3 (clay) values (Fig. 2.4, Tab. 2.2), which are slightly higher compared to recent sand flat deposits (SiO_2=88%, Al_2O_3=3.5%, Dellwig et al., 2000) from the backbarrier area of Spiekeroog, the island located eastwards of Langeoog. Exceptions are for instance the comparatively low SiO_2 content of 77% in 0.0 m NN depth at site L3 with concomitant higher Al_2O_3 content (3.7%) as well as the lower SiO_2 content of 78% in 0.95 m NN depth at site L6. However, the Zr contents (Fig. 2.4, Tab. 2.2) are significantly below those of the relocated beach sands and the Zr/Al ratios shows low variations. The only exception forms the lower portion of the relocated beach sands of L6 where a similar level for both facies is seen. The observed TiO_2 contents (Table 2) are still comparable to recent sand flat deposits (TiO_2=0.29%, Dellwig et al., 2000). The Fe_2O_3 contents (Fig. 2.4, Tab. 2.2) are distinctly lower compared to 0.8% Fe_2O_3 for recent sand flat deposits (Dellwig et al., 2000) with the exception of 1.7% Fe_2O_3 in 0.0 m NN at site L3. The Fe/Al ratios reveal little variation and show no clear spatial trend within the study transect (Fig. 2.4). Compared to recent sand flat deposits (Fe/Al=0.4, Dellwig et al., 2000) the Fe/Al ratios are in the same range. The Mn contents and the Mn/Al ratios (Fig. 2.4, Tab. 2.2) are partly comparable to those of recent tidal flat sediments (Mn=124±59 µg/g, Mn/Al=$64 \cdot 10^{-4} \pm 26 \cdot 10^{-4}$) of the Spiekeroog backbarrier area (Hinrichs et al., 2002). The Mn

contents and Mn/Al ratios of the sand flat deposits show no spatial variation (Fig. 2.4). Like the

relocated beach sands the sand flat deposits reveal low TS and TC contents (Tab. 2.2).

Tab. 2.2: Average values of bulk parameters [%] and selected major elements and element/element ratios for marsh soil, relocated beach sands, sand flat and mixed flat (# number of samples); data based on the four study sites L3, L4, L5, and L6, complemented by average shale values (Wedepohl, 1971)

	Marsh soil (#9)		Relocated beach sands (#51)		Sand flat (#71)		Mixed flat (#7)		Average shale
[%]	avg.	range	avg.	range	avg.	range	avg.	range	
SiO_2	79	(52-94)	93	(86-96)	92	(77-95)	83	(76-93)	58
Al_2O_3	5.4	(1.6-11.1)	1.9	(1.2-2.9)	1.9	(1.2-3.7)	3.9	(1.8-5.3)	16.8
TiO_2	0.47	(0.18-0.70)	0.55	(0.07-2.4)	0.20	(0.09-0.38)	0.33	(0.18-0.43)	0.78
Fe_2O_3	2.3	(0.4-5.2)	0.8	(0.2-2.8)	0.5	(0.2-1.7)	1.3	(0.4-1.9)	6.9
CaO	0.74	(0.2-1.9)	0.39	(0.2-0.9)	0.88	(0.3-7.6)	2.3	(0.6-3.4)	2.3
TS	0.1	(0.014-0.32)	0.02	(0.002-0.087)	0.1	(0.038-0.48)	0.4	(0.07-0.61)	0.2
TC	2.7	(0.18-8.3)	0.09	(0.0004-0.52)	0.3	(0.04-2.3)	0.9	(0.12-1.4)	
[µg/g]									
Mn	342	(39-875)	231	(23-1069)	53	(8-240)	129	(31-201)	850
Zr	480	(216-770)	1015	(91-4907)	295	(108-752)	394	(259-493)	200
Sr	61	(30-122)	35	(22-54)	47	(23-229)	92	(41-128)	230
Si/Al	25	(4-52)	46	(26-71)	47	(18-72)	22	(13-45)	3
Fe/Al	0.49	(0.34-0.63)	0.55	(0.23-1.2)	0.34	(0.22-0.60)	0.42	(0.26-0.50)	0.54
Fe/Ti	4.1	(0.3-8.9)	1.9	(0.3-4.0)	2.3	(0.2-5.3)	3.7	(0.4-6.4)	10.3
Fe/Zr	41	(6-167)	8	(4-20)	13	(6-36)	24	(10-48)	302
$Mn/Al \cdot 10^{-4}$	104	(37-210)	206	(25-689)	50	(9-137)	60	(32-72)	96
$Mn/Ti \cdot 10^{-4}$	913	(121-2008)	584	(245-899)	316	(39-1168)	558	(138-864)	1818
Mn/Zr	0.78	(0.14-2.9)	0.23	(0.12-0.53)	0.16	(0.04-0.52)	0.33	(0.12-0.65)	4.26
$Zr/Al \cdot 10^{-4}$	274	(37-690)	915	(144-3164)	307	(112-807)	205	(103-270)	22

Mixed flat: The mixed flat deposits (not occurring in L6) are characterised by SiO_2 (quartz) and Al_2O_3 (clay) (Tab. 2.2) which are comparable to recent mixed flat deposits (SiO_2=76%, Al_2O_3=5.5%; Dellwig et al., 2000). In comparison to Zr values of 414 µg/g reported for recent mixed flat deposits by Dellwig et al. (2000) the Zr contents (Fig. 2.4, Tab. 2.2) are in the same range. Regarding the Zr/Al ratios (Fig. 2.4, Tab. 2.2) no differences to the sand flat deposits are obvious. The mixed flat deposits show a decreasing trend with depth for Fe_2O_3 contents and after an initial peak the Fe/Al ratios from L3 to L5 (Fig. 2.4). The Fe_2O_3 contents and the Fe/Al ratios (Tab. 2.2) are comparable to those described for recent mixed flats by Dellwig et al. (2000) (Fe_2O_3=1.8 %, Fe/Al=0.41). Mn contents are generally low (Fig. 2.4, Tab. 2.2), but comparable to values reported for tidal flat sediments by Hinrichs et al. (2002). The same holds true for Mn/Al ratios (Tab. 2.2) of the mixed flat deposits. The mixed flat deposits show intermediate TC (0.9%) and TS (0.4%) contents (Tab. 2.2).
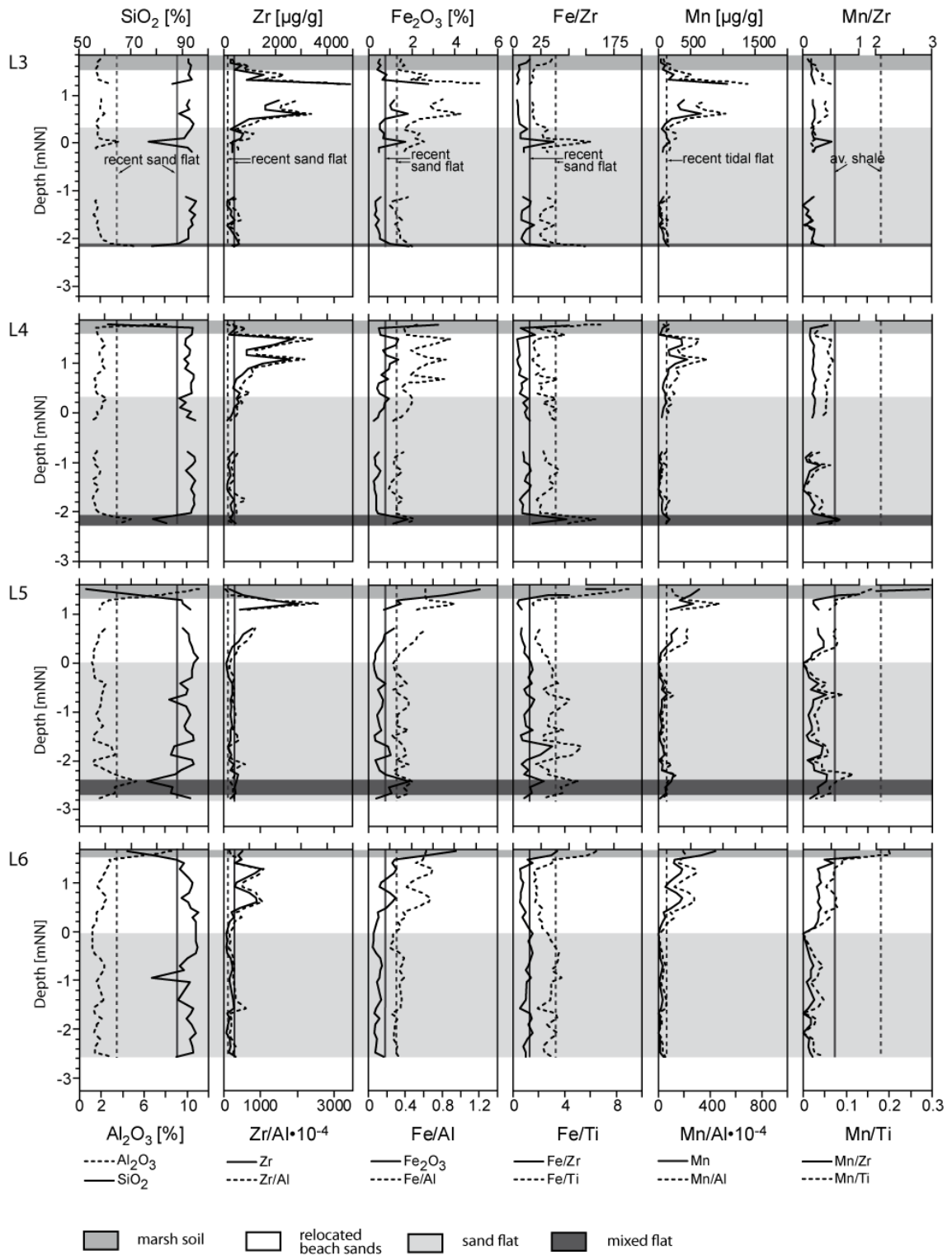
Fig. 2.4: Depth profiles of sediment geochemistry of hammer cores L3-L6 (from left to right): SiO$_2$ and *Al$_2$O$_3$* content, Zr content and *Zr/Al* ratio; Fe$_2$O$_3$ content and *Fe/Al* ratio; Fe/Zr and *Fe/Ti* ratio; Mn content and *Mn/Al* ratio; Mn/Zr and *Mn/Ti* ratio (top scale, *bottom scale*), vertical lines mark different comparative values (recent sand flat from Dellwig et al. (2000); recent tidal flat from Hinrichs et al. (2002); average shale from Wedepohl (1971)); dashed and solid lines correspond to the respective plot parameters; sampling sites are sorted in N-S direction; line gaps mark loss of core

2.4.4 SEM-EDX

The heavy mineral composition was measured in five selected sediment samples by SEM-EDX. These samples were chosen as bulk geochemical analyses suggested a high abundance of heavy minerals. Examples of SEM-photographs of heavy minerals along with their main geochemical composition derived from EDX are presented in Figure 2.5. The heavy mineral grains are rounded in shape as a result of transport in high-energy environments.

Table 2.3 shows the results of the automated particle analyses by SEM-EDX. The most abundant heavy minerals are ilmenite, zircon, and garnets (almandine and grossular). Zircon as the only Zr-bearing phase was determined in all samples with relative abundance reached up to 25.6% (site L3). Ti-bearing phases are ilmenite and rutile with the first being the dominant heavy mineral. While ilmenite occurs in a relative abundance of up to 37.0% at site L3 (Tab. 2.3), rutile reaches only a maximum value of 7.0% at this site. Such ilmenite dominance is also true for the other investigated sites L4 and L5. In addition to ilmenite, the most abundant Fe-bearing phases is almandine (from 15.9% at site L3 to 19.9% at site L5, Tab. 2.3) while fayalite is almost negligible. Fe-oxides, such as haematite and magnetite, are subordinate (max. 5.7%, Tab. 2.3) as well. Heavy minerals with Mn as a major component, e.g. pyrophanite ($MnTiO_3$) or hausmannite (Mn_3O_4) are not found. Mn was only recorded as a minor component of ilmenite (Fig. 2.5).

Tab. 2.3: Heavy mineralogical composition and relative abundance of heavy minerals of selected sediment samples from sites L3, L4, and L5

mineral		Relative abundance [%]				
	site	L3	L3	L4	L5	L5
	depth [m NN]	1.30-1.20	0.65-0.60	1.15-1.10	1.50-1.45	1.30-1.20
ilmenite	$FeTiO_3$	37.0	33.2	22.7	25.5	28.8
zircon	$ZrSiO_4$	18.5	25.6	10.2	14.2	18.9
rutile	TiO_2	4.8	7.0	6.8	2.1	3.8
haematite/ magnetite	Fe_2O_3/Fe_3O_4	0.7	1.3	5.7	4.3	1.5
monazite	$CePO_4$	2.1	0.9	5.7	6.4	4.5
chromite	$(Mg,Fe)(Cr,Al,Fe)_2O_4$	1.4	0.9	0.0	0.7	0.8
cassiterite	SnO_2	0.0	0.0	3.4	0.0	0.0
almandine	$Fe_3Al_2[SiO_4]_3$	18.5	18.7	15.9	19.9	16.7
grossular	$Ca_3Al_2Si_3O_{12}$	13.7	9.8	18.2	19.1	19.7
pyrope	$Mg_3Al_2[SiO_4]_3$	0.7	0.6	1.7	2.8	2.3
fayalite	$Fe_2[SiO_4]$	0.0	0.6	1.1	0.7	0.0
hornblende	$Ca_2Na(Mg,Fe)_4(Al,Fe)[(Si,Al)_4O_{11}]_2[OH]_2$	2.7	0.9	6.8	3.5	3.0
hedenbergite	$CaFe[Si_2O_6]$	0.0	0.0	0.0	0.7	0.0
diopside	$CaMg[Si_2O_6]$	0.0	0.3	2.3	0.0	0.0
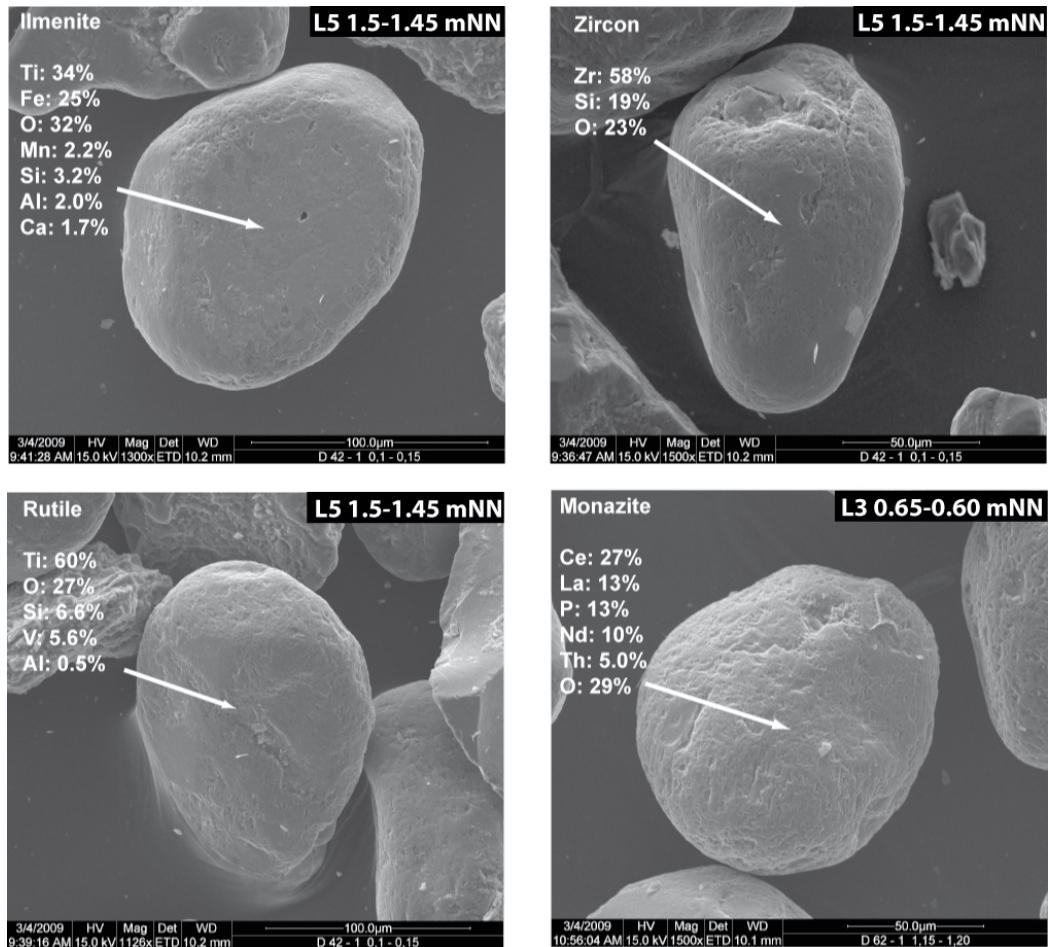
Fig. 2.5: SEM photographs of selected heavy mineral grains (ilmenite, zircon, rutile, and monazite) and their chemical compositions

2.5 Discussion

2.5.1 Sediment geochemistry as a tracer for heavy mineralogical composition, a proxy for depositional energy

As heavy minerals like zircon, ilmenite, or rutile are known as indicators for high depositional energy conditions, enrichments in Zr, Ti, Fe, and Mn may serve as geochemical proxies for depositional energy (e.g. Buynevich et al., 2004; Dellwig et al., 2000; Hinrichs et al., 2002). As demonstrated by the Fe/Al and Mn/Al depth profiles (Fig. 2.4), the relocated beach sands reveal distinct Fe- and Mn-enrichments which correspond to the Zr/Al profiles. We infer from this fact that higher amount of Fe- and Mn-bearing heavy minerals (e.g. ilmenite) are present. In order to support this assumption Fe and Mn contents are normalised to Zr and Ti (Hild, 1997) as common elements for heavy minerals (Fig. 2.4). Through this normalisation the

pronounced peaks seen in the Fe/Al and Mn/Al profiles disappear, which strongly indicates the presence of Fe- and Mn-bearing heavy minerals in the relocated beach sands. This assumption is confirmed by SEM-EDX particle analyses. Thus, the relocated beach sands reveal significant amounts of zircon, ilmenite and almandine (Tab. 2.3) with ilmenite and almandine representing Fe-bearing minerals. Figure 2.6 shows the relation between Fe and Ti for the four sedimentary facies along with data for recent tidal flat sediments from the literature. Especially the relocated beach sands plot particularly close to the ilmenite-line (Fig. 2.6b), reflecting the presence of this heavy mineral. The occurrence of elevated amounts of ilmenite in relocated beach sands is supported by heavy mineral studies in the southern North Sea by Ludwig and Figge (1979) and Schüttenhelm and Laban (2005). In contrast, the marsh soil deposits, and in part the mixed flat deposits, plot closer to the average shale-line (Figs. 2.6a and d), indicating low depositional energy conditions. This result is supported by Fe/Zr and Fe/Ti ratios (Fig. 2.4) showing that Fe is not primarily fixed in heavy minerals in the marsh soil deposits. Further evidence is provided by Fe/Al ratios (Fig. 2.4) which suggest that Fe is predominantly associated with clay minerals most likely resulting from intense redox processes (e.g. Carey and Taillefert, 2005; Kostka et al., 2002; Luther et al. 1992). Based on this reasoning the sand flat deposits represent a transitional stage: their depositional energy is lower than that of the relocated beach sands and higher than that of the marsh soil and mixed flat deposits (Fig. 2.6c). Fe-containing phases are not as clearly defined as they are for the relocated beach sands (Fig. 2.4). Intercalated clayey layers and lenses reflect the presence of clay minerals hosting a significant Fe-fraction which further indicate fluctuating depositional energy conditions.

A strong correlation between MnO and TiO_2 is seen especially for the relocated beach sands (Fig. 2.7b) due to the fact, that ilmenite may contain Mn (Deer et al., 1972) whereas pure rutile forms only a minor component in the study area (Tab. 2.3). Additionally, FeO and MnO of the relocated beach sands correlate very well, thus reflecting the incorporation of Mn into ilmenite (Fig. 2.8). However, the differences between the lithological units in MnO-TiO_2-correlation are less pronounced when compared with Figure 2.6. The mixed and sand flat deposits plot on the high energy line as defined by the linear regression of the relocated beach sands samples (Figs. 2.7b-d). The incorporation of Mn into the heavy mineral fraction is also supported by the Mn/Zr and Mn/Ti ratios (Fig. 2.4) as well as by SEM-EDX analyses which evidence Mn as a minor component of ilmenite (Fig. 2.5).
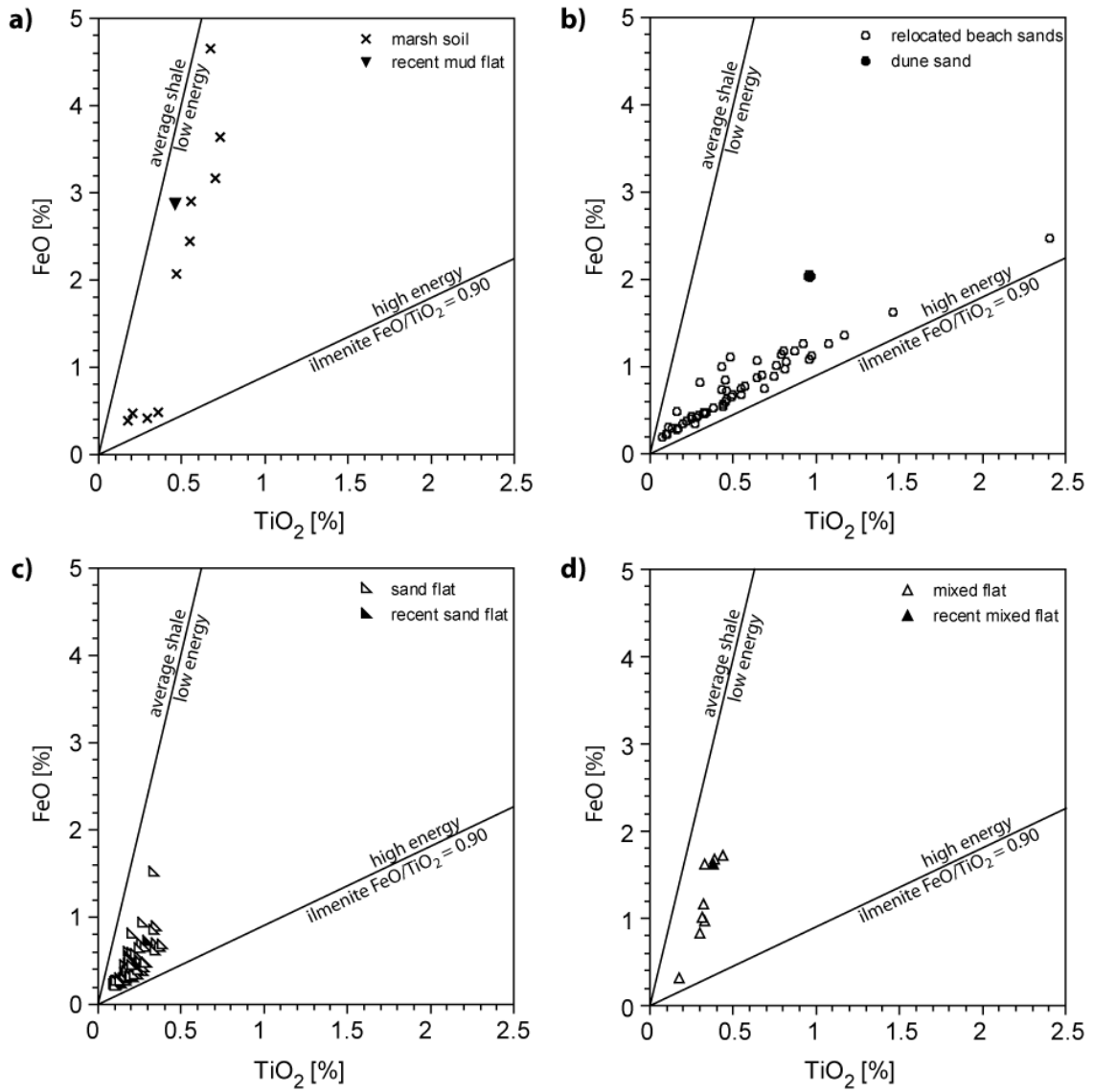
Fig. 2.6: Scatter plot of FeO versus TiO$_2$ of the a) marsh soil, b) relocated beach sand, c) sand flat, and d) mixed flat deposits; comparative values of recent mud, mixed and sand flat from Dellwig et al. (2000), average shale from Wedepohl (1971)
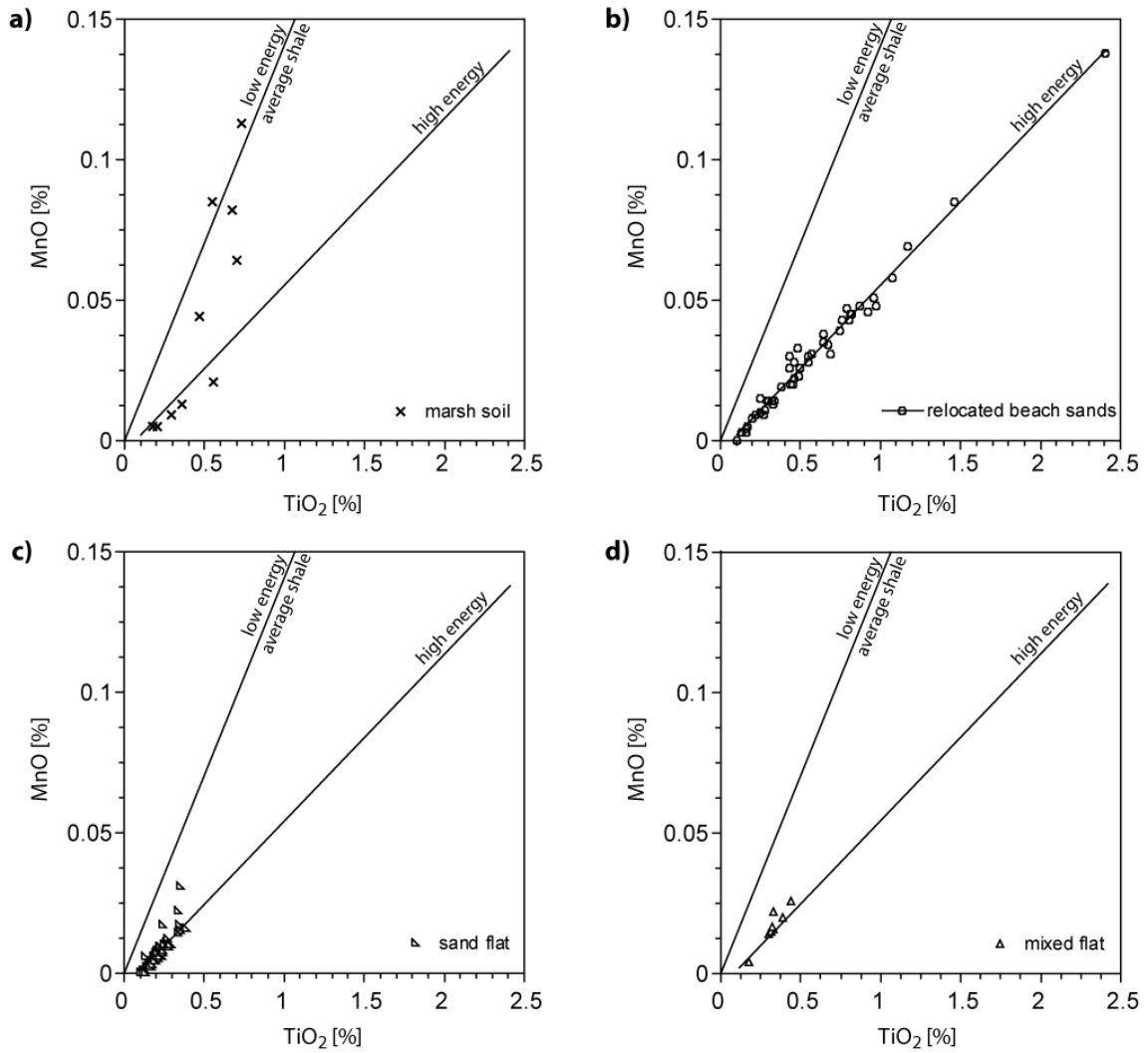
Fig. 2.7: Scatter plot of MnO versus TiO_2 of the a) marsh soil, b) relocated beach sand, c) sand flat, and d) mixed flat deposits; comparative values of average shale from Wedepohl (1971)
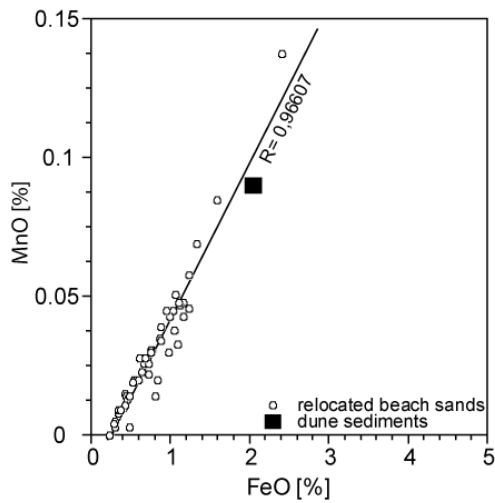
Fig. 2.8: Scatter plot of MnO versus FeO of the relocated beach sand deposits, the solid line marks the regression between MnO and FeO, the black square marks the dune sediments described by Saye and Pye (2006)

Additionally, relations between major oxides SiO_2, Al_2O_3, and TiO_2, and the trace element Zr are visualised in the ternary plots of Figures 2.9a and b in order to highlight the relationship between sediment geochemistry and depositional energy. In these plots the clay fraction is represented by Al_2O_3, the quartz/sand fraction by SiO_2 and the heavy mineral fraction by TiO_2 and Zr (factors are used for visualisation). The grey arrows in the ternary plots reflect a trend of increasing depositional energy complemented by values from the literature. Low depositional energy is characterised by high Al_2O_3 and low amounts of SiO_2 and Zr. In contrast, decreasing Al_2O_3, increasing SiO_2, and constant but low Zr contents reflect increasing depositional energy. Constant but high SiO_2 and concomitant low Al_2O_3 as well as increasing Zr mark high depositional energy conditions. For instance, the maximum Zr content of about 4,900 µg/g at site L3 (Fig. 2.4) is equivalent to a zircon ($ZrSiO_4$) content of about 1% for the relocated beach sands. Following the grey arrow in Figure 2.9a, the investigated lithological units show the above postulated trends in depositional energy. A significant fraction of TiO_2 in average shale and marsh soil (Fig. 2.9b) may be explained by Ti incorporation into clay minerals (Skrabal and Terry, 2002; Zhang et al., 2002; Zuther et al., 2000). Nevertheless, the studied lithological units demonstrate a similar trend of increasing depositional energy as seen in Figure 2.9a. The sand flat deposits and the relocated beach sands show certain overlaps in bulk composition close to the SiO_2 pole in Figure 2.9 due to the quartz dominance in these samples.
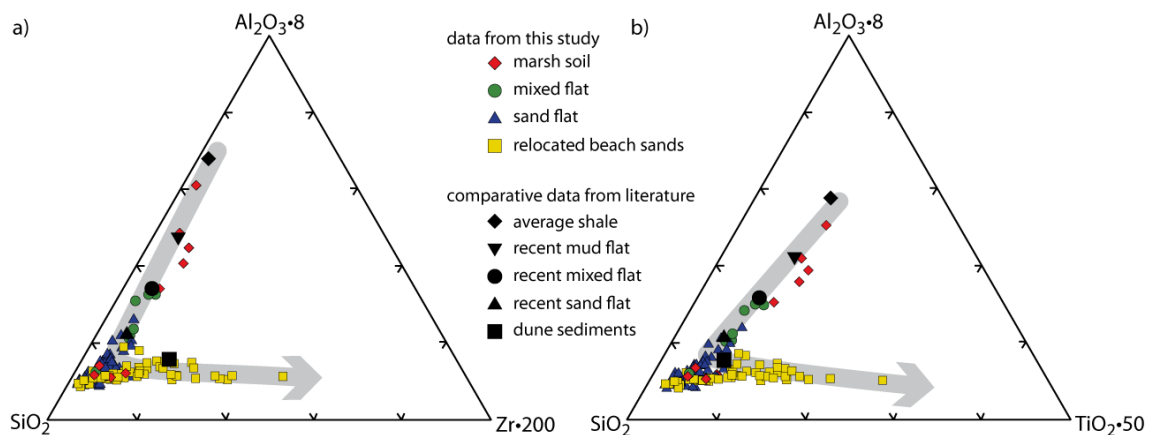
Fig. 2.9: Ternary plot a) $Al_2O_3 \cdot 8$, SiO_2, $Zr \cdot 200$, b) $Al_2O_3 \cdot 8$, SiO_2, $TiO_2 \cdot 50$; the grey line marks direction of increasing depositional energy; comparative values of average shale from Wedepohl (1971), recent mud, mixed, and sand flat from Dellwig et al. (2000), and dune sediments from Saye and Pye (2006)

2.5.2 Relation between diatom abundance and sediment geochemistry

Figure 2.10 shows the Si/Al and Zr/Al values of cores L1 and L2, the TDV, a synthetic lithological profile, and the percentage of three halobous diatom groups (polyhalobous, mesohalobous, and oligohalobous). In general, high Si/Al and Zr/Al values are associated with low TDV. In case of low TDV less variation in the number of diatom valves of one of the halobous groups leads to high variations in the percentage of this group. Thus, these results should be handled in a more qualitative than quantitative way. Allochthonous diatom input of resistant marine planktonic and tychoplanktonic species can be high in any tide-influenced environment and even mask the autochthonous diatom species (Simonsen, 1962; Vos and De Wolf, 1993, 1994), which may complicate environmental reconstructions. The Si/Al and Zr/Al ratios in Figure 2.10 correspond to the respective lithological units of site L3 to L6 (Tab. 2.2, Figs. 2.2 and 2.4) and reflect the depositional energy as well.

The occurrence of weakly silicified, fragile diatoms (e.g. *Scolioneis tumida*, Fig. 2.3) confirms the low depositional energy of the marsh soil. *Scolioneis tumida* belongs to the benthic epipelic diatoms which are related to fine-grained sediments (Vos and De Wolf, 1993). As described in section 2.4.1, the marsh soil deposits chiefly contain silt and clay. The low Si/Al ratio of 8 (Fig. 2.10) of the marsh soil samples reflects this observed sedimentology. The marine planktonic and tychoplanktonic species within the marsh soil are assigned to be allochthonous diatom input. The high abundance of mesohalobous, aerophilous diatom species (*Diploneis interrupta* = 41.5%, Fig. 2.3) indicates the transition from tidal flat to salt marsh sedimentation.

The relocated beach sands reveal no complete diatoms but contain the highest numbers of fragments (Figs. 2.3 and 2.10). Even strongly silicified diatoms with high preservation potential are missing as complete frustules. Thus, the high depositional energy of the relocated beach sands is additionally confirmed.

Within the sand flat deposits three distinct peaks in TDV are found while the remaining sand flat sediments are comparatively poor in diatoms. The higher abundance of species partly coincide with decreasing Si/Al ratios due to occurrence of intercalated silty/clayey layers or lenses, finally indicating lower depositional energy (Fig. 2.10). The absence of significant abundances of the sand flat species *Achnanthes delicatula* (Vos and De Wolf, 1993, 1994; Zong and Horton, 1999), which is a strongly silicified and thus well conservable species, reflects higher depositional energy conditions.
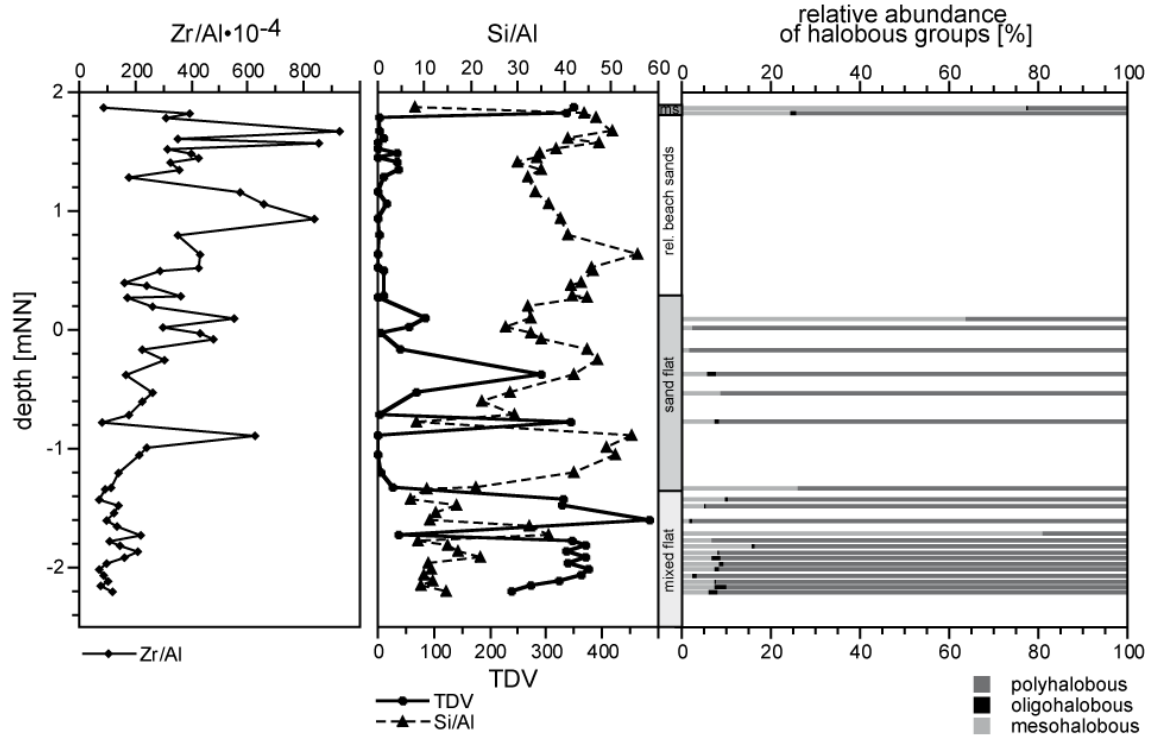
Fig. 2.10: left: Zr/Al ratio, Si/Al ratio of the sediment of L1 and L2, the total number of diatom valves (TDV), middle: simplified lithology (ms=marsh soil), right: relative abundance of polyhalobous, mesohalobous, and oligohalobous diatoms

Within the mixed flat deposits higher TDV values and lower numbers of diatom fragments occur. The abundance of the fragile marine diatom *Raphoneis amphiceros* (Fig. 2.3) underlines the postulated low depositional energy of the mixed flat deposits very well. The mixed and sand flat deposits are dominated by polyhalobous diatoms, especially (tycho)planktonic species. Some of the polyhalobous diatoms, especially the strongly silicified species (e.g. *Paralia sulcata*) are allochtonous and therefore not very diagnostic for these deposits. Nevertheless, their variation in abundance likely reflects changes in depositional energy. The abrupt change from high TDV (mixed flat) to low TDV (sand flat) point out to an inferred increase in depositional energy and coupled deterioration in diatom valve preservation (Fig. 2.10). In comparison to sand and mixed flat deposits, the marsh soil sediments reveal significant differences in diatom composition as mesohalobous, aerophilous diatoms are highly abundant in the marsh soils due to irregular flooding events during the onset of salt marsh deposition.

2.5.3 Reconstruction of sedimentary conditions

The combination of geochemical and diatom analyses allows the reconstruction of the sedimentary history of the studied sediments (Dellwig et al., 1999).

The investigated sediments on Langeoog island belong to the seaward side of the Holocene accumulation wedge (Hoselmann and Streif, 2004; Streif, 1990, 2004) which resulted from cyclic alternation of transgressive and regressive phases of the sea-level rise. Transgressive phases are characterised by brackish and marine deposits overlying limnic to semi-terrestrial peats while peats overlying brackish and marine sediments define regressive phases (Dellwig et al., 2001; Hoselmann and Streif, 2004; Streif, 1990). As shown by Streif (2004) such alternations are less developed within the barrier island areas when compared with the near-coastal zones. Nevertheless, Holocene sediments from Langeoog are classified as a marine-littoral sediment sequence by the appearance of the "*Hydrobia*-layer" marker stratum (Barckhausen, 1969; Streif, 1990) within the sand flat deposits.

The sequence starts with an alternation of fine sand and silt/clay. The marine origin of these deposits is supported by high abundances of marine (tycho)planktonic diatoms. The geochemical composition of this unit leads to classification as mixed flat deposits (Dellwig et al., 2000). Based on their geochemistry the mixed flat deposits are assigned to low depositional energy conditions (Figs. 2.6 and 2.9) this interpretation is supported by low numbers of diatom fragments (Fig. 2.3). The overlying unit consists of fine sand with intercalated small clayey/silty layers and lenses and thus defined as sand flat. As low TDV values complicate microfacies classification microfacies analyses are less well applicable than geochemical analyses for this unit. The higher depositional energy of the sand flat deposits is mainly identified by its geochemical composition (Figs. 2.6, 2.9 and 2.10; Tab. 2.2). The *Hydrobia* layer within the sand flat deposits serves as a marker stratum. Freund and Streif (1999) dated *Hydrobia ulvae* on the barrier island Borkum (Fig. 2.1a) at a similar elevation level with an age of 2,090 ± 115 BP. Thus, the formation of the *Hydrobia* layer on Langeoog island can be assigned to the transition between the transgression Dunkirk Ib and the Regression 4 concerning to Behre (2003). The *Hydrobia* layer marks the southern edge of the initial sand plate formed during the earliest stage of the development of Langeoog island. Although, this sand plate was above mean high tide level it was still lacking a closed vegetation cover (Barckhausen, 1969).

The marsh soil deposits at the top of the sequence are dominated by silt and clay. They represent the transition from tidal flat sedimentation with regular tidal flooding to salt marsh sedimentation with irregular tidal flooding. This is confirmed by the occurrence of the diatom *Diploneis interrupta*, which is adapted to irregular flooding. Vos and De Wolf (1993, 1994) and Zong and Horton (1999) stated that marine/brackish aerophilous diatoms such as *Diploneis interrupta* are related to salt marshes around MHW (mean high water) with relative abundances of up to 40% and to salt marshes above MHW of up to 95%. The abundance of fragile diatoms like *Scolioneis tumida* or *Navicula peregrina* indicate low energy conditions. The calmer sedimentation conditions are also reflected in geochemical patterns, as seen in increasing Al_2O_3 and decreasing SiO_2 contents, respectively (Fig. 2.4).

The relocated beach sands (Fig. 2.2) on Langeoog island are situated close to several dune breaches (Fig. 2.1b) which occurred after storm surge events in 1717 and 1825 (Obstfeld, 2001). These events produced the pathway for the accumulation of beach and dune sands by eroding and overlying the upper part of the sand flat and the entire marsh soil deposits of the former undisturbed Holocene sequence. Therefore, the relocated beach sands deposited in the study area reflect a mixture of sandy material originating from the dunes and the beach on the seaward site of the dunes. This multi end member composition of the relocated beach sands is also seen in their geochemical characteristics (Tab. 2.2) as certain similarities with sediments of different genesis are evident. For instance, Huisman et al. (2000) reported comparable contents of several major components in Pleistocene sands (SiO_2=88%, Al_2O_3=3.7%, TiO_2=0.19%; Fe_2O_3=1.5%, Mn=233 µg/g). In comparison to marine surface sands from the Barents Sea (SiO_2= 85%, Al_2O_3=7.7%, TiO_2=0.16%, Fe_2O_3=1.6%) and the upper continental crust (SiO_2=66%, Al_2O_3=15.2%, TiO_2=0.68%, Fe_2O_3=5%, Mn=600 µg/g, Zr=190 µg/g) further similarities in geochemical composition are obvious (McLennan, 2001; Taylor and McLennan, 1985). Furthermore, the geochemical composition of dune sediments (SiO_2 89.2-92.5%, Al_2O_3 2.0-3.1%, TiO_2 0.3-2.2%; Fe_2O_3 0.8-4.6%, Mn 232-1,472 µg/g, Zr 310-3,121 µg/g) of Jutland, Denmark (Saye and Pye, 2006) corresponds well with the relocated beach sands.

On the other hand, the relocated beach sands differ from sand flats, for example, by extremely high Zr/Al ratios (Figs. 2.4 and 2.10; Tab. 2.2) or the amount of heavy minerals (e.g. ilmenite, zircon) characterising the high energy conditions during deposition (Figs. 2.6 and 2.9). The decreasing Zr/Al ratios of the relocated beach sands from L3 to L6 (Fig. 2.4) may be

explained by the proximity of site L3 and the larger distance of site L6 to the breached dunes (Fig. 2.2). The significant double peak found in the Zr/Al, Fe/Al and Mn/Al profiles possibly reflects the dune breaching events in 1717 and 1825 reported by Obstfeld (2001). The geochemical composition of the relocated beach sands is comparable to Pleistocene sands (Huisman et al., 2000) as well as dune sediments (Saye and Pye, 2006), and reflects the heavy mineral pattern of the southern North Sea (e.g. Ludwig and Figge, 1979). The dune breaches within the study transect area were not completely closed until 1906 (Obstfeld, 2001). This offers a possible explanation for the relatively thin marsh soil deposits, especially at the northernmost site L3. The original marsh soil was eroded and the present marsh soil development started in 1906 at the earliest.

2.6 Conclusions

This study combines geochemical and diatom investigations of sediments from the East Frisian barrier island Langeoog to provide a better understanding of the depositional conditions during Holocene evolution.

Correlations between FeO and TiO_2 along with SEM-EDX analyses prove the dominating presence of the heavy mineral ilmenite within the study area and allow the characterisation of depositional energy conditions. Ternary plots visualise the relationship between sediment geochemistry (represented by the major oxides SiO_2, Al_2O_3, TiO_2 and the trace element Zr) and depositional energy for the investigated marine-terrestrial sediments and are assumed to be applicable to other sedimentary systems.

The combination of diatom analyses and geochemical data document the barrier island development as well as the varying energetic conditions during deposition. Sediments deposited under high depositional energy conditions reveal low to no diatom abundances and concomitant high number of diatom fragments. Sediments deposited under low depositional energy are characterised by high diatom abundances and low number of diatom fragments.

The studied Holocene sediment sequence starts with mixed flat deposits on its base accumulated under low energy and marine depositional conditions followed by sand flat deposits of higher energy and marine depositional conditions. The highest depositional energy conditions are recorded in the adjacent relocated beach sands which were accumulated after

several dune-breaching events. The sequence is overlain by marsh soil deposits of low energy and marine-terrestrial conditions.

Acknowledgements

3. Salt marsh sedimentation during simulated sea-level rise and its relation to Holocene coastal development of NW Germany

Kerstin Kolditz, Olaf Dellwig, Jan Barkowski, Holger Freund, Hans-Jürgen Brumsack

Abstract

De-embankment in the salt marshes of the East Frisian island of Langeoog (Southern North Sea) was carried out in 2004, thereby inducing an artificial transgression within an area of 2.2 km^2. The removed dike was rebuilt about max. 620 m northwards of its former position. Samples from three sediment settling traps (SST) located along a N-S transect across the salt marsh were collected monthly during a 13 month period. SST material was analysed for geochemical (major and trace elements) and sedimentological (grain size, sedimentation rates) parameters. Additionally, surface pressure was determined continuously during the sampling period thus revealing tidal inundation frequency and inundation water level.

The imported sediment is dominated by silt and exhibits a geochemical composition comparable to suspended particulate matter (SPM) from the adjacent Wadden Sea thus indentifying SPM as an essential contributor to salt marsh accumulation. Biogeochemical processes occurring in the open water column, e.g. non-conservative behaviour of Mo (Dellwig et al., 2007a; Kowalski et al., 2009), are reflected in SST.

The comparison with older Holocene coastal deposits reveals a mixed geochemistry of the SST. Both the geochemical composition of Holocene brackish and tidal flat sediments is reflected in the SST. Therefore, the investigated SST samples from Langeoog Island reflect an early stage of sea-level rise and document the development from a terrestrial towards a marine dominated system. Sedimentation rates range from 3.8 to 7.2 mm/yr and are higher than the local sea-level rise evidencing vertical salt marsh growth. Extreme events as storm surges deliver highest amounts of sediment and play an important role in salt marsh accumulation within the study area.

3.1 Introduction

The Holocene coastal deposits of NW Germany were formed during the sea-level rise after the Weichselian Glacial. The rising North Sea pushed sedimentary material landwards („bulldozing effect", Hagemann, 1969) which led to the formation of the so-called Holocene accumulation wedge in the coastal area of Lower Saxony, NW Germany. The development of the barrier islands, tidal flats, and coastal marshlands along the North Sea coast of Lower Saxony started at about 7,500 BP (Hoselmann and Streif, 2004; Streif, 1990, 2004). Sediments of the seafloor (Veenstra, 1982), i.e. eroded Pleistocene deposits and Holocene marine sediments from the North Sea (Hoselmann and Streif, 2004) chiefly account for the sediments of the Holocene sedimentary wedge. Hoselmann and Streif (2004) reported that 90% are delivered from marine sources and only 10% by rivers. A detailed description of the Holocene evolution is given by, e.g., Long et al. (1988); Streif (2004).

The coastal deposits contain a large number of different sediment facies which range from lagoonal to tidal flat sediments depending on exposition to the open sea. According to Eisma and Kalf (1987) the Wadden Sea is one of the few areas of the North Sea in which accumulation and deposition of suspended particulate matter occurs. Eisma (1981) reported that the tidal flats of the Wadden Sea and the Wash embayment in eastern England account for 12-18% of the total amount of suspended matter deposited in the North Sea area. However, studies by Dellwig et al. (2002), Flemming and Nyandwi (1994), Flemming and Ziegler (1995), and Hinrichs et al. (2002) document a loss of fine grained components in the tidal flat sediments of the Wadden Sea in recent times. The authors attributed this trend to higher energy levels caused by dike-building which alters the hydrodynamic regime and sedimentation conditions. Land reclamation and dike construction along the mainland coast of NW Germany inhibit the deposition of sediments with settling velocities <0.5 m/s corresponding to a settling diameter of 0.088 mm and finer (Flemming and Nyandwi, 1994; Flemming and Ziegler, 1995). Furthermore, dike construction reduces vegetation areas in the sub- and supratidal zone which act as efficient sediment traps and lower the velocity of currents (Hoselmann and Streif, 2004). In contrast, during the Holocene the coastland of NW Germany was characterised by the occurrence of extended areas of marshlands vegetated by e.g. *Phragmites australis* (Dellwig et al., 2001, 2002). As a result of dike construction no modern analogues are found along the coast of NW Germany (Dellwig et al., 2001).

After a de-embankment in 2004 on the landwards side of the East Frisian barrier Island Langeoog (Fig. 3.1a) 2.2 km^2 of salt marshes are now exposed to regular tidal flooding (Kolditz et al., 2009b) thereby simulating a "natural" transgression in a discrete area. This de-embankment includes the removal of a summer dike and the build-up of a new dike further inland (Fig. 3.1b), thus, allowing investigation of processes occurring during a rising sea level.
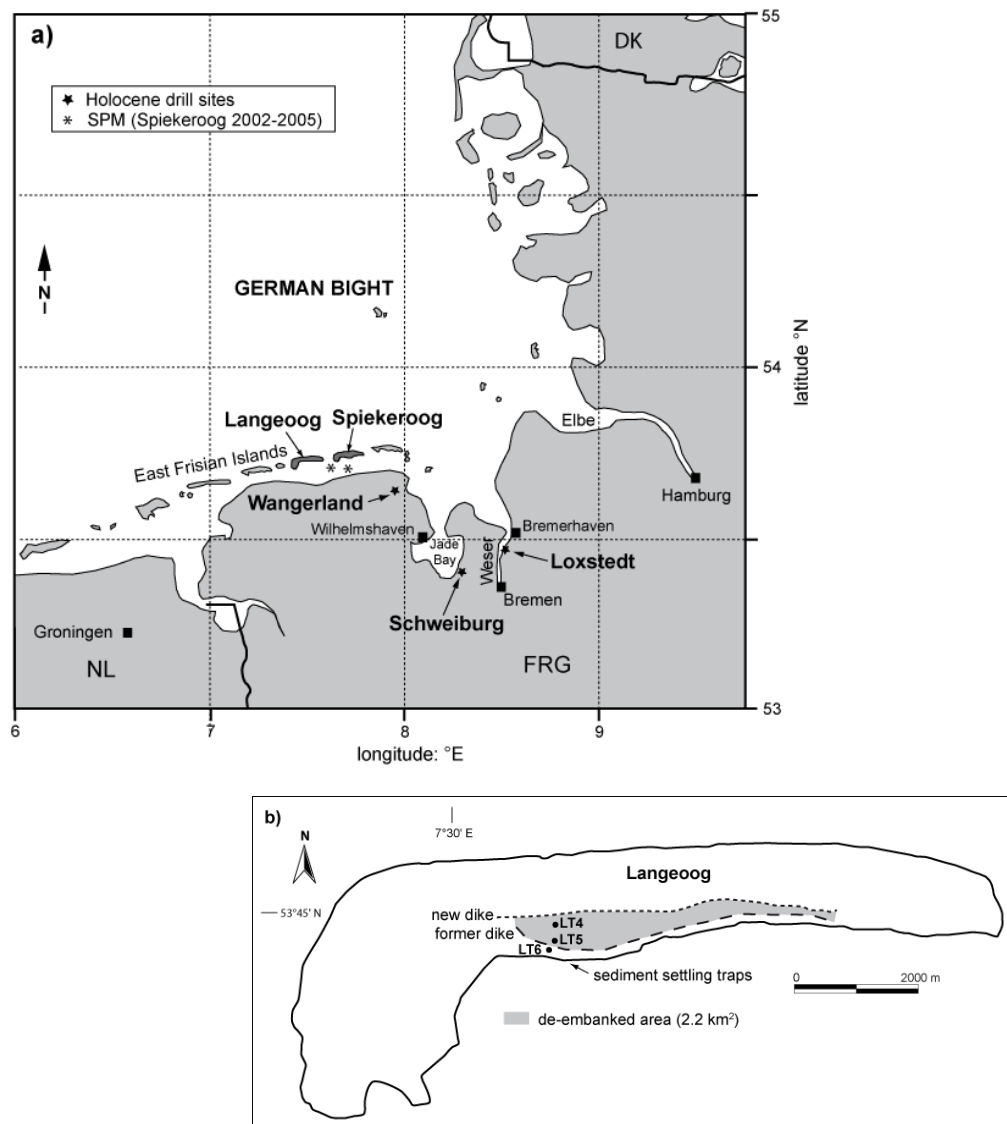
Fig. 3.1: a) Map of the study area showing the sampling sites for suspended particulate matter in the backbarrier area of Spiekeroog Island and the drill sites of the Holocene coastal deposits (Loxstedt, Schweiburg, Wangerland). b) detailed map of the East Frisian barrier island of Langeoog showing the sites of the sediment settling traps and the de-embanked area.

This study combines geochemical analyses of freshly deposited sediment material on the de-embanked salt marsh area, of suspended particulate matter from the adjacent Wadden Sea, and of older Holocene coastal deposits from NW Germany. The major goals of this work

are the geochemical characterisation of the deposited material, the determination of the major sources, and the comparison of deposited material and Holocene coastal sediments in order to improve our knowledge about sedimentation processes under transgressive conditions, finally, leading to a balance of the imported material and compounds to the de-embanked area. Furthermore, the seasonal behaviour of the redox-sensitive trace metals Mo and Mn was investigated as both metals reveal significant changes in their seasonal patterns in the open water column (Dellwig et al., 2007a, b) which are likely also reflected in the material deposited in the salt marshes.

3.2 Geological setting and study area

Langeoog Island forms part of the East Frisian barrier island system of NW Germany (Fig. 3.1a) which developed during the Holocene sea-level rise app. 7,500 BP (Streif, 1990). The Holocene sediments on Langeoog Island belong to the seaward side of the Holocene accumulation wedge (Hoselmann and Streif, 2004; Streif, 1990, 2004) consisting of a marine-littoral sequence and salt marsh deposits on the top (Freund et al., 2004; Kolditz et al.; 2009a; Streif, 1990, 2004).

The study site on Langeoog Island is situated on the landward side of the island close to the back barrier tidal flats (Fig. 3.1b). Semidiurnal tides with a tidal range of on average 2.7 m dominate the hydrodynamic situation. The mean high water reaches a height of 1.4 m NN (german zero datum). This study bases on three locations, two within the above mentioned de-embanked salt marsh area (LT4 and LT5) and a further location close to the former dike (LT6). Sites LT5 and LT6 are inundated 260 to 280 times per year, whereas site LT4 shows only about 100 inundations per year (appendix A 3, Barkowski et al., 2009). All sites are vegetated with site LT4 being characterised by the occurrence of high marsh species (e.g. *Festuca rubra*) and low marsh species (e.g. *Atriplex portulacoides*) at site LT5 and LT6 (appendix A 3, Barkowski et al., 2009).

Suspended particulate matter samples originate from the easterly located back barrier area of the Island of Spiekeroog (Fig. 3.1a). The samples were taken from surface waters during 12 cruises with RV "Senckenberg" between February 2002 and November 2005. The tidal and seasonal behaviour of the redox-sensitive trace metals Mn and Mo in from this area has been described in detail by Dellwig et al. (2007a, b).

The drilling sites of the Holocene coastal deposits are Loxstedt, Schweiburg, and Wangerland (Fig. 3.1a) which are comprehensively described in several sedimentary and geochemical studies (e.g. Dellwig et al., 1998, 1999, 2000, 2001, 2002; Hinrichs et al., 2002). The cores were drilled with a drilling device (Merkt and Streif, 1970) of the Geological Survey of the Federal State of Lower Saxony, Hannover (Germany). The Loxstedt drill site is located about 20 km SW of Bremerhaven close to the river Weser (Fig. 3.1a) and consists of two parallel cores (Archive No. GE 430, 432), which were combined to one composite profile. The upper part of this site is located in the funnel-like Pleistocene watercourse of the river Weser (Müller, 1977) thus reflecting a river influenced intertidal system. The drill site Schweiburg (Archive No. GE 707) from the Jade Bay (Fig. 3.1a) represents an open tidal flat area during Holocene sea-level rise.The third location in the marshlands of the Wangerland about 18 km NW of Wilhelmshaven (Fig. 3.1a) consists of a transect (about 3 km in length) of five drill cores (Archive No. W1=KB5552, W2=KB5156, W3=KB5750, W4=KB5752, W5=KB5950). This area was formerly a sheltered so-called Crildumer Bay which was presumably divided by a peninsula into a northern and a southern part (Petzelberger, 1997). The transect is located in the southern part of this bay.

3.3 Material and Methods

3.3.1 Material from sediment settling traps

Sediment settling traps (SST) (Fig. 3.2) were installed in the salt marsh area at three different sites. The higher and the lower salt marsh locations (LT4 and LT5) are situated within the de-embanked area. The location at the transition from lower salt marsh to the tidal flats (LT6) was not embanked and is located close to the removed dike (Fig. 3.1b).The inner tube is filled with saline water from the surroundings. During inundation suspended particles can settle within the inner tube. The sediment traps were sampled almost monthly between February 2006 and February 2007. Sediment material in the inner tube was filled in polyvinyl chloride (PVC) bottles and stored at 4°C until further preparation in the laboratory.
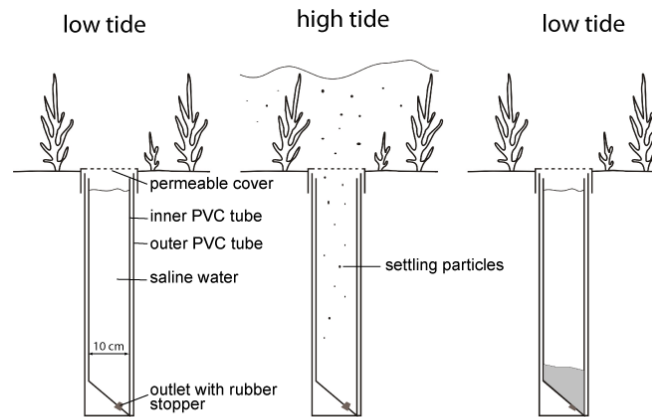
Fig. 3.2: Sketch of the sediment settling traps showing the design and the operation during a tidal cycle.

3.3.2 Sediment amount and grain size analyses

Material from the SST was sieved (mesh size: 250 µm) and dried at 40°C for bulk parameter and multi-element analyses. Sediment amount (n=39) was determined by weighting the <250 µm fraction. For grain size analyses subsamples were dried at 525°C for 5h. Grain size analyses (n=32) required not less than 5 g sediment and were performed in triplicate of each sample by a laser particle sizer (Fritsch Analysette 22) using the software Analysette 22. Grain sizes were grouped in three major fractions: clay (<2µm), silt (2-63 µm), and sand (> 63 µm). Additionally, the silt fraction was subdivided into fine silt (2-6.3 µm), medium silt (6.3-20 µm), and coarse silt (20-63 µm).

3.3.3 Surface pressure measurements

Pressure sensors were installed near the sediment surface at the high marsh site LT4 and the low marsh site LT6. Pressure data were collected with an ALMEMO System (Ahlborn, Holzkirchen, Germany). Pressure data were recorded by a connected data logger in 10 min intervals from October 2006 to February 2007 at site LT4 and from June 2006 to February 2007 at site LT6. The data were monthly downloaded.

3.3.4 Geochemical analyses

Sediment settling traps: Total organic carbon (TOC) of the SST (n=28) was calculated as the difference between total carbon (TC) and total inorganic carbon (TIC). The TC contents were determined by using a C/S element analyser (Eltra CS 500). The TIC content was

determined with a UIC Coulometrics Inc. CM5014 CO_2 coulometer coupled to a CM5130 acidification module (Engleman et al., 1985; Huffman, 1977). Major components (Ti, Al, Fe, Mg, Ca, K, P) and trace metals (Mn, Mo, Sr, Zr) were measured by ICP-OES (iCAP 6300 DUO, Thermo Scientific) from $HClO_4$/HF digestions. Acid digestions were performed after Heinrich and Hermann (1990) in closed teflon vessels (PDS-6; Heinrichs et al., 1986) heated for 6 h at 180°C by treating 500 mg sample with 4 ml HF + 4 ml $HClO_4$. After digestion the acids were evaporated using a heated metal block (180°C) and were re-dissolved and fumed off three times with 3 ml half-concentrated HCl, followed by re-dissolution with 0,2 ml conc. HNO_3 and dilution to 10 ml. Corrections for residual salt were necessary for the samples of LT4 in April, June August, and October 2006 as seen in unusual high Na values.

Suspended particulate matter from the Wadden Sea: Surface water sampling was performed in intervals of 20-60 min during 12 cruises with RV Senckenberg (2002, 2003, 2005). A comprehensive description of the sampling procedure and the geochemical analyses is given by Dellwig et al. (2007a, b). Generally, major and trace elements were determined from acid digestions (see paragraph *sediment settling traps*) by ICP-OES (Optima 3000XL, Perkin Elmer) and ICP-MS (Element I and II, Thermo Scientific).

Holocene deposits: Sampling was performed on the Holocene drill cores at 5 to 10 cm intervals depending on lithology. The samples (n=349) were analysed for major elements and trace metals by XRF (Philips PW 2400, equipped with a Rh-tube). Mo was measured by using ICP-MS (Element I, Thermo Finnigan). Total carbon (TC) was determined by combustion using an IR-analyser Leco SC-444 and inorganic carbon (TIC) with a UIC coulometer. Further Details about the Holocene sediment samples are given by Dellwig et al. (1999, 2002) and Hinrichs et al. (2002).

Accuracy and precision of all geochemical analyses were checked by parallel measurements of international reference materials (GSD-10, SDO-1) and in-house standards (TW-TUC: shale, Loess: aeolian material) and were <6%.

3.4 Results

3.4.1 Accumulation rates of SST

As the design of the sediment settling traps (Fig. 3.2) does not consider sediment loss by erosion, the present data has to be regarded as maximum sediment import values. Sediment

amounts collected from SST ranged on average from 0.7 to 1.0 kg m^{-2} month^{-1} for sites LT4-6 (Tab. 3.1) showing a high seasonal variability with a minimum value of 0.1 kg m^{-2} month^{-1} in May 2006 at site LT5 and a maximum amount of 3.4 kg m^{-2} month^{-1} at site LT6 in November 2007 (Fig. 3.3a). Generally, sediment amounts are elevated in autumn and winter due to more pronounced tidal inundations and storm activities. During summer and partly spring, sediment amounts are lowest, except for site LT4 in June and August 2006. Elevated sediment amounts during these months are caused by human activities (construction works) near the sediment trap. While sites LT5 and LT6 show a similar pattern during the entire sampling period, site LT4 reveals lower sediment amounts especially from November 2006 to February 2007.

Tab. 3.1: Average amount of material and percentage of the grain size fractions clay (T), silt (U), and sand (S) from sediment settling traps (SST). Geochemical characteristics (bulk parameters, major and trace elements, element/Al ratios) of SST material are compared to recent suspended particulate matter (SPM) from the Wadden Sea (Spiekeroog Island), Holocene coastal sediments (lagoonal, brackish, and tidal flat deposits), and the average shale after Wedepohl (1971, 1991).

parameter	SST			recent	Holocene			av. shale
	LT4	LT5	LT6	SPM	lagoonal	brackish	tidal flat	
SST [kg m^{-2} month^{-1}]	0.7	1.0	1.0					
T (<2 µm) [%]	12	10	11					
U (<2-63 µm) [%]	88	89	89					
S (<63-250 µm) [%]	0.7	0.5	1.0					
TOC [%]	7.0	4.1	4.5	4.6	6.3	2.2	1.3	0.2
TIC	2.3	1.2	1.0	1.5	0.02	1.1	1.2	0.15
Ti	0.14	0.3	0.25	0.32	0.41	0.38	0.32	0.47
Al	2.0	5.1	4.9	5.1	6.4	5.7	4.2	8.9
Fe	1.2	3.1	2.6	3.3	4.0	3.7	2.4	4.8
Ca	6.9	5.3	6.1	5.1	0.5	3.7	3.9	1.6
K	0.76	1.6	1.4	1.8	2.0	1.9	1.6	2.8
P	0.54	0.27	0.27	0.17	0.05	0.06	0.05	0.07
Mn [mg kg^{-1}]	189	447	397	1044	348	449	387	850
Mo	4.0	2.7	3.3	6.4	8	n.d.	n.d.	1.3
Sr	884	331	399	245	92	143	165	230
Zr	81	119	105	150	196	214	328	160
TOC/Al	3.5	0.8	1.0	0.90	0.98	0.37	0.31	0.02
TIC/Al	1.2	0.2	0.2	0.3	0.003	0.2	0.3	0.02
Ti/Al	0.07	0.06	0.05	0.06	0.06	0.07	0.08	0.05
Fe/Al	0.60	0.61	0.53	0.65	0.63	0.65	0.57	0.54
Ca/Al	3.5	1.0	1.2	1.0	0.08	0.65	0.93	0.18
K/Al	0.38	0.31	0.29	0.35	0.31	0.33	0.38	0.31
P/Al	0.27	0.05	0.05	0.03	0.008	0.01	0.01	0.008
Mn/Al*10^{-4}	95	88	84	205	54	79	92	96
Mo/Al*10^{-4}	2.0	0.5	0.7	1.3	1.3	n.d.	n.d.	0.15
Zr/Al*10^{-4}	41	24	22	29	31	38	78	18
Ca/Sr*10^{4}	78	160	153	208	54	259	236	71

The relation between sediment amount and inundation frequency is presented in Figures 3.3b and c for sites LT4 and LT6. Near surface pressure data at these sites reflect the number of tidal inundations and the tidal range. It is clearly seen that higher inundation frequencies and tidal ranges are accompanied by higher sediment amounts. Distinct storm surge events are seen in November 2006 and January 2007. During these events, the

maximum height of the water column overlying the salt marshes reached levels of about 2.3 m (LT4) and 2.4 m (LT6) in November 2006 and 1.8 m (LT4) and 1.6 m (LT6) in January 2007.
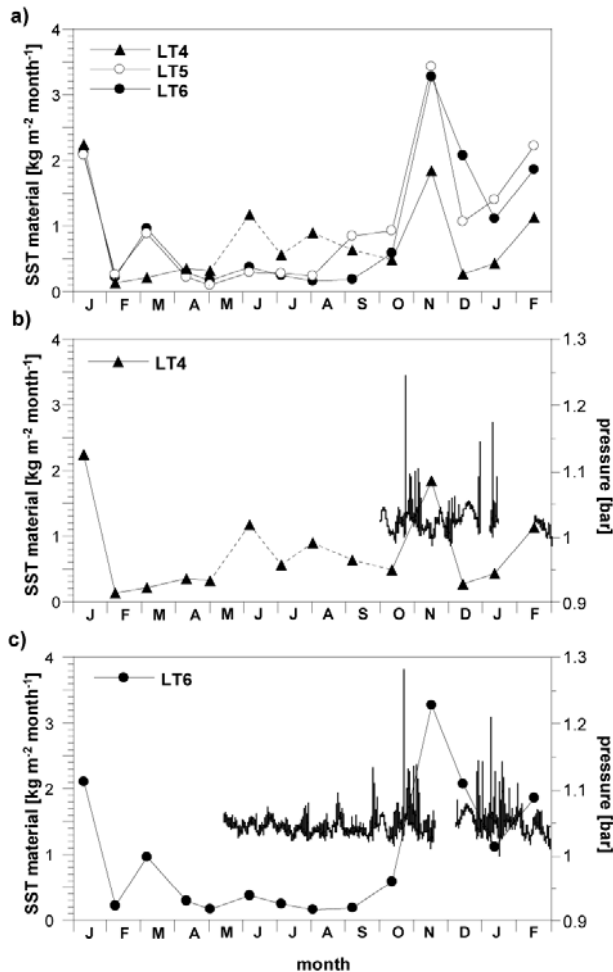
Fig. 3.3: a) monthly material accumulation in the sediment settling traps (SST) from sites LT4-6 during sampling period from February 2006 to February 2007. The dashed line for site LT4 marks man-made disturbances resulting in artificially high sediment amount. b) sediment amount (February 2006-February 2007) and surface pressure data (October 2006-February 2007) of site LT4, c) sediment amount (February 2006-February 2007) and surface pressure data (June 2006-February 2007) of site LT6. Surface pressure data are not air-pressure corrected.

3.4.2 Sedimentological properties of SST

The average grain sizes of SST material reveal only small variations when comparing the sites LT4-LT6 (Tab. 3.1). The material is dominated by silt followed by clay whereas the sand fraction plays only a minor role. However, distinct seasonal trends are seen in the grain size distribution throughout the sampling period. Generally, an increasing abundance of clay is observed towards summer which is most pronounced at site LT6 (Figs. 3.4a-c). Regarding the silt fraction, which has been subdivided in fine (fU), medium (mU), and coarse grained (gU) silt, decreasing values in the coarse fraction are seen during summer while highest abundances occur in winter and autumn. This variation in the coarse grained silt is compensated by an increasing percentage of the fine silt fraction whereas the medium fraction reveals an irregular behaviour.
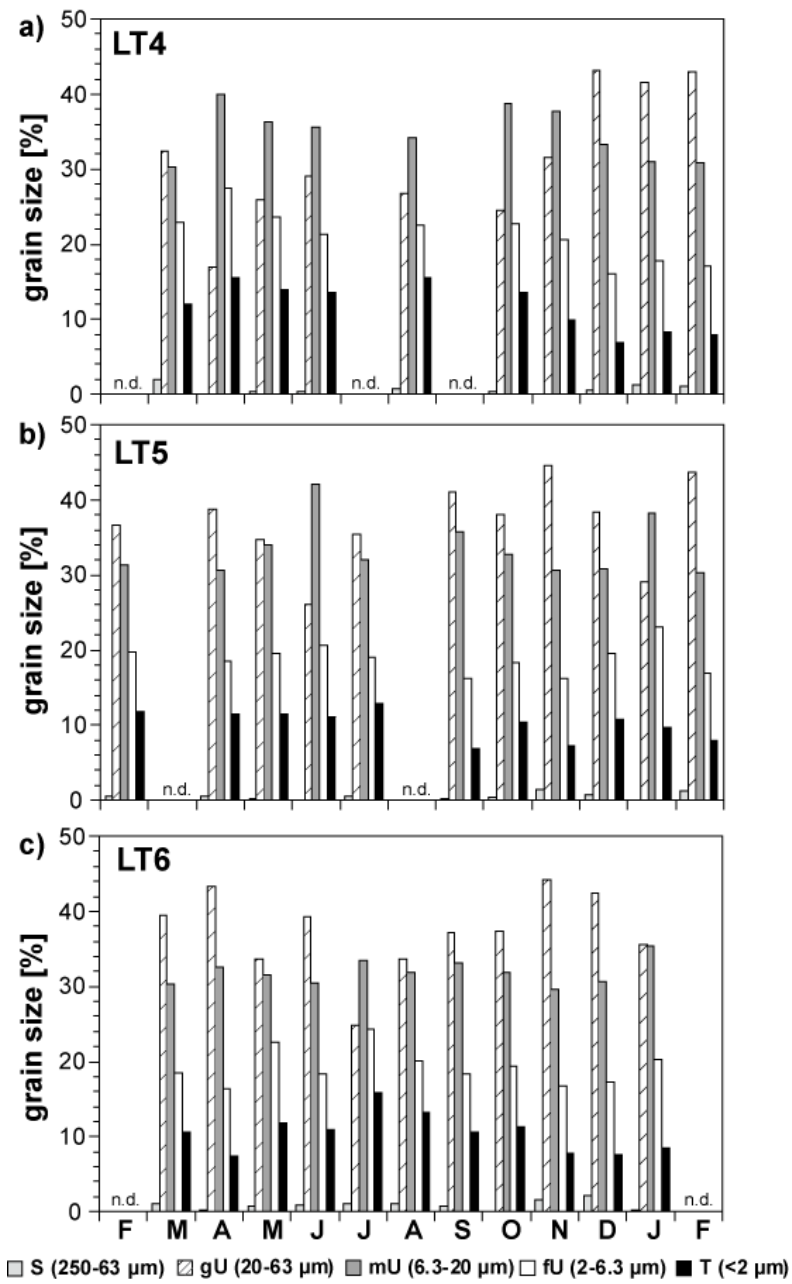
Fig. 3.4: Grain size distribution of the SST material for sites LT4-6 from February 2006 to February 2007 (S=sand, gU=coarse silt, mU=medium silt, fU=fine silt, T=clay, n.d.=not determined).

3.4.3 Geochemical properties of SST and SPM

Table 3.1 provides an overview about geochemical properties of the studied materials. In addition to absolute contents normalisation to aluminium was chosen to eliminate dilution effects caused by quartz, carbonates, and organic matter. The geochemical composition of SST material from sites LT5 and LT6 is almost similar to each other (Tab. 3.1) and is for most parameters in accordance with suspended particulate matter (SPM) from the open water column (compare Chapter 3.4.4). In comparison to the geogenic background as reflected by the average shale (Wedepohl, 1971, 1991) significant differences are seen for TOC/Al, TIC/Al, Ca/Al, P/Al, and Mo/Al ratios due to presence of organic matter and biogenic carbonates. Differences between SST and SPM are seen especially for Mn/Al which shows the highest average content in SPM of all studied materials. Distinct differences are also seen for site LT4 as this material is characterized by highest TOC/Al, TIC/Al, P/Al, and Mo/Al ratios. The Ca/Sr ratios, which allow differentiation between marine and terrigenous material (Dellwig et al., 1999), differ significantly between SPM and SST samples (Table 1). While the value of SPM clearly indicates the presence of marine carbonates (Ca/Sr>200; Pingitore and Eastman, 1985; Dellwig et al., 1998), the SST ratios from sites LT5 and 6 reflect a transient position between both endmembers and the geogenic background, respectively. The ratio of site LT4 is almost identical to the geogenic background.

The seasonal pattern of SST for selected parameters is shown in Figures 3.5a-d. All sites show a similar seasonal pattern of TOC/Al ratios (Fig. 3.5a) with maxima in summer and minima in winter with generally the highest level at site LT4. The P/Al ratios (Fig. 3.5b) at all sites reveal similar patterns as observed for TOC/Al. The Fe/Al ratios (Fig. 3.5c) fluctuate close to the average shale value. While Mn/Al ratios of sites LT5 and 6 reveal an irregular behaviour close to the average shale level, site LT4 shows maximum values in summer (Fig. 3.5d). Furthermore, the level of Mn/Al ratios of site LT4 is about 4fold higher when compared with the other sites. The Mo/Al ratios (Fig. 3.5e) reveal clearly increasing values from early summer until early autumn again with the highest level at site LT4 (Mo/Al=9.7 in August). In winter and spring Mo/Al ratios are on low levels at all sites.
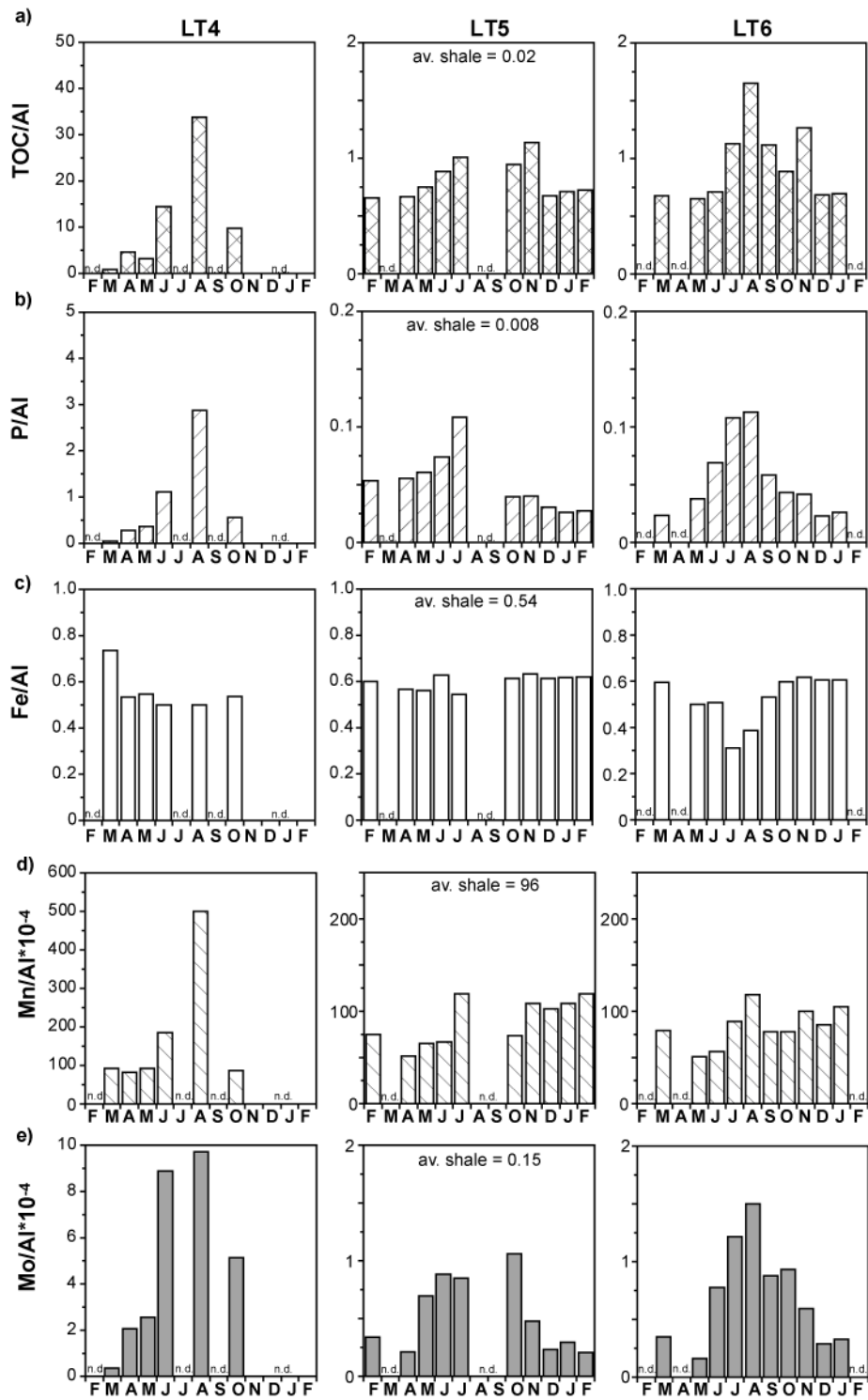
Fig. 3.5: Seasonal variations of a) TOC/Al, b) P/Al, c) Fe/Al, d) Mn/Al, and e) Mo/Al ratios of the SST material of sites LT4-6 from February 2006 to February 2007, n.d.=not determined, average shale data from Wedepohl (1971, 1991)

3.4.4 Geochemistry of Holocene coastal sediments

The major clastic facies of the Holocene coastal deposits are tidal flat, brackish, and lagoonal sediments, which can be distinguished by varying proportions of the main components quartz, clay, carbonate, and organic matter due to varying depositional energy and palaeosalinity (e.g. Dellwig et al., 1999; Streif, 1990).

In comparison to the Holocene lagoonal and brackish sediments the tidal flat sediments contain elevated amounts of heavy minerals as seen in elevated Zr/Al ratios (Tab. 3.1) caused by higher depositional energy (Dellwig et al., 2000; Hinrichs et al., 2002). This pattern is also seen in slightly increasing Ti/Al and K/Al ratios due to the presence of ilmenite, rutile, and K-feldspars. The majority of carbonate found in the brackish and tidal flat sediments can be attributed almost exclusively to the occurrence of mussel shells whereas the amounts of authigenic carbonates are negligible (Irion, 1994). Thus, typical mussel species as *Cerastoderma edule*, *Scrobicularia plana*, *Macoma balthica*, *Mytilus edulis* has been identified during visual core description. This finding is also supported by Ca/Sr ratios which are in accordance with the appearance of biogenic carbonate and marine influence, respectively. In contrast, the lagoonal sediments reflect an almost carbonate-free facies formed under lower depositional energy and salinity. The higher availability of organic matter in the lagoonal sediments as indicated by the higher TOC content encouraged the formation of pyrite thereby explaining enrichments in Mo when compared with average shale.

3.5. Discussion

3.5.1 Salt marsh accretion

It is well documented that vertical salt marsh growth occurs in salt marshes with a positive accretionary balance (Goodman et al., 2007; Orson et al., 1985, 1998; Reed, 1990), i.e. the sediment accumulation rates are equal to or greater than the local relative sea-level rise. This salt marsh accretion depends on a number of interconnected factors as for instance local hydrodynamics (tidal range, flooding regime, storm activities, relative sea level rise, Goodman et al., 2007; Orson et al., 1985, 1998; Quaresma et al., 2007; Reed, 1995; Voulgaris and Meyers, 2004), sediment supply (French and Spencer, 1993; Murphy and Voulgaris, 2006; Oenema and DeLaune, 1988; Reed, 1988), elevation (Bricker-Urso et al., 1989; Chmura et al.,

2001; French and Spencer, 1993; Paquette et al., 2004; Richard, 1978), and vegetation cover (Reed, 1988; Stumpf, 1983).

The vegetation cover promotes sediment accumulation by trapping suspended material via adherence to stems and leaves (Stumpf, 1983), by protection against erosion (Quaresma et al., 2007), and by the organic matter supply due to in-situ below-ground production (Reed, 1990). As all study sites are vegetated with site specific species (e.g. low marsh - LT5 and LT6: *Atriplex portulacoides*, high marsh – LT4: *Festuca rubra*, Barkowski et al., 2009) it can be concluded that the vegetation cover positively affects the sediment accumulation in the study area. Additionally, rain events are also periods influencing sediment accumulation within the salt marsh (Murphy and Voulgaris, 2006) as rainfall may wash sediment from the vegetation to the bed (Stumpf, 1983). However, rainfall does not significantly erode consolidated substrate from the salt marsh surface. It mobilizes only recently deposited, non-consolidated sediment (Voulgaris and Meyers, 2004). When considering the number of tidal inundations, which are 260-280 a^{-1} at sites LT5 and 6 and about 100 a^{-1} at site LT4 (appendix A 3, Barkowski et al., 2009), suspended matter from the water column of the backbarrier area appears as the most important factor contributing to the sediment supply of the salt marshes.

The sediment traps used in this study reveal sediment supply to the salt marshes on Langeoog Island during the entire sampling period of 13 months (Fig. 3.3a). Significant seasonal variations are observed. While the sediment amount in spring and summer does not exceed 0.37 kg m^{-2} month^{-1} at sites LT5 and 6, the autumn and winter months show distinctly higher sediment accumulation reaching a maximum value of 3.4 kg m^{-2} month^{-1} at site LT5 in November 2006. Such elevated import rates result from more frequent and longer inundation events (Figs. 3.3b and c). As autumn and winter times are characterised by elevated storm activities a clear relationship between storm activity and increasing sediment import is found. Thus, pressure measurements (Figs. 3.3b-c) reveal distinct storm flood events in November 2006 and January 2007 causing an overlying water column of max. 2.4 m in November 2006 and enhanced sediment supply, respectively. As the elevation of the sites plays an important role (French and Spencer, 1993) sediment accumulation is distinctly reduced at the high salt marsh site LT4 during this period (1.8 kg m^{-2} month^{-1}) which is located at an elevation 0.35 m and 0.25 m higher than sites LT5 and LT6. Therefore, site LT4 is subject to less frequent

inundations, shorter duration of tidal submergence, and a shallower overlying water column (Chmura et al., 2001; Richard, 1978) finally resulting in a lowered sediment supply.

A further factor influencing the amount of material supplied to the salt marshes forms the SPM concentration within the open water column itself. Besides depositional energy and water temperature the SPM concentration is also controlled by aggregation of particles during the breakdown of algae blooms along with the corresponding microbial processes (appendix A 1, Dellwig et al., 2007a; Lunau et al., 2006). The formation of large aggregates and flocs in summer with settling velocities >0.5 cm/s (hydraulically equivalent to the local sands) enables the deposition of fine-grained material while smaller particles dominate in winter (Chang et al., 2006a, b; Lunau et al., 2006). Therefore, the sediment distribution pattern in the tidal flats is clearly controlled by particle aggregation and disaggregation in response to seasonal changes in energy flux, water temperature, and microbial activity. As the deposition of aggregates significantly influences the SPM concentration within the open water column, Chang et al. (2006b) observed an inverse relationship between the mean floc size and suspended sediment concentrations, i.e. lower SPM concentrations during summer.

3.5.2 Sediment and elemental budget estimates

As a rough estimate the average sediment supply amounts to 10.8 kg m^{-2} a^{-1} which corresponds to a total supply of 23,900 t a^{-1} when considering the entire de-embanked area (2.2 km^2). Assuming an average dry density of 1.25 t m^{-3} (Dellwig et al., 2000) a sediment volume of 19,000 m^3 was deposited in the de-embanked area which approximates a sedimentation rate of 8.6 mm a^{-1}. Although, the sediment traps reflect only the maximum level of sediment supply due to lacking erosion, this value is close to sedimentation rates calculated on the basis of changing surface elevation by Barkowski et al. (in prep.). The authors reported an average sedimentation rate of 5.4 mm a^{-1} (site LT4: 3.8 mm a^{-1}; site LT5: 5.1 mm a^{-1}; site LT6: 7.2 mm a^{-1}), thus implying a reduction of the total sediment supply by a factor of 1.6 leading to a value of about 15,000 t a^{-1}. As the sedimentation rates are higher than the relative sea-level rise of 1.0-3.0 mm a^{-1} for north-west Europe (Wolters et al., 2005) and the global sea level rise of 1.5-2.5 mm a^{-1} (Miller and Douglas, 2004) the salt marshes on Langeoog Island currently have a positive accretionary balance. Therefore, the resulting vertical salt marsh growth is comparable to transgressive periods in the late Holocene of the study area (Behre, 2007; Streif, 1990).

However, it should be considered that the mainland dikes in the study area cause a higher depositional energy level in the water column of the Wadden Sea (Flemming and Nyandwi, 1994; Flemming and Ziegler, 1995) resulting in a higher SPM load of the open water column when compared with the Holocene situation (Dellwig et al., 2000; Hinrichs et al., 2002). Therefore, a higher amount of sedimentary material is available for deposition in the salt marsh area at present.

By using the yearly sediment supply of 15,000 t and the average geochemical composition of SST material an input of 780 t TOC a^{-1}, 54 t P a^{-1}, 5.2 t Mn a^{-1}, and 0.05 t Mo a^{-1} can be calculated for the de-embanked area. Such numbers imply that the former sandy deposits of the de-embanked area (Kolditz et al., 2009a, b) currently receive significant amounts of reactive organic-rich material thereby favouring (micro)biological activity. Deposition of organic matter presumably initiates sulphide reduction and intensifies biogeochemical cycling of nutrients and certain trace metals. Therefore, the de-embanked salt marshes act as a temporal depo-centre for material mainly of brackish/marine origin. For instance, imported particulate Mn may be stored until reduction by H_2S or microbes and is likely released again to the Wadden Sea via small tidal creeks preferentially during summer when microbial activity is highest. Additionally, as seen in pore water analyses carried out by (Kolditz et al., 2009b), tidal inundation and especially storm events favour significant release of nutrients and certain trace metals. Thus, the de-embanked salt marsh of this work forms an important component within the entire "bio-reactor" Wadden Sea. As such ecosystems are nowadays extremely rare due to dike-building, elevated amounts of reactive suspended matter are exported from the Wadden Sea, thereby transferring the aforementioned biogeochemical processes towards offshore zones.

3.5.3 Relations between SST, SPM, and Holocene coastal deposits

The simulated sea-level rise on Langeoog Island caused by the de-embankment in 2004 enables a geochemical characterisation of sediments deposited under transgressive conditions. SPM from the backbarrier area essentially contributes to the salt marsh deposition at the de-embanked area of Langeoog Island as reflected in a comparable major element composition of SPM and SST material from sites LT5 and 6 (Tab. 3.1). However, differences are found especially concerning the trace metals Mn and Mo which are stronger enriched in

SPM when compared with SST from sites LT5 and 6. Such differences are most likely due to certain fractionation during particle transport. While higher depositional energy conditions characterise sites LT5 and 6, the higher salt marsh at site LT4 reflects calmer conditions. Consequently, more shale-like detrital material is deposited at the lower salt marsh sites. In contrast, freshly formed Mn-oxides, which likely appear to a certain degree as colloids are transported until the high salt marsh. This assumption is in accordance with the lacking seasonal pattern of Mn at sites LT5 and 6 (Fig. 3.6), whereas distinct Mn enrichments are seen in summer at site LT4 when microbial oxidation of Mn^{2+} is most pronounced (Dellwig et al., 2007b). In a first approximation, this fractionation seems to contradict with the average grain sizes of the SST material (Tab. 3.1) which reveal a comparable composition. However, when excluding the periods of elevated storm activity, site LT4 is dominated by medium silt (Fig. 3.4) whereas sites LT5 and 6 are characterised by a higher abundance of the coarse-grained silt fraction.

Such fractionation is also relevant for Mo which shows a seasonal pattern clearly approving a strong relation to the TOC content (Fig. 3.5). This relation is most pronounced at the higher located site LT4 showing extremely high enrichments of organic-rich material and Mo which even exceed the SPM level significantly (Tab. 3.1, Fig. 3.6). As suggested by Dellwig et al. (2007a) Mo enrichments on coastal suspended particulate matter results from a tight coupling of (micro)biological and geochemical processes during breakdown of algae blooms. Therefore, the seasonal pattern of Mo in SST reflects biogeochemical processes occurring in the open water column thereby highlighting SPM as an important sediment source in the investigated salt marshes.
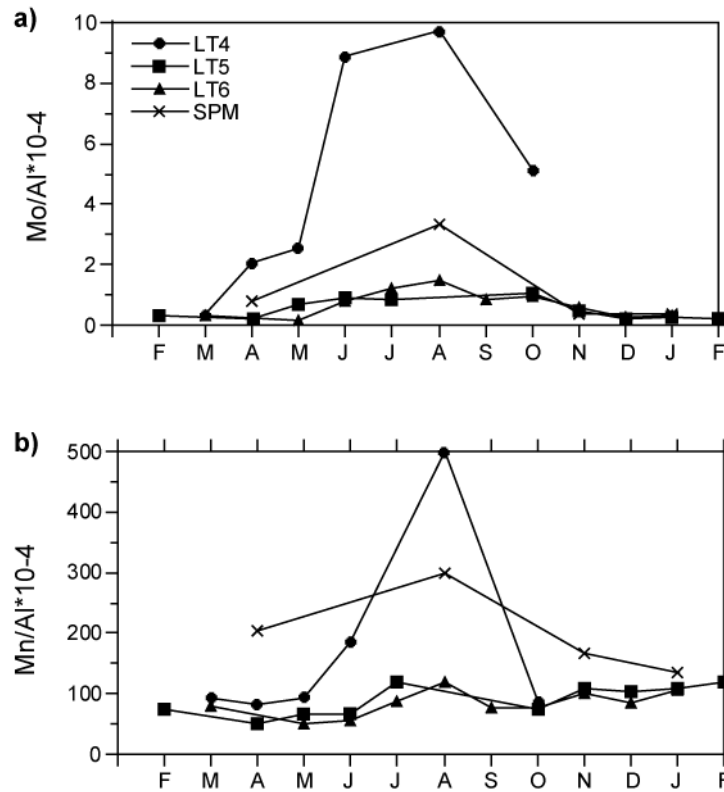
Fig. 3.6: Seasonal variations of a) Mo/Al and b) Mn/Al ratios of material from the sediment settling traps (sites LT4-6) and the suspended particulate matter (SPM) of the Wadden Sea SPM values are seasonal averages of the cruises in 2002, 2003, and 2005

Since the Holocene coastal development in NW Germany was controlled by transgressive and regressive phases (e.g. Dellwig et al., 1998; Streif, 2004) parallels in the geochemistry of SST material deposited under transgressive conditions and the Holocene coastal deposits may also exist. Depending on salinity, depositional energy, and morphological aspects the Holocene deposits of the investigated area are generally divided into lagoonal, brackish, and tidal flat sediments (Streif, 1990). While the lagoonal sediments were formed under comparatively calm and low-salinity conditions, brackish and especially tidal flat sediments were subjected to a pronounced marine influence.

As seen above, the SST site LT4 possesses an exceptional position when comparing its geochemical composition. For instance, TOC contents are comparable to the lagoonal sediments, whereas the TOC/Al ratios reveal a much higher enrichment for the SST material. Despite fractionation processes during material transport, the sediment from site LT4 may also contain a certain amount of eolian material as indicated by slightly higher Zr/Al ratios (Schnetger, 1992). Regarding the TOC/Al ratios, the lagoonal sediments are in accordance with SST sites LT5 and 6 as well as SPM. In contrast, TIC/Al and Ca/Al ratios show a stronger

relation to the brackish and tidal flat sediments. This difference is due to the amount of fresh organic matter significantly contributing to SST and SPM while older Holocene deposits were subjected to pronounced decomposition of organic matter. This is also seen in P as a major component of organic matter. Thus, P/Al ratios of the SST material and SPM are distinctly higher when compared with the Holocene deposits due to preferential decomposition of fresh marine organic matter. The relation of the SST sites LT5 and 6 to the Holocene brackish/tidal flat sediments is also seen in Ca/Sr ratios (Tab. 3.1), which clearly exceed the value of the lagoonal deposits. However, the Ca/Sr ratios of both sites do not completely reach SPM or the brackish/tidal flat sediments, which indicate biogenic calcite. Thus, the Ca/Sr ratio of SST points towards a certain contribution of terrigenous matter which is most pronounced at site LT4.

Overall, we suggest that the varying geochemical signatures of the SST indicate on the one hand the rising marine influence and on the other hand the still existing brackish conditions in the study area. Since the de-embankment dates back only about 2 years, the transgression on the salt marshes at Langeoog Island is in a very initial stage of development. The importance of SPM as a material source for recent and Holocene coastal development is however documented by comparable geochemical signatures of the different investigated materials. Therefore, the study area of this contribution provides the opportunity for performing detailed studies on the geochemical, sedimentological, and biological evolution of transgressive coastlines.

3.6 Conclusions

A de-embankment on Langeoog Island (NW Germany) caused a simulated a sea-level rise in a definite salt marsh area of 2.2 km^2. Sediment material imported under transgressive conditions was sampled by using sediment settling traps (SST). This area currently has a positive accretionary balance resulting in vertical salt marsh growth comparable to transgressive periods in the late Holocene. Sediment supply is highest in autumn and winter especially during storm events whereas the late spring and summer level is distinctly lower. Although, the SST reflect only maximum deposition because of lacking erosion, a calculated sedimentation rate coincide well with measured rates (Barkowski et al., in prep.).

The geochemical composition of the material from the SST emphasise suspended particulate matter from the adjacent Wadden Sea as a major sediment source. TOC, P and Mo

show a clear seasonal behaviour with maximum contents during summer, thus reflecting biogeochemical processes occurring in the open water column. Accumulation rates of TOC, P, Mn, and Mo highlight the investigated salt marsh as an important depo-centre for particulate matter from the Wadden Sea, thereby driving biogeochemical processes within the salt marsh ecosystem.

The comparison with Holocene coastal deposits reveals similarities of the freshly deposited material on Langeoog Island and Holocene brackish and tidal flat and sediments. Therefore, we suggest that this situation is inferred to be an example for an early stage of transgression which provides the opportunity for future interdisciplinary studies focussing on the coastal development under transgressive conditions.

Acknowledgements

4. Effects of De-Embankment on Pore Water Geochemistry of Salt Marsh Sediments

K. Kolditz, O. Dellwig, J. Barkowski, M. Beck, H. Freund, H.-J. Brumsack

Abstract

Salt marshes form part of the widely distributed intertidal landscape. The salt marshes of the East Frisian barrier island Langeoog (NW Germany) belong to the barrier-connected salt marsh type and were protected by a summer dike, which was removed in 2004. In this study pore water and sediment data were combined to investigate the effects of the de-embankment along a transect, including sites on seawater-influenced grassland, high and low salt marsh, and transition zone tidal flat/low salt marsh. Pore waters were sampled with in-situ pore water samplers for 13 months and analysed for trace metals (Fe, Mn), nutrients (NH_4^+, PO_4^{3-}), dissolved organic carbon, and sulphate. Additionally, on site measurements of pH and salinity were carried out. Pore water ultrafiltration experiments with 5 kDa MWCO (molecular weight cut off) complemented the water analyses. Sediment samples were taken from hammer corings and were analysed for bulk parameters (TC, TIC, TOC, TS) and selected major elements (Si, Al, Fe, Mn). Additionally reactive iron and manganese were analysed.

Sediments along the study transect are characterised by quartz dominance and very low TC (TOC and TIC) and TS contents. The iron content is comparable to other salt marsh sediments. The high percentage of reactive iron (up to 40%) indicates that salt marsh sediments form an important iron source for pore waters, as confirmed by high pore water concentrations of dissolved iron (up to 583 µM). Dissolved iron in pore waters most likely results from reduction and dissolution of oxidized iron minerals by organic ligands or Fe(II) organic complexes. Iron complexation by humic substances and siderophores in combination with circum-neutral pH values keeps iron in solution. Therefore, the studied salt marshes presumably form an important iron reservoir, which may account for elevated pyrite contents frequently observed in Holocene coastal peats.

Flooding of the salt marsh during a storm surge resulted in a considerable increase in pore water iron (8-fold), manganese (21-fold), phosphate (5-fold), and ammonia (7-fold) concentrations. These results show that seawater restoration (de-embankment) should be handled very carefully, especially with regard to nutrient release and subsequent changes in pore water quality.

4.1 Introduction

Salt marshes are mudflats and periodically seawater inundated marine and estuarine grassland mainly covered by halophytic vegetation (Allen, 2000; Beeftink and Rozema, 1988). Salt marshes at the coastline of the North Sea belong to the foreland and barrier-connected salt marsh types (Beeftink and Rozema, 1988). The salt marshes of the Frisian Islands, including the island of Langeoog, which is subject of this study, belong to the open-coastal back-barrier salt marsh type. This salt marsh type is defined as a sandy-muddy system on the sheltered landwards side of coastal barrier islands and spits (Allen, 2000). Sandy salt marshes are developed especially on the barrier islands (Stock, 2003).

The area of the salt marshes in the Wadden Sea of Lower Saxony (NW Germany) amounts to 26.4 km^2 on the East Frisian barrier islands, 54.6 km^2 in the mainland coastal zone, and 19 km^2 within summer polders. In Europe salt marshes are endangered habitats as human activities like dike building, land reclamation, and drainage significantly change these ecosystems. In Germany they are legally protected habitats and belong to the Wadden Sea National Park of Lower Saxony (Stock, 2003). Nevertheless, the salt marshes of Lower Saxony are largely embanked areas or highly influenced by their proximity to coastal embankments. In the past salt marshes were embanked because agriculture and cattle grazing on summer polders were very profitable. For this reason natural salt marsh systems in Lower Saxony are rarely found (Stock, 2003). Today salt marsh protection aims to promote the development of natural salt marshes. This is achieved by the termination of cattle grazing and drainage. Additionally de-embankments of previously reclaimed salt marshes and summer polders are carried out in Lower Saxony to enlarge salt marsh areas. A certain fear existed that salt marsh erosion might follow de-embankment. But it could be shown that sediment is supplied by regular tidal flooding (Stock, 2003).

Salt marshes are highly productive areas. A large portion of their productivity occurs subsurface in the form of roots and rhizomes (Schubauer and Hopkinson, 1984; Valiela et al., 1976). The salt marsh vegetation, e.g. *Spartina alterniflora*, oxidises the sediments (Howes et al., 1981), which results in organic matter degradation via aerobic respiration (e.g. Howes et al., 1984). Several recent studies suggested that ferric iron reduction may account for a significant fraction of organic matter re-mineralization in salt marsh sediments (e.g. Bull and Taillefert, 2001; Carey and Taillefert, 2005; Kostka et al., 2002; Luther et al., 1992; Taillefert et al., 2007) resulting in an intensification of the iron cycle. The presence of both macrophytic roots/rhizomes and fungi/bacteria and their resulting interaction with the sediment play an important role in salt marsh iron cycling (Buyer and Sikora, 1990; Carrasco et al., 2007; Crowley et al., 1991; Lindsay, 1991; Luther et al., 1992; Winkelmann, 2007) and the presence of humic substances in pore waters as well (Cesco et al., 2000; Luther et al., 1992; Violante et al., 2003). Ferric iron reduction is promoted by siderophores, exuded by plant roots, fungi and bacteria (Amon and Benner, 1996; Buyer and Sikora, 1990; Crowley et al., 1991; Hersman et al., 1995; Kraemer, 2004; Neilands, 1981) as well as by humic substances (Cesco et al., 2000; Francois, 1990; Van Dijk, 1971).

Near surface anoxic conditions are common for salt marshes (Hines et al., 1989; Howarth and Giblin, 1983; Howarth and Teal, 1979) because of high rates of organic carbon oxidation in the uppermost centimetres of the sediment (Koretsky et al., 2005). This is fuelled by the high productivity of these areas and generally attributed to microbial sulphate reduction (Canfield, 1989; Howarth and Teal, 1979; Kostka et al., 2002). During early diagenesis sulphate reduction and the release of hydrogen sulphide as an by-product could lead to the formation of iron monosulphides and pyrite in the presence of dissolved Fe^{2+} (e.g. Giblin, 1988; Hines et al., 1989; Howarth and Teal, 1979; Lord and Church, 1983; Otero and Macias, 2002).

In this study a combination of pore water data, which were sampled monthly from January 2006 to January 2007, and geochemical sediment properties from hammer corings in April 2007 are presented for four salt marsh sites on Langeoog Island, NW Germany (Fig. 4.1a). This study deals with small-scale marine inundations in the salt marsh area caused by de-embankment. In view of the present discussion on climate change and resulting sea-level rise this study reveals the biogeochemical consequences of the inundation of coastal areas and forms an important basis for de-embankment management.
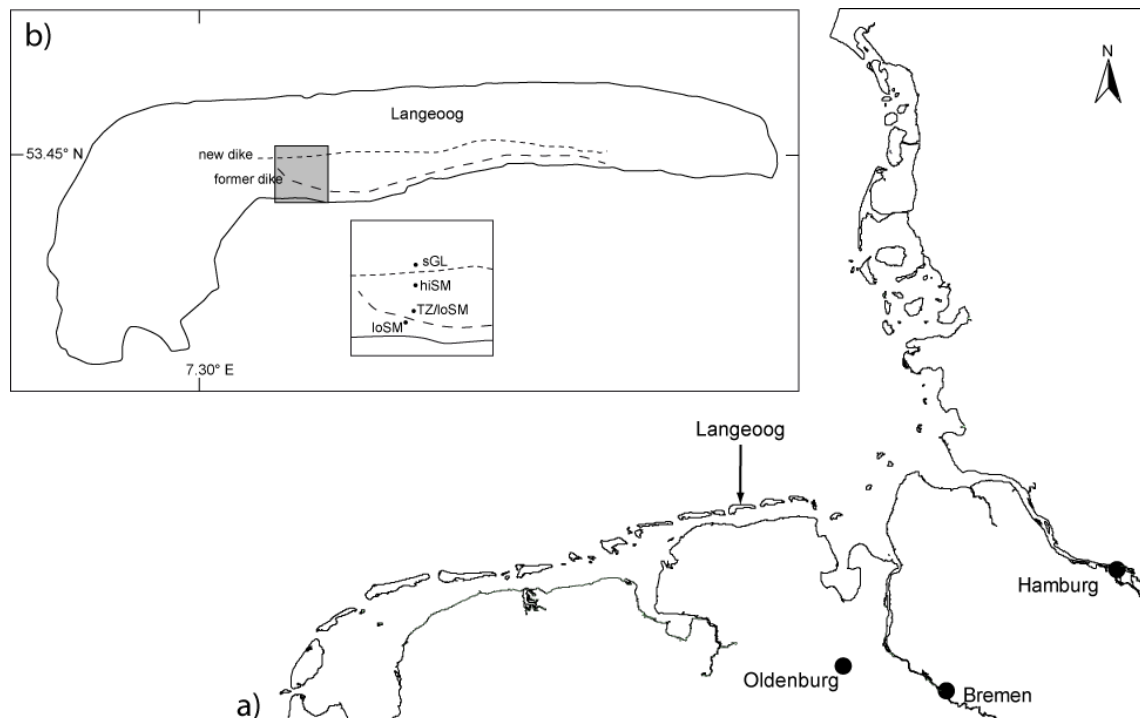
Fig. 4.1: a) Study area: East Frisian barrier island Langeoog, NW Germany; b) study transect on Langeoog island marked by rectangle

4.2 Environmental setting

Langeoog Island belongs to the East Frisian barrier island system of NW Germany (Fig. 4.1a) which formed during the Holocene sea-level rise app. 7,500 BP (Streif, 1990). The recent deposits of Langeoog Island are characterised by a marine-littoral sediment sequence. The basal part of this sequence is a marker stratum, primarily composed of *Hydrobia ulvae Pennent*. The following main part is made up of clastic lithofacies from tidal channels, tidal flats, brackish lagoons, and fluvial levees associated with intercalated peat layers. Salt marsh deposits form the top of the coastal Holocene succession (Freund et al., 2004; Streif, 1990, 2004).

The study area includes sites of seawater-influenced grassland (sGL), high salt marsh (hiSM), low salt marsh (loSM) and transition zone tidal flat/low salt marsh (TZ/loSM) along a N-S directed transect on Langeoog Island (Fig. 4.1b). This classification of the study sites is based on the altitude relative to sea level and on vegetation mappings carried out in August 2005 and August 2006.

Sites sGL, hiSM and TZ/loSM were protected by a summer dike until 2004 (Fig. 4.1b). The embankment assured agricultural use, primarily cattle grazing, of the so-called summer polder and inhibited regular tidal flooding. The dike crest height ranged between +2.0 mNN (m

above mean sea level at high tide) and +2.25 mNN (Ahlhorn and Kunz, 2002) and only allowed seawater flooding during storm surges. The summer polder area was also crossed by a regular pattern of small creeks to support seawater drainage after flooding events. The summer dike was partially removed (about 2 km; total dike length 5.5 km) and rebuilt approximately 120 to 460 m further north (Fig. 4.1b) to compensate for the loss of nature areas in the cause of the construction of the gas pipes EUROPIPE I and II within the Wadden Sea National Park of Lower Saxony. The de-embankment was carried out in several steps. In 2003 three flood-protecting gates of the embanked area were removed allowing first regular tidal influences within the summer polder area. The summer dike removal began in spring 2004 on the western end of the dike, interrupted during the main breeding-season from April to August 2004. The main part of the summer polder is situated in the Wadden Sea National Park of Lower Saxony and belongs to the restricted zone of the national park. Dike removal was completed in autumn 2004. Dike rebuilding further to the North occurred simultaneously.

Presently site sGL is still protected by the rebuilt dike (Fig. 4.1b), whereas site loSM is always influenced by the regular tide. The hiSM and TZ/loSM sites are affected by the regular tidal flooding since de-embankment.

4.3 Methods and Material

4.3.1 Sampling and Sample Preparation

Monthly pore water sampling started in January 2006 at four sites for a time period of 13 months along the N-S directed transect. In April 2007, single hammer corings were carried out at each site for sediment characterisation.

Permanent lances for pore water sampling were installed in the sediments in a depth of up to 5 m. These pore water samplers were similar in design to those described in Beck et al. (2007). Pore water samples were taken with pre-cleaned PE-syringes. Depending on analysed parameters pore water was filtered with 0.45 µm SCFA filters for dissolved metals and with 1.2 µm GF/C Whatman glass microfibre filters for nutrients and dissolved organic carbon. Samples for dissolved metal analysis were acidified to 1 vol.% HNO_3 in pre-cleaned PE-bottles. Samples for dissolved organic carbon analysis (30 mL sample volume) were acidified with 200 µL of 50 vol.% HCl in pre-cleaned brown glass bottles. Samples for nutrient analysis were filtered in pre-

cleaned LDPE-bottles without acid treatment. All pore water samples were stored at 4°C for subsequent analyses.

Sediment samples were taken at about 10 cm intervals from hammer corings on each site in April 2007. Samples were stored in LDPE-bottles and immediately frozen after return to the laboratory. After freeze-drying the samples were grinded and homogenised in an agate mortar.

4.3.2 Pore Water Analyses

The pH values were measured on site during sampling with a pH electrode (SenTix 20) coupled to a combined WTW pH/Cond 340i instrument.

Nutrients (phosphate and ammonia) were determined by a Spekol 1100 photometer (Analytik Jena) as described by Grasshoff et al. (1999). Dissolved organic carbon was determined by a multi N/C 3000 analyser (Analytik Jena). Determination of chloride and sulphate were carried out by ion chromatography (Dionex DX 300). Iron and manganese were measured by ICP-OES (Perkin-Elmer Optima 3000XL) and subsequently by ICP-MS (Thermo Finnigan ELEMENT 1 and ELEMENT 2) if element concentrations were below 17.9 µM Fe and 18.2 µM Mn. Measurements by ion chromatography, ICP-OES and ICP-MS were checked by international standard solutions. Atlantic Seawater (OSIL) was used as reference for chloride and sulphate, whereas Cass-4 (Canada) was used as reference for iron and manganese. A spike solution with a final concentration of 36.4 µM Mn and 35.8 µM Fe for ICP-OES and 3,640 nM Mn and 3,581 nM Fe for ICP-MS was added to the Cass-4 reference standard as the concentrations for Mn and Fe in the Langeoog pore waters were much higher than in the original reference standard.

Pore water ultrafiltration experiments were accomplished using vivaspin 500 ultrafiltration units (Sartorius) with a 5,000 Da molecular weight cut off (MWCO). Samples were pre-filtered with 0.45 µm SCFA filters. Subsamples of 600 µL of the pre-filtered pore water were filled into each ultrafiltration unit and centrifuged (Biofuge 15R) for 30 min at 10,000 rpm (~ 7,800 g). Ultrafiltered samples were filled in pre-cleaned 2 mL Eppendorf cups and acidified to 1vol.% HNO_3. Remaining pre-filtered pore water samples were also acidified in the same manner. Both, the ultrafiltered and the pre-filtered pore water samples were analysed for iron

and manganese by ICP-OES and ICP-MS. Accuracy and precision for pore water measurements are listed in Tab. 4.1.

4.3.3 Sediment Analyses

A total number of 138 sediment samples was analysed for major elements (Al, Fe, Mn, Si) by XRF (Philips PW 2400) using fused di-lithiumtetraborate/lithiumtetraborate (50%/50%) glass discs. Total carbon (TC) and total sulphur (TS) contents were determined by using a C/S element analyser (Eltra CS 500). Total inorganic carbon (TIC) content was determined with a UIC Coulometrics Inc. CM5014 CO_2 coulometer coupled to a CM5130 acidification module (Engleman et al., 1985; Huffman, 1977). A large number of samples (74) was not analysed for TIC, because their TC content was too low (<0.4%) to gain reliable results, especially in the relocated beach sand and sand flat deposits. From the remaining samples total organic carbon (TOC) content was calculated as the difference between TC and TIC.

Leaching experiments for iron and manganese were carried out on 44 samples with 1 N HCl according to the method described in Leventhal and Taylor (1990). Leachates were analysed by ICP-OES (Perkin-Elmer Optima 3000XL).

Accuracy and precision for all sediment measurements (Tab. 4.1) were checked by parallel analysis of in-house standards (TW-TUC shale type material, Loess, UT-S)

Tab. 4.1: Precision and accuracy of sediment and pore water analyses

Analyte	Method	Precision %	Accuracy %
TS	IR Analyser	5.1	3.0
TC		0.7	-0.2
TIC	Coulometry	2.0	-1.2
Si	XRF	0.7	-1.6
Al		0.8	-2.7
Fe		0.6	-1.3
Mn		0.9	-5.3
phosphate	Photometry	6.5	0.1
ammonia		5.9	-0.1
chloride	Ion chromatography	1.0	-0.5
sulphate		1.1	-4.6
DOC		0.8	0.7
Fe	ICP-OES	1.2	-2.3
Mn		2.3	-1.7
Fe	ICP-MS	4.1	0.8
Mn		1.2	3.3

4.4 Results

4.4.1 Sediment Properties

Hammer corings were accomplished close to the four pore water sampling sites along the studied transect. Sediment lithology was described on-site and subsequent sampling was done in 10 cm intervals.

Four lithological units, termed A to D from top to basis of the sediment sequence, are distinguishable. Unit A reaches a maximum thickness of 0.30 m and consists mainly of silt and clay and partly contains medium sand. Unit B comprises relocated fine sands from the northwards situated dunes, which were breached during extreme storm surge events in 1717 and 1825 (Obstfeld, 2001), and the beach behind these dunes. The thickness of unit B varies between 1.20-2.03 m depending on the distance to the dune breaches. Unit C also is composed of fine sands including the marker stratum of the marine snail *Hydrobia ulvae Pennant.* In contrast to unit B shell debris or remnants of echinoderms do occur. The thickness of unit C varies between 1.72 m and 2.43 m. Unit D consists of alternating fine sand and silt/clay or silt/clay lenses within fine sand deposits. Unit D has a thickness of 0.06 to 0.43 m, depending on the thickness of the overlaying strata.

4.4.2 Sediment Geochemistry

The sediment geochemistry is very similar when comparing the studied sites. Thus the geochemical characterisation focuses on the four lithological units described before.

The sediments are dominated by quartz (SiO_2 predominately >90%, Tab. 4.2). Based to their SiO_2 content and the geochemical classification postulated by Dellwig et al. (2000) unit C is identified as sand flat deposits. Unit D with an average SiO_2 content of 83.1% (Tab. 4.2) is classified as mixed flat deposits (Dellwig et al., 2000). Unit A is defined as marsh soil. Units B-D are also characterised by very low total sulphur (TS) and total carbon (TC) contents (Tab. 4.2). Unit A and sediments close to the marker stratum in unit C reveal higher TC contents (Tab. 4.2, Fig. 4.2). TS contents (Fig. 4.2) vary from 0.002% to 0.6% (median 0.05%) with highest values in unit D. Further slight enrichments in TS were detected in silty and clayey layers of unit C. The observed TS contents (average 0.1 %, Tab. 4.2) in unit A are very low when compared with

other studies on salt marsh sediments, e.g. diked seasonally flooded salt marshes at North Sunken Meadow, Eastham (Portnoy and Giblin, 1997).

Tab. 4.2: Average, minimum and maximum values of bulk parameters [%] and selected major elements [%] (Mn in µg/g) for sediment unit A-D (# number of samples); results of leaching experiments: HCl-extractable iron (Fe_{HCl}) and manganese (Mn_{HCl}) and their percentage of total iron and manganese sediment content; merge data of the four study sites

	Unit A Marsh soil (#9)			Unit B Relocated beach sands (#51)			Unit C Sand flat (#71)			Unit D Mixed flat (#7)		
	av	min	max	av	min	max	av	min	max	av	min	max
SiO_2	78.5	52.5	94.1	92.6	86.1	96.1	91.9	77.1	95.2	83.1	76.2	93.0
Al_2O_3	5.4	1.6	11.1	1.9	1.2	2.9	1.9	1.2	3.7	3.9	1.8	5.3
Fe_2O_3	2.3	0.5	5.2	0.8	0.2	2.8	0.5	0.2	1.7	1.3	0.4	1.9
Mn [µg/g]	342	<155	875	232	<155	1069	<155	<155	240	155	<155	201
TC	2.7	0.2	8.3	0.09	0	0.5	0.3	0.04	2.4	0.9	0.1	1.4
TS	0.1	0.01	0.3	0.02	0.002	0.09	0.1	0.04	0.5	0.4	0.07	0.6
Leaching	(#5)			(#18)			(#17)			(#4)		
Fe_{HCl}	0.82	0.098	1.43	0.091	0.042	0.26	0.079	0.049	0.16	0.21	0.06	0.31
%Fe_{HCl} of total Fe	33.6	26.4	39.6	18.2	7.2	30.4	23.7	19.0	28.7	23.0	22.5	23.4
Mn_{HCl} [µg/g]	303	11	634	19.5	7	82	19.5	10	54	65	18	106
%Mn_{HCl} of total Mn	57.9	28.2	81.2	14.2	2.9	70.1	43.9	19.9	70.0	53.1	50.0	59.1

The total carbon contents reveal a similar pattern (Fig. 4.2) and are on average low as well (av. 0.13%, range 0.02-8.26%). TIC ranges from 0.06% to 0.97% with maximum values in the *Hydrobia* layer. Highest TOC contents (1.43%-8.26%) are typical of unit A, whereas unit D show intermediate TOC contents of up to 0.82% due to elevated silt and clay contents. Such TOC contents are comparable to those of recent mixed flat deposits of the Swinnplate (backbarrier area of the East Frisian island Spiekeroog, eastward neighbour island to Langeoog) where average values of 1.3% were reported (Dellwig et al., 2000). Unit C is characterised by the lowest values (av. 0.20%) and shows a similar range like recent sand flat deposits (0.30%) (Dellwig et al., 2000).

Average iron contents (Tab. 4.2) vary in a range of 0.5% (unit C) to 2.3% (unit A). The iron content of unit A is comparable to values (2.2-6.5%) reported for salt marsh sediments of the tidal flat sedimentary regime of the Wash area, England (Macleod, 1973; Suttill et al., 1982). Iron contents of unit B (0.8%) and C (0.5%) are within the range of deeper sand flat sediments

(0.5%) and recent surface sand flat sediments of the Swinnplate, Spiekeroog backbarrier area (0.8% Fe_2O_3; Dellwig et al., 2000).

In comparison to the assumed geogenic background (expressed by average shale Fe/Al=0.54; Wedepohl, 1971) Fe/Al ratios (Fig. 4.2) of unit B exceed the shale value mainly at sites sGL and hiSM (1.2 and 0.8). Unit C is characterised by Fe/Al ratios of 0.22-0.60 (average 0.34), and plots distinctly below the average shale value, but is comparable to Fe/Al ratios of 0.30 for recent sand flat deposits (Dellwig et al., 2000) and 0.18-0.29 for the Janssand in the Spiekeroog backbarrier area. Slightly higher values were determined for unit D at sGL (0.47), hiSM (0.45) and TZ/loSM (0.39), which are comparable to recent mixed flat deposits (Fe/Al 0.43; Dellwig et al., 2000).

Manganese contents (Mn) of the sediment samples are generally very low (Tab. 4.2). This is especially true for units C and D. The Mn/Al ratios (Fig. 4.2) of unit A reach average values of $104 \cdot 10^{-4}$ and thus are comparable to the average shale Mn/Al ratio of $96 \cdot 10^{-4}$ (Wedepohl, 1971). Distinct manganese enrichments are found in unit B (average Mn/Al ratio of $206 \cdot 10^{-4}$, maximum value $689 \cdot 10^{-4}$ at site sGL) similar to the iron enrichments of this unit. Units C and D are characterised by average Mn/Al ratios of $51 \cdot 10^{-4}$ and $60 \cdot 10^{-4}$, respectively, which are comparable to Mn/Al ratios of $64 \cdot 10^{-4}$ for recent tidal flat sediments (Hinrichs et al., 2002).

4.4.3 Leaching Experiments

Several sediment samples from all sites were selected for iron/manganese leaching experiments. These experiments were carried out to determine the percentage of reactive iron and manganese in the solid phase. Reactive iron was defined by Canfield (1989) as mainly non-silicate-bound iron, including amorphous iron oxides, oxyhydroxides, and some crystalline oxides, besides FeS. The HCl-extractable iron (Fe_{HCl}) contents vary in a range of 7-40% of total sediment iron content (Tab. 4.2). The HCl-extractable Manganese (Mn_{HCl}) contents reach values of 3-81% of total sediment manganese contents (Tab. 4.2). Unit A shows the highest values for Fe_{HCl} and Mn_{HCl} (avg. 34% and 58%) while minimum percentages are found in unit B (avg. 18% and 14%). Units C and D show intermediate Fe_{HCl} contents of 19-29%. Larger variations were observed for Mn_{HCl} contents (20-70%).

In general, the percentage of Mn_{HCl} exceeds the percentage of Fe_{HCl} within unit A, C, and D. The opposite ($Fe_{HCl} > Mn_{HCl}$) is predominately seen in unit B.
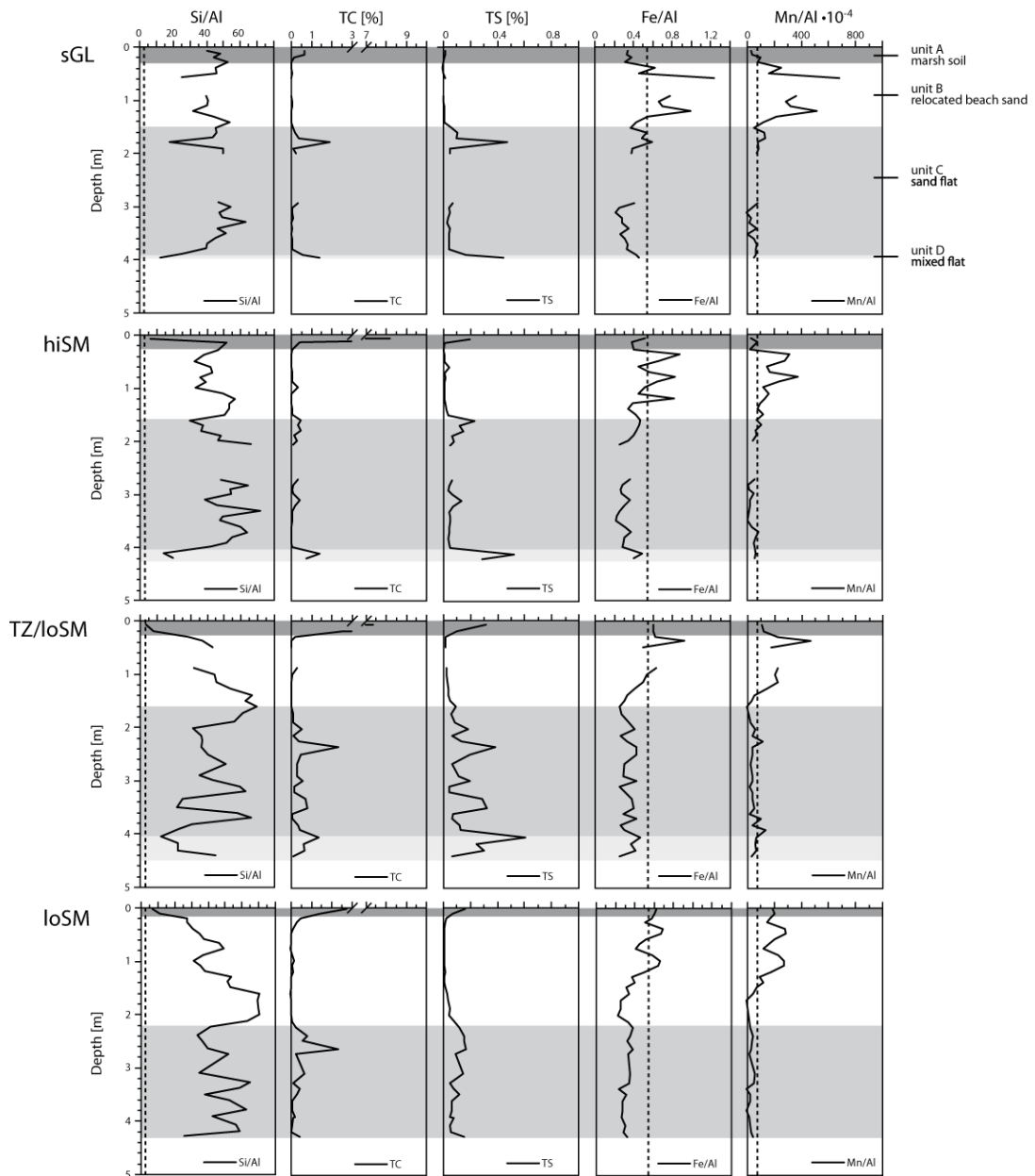
Fig. 4.2: Salt marsh sediment parameters: Si/Al ratios, total carbon content (TC), total sulphur content (TS), Fe/Al ratios, Mn/Al ratios (from left to right), dashed line = average shale values (Wedepohl, 1971); sampling sites are sorted in N-S direction: sGL=seawater-influenced grassland, hiSM=high salt marsh, TZ/loSM=Transition zone tidal flat/low salt marsh, loSM=low salt marsh; line gaps mark loss of core

4.4.4 Pore Water Geochemistry

The number of pore water samples and measurements differed in time and depth resolution at each site depending on pore water availability and sample volume. This is especially true for the uppermost meter at sites loSM, hiSM, and sGL as well as for depths exceeding 1.5 m at site TZ/loSM.

Salinity: From a spatial point of view, a distinct gradient in pore water salinity is observed (Fig. 4.3) with decreasing values from the loSM site in the south (avg. 29 psu) to the sGL site in the north (avg. 7 psu). The sites within the summer polder area are characterised by

medium values (avg. 25 psu TZ/loSM; avg. 18 psu hiSM). Variations in salinity are presumably not influenced by altitude of the sites, but controlled by the flooding regime. Profiles at each site show no significant seasonal trend below 1 m depth. They are quite stable over time and depth. In contrast, pronounced seasonal variations due to higher precipitation in fall and desiccation effects in summer are observed in the uppermost meter. Evidence for fresh groundwater discharge in the form of lower salinities was not found, even at greater depths.
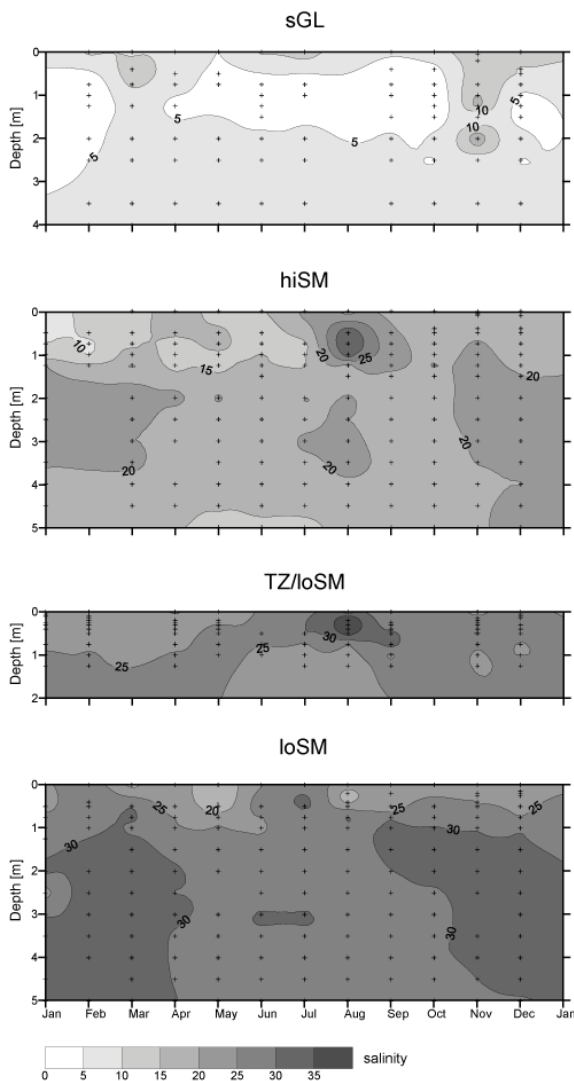
Fig. 4.3: Pore water salinity along the study transect (sGL=seawater-influenced grassland, hiSM=high salt marsh, TZ/loSM=Transition zone tidal flat/low salt marsh, loSM=low salt marsh), sampling period from January 2006 to January 2007, each black cross marks one sample

70
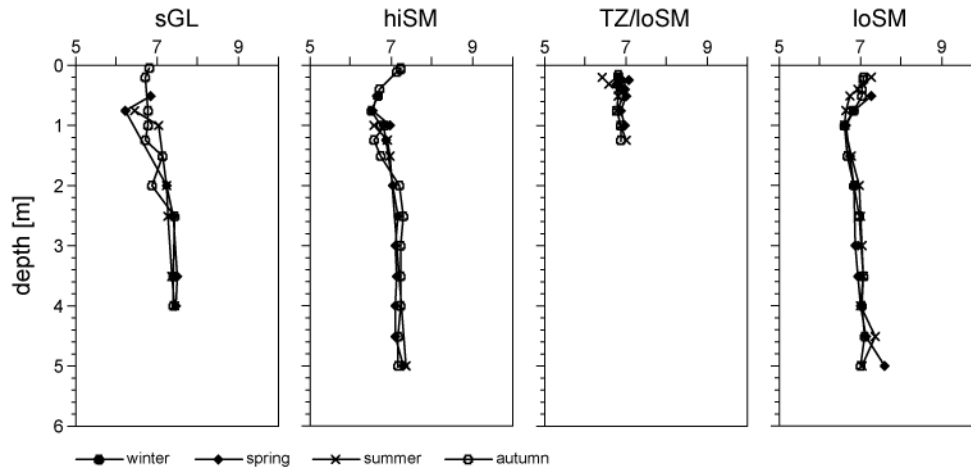
Fig. 4.4: Pore water pH values along the study transect (sGL=seawater-influenced grassland, hiSM=high salt marsh, TZ/loSM=Transition zone tidal flat/low salt marsh, loSM=low salt marsh) for spring, summer, autumn, and winter situation in 2006

pH: The pH measurements show no spatial or seasonal variation (Fig. 4.4). At each site pH reaches values of about 7. There was a slight variability with greater depth but pH rarely exceeded 7.5 or fell below a value of 6.5.

Sulphate/chloride ratios: The sulphate-chloride ratios were calculated for all pore water samples (Fig. 4.5). At three sites (loSM, TZ/loSM, and hiSM) sulphate-chloride ratios behave almost constant with an average seawater-like value of about 0.05. While, the aforementioned sites are regularly inundated by tides, sulphate-chloride ratios are often above the seawater value and reach a maximum of 0.19 at site sGL, which is located behind the new dike.

Dissolved organic carbon (DOC): The concentrations of DOC generally increase in south-north direction (Fig. 4.5). At site loSM DOC concentrations (0.25 - 0.5 mM) are more or less stable with depth and season in 2006. A certain seasonal variation is observed at site TZ/loSM where DOC concentrations change from higher values of 2-2.5 mM in July-September 2006 at 1 m and 1.25 m depth to values <1.5 mM in the remaining depth intervals. At site hiSM DOC concentrations vary with depth in the range of 1 to 2.3 mM but without seasonal trends. Behind the new dike (site sGL) the highest DOC concentrations (max. 22 mM) are observed primarily at 1 to 1.5 m depth. At depths below 2 m DOC ranges between 2.3 and 3.8 mM.
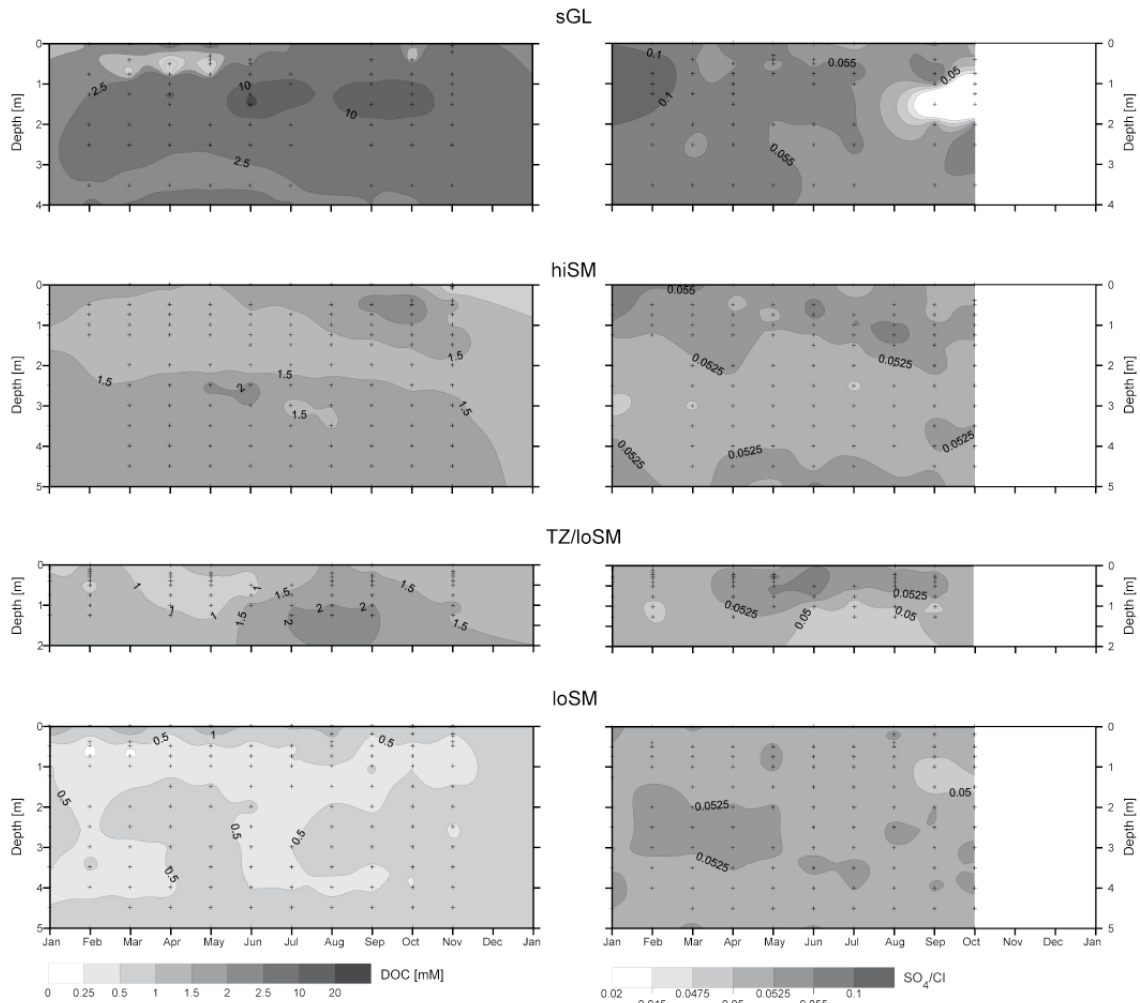
Fig. 4.5: Pore water dissolved organic carbon concentrations (left column) and pore water SO$_4$/Cl ratios (right column) along the study transect (sGL=seawater-influenced grassland, hiSM=high salt marsh, TZ/loSM=Transition zone tidal flat/low salt marsh, loSM=low salt marsh) for sampling period from January 2006 to January 2007 (October 2006 for SO$_4$/Cl ratio, respectively), each cross mark one sample

Iron: At site sGL iron concentrations (Fig. 4.6) vary down to 2 m depths in a range of 0.8 to 583 µM (avg. 86 µM), but no clear seasonal trend was found. The highest concentration of 583 µM occurs in November 2006 at 1.25 m depth after a storm surge event inundated this dike-protected site. At depths greater than 2 m iron shows smaller variations over time and depth with concentrations between 22 and 102 µM.

A general trend of increasing iron concentrations with increasing depth is observed at site hiSM (avg. 98 µM; range 0.6 – 340 µM). For site TZ/loSM samples were, however, only available for the upper 2 m. In this depth interval iron reaches high concentrations (e.g. 126-271 µM in September 2006) at depths between 0.25 m and 0.5 m. These concentration maxima are observed over the entire sampling period but the iron concentration is not always the same. At greater depths iron concentrations are significantly lower (≤100 µM).

Site loSM shows the lowest iron concentrations compared to the other sites, mainly in the uppermost meter. Here, iron values often are below 1 µM. However, there are also distinct concentration peaks at greater depths, e.g. at 3.5 m and partly at 2.5 m depth.

Iron concentrations show no correlation with the described gradient in salinity. The observed iron values in the uppermost sediment are comparable to iron concentrations at creek bank and levee salt marsh sites on Sapelo Island, Georgia, USA (Koretsky et al., 2005) as well as to drained-diked salt marshes of the eastern shore of Cape Cod Bay, USA (Portnoy and Giblin, 1997).
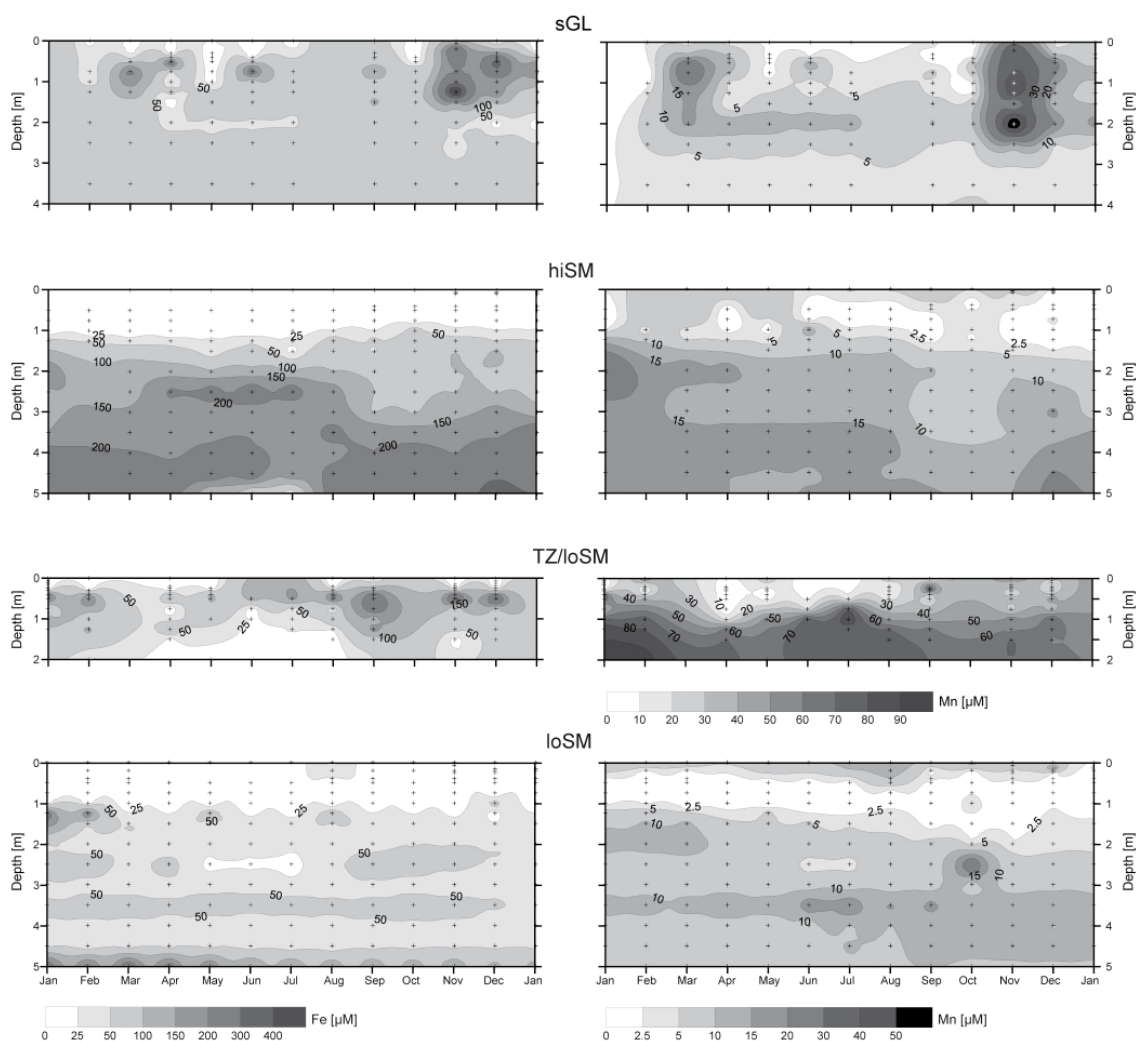
Fig. 4.6: Pore water iron concentrations (left column) and manganese concentrations (right column) along the study transect (sGL=seawater-influenced grassland, hiSM=high salt marsh, TZ/loSM=Transition zone tidal flat/low salt marsh, loSM=low salt marsh) for sampling period from January 2006 to January 2007, each cross marks one sample; Please note the different manganese concentration scale for site TZ/loSM

Manganese: Pore water profiles at site sGL show distinct maxima in manganese (Fig. 4.6, please note the two different concentration scales) at 0.5 m depths (31 µM in March, 14 µM in April and 17 µM in June 2006) and at 2 m depth within a range of 10-17 µM (March-July 2006).

After a storm surge event in November 2006 manganese reached the highest values observed within the entire sampling period at this site (up to 63 µM) in the uppermost 1.25 m and at 2 m depth.

Site hiSM is mainly characterised by low manganese concentrations (< 10 µM) in the uppermost meter in 2006. Manganese concentrations increase below 1 m depth and reach a maximum at 2 m depth.

The highest manganese concentrations of 95 µM were found at site TZ/loSM within 2 m depths in February 2006. Generally manganese shows an increasing trend with depth at this site. Manganese concentrations at site loSM usually do not exceed 20 µM. The uppermost meter is distinguished by concentration levels <5 µM, frequently <1 µM. Concentration maxima are observed at 3.5 m depth over the entire sampling period and additionally from July 2006 at greater depths. Compared to other studies manganese concentrations are in a similar range at lower sediment depths like in salt marshes (23-30 µM at 0.03-0.29 m depth) of the Barataria Basin, Louisiana, USA (Feijtel et al., 1988). Manganese concentration maxima of this study are comparable to values reported for created marsh soils (0.6% organic matter, Mn 50-75 µM) of the Pamlico River estuary, North Carolina, USA and distinctly exceed the manganese concentrations of natural marsh soils (Craft et al., 1991).

Size fractionation: The pore water filtration experiments show that in most samples dissolved Fe concentrations decrease dramatically after filtration, in part up to almost 100% (Tab. 4.3). By contrast, Mn concentrations did not change. This leads to the assumption, that most of the dissolved Fe in pore water is present as an organic complex in the molecular weight fraction >5,000 Da, whereas dissolved Mn is not.

Nutrients: In Figure 4.7 ammonia (NH_4^+) and phosphate (PO_4^{3-}) concentrations for site sGL are presented. Ammonia concentrations predominately lie below the detection limit of 0.05 µM. Greater variations are seen in November 2006. This month shows a significant increase in NH_4^+ (max. 0.42 µM at 1 m depth) in different depth. Sampling took place a few days after a storm surge event, which caused inundation of this normally dike-protected site. Phosphate is

affected by this event as well. Highest concentrations (132 µM) are found in November 2006 at 0.2 m depth. Usually PO_4^{3-} concentrations at this site varied between 0.3 and 61 µM (avg. 15 µM) without clear trends with depth or season.

Tab. 4.3: Pore water ultrafiltration experiments

Study site	Depth [m]	Fe_{diss} [µM]	Fe_{diss} [µM] <5k Da	Percentage Fe_{diss} <5k Da [%]	Mn_{diss} [µM]	Mn_{diss} [µM] <5k Da	Percentage Mn_{diss} <5k Da [%]
sGL	0	18	0	100	2.8	2.8	0
	1.25	385	94	76	22	22	0
	1.5	492	34	93	35	35	0
	4.0	51	0	100	3.6	3.6	0
hiSM	0	1	0	100	0.8	0.7	12.5
	0.5	1	0	100	0.09	0.09	0
	1.0	1	0.5	50	0.5	0.5	0
	2.0	83	0	100	6.2	6.2	0
TZ/loSM	0.5	199	8	96	9.7	9.9	0
	5.0	132	0	100	120	118	1.7
loSM	0	1	0	100	1.6	1.6	0
	0.5	10	4	60	5.2	5.1	1.9
	1.25	59	0	100	6.5	6.5	0
	1.5	63	8	87	23	24	0
	2.0	48	6	88	9.3	9.6	0
	5.0	109	4	96	9.3	9.9	0
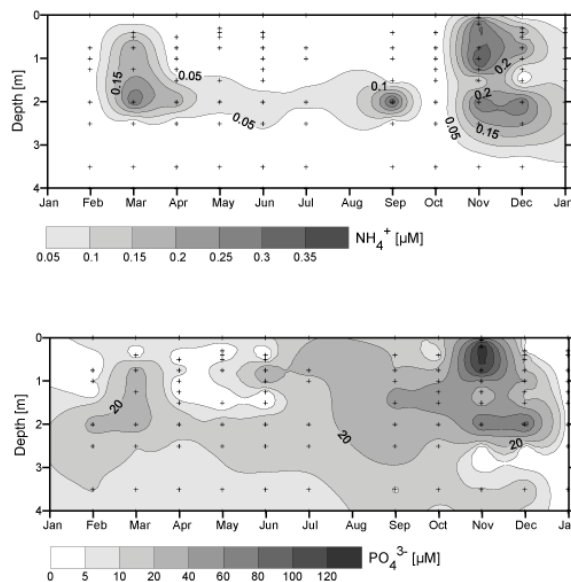
Fig. 4.7: Pore water nutrient concentrations (ammonia and phosphate) for site sGL=seawater-influenced grassland; sampling period from January 2006 to January 2007, each black cross marks one sample

4.5 Discussion

4.5.1 Iron and Manganese Geochemistry

High iron concentrations in pore waters are typical for the studied sites. Pore water iron concentrations undergo little seasonal variation. However, the individual study sites differ in iron concentration depth trends (Fig. 4.6). The sediment is assumed as iron source for the pore waters. The Fe/Al ratios show significant iron enrichments in unit B. These iron enrichments correlate with the spotted red-brownish colour of unit B indicating the presence of oxidised iron minerals. Slight iron depletions are found in units A, C, and D (Fig. 4.2). The sediments along the study transect possess a high potential of reactive iron as shown by the leaching experiments. The percentages of reactive iron vary mostly between 20-40% with highest values in unit A. Along the study transect the reactive iron potential is on a similar level.

In several previous studies it was concluded that iron cycling in salt marshes is controlled by sulphate reduction and sediment oxidation (Giblin, 1988; Giblin and Howarth, 1984; Hines et al., 1989; Kostka and Luther, 1995; Luther and Church, 1988). In our study area the presence of iron oxides seems to inhibit sulphate reduction since organic matter oxidation with iron oxides provides more energy for microorganisms than using sulphate as an electron acceptor (Bull and Taillefert, 2001; Kostka et al., 2002; Taillefert et al., 2007). In this study only few indications for sulphate reduction were found. The SO_4/Cl ratios reach values close to or above the seawater ratio (Fig. 4.5). In contrast, the higher SO_4/Cl ratios, especially at site sGL provide evidence for sulphide mineral oxidation. The relatively low sedimentary sulphur values (Fig. 4.2) indicate that the formation of pyrite or other iron (mono)sulphides plays only a minor role in the investigated environment. The absence of iron sulphides is caused by the lack of organic matter in the predominantly sandy sediments and the restricted supply of organic matter by tidal inundations, which seems to inhibit microbial activity like sulphate reduction which would provide H_2S for sulphide formation. The studied sites, particularly the seawater-influenced grassland site, are less frequently inundated than e.g. permeable intertidal flat sediments in the backbarrier area of Spiekeroog Island, NW Germany (Beck et al., 2008a, b). Beck et al. (2008a) termed these sediments a "bio-reactor" where sulphate reduction is the most important pathway for anaerobic organic matter remineralisation, and DOC and nutrients are released. Rapid organic matter remineralisation reported for permeable, organic-poor marine sands e.g. by

Jahnke et al. (2005) and Rao et al. (2007) can not be excluded completely during tidal inundations.

Furthermore, the light yellow to brown colour of the pore waters, especially at sites hiSM and sGL, indicate the presence of humic substances. Humic substances are known for their metal complexation properties (Cesco et al., 2000; Van Dijk, 1971) and their reducing power which increases with pH (Francois, 1990). The combination of these pore water properties and the high DOC concentrations lead to the assumption that iron may be organically complexed by humic substances. The ultrafiltration experiments in this study confirm this assumption and document that iron is complexed by the high molecular weight fraction >5k Da (Tab. 4.3). The circum-neutral pH values of pore waters enable humic high molecular weight Fe organic complexes to be kept in solution (Luther et al., 1996).

The high DOC concentrations most likely result from organic matter breakdown pathways described in the pore water-size/reactivity model (Burdige and Gardner, 1998; Weston et al., 2006) and its selective preservation and accumulation with depth because of its refractory character (Amon and Benner, 1996; Burdige and Gardner, 1998). Luther et al. (1992) describe an iron cycle in salt marsh sediments, which is based on iron complexation by organic ligands. This iron cycle works as long as plants and/or bacteria produce organic ligands and sulphate reduction rates are low. Penetration of O_2 into subsurface sediments was also considered.

Organic ligands are supplied by the vegetation cover and by exudation of siderophores from the rhizosphere, bacteria or fungi (Amon and Benner, 1996; Buyer and Sikora, 1990; Crowley et al., 1991; Lindsay, 1991). Such organic ligands are released in unit A and the uppermost unit B. Siderophores are known for their extremely high affinity to ferric ion (Neilands, 1981) and thus can initialize the iron cycle by solubilisation of oxidised Fe(III) minerals forming Fe(III) organic complexes (Luther et al., 1992).

Periodically O_2 penetration could occur during restored tidal flooding. Significant sediment desiccations in summer lead to aeration of the marsh soil. The coexistence of reduced and oxidised iron minerals in salt marsh sediments is well documented (Feijtel et al., 1988; Giblin, 1988; Howarth and Giblin, 1983; Lord and Church, 1983). Sediment O_2 penetration may oxidise Fe(II) to Fe(III) with subsequent formation of Fe(III) (oxy)hydroxides. Several authors

state that in the absence of O_2 Fe(III) is the dominating oxidant in pyrite oxidation in salt marsh sediments (Carey and Taillefert, 2005; Luther and Church, 1988; Luther et al., 1992).

Manganese oxides are usually found in close association with sedimentary iron oxides as reflected by the similar shape of the Fe/Al and Mn/Al profiles (Fig. 4.2). It is assumed that these minerals generally appear in amorphous structure as coatings on inorganic or biogenic sediment particles (Burdige, 1993). Incubation experiments with salt and brackish marsh sediments (Guo et al., 2000) showed that Mn(IV) and Fe(III) reduction occur almost simultaneously with a lower release of Mn(II) when compared to Fe(II). We can confirm this observation by our study. Increased pore water manganese concentrations correlate with increased iron concentration, e.g. at site loSM at 3.5 m depth almost over the entire sampling period (Fig. 4.6). On the other hand there are also indications for the classical vertical stratification of Mn and Fe release in pore waters especially within the upper 1.0 m sediment at site TZ/loSM.

4.5.2 Implications for Holocene pyrite formation

The pore waters of the investigated salt marsh deposits are extremely rich in dissolved Fe. Additionally, high amounts of dissolved organic matter cause complexation of Fe thereby keeping Fe in solution. As the deposits mainly consist of sandy material with an elevated pore space, transport of pore water and its constituents via advection (e.g. tidal pumping) or diffusion seems to be likely.

Dellwig et al. (2001) drew a hypothesis about pyrite formation in Holocene coastal peats, which formed during regressive phases of the Holocene sea-level rise. Within the geological record, highest enrichments of authigenic pyrite of up to 50.3 wt% were observed in reed peats (*Phragmites australis*), which were intercalated between brackish and lagoonal sediments.

The conceptual model of these authors is based on the interaction of different element sources in a system forming a transition zone between the marine and terrestrial realm. On one hand, sulphate for the production of reduced sulphur species by sulphate reducing bacteria is delivered by seawater and the tides. On the other hand, an elevated Fe input can only be provided by terrestrial or semi-terrestrial sources. Possible Fe sources are for instance small coastal tributaries partly carrying unusually high amounts of dissolved Fe and other trace metals

like Mn (Dellwig et al., 2002). The Fe-rich pore water investigated in our study forms an additional Fe source. Advection or diffusion may transport dissolved/complexed Fe to peat forming environments where authigenic H_2S is able to trap the delivered Fe as pyrite. For this reason the investigated salt marsh deposits, which are re-exposed to natural sea level fluctuations may form the missing link in pyrite formation which occurred in Holocene coastal peats.

4.5.3 Effects of de-embankment

Further aspects seen in pore water geochemistry are the implications of the restored regular tidal flooding at sites TZ/loSM and hiSM in the course of the de-embankment. Portnoy and Giblin (1997) describe possible effects of seawater flooding restoration after decades of embankment as follows: "A rapid decrease in redox potential, increasing pH and cation exchange may cause short-term release of certain compounds like nutrients and metals." The data of this study (Fig. 4.7) show very low ammonia concentrations in the pore water (mostly <0.05 mM) whereas phosphate predominately varies in a range of 0.3 – 61 µM (avg. 15 µM). Sampling already started in June 2005 (data not shown) nearly one year after the de-embankment. Thus, a possible ammonia release as proposed by Portnoy and Giblin (1997) could be at most short-termed. The distinct ammonia increase at sGL (Fig. 7) after the storm surge event in November 2006 (max. 0.42 mM at 1m depth, 7-fold increase compared to October), which is well documented in pressure data from the sediment surface and from 5 m sediment depth (Fig. 4.8), supports the assumption of Portnoy and Giblin (1997), that restored seawater flooding could lead to short-term ammonia release. The ammonia release at sGL in November 2006 lasted until January 2007 (max. 0.11 mM at 1m depth). The same effect of the storm surge event is observed for phosphate at site sGL (Fig. 4.7). In November 2006 the phosphate concentrations increased 5-fold at 0.75 m compared to October and rapidly decreased by a factor of 6 in December. Additionally, pore water was available at 0.05 m and 0.2 m depth. Normally at these depths pore water could not be sampled. Phosphate at both depths showed similar concentrations as at 0.75 m depth. Increase in pore water phosphate concentrations most likely results from P-desorption from iron oxides (Krom and Berner, 1980; Slomp et al., 1996; Slomp and Van Raaphorst, 1993). These results further support the presumed effects of de-embankment as postulated by Portnoy and Giblin (1997) and Portnoy

(1999). Furthermore, the authors predicted an iron release as a result of restored seawater flooding. After the storm surge event this effect is also observed in this study at site sGL (Fig. 4.6). Iron concentrations increase 8-fold e.g. at 1.25 m depth from 75 µM in October to 583 µM in November. Iron concentration decrease to the October level within two months. The seawater impact at sGL affects manganese pore water concentrations as well (Fig. 4.6). A 3 to 21-fold increase in manganese concentrations is found between 0.75 and 2.5 m depth. Manganese is still enriched in December and only reaches the pre-seawater intrusion level in January 2007.
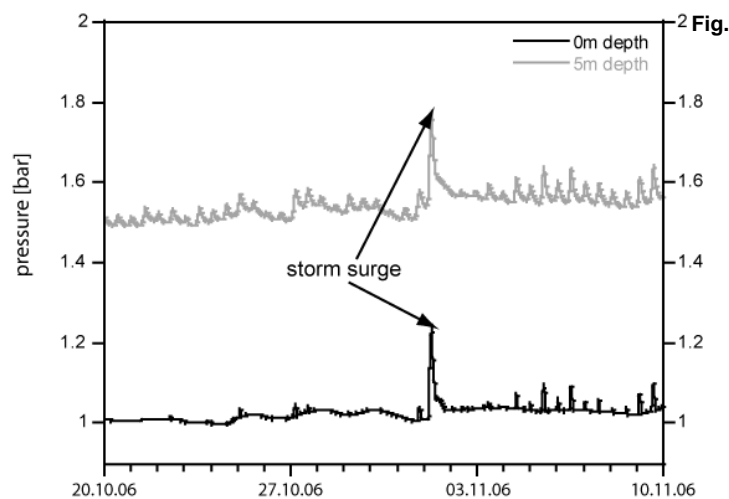
Fig. 4.8: Pressure data (air-pressure uncorrected) at site hiSM=high salt marsh from 20.10.-10.11.06, sediment surface – black line, 5 m sediment depth – grey line, storm surge event marked by black arrows

Especially the observed huge nutrient release (ammonia and phosphate) within a few days could have an impact on water quality. The decline in nutrient concentrations within one month indicates that the released nutrients most likely are exported from the salt marsh pore water system via hydrological gradients (proximity to drainage ditches or creeks) or advection (e.g. tidal pumping). A nutrient uptake by perennial plants can not be excluded for this study. However, the huge nutrient and trace metal releases are seen during an on-off event in November 2006, but are also described in previous studies (Portnoy, 1999; Portnoy and Giblin, 1997). The results of our study may also be important for sea-level rise scenarios and transgression scenarios, respectively. A continuing seawater influence through transgression could lead to enhanced nutrient and trace metal release to pore waters as observed in this study. Under appropriate conditions pyrite formation could be intensified through the release of iron. Nevertheless, more detailed investigations on pore water quality (nutrients and trace

metals) are indispensable to improve knowledge about long- and short-term implications of de-embankments.

4.6 Conclusions

Our combined pore water and solid phase geochemical approach leads to a better understanding of processes associated with inundation of formerly flood-protected coastal areas. It not only may serve as a basis for future sea level rise scenarios, but also helps re-interpreting geochemical signatures seen in Holocene coastal sedimentary sequences.

The quartz-dominated sand flat-type deposits along the studied salt marsh transect are characterised by very low carbon and sulphur contents, except for the upper 0.29 m sediment. The sedimentary iron content is comparable to other salt marsh and tidal flat sediments with Fe/Al ratios partly exceeding average shale values (relocated beach sand deposits). Elevated manganese contents only occur in the marsh soil and relocated beach sand deposits with Mn/Al ratios near average shale values.

The high percentage of reactive iron suggests that the salt marsh sediments act as iron source for pore waters. Salt marsh pore water iron is dominated by organically complexed iron in the high molecular weight class >5,000 Da, partly at high concentration levels (up to 583 µM). Iron complexation is most likely controlled by humic substances, and is accompanied by siderophores in the rhizosphere. The circum-neutral pore water pH value keeps the complexed iron in solution. Thus the salt marsh pore waters may serve as significant sources of dissolved iron, which can be exported and precipitated e.g. as pyrite under appropriate conditions.

The restoration of regular tidal flooding (de-embankment) results in considerable increases in pore water iron, manganese, phosphate, and ammonia concentrations as observed in this study after a storm surge. This was already predicted by some authors (Portnoy, 1999; Portnoy and Giblin, 1997) but served as management implication for sea water restoration. Nevertheless, the specific time scale of nutrient and trace metal release caused by de-embankments still remains unclear and requires further detailed investigations.

Acknowledgements

5.   Conclusions and perspectives

A de-embankment on the East Frisian barrier island Langeoog (NW Germany) caused a simulated a sea level rise in a definite salt marsh area of 2.2 km^2. This study combines solid phase and pore water investigations of the de-embanked salt marshes from Langeoog Island to provide a better understanding of the depositional conditions during a rising sea level. Furthermore, this study improves the knowledge of geochemical and sedimentary processes associated with inundation of formerly flood-protected coastal areas. It not only may serve as a basis for future sea level rise scenarios, but also helps re-interpreting geochemical signatures seen in Holocene coastal sedimentary sequences.

The studied Holocene sediment sequence on Langeoog Island starts with mixed flat deposits on its base accumulated under low energy and marine depositional conditions followed by sand flat deposits of higher energy and marine depositional conditions. The highest depositional energy conditions are recorded in the adjacent relocated beach sands which were accumulated after several dune-breaching events. The sequence is overlain by marsh soil deposits of low energy and marine-terrestrial conditions. Correlations between FeO and TiO$_2$ content of the Holocene sediment sequence on Langeoog Island along with SEM-EDX analyses give evidence of the dominating presence of the heavy mineral ilmenite within the study area and allow the characterisation of depositional energy conditions. The relationship between sediment geochemistry (represented by the major oxides SiO$_2$, Al$_2$O$_3$, TiO$_2$ and the trace element Zr) and depositional energy for the investigated marine-terrestrial sediments is visualised in ternary plots. This relationship is assumed to be applicable to other sedimentary systems. Further, the combination of diatom analyses and geochemical data document the barrier island development as well as the varying energetic conditions during deposition. Sediments deposited under high depositional energy conditions reveal low to no diatom abundances and concomitant high number of diatom fragments. Sediments deposited under low depositional energy are characterised by high diatom abundances and low number of diatom fragments.

Sediment material imported under transgressive conditions to the study area was sampled by using sediment settling traps (SST). The de-embanked salt marsh area on Langeoog Island currently has a positive accretionary balance resulting in vertical salt marsh

growth comparable to transgressive periods in the late Holocene. Sediment supply is highest in autumn and winter especially during storm events whereas the late spring and summer level is distinctly lower. Although, the SST reflect only maximum deposition because of lacking erosion, a calculated sedimentation rate coincide well with measured rates (Barkowski et al., 2009b). The geochemical composition of the material from the SST emphasise suspended particulate matter from the adjacent Wadden Sea as a major sediment source. Clear seasonal behaviour is shown by TOC, P and Mo with maximum contents during summer, thus reflecting biogeochemical processes occurring in the open water column. Accumulation rates of TOC, P, Mn, and Mo highlight the investigated salt marshes on Langeoog Island as an important depo-centre for particulate matter from the Wadden Sea, thereby driving biogeochemical processes within the salt marsh ecosystem. The comparison with Holocene coastal deposits reveals similarities of the freshly deposited material on Langeoog Island and Holocene brackish and tidal flat and sediments. Therefore, this situation is inferred to be an example for an early stage of transgression which provides the opportunity for future interdisciplinary studies focussing on the coastal development under transgressive conditions.

The quartz-dominated sand flat-type deposits within the study area on Langeoog Island are characterised by very low carbon and sulphur contents, except for the upper 0.29 m sediment (marsh soil deposits). The sedimentary iron content is comparable to other salt marsh and tidal flat sediments with Fe/Al ratios partly exceeding average shale values (relocated beach sand deposits). Elevated manganese contents only occur in the marsh soil and relocated beach sand deposits with Mn/Al ratios near average shale values. The high percentage of reactive iron suggests that the salt marsh sediments act as iron source for pore waters. Salt marsh pore water iron is dominated by organically complexed iron in the high molecular weight class >5,000 Da, partly at high concentration levels (up to 583 µM). Iron complexation is most likely controlled by humic substances, and is accompanied by siderophores in the rhizosphere. The circum-neutral pore water pH value keeps the complexed iron in solution. Thus the salt marsh pore waters may serve as significant sources of dissolved iron, which can be exported and precipitated e.g. as pyrite under appropriate conditions.

The restoration of regular tidal inundation (de-embankment) results in considerable increases in pore water iron, manganese, phosphate, and ammonia concentrations as observed in this study after a storm surge. This was already predicted by some authors (Portnoy, 1999;

Portnoy and Giblin, 1997) but served as management implication for sea water restoration. Nevertheless, the specific time scale of nutrient and trace metal release caused by de-embankments still remains unclear and requires further detailed investigations.

6.   References

Ahlhorn, F. and Kunz, H., 2002. The future of historically developed summerdikes and polders: a saltmarsh use conflict*Littoral*.

Allen, J.R.L., 2000. Morphodynamics of Holocene Salt marshes: a review sketch from the Atlantic and Southern North Sea coasts of Europe. *Quaternary Science Reviews* 19, 1155-1231.

Amon, R.M.W. and Benner, R., 1996. Bacterial utilization of different size classes of dissolved organic matter. *Limnology and Oceanography* 41, 41-51.

Barckhausen, J., 1969. Entstehung und Entwicklung der Insel Langeoog. *Oldenburger Jahrbuch Bd. 68*, 239-281.

Barkowski, J., Kolditz, K., Brumsack, H.J. and Freund, H., 2009. The impact of tidal inundation on salt marsh vegetation after de-embankment on Langeoog Island, Germany - Six years time series of permanent plots. *Journal of Coastal Conservation: Planning and Management* 13, 182-206.

Barkowski, J., Kolditz, K., Brumsack, H.J. and Freund, H., (in prep.). Sediment accumulation on a salt marsh after de-embankment on Langeoog Island, Germany. *Estuarine, Coastal and Shelf Science*.

Beck, M., Dellwig, O., Holstein, J.M., Grunwald, M., Liebezeit, G., Schnetger, B. and Brumsack, H.J., 2008a. Sulphate, dissolved organic carbon, nutrients and terminal metabolic products in deep pore waters of an intertidal flat. *Biogeochemistry* 89, 221-238.

Beck, M., Dellwig, O., Kolditz, K., Freund, H., Liebezeit, G., Schnetger, B. and Brumsack, H.J., 2007. In situ pore water sampling in deep intertidal flat sediments. *Limnology and Oceanography-Methods* 5, 136-144.

Beck, M., Dellwig, O., Liebezeit, G., Schnetger, B. and Brumsack, H.J., 2008b. Spatial and seasonal variations of sulphate, dissolved organic carbon, and nutrients in deep pore waters of intertidal flat sediments. *Estuarine, Coastal and Shelf Science* 79, 307-316.

Beeftink, W.G. and Rozema, J., 1988. The nature and functioning of Salt Marshes. In: Salomons, W., Bayne, B.L., Duursma, E.K. and Förstner, U. Eds.), *Pollution of the North Sea: An assessment*. Springer.

Behre, K.E., 2003. Eine neue Meeresspiegelkurve für die südliche Nordsee: Transgressionen und Regressionen in den letzten 10.000 Jahren. *Probleme der Küstenforschung im südlichen Nordseegebiet* 28, 9-63.

Behre, K.E., 2004. Coastal development, sea-level change and settlement history during the later Holocene in the Clay District of Lower Saxony (Niedersachsen), northern Germany. *Quaternary International* 112, 37-53.

Behre, K.E., 2007. A new Holocene sea-level curve for the southern Noth Sea. *Boreas* 36, 82-102.

Bricker-Urso, S., Nixon, S.W., Cochran, J.K., Hirschberg, D.J. and Hunt, C., 1989. Accretion rates and sediment accumulation in Rhode Island salt marshes. *Estuaries* 12, 300-317.

Bull, D.C. and Taillefert, M., 2001. Seasonal and topographic variations in porewaters of a southeastern USA salt marsh as revealed by voltammetric profiling. *Geochemical Transactions* 2, 104ff.

Burdige, D.J., 1993. The Biogeochemistry of Manganese and Iron Reduction in Marine-Sediments. *Earth-Science Reviews* 35, 249-284.

Burdige, D.J. and Gardner, K.G., 1998. Molecular weight distribution of dissolved organic carbon in marine sediment pore waters. *Marine Chemistry* 62, 45-64.

Buyer, J.S. and Sikora, L.J., 1990. Rhizosphere Interactions and Siderophores. *Plant and Soil* 129, 101-107.

Buynevich, I.V., FitzGerald, D.M. and van Heteren, S., 2004. Sedimentary records of intense storms in Holocene barrier sequences, Maine, USA. *Marine Geology* 210, 135-148.

Cameron, T.D.J., Stoker, M.S. and Long, D., 1987. The history of quaternary sedimentation in the UK sector of the North Sea Basin. *Journal Geological Society London* 144, 43-58.

Canfield, D.E., 1989. Reactive Iron in Marine-Sediments. *Geochimica Et Cosmochimica Acta* 53, 619-632.

Carey, E. and Taillefert, M., 2005. The role of soluble Fe(III) in the cycling of iron and sulfur in coastal marine sediments. *Limnology and Oceanography* 50, 1129-1141.

Carrasco, N., Kretzschmar, R., Pesch, M.L. and Kraemer, S.M., 2007. Low concentrations of surfactants enhance siderophore-promoted dissolution of goethite. *Environmental Science & Technology* 41, 3633-3638.

Cesco, S., Romheld, V., Varanini, Z. and Pinton, R., 2000. Solubilization of iron by water-extractable humic substances. *Journal of Plant Nutrition and Soil Science-Zeitschrift fuer Pflanzenernaehrung und Bodenkunde* 163, 285-290.

Chang, T.S., Bartholomä, A. and Flemming, B.W., 2006a. Seasonal dynamics of fine-grained sediments in a back-barrier tidal basin of the German Wadden Sea (Southern North Sea). *Journal of Coastal Research* 22, 328-338.

Chang, T.S., Joerdel, O., Flemming, B.W. and Bartholoma, A., 2006b. The role of particle aggregation/disaggregation in muddy sediment dynamics and seasonal sediment turnover in a back-barrier tidal basin, East Frisian Wadden Sea, southern North Sea. *Marine Geology* 235, 49-61.

Chmura, G.L., Coffey, A. and Crago, R., 2001. Variation in surface sediment deposition on salt marshes in the Bay of Fundy. *Journal of Coastal Research* 17, 221-227.

Craft, C.B., Seneca, E.D. and Broome, S.W., 1991. Porewater Chemistry of Natural and Created Marsh Soils. *Journal of Experimental Marine Biology and Ecology* 152, 187-200.

Crowley, D.E., Wang, Y.C., Reid, C.P.P. and Szaniszlo, P.J., 1991. Mechanisms of Iron Acquisition from Siderophores by Microorganisms and Plants. *Plant and Soil* 130, 179-198.

Cundy, A.B. and Croudace, I.W., 1995. Sedimentary and Geochemical Variations in a Salt-Marsh Mud Flat Environment from the Mesotidal Hamble Estuary, Southern England. *Marine Chemistry* 51, 115-132.

Deer, W.A., Howie, R.A. and Zussman, J., 1972. *An introduction to the rock-forming minerals.* Longman Group Limited, London,

Dellwig, O., Beck, M., Lemke, A., Lunau, M., Kolditz, K., Schnetger, B. and Brumsack, H.J., 2007a. Non-conservative behaviour of molybdenum in coastal waters: Coupling geochemical, biological, and sedimentological processes. *Geochimica Et Cosmochimica Acta* 71, 2745-2761.

Dellwig, O., Bosselmann, K., Kölsch, S., Hentscher, M., Hinrichs, J., Böttcher, M.E., Reuter, R. and Brumsack, H.J., 2007b. Sources and fate of manganese in a tidal basin of the German Wadden Sea. *Journal of Sea Research* 57, 1-18.

Dellwig, O., Böttcher, M.E., Lipinski, M. and Brumsack, H.J., 2002. Trace metals in Holocene coastal peats and their relation to pyrite formation (NW Germany). *Chemical Geology* 182, 423-442.

Dellwig, O., Gramberg, D., Vetter, D., Watermann, F., Barckhausen, J., Brumsack, H.J., Gerdes, G., Liebezeit, G., Rullkötter, J., Scholz-Böttcher, B.M. and Streif, H., 1998. Geochemical and microfacies characterization of a Holocene depositional sequence in northwest Germany. *Organic Geochemistry* 29, 1687-1699.

Dellwig, O., Hinrichs, J., Hild, A. and Brumsack, H.J., 2000. Changing sedimentation in tidal flat sediments of the southern North Sea from the Holocene to the present: a geochemical approach. *Journal of Sea Research* 44, 195-208.

Dellwig, O., Watermann, F., Brumsack, H.J. and Gerdes, G., 1999. High-resolution reconstruction of a holocene coastal sequence (NW Germany) using inorganic geochemical data and diatom inventories. *Estuarine Coastal and Shelf Science* 48, 617-633.

Dellwig, O., Watermann, F., Brumsack, H.J., Gerdes, G. and Krumbein, W.E., 2001. Sulphur and iron geochemistry of Holocene coastal peats (NW Germany): a tool for palaeoenvironmental reconstruction. *Palaeogeography Palaeoclimatology Palaeoecology* 167, 359-379.

Eisma, D., 1981. Supply and deposition of suspended matter in the North Sea. *Special Publication of the International Association of Sedimentologists* 5, 415-428.

Eisma, D. and Kalf, J., 1987. Dispersal, Concentration and Deposition of Suspended Matter in the North-Sea. *Journal of the Geological Society* 144, 161-178.

Engleman, E.E., Jackson, L.L. and Norton, D.R., 1985. Determination of Carbonate Carbon in Geological-Materials by Coulometric Titration. *Chemical Geology* 53, 125-128.

Feijtel, T.C., Delaune, R.D. and Patrick, W.H., 1988. Seasonal Pore Water Dynamics in Marshes of Barataria Basin, Louisiana. *Soil Science Society of America Journal* 52, 59-67.

Flemming, B. and Ziegler, K., 1995. High resolution grain size distribution patterns and textural trends in the backbarrier environment of Spiekeroog Island (Southern North Sea). *Senckenbergiana maritima* 26, 1-24.

Flemming, B.W. and Nyandwi, N., 1994. Land reclamation as a cause of fine-grained sediment depletion in backbarrier tidal flats (southern North Sea). *Netherlands Journal of Aquatic Ecology* 28, 299-307.

Francois, R., 1990. Marine Sedimentary Humic Substances - Structure, Genesis, and Properties. *Reviews in Aquatic Sciences* 3, 41-80.

French, J.R. and Spencer, T., 1993. Dynamics of sedimentation in a tide-dominated backbarrier salt marsh, Norfolk, UK. *Marine Geology* 110, 315-331.

Freund, H., 2003. *Die Dünen- und Salzwiesenvegetation auf Juist und deren Änderung als Indikator für die Entwicklung der Insel seit dem Frühen Mittelalter.* Isensee Verlag, Oldenburg,

Freund, H., Gerdes, G., Streif, H., Dellwig, O. and Watermann, F., 2004. The indicative meaning of diatoms, pollen and botanical macro fossils for the reconstruction of palaeoenvironments and sea-level fluctuations along the coast of Lower Saxony; Germany. *Quaternary International* 112, 71-87.

Freund, H., Petersen, S. and Pott, R., 2003. Investigations on recent and subfossil salt-marsh vegetation of the East Frisian barrier islands in the southern North Sea (Germany). *Phytocoenologia* 33, 349-375.

Freund, H. and Streif, H., 1999. Natürliche Pegelmarken für Meeresspiegelschwankungen der letzten 2000 Jahre im Bereich der Insel Juist. *Petermanns Geographische Mitteilungen* 143.

Giblin, A.E., 1988. Pyrite Formation in Marshes During Early Diagenesis. *Geomicrobiology Journal* 6, 77-97.

Giblin, A.E. and Howarth, R.W., 1984. Porewater Evidence for a Dynamic Sedimentary Iron Cycle in Salt Marshes. *Limnology and Oceanography* 29, 47-63.

Goodman, J.E., Wood, M.E. and Gehrels, W.R., 2007. A 17-yr record of sediment accretion in the salt marshes of Maine (USA). *Marine Geology* 242, 109-121.

Grasshoff, K., Kremling, K. and Ehrhardt, M., 1999. *Methods of seawater analysis.* Wiley-VCH, New York,

Guo, T.Z., DeLaune, R.D. and Patrick, W.H., Jr., 2000. Iron and manganese transformation in Louisiana salt and brackish marsh sediment. *Communications in Soil Science and Plant Analysis* 31, 2997-3009.

Hagemann, B.P., 1969. Development of the western part of the Netherlands during the Holocene. *Geologie en Mijnbouw* 48, 373-388.

Hanisch, J., 1980. Neue Meeresspiegeldaten aus dem Raum Wangerooge. *Eiszeitalter und Gegenwart* 30, 221-228.

Hartley, B., 1996. *An atlas of British Diatoms.* Biopress Ltd, Bristol, 601pp.

Heinrich, H. and Hermann, A.G., 1990. *Praktikum der Analytischen Geochemie.* Springer-Verlag, Berlin,

Heinrichs, H., Brumsack, H.J., Loftfield, N. and König, N., 1986. Verbessertes Druckaufschlusssystem für biologische und anorganische Materialien. *Zeitschrift für Pflanzenernährung und Bodenkunde* 149, 350-353.

Hersman, L., Lloyd, T. and Sposito, G., 1995. Siderophore-Promoted Dissolution of Hematite. *Geochimica Et Cosmochimica Acta* 59, 3327-3330.

Hild, A., 1997. Geochemie der Sedimente und Schwebstoffe im Rückseitenwatt von Spiekeroog und ihre Beeinflussung durch biologische Aktivität. *Forschungszentrum Terramare Berichte* 5.

Hines, M.E., Knollmeyer, S.L. and Tugel, J.B., 1989. Sulfate Reduction and Other Sedimentary Biogeochemistry in a Northern New-England Salt-Marsh. *Limnology and Oceanography* 34, 578-590.

Hinrichs, J., Dellwig, O. and Brumsack, H.J., 2002. Lead in sediments and suspended particulate matter of the German Bight: natural versus anthropogenic origin. *Applied Geochemistry* 17, 621-632.

Hoselmann, C. and Streif, H., 2004. Holocene sea-level rise and its effect on the mass balance of coastal deposits. *Quaternary International* 112, 89-103.

Howarth, R.W. and Giblin, A.E., 1983. Sulfate Reduction in the Salt Marshes at Sapelo Island, Georgia. *Limnology and Oceanography* 28, 70-82.

Howarth, R.W. and Teal, J.M., 1979. Sulfate Reduction in a New-England Salt-Marsh. *Limnology and Oceanography* 24, 999-1013.

Howes, B.L., Dacey, J.W.H. and King, G.M., 1984. Carbon Flow through Oxygen and Sulfate Reduction Pathways in Salt-Marsh Sediments. *Limnology and Oceanography* 29, 1037-1051.

Howes, B.L., Howarth, R.W., Teal, J.M. and Valiela, I., 1981. Oxidation-Reduction Potentials in a Salt-Marsh - Spatial Patterns and Interactions with Primary Production. *Limnology and Oceanography* 26, 350-360.

Huffman, E.W.D., 1977. Performance of a New Automatic Carbon-Dioxide Coulometer. *Microchemical Journal* 22, 567-573.

Huisman, D.J., Weijers, J.P., Dijkshoorn, L. and Veldkamp, A., 2000. Spatial prediction of the variability of Early Pleistocene subsurface sediments in the Netherlands-Part 2: Geochemistry. *Geologie en Mijnbouw / Netherlands Journal of Geosciences* 79, 381-390.

Irion, G., 1994. Morphological, sedimentological and historical evolution of the Jade Bay, Southern North Sea. *Senckenbergiana maritima* 24, 171-186.

Jahnke, R., Richards, M., Nelson, J., Robertson, C., Rao, A. and Jahnke, D., 2005. Organic matter remineralization and porewater exchange rates in permeable South Atlantic Bight continental shelf sediments. *Continental Shelf Research* 25, 1433-1452.

Kolditz, K., Barkowski, J., Dellwig, O., Bahlo, R., Leipe, T., Freund, H. and Brumsack, H.J., 2009a. Geochemistry of Holocene salt marsh and tidal flat sediments on a barrier island in the southern North Sea (Langeoog, NW Germany). *Sedimentology* in review.

Kolditz, K., Dellwig, O., Barkowski, J., Beck, M., Freund, H. and Brumsack, H.J., 2009b. Effects of de-embankment on pore water geochemistry of salt marsh sediments. *Journal of Coastal Research* 25, 1222-1235.

Koretsky, C.M., Van Cappellen, P., DiChristina, T.J., Kostka, J.E., Lowe, K.L., Moore, C.M., Roychoudhury, A.N. and Viollier, E., 2005. Salt marsh pore water geochemistry does not correlate with microbial community structure. *Estuarine Coastal and Shelf Science* 62, 233-251.

Kostka, J.E. and Luther, G.W., III., 1995. Seasonal Cycling of Fe in Salt-Marsh Sediments. *Biogeochemistry* 29, 159-181.

Kostka, J.E., Roychoudhury, A. and Van Cappellen, P., 2002. Rates and controls of anaerobic microbial respiration across spatial and temporal gradients in saltmarsh sediments. *Biogeochemistry* 60, 49-76.

Kowalski, N., Dellwig, O., Beck, M., Grunwald, M., Fischer, S., Piepho, M., Riedel, T., Freund, H., Brumsack, H.J. and Böttcher, M.E., 2009. Trace metal dynamics in the water column and pore waters in a temperate tidal system: response to the fate of algae-derived organic matter. *Ocean Dynamics* 59, 333-350.

Kraemer, S.M., 2004. Iron oxide dissolution and solubility in the presence of siderophores. *Aquatic Sciences* 66, 3-18.

Krammer, K. and Lange-Bertalot, H., 1997a. *Süßwasserflora Mitteleuropas 2/2: Bacillariophyceae Bacillariaceae, Epithemiaceae, Surirellaceae*. Spektrum Akademischer Verlag, Heidelberg, Berlin, 612pp.

Krammer, K. and Lange-Bertalot, H., 1997b. *Süßwasserflora Mittelweuropas 2/1: Bacillariophyceae Naviculaceae*. Spektrum Akademischer Verlag, Heidelberg, Berlin, 876pp.

Krammer, K. and Lange-Bertalot, H., 2000. *Süßwasserflora Mitteleuropas 2/3: Bacillariophyceae Centrales, Fragilariaceae, Eunotiaceae*. Spektrum Akademischer Verlag, Heidelberg, Berlin, 600pp.

Krom, M.D. and Berner, R.A., 1980. Adsorption of Phosphate in Anoxic Marine-Sediments. *Limnology and Oceanography* 25, 797-806.

Leventhal, J. and Taylor, C., 1990. Comparison of Methods to Determine Degree of Pyritization. *Geochimica Et Cosmochimica Acta* 54, 2621-2625.

Lindsay, W.L., 1991. Iron-Oxide Solubilization by Organic-Matter and Its Effect on Iron Availability. *Plant and Soil* 130, 27-34.

Long, D., Laban, C., Streif, H., Cameron, T.D.J. and Schuettenhelm, R.T.E., 1988. The sedimentary record of climatic variation in the Southern North Sea. *Philosophical Transactions of the Royal Society of London* B318.

Lord, C.J., III. and Church, T.M., 1983. The Geochemistry of Salt Marshes - Sedimentary Ion Diffusion, Sulfate Reduction, and Pyritization. *Geochimica Et Cosmochimica Acta* 47, 1381-1391.

Ludwig, G. and Figge, K., 1979. Schwermineralvorkommen und Sandverteilung in der Deutschen Bucht. *Geologisches Jahrbuch* D 32, 23-68.

Lunau, M., Lemke, A., Dellwig, O. and Simon, M., 2006. Physical and biogeochemical controls of microaggregate dynamics in a tidally affected coastal ecosystem. *Limnology and Oceanography* 51, 847-859.

Luther, G.W., III and Church, T.M., 1988. Seasonal cycling of sulfur and iron in porewaters of a Delaware salt marsh. *Marine Chemistry* 23, 295-309.

Luther, G.W., III., Kostka, J.E., Church, T.M., Sulzberger, B. and Stumm, W., 1992. Seasonal Iron Cycling in the Salt-Marsh Sedimentary Environment - the Importance of Ligand Complexes with Fe(Ii) and Fe(Iii) in the Dissolution of Fe(Iii) Minerals and Pyrite, Respectively. *Marine Chemistry* 40, 81-103.

Luther, G.W., III., Shellenbarger, P.A. and Brendel, P.J., 1996. Dissolved organic Fe(III) and Fe(II) complexes in salt marsh porewaters. *Geochimica Et Cosmochimica Acta* 60, 951-960.

Macleod, D.A., 1973. Iron, Manganese and Sulphur Forms in Salt Marsh Soils of the Wash, E. England, and Changes Resulting from Reclamation. In: Schlichting, E. and Schwertmann, U. Eds.), *Pseudogley and gley. Genesis and use of hydromorphic soils. Transactions of commissions V and VI of the International Society of Soil Sciences.* Verlag Chemie, Weinheim.

McLennan, S.M., 2001. Relationship between the trace element composition of sedimentary rocks and the upper continental crust. *Geochemistry Geophysics Geosystems* 2.

Menke, B., 1976. Befunde und Überlegungen zum nacheiszeitlichen Meeresspiegelanstieg. *Probleme der Küstenforschung im südlichen Nordseegebiet* 11, 145-161.

Merkt, J. and Streif, H., 1970. Stechrohr-Bohrgeräte für limnische und marine Lockersedimente. *Geologisches Jahrbuch* 88, 137-148.

Miller, L. and Douglas, B.C., 2004. Mass and volume contributions to twentieth-century global sea level rise. *Nature* 428, 406-409.

Müller, W., 1977. Geologie. In Exkursion A (=E) Wesermarsch. *Mitteilungen der Deutschen Bodenkundlichen Gesellschaft* 24, 15-29.

Murphy, S. and Voulgaris, G., 2006. Identifying the role of tides, rainfall and seasonality in marsh sedimentation using long-term suspended sediment concentration data. *Marine Geology* 227, 31-50.

Neilands, J.B., 1981. Microbial iron compounds. *Annual Review of Biochemistry* 50, 715-731.

Obstfeld, I., 2001. *Langeoog - Chronik einer ostfriesischen Insel.* Eigenverlag, Langeoog, 72pp.

Oenema, O. and DeLaune, R.D., 1988. Accretion rates in salt marshes in the eastern Scheldt, south-west Netherlands. *Estuarine Coastal and Shelf Science* 26, 379-394.

Orson, R.A., Panageotou, W. and Leatherman, S.P., 1985. Response of tidal salt marshes of the U.S. Atlantic and Gulf coasts to rising sea levels. *Journal of Coastal Research* 1, 29-37.

Orson, R.A., Warren, R.S. and Niering, W.A., 1998. Interpreting sea-level rise and rates of vertical accretion in a Southern New England tidal salt marsh. *Estuarine, Coastal and Shelf Science* 47, 419-429.

Otero, X.L. and Macias, F., 2002. Variation with depth and season in metal sulfides in salt marsh soils. *Biogeochemistry* 61, 247-268.

Pankow, H., 1990. *Ostsee-Algenflora.* Gustav Fischer Verlag, Jena, 648pp.

Paquette, C.H., Sundberg, K.L., Boumans, R.M.J. and Chmura, G.L., 2004. Changes in saltmarsh surface elevation due to variability in evapotranspiration and tidal flooding. *Estuaries* 27, 82-89.

Petzelberger, B.E.M., 1997. Geologische Untersuchungen zur Landschaftsgeschichte des jüngeren Holozäns in der ehemaligen Crildumer Bucht im Wangerland, Ldkr. Friesland. *Probleme der Küstenforschung im südlichen Nordseegebiet* 24, 301-309.

Pingitore, N.E. and Eastman, M.E., 1985. Barium partitioning during transformation of corals from aragonite to calcite. *Chemical Geology* 48, 183-187.

Portnoy, J.W., 1999. Salt marsh diking and restoration: Biogeochemical implications of altered wetland hydrology. *Environmental Management* 24, 111-120.

Portnoy, J.W. and Giblin, A.E., 1997. Effects of historic tidal restrictions on salt marsh sediment chemistry. *Biogeochemistry* 36, 275-303.

Prakash Babu, C., Brumsack, H.J. and Schnetger, B., 1999. Distribution of organic carbon in surface sediments along the eastern Arabian Sea: a revisit. *Marine Geology* 162, 91-103.

Quaresma, V.d.S., Bastos, A.C. and Amos, C.L., 2007. Sedimentary processes over an intertidal flat: A field investigation at Hythe flats, Southampton Water (UK). *Marine Geology* 241, 117-136.

Rao, A., McCarthy, M.J., Gardner, W.S. and Jahnke, R.A., 2007. Respiration and denitrification in permeable continental shelf deposits on the South Atlantic Bight: Rates of carbon and nitrogen cycling from sediment column experiments. *Continental Shelf Research* 27, 1801-1819.

Reed, D.J., 1988. Sediment dynamics and deposition in a retreating coastal salt marsh. *Estuarine, Coastal and Shelf Science* 26, 67-79.

Reed, D.J., 1990. The impact of sea-level rise on coastal salt marshes. *Progress in Geography* 14, 465-481.

Reed, D.J., 1995. The response of coastal marshes to sea-level rise: Survival or submergence? *Earth Surface Processes and Landforms* 20, 39-48.

Richard, G.A., 1978. Seasonal and environmental variations in sediment accretion in a Long Island salt marsh. *Estuaries* 1, 29-35.

Saye, S.E. and Pye, K., 2006. Variations in chemical composition and particle size of dune sediments along the west coast of Jutland, Denmark. *Sedimentary Geology* 183, 217-242.

Schnetger, B., 1992. Chemical composition of loess from a local and worldwide view. *Neues Jahrbuch der Mineralogischen Abhandlungen* Monatshefte H1, 29-47.

Schrader, H.J., 1973. Proposal for a standardized method of cleaning diatom-bearing deepsea and land-exposed marine sediments. *Nova Hedwigia Beihefte* 45.

Schubauer, J.P. and Hopkinson, C.S., 1984. Above- and Belowground Emergent Macrophyte Production and Turnover in a Coastal Marsh Ecosystem, Georgia. *Limnology and Oceanography* 29, 1052-1065.

Schüttenhelm, R.T.E. and Laban, C., 2005. Heavy minerals, provenance and large scale dynamics of seabed sands in the Southern North Sea: Baaks (1936) heavy mineral 179 study revisited. *Quaternary International* 133-34, 179-193.

Simonsen, R., 1962. *Untersuchungen zur Systematik und Ökologie der Bodendiatomeen der westlichen Ostsee*. Akademie-Verlag, Berlin, 147pp.

Sindowski, K.-H. and Streif, H., 1974. Geschichte der Nordsee am Ende der letzten Eiszeit und im Holozän. In: Wohlstedt, P. and Duphorn, K. Eds.), *Norddeutschland und angrenzende Gebiete im Eiszeitalter*. Köhler, Stuttgart.

Skrabal, S.A. and Terry, C.M., 2002. Distributions of dissolved titanium in porewaters of estuarine and coastal marine sediments. *Marine Chemistry* 77, 109-122.

Slomp, C.P., Van der Gaast, S.J. and Van Raaphorst, W., 1996. Phosphorus binding by poorly crystalline iron oxides in North Sea sediments. *Marine Chemistry* 52, 55-73.

Slomp, C.P. and Van Raaphorst, W., 1993. Phosphate Adsorption in Oxidized Marine-Sediments. *Chemical Geology* 107, 477-480.

Stock, M., 2003. Salzwiesenschutz im Wattenmeer. In: Lozan, J.L. (Ed.), *Warnsignale aus Nordsee & Wattenmeer: Eine aktuelle Umweltbilanz*. Wissenschaftliche Auswertungen, Hamburg.

Streif, H., 1986. Zur Altersstellung und Entwicklung der Ostfriesischen Inseln. *Offa* 43, 29-44.

Streif, H., 1990. *Das ostfriesische Küstengebiet - Nordsee, Inseln, Watten und Marschen*. Borntraeger, Berlin-Stuttgart, 376pp.

Streif, H., 2004. Sedimentary record of Pleistocene and Holocene marine inundations along the North Sea coast of Lower Saxony, Germany. *Quaternary International* 112, 3-28.

Stumpf, R.P., 1983. The process of sedimentation on the surface of a salt marsh. *Estuarine Coastal and Shelf Science* 17, 495-508.

Suttill, R.J., Turner, P. and Vaughan, D.J., 1982. The Geochemistry of Iron in Recent Tidal-Flat Sediments of the Wash Area, England - a Mineralogical, Mossbauer, and Magnetic Study. *Geochimica Et Cosmochimica Acta* 46, 205-217.

Taillefert, M., Neuhuber, S. and Bristow, G., 2007. The effect of tidal forcing on biogeochemical processes in intertidal salt marsh sediments. *Geochemical Transactions* 6.

Taylor, S.R. and McLennan, S.M., 1985. *The continental crust: Its composition and evolution*. Blackwell, Oxford, 312pp.

Töppe, A., 1994. Deutsche Nordseeküste - Beschleunigter Meersspiegelanstieg. *HANSA* 131, 78-82.

Valiela, I., Teal, J.M. and Persson, N.Y., 1976. Production and Dynamics of Experimentally Enriched Salt-Marsh Vegetation - Belowground Biomass. *Limnology and Oceanography* 21, 245-252.

Van Dijk, H., 1971. Cation Binding of Humic Acids. *Geoderma* 5, 53-67.

Veenstra, H.J., 1982. Size, shape and origin of the sands of the east frisian islands (North Sea, Germany). *Geologie en Mijnbouw* 61, 141-146.

Violante, A., Barberis, E., Pigna, M. and Boero, V., 2003. Factors affecting the formation, nature, and properties of iron precipitation products at the soil-root interface. *Journal of Plant Nutrition* 26, 1889-1908.

Vos, P.C. and de Wolf, H., 1993. Diatoms as a tool for reconstructing sedimentary environments in coastal wetlands; methodological aspects. *Hydrobiologia* 269/270.

Vos, P.C. and De Wolf, H., 1994. Paleoenvironmental research on diatoms in early and middle Holocene deposits in central North Holland (the Netherlands). *Netherlands Journal of Aquatic Ecology* 28, 97-115.

Voulgaris, G. and Meyers, S.T., 2004. Net effect of rainfall activity on salt-marsh sediment distribution. *Marine Geology* 207, 115-129.

Wedepohl, K.H., 1971. Environmental influences on the chemical composition of shales and clays. In: Press, L.H., Ahrens, F., Runcorn, S.K. and Urey, H.C. Eds.), *Physics and Chemistry of the Earth 8*. Pergamon, Oxford.

Wedepohl, K.H., 1991. The compositionof the upper earth's crust and the natural cycles of selected metals. Metals in natural raw materials. Natural resources. In: Merian, E. (Ed.), *Metals and their Compounds in the Environment*. VCH, Weinheim.

Weston, N.B., Porubsky, W.P., Samarkin, V.A., Erickson, M., Macavoy, S.E. and Joye, S.B., 2006. Porewater stoichiometry of terminal metabolic products, sulfate, and dissolved organic carbon and nitrogen in estuarine intertidal creek-bank sediments. *Biogeochemistry* 77, 375-408.

Winkelmann, G., 2007. Ecology of siderophores with special reference to the fungi. *Biometals* 20, 379-392.

Wolters, M., Garbutt, A. and Bakker, J.P., 2005. Salt-marsh restoration: evaluating the success of de-embankments in north-west Europe. *Biological Conservation* 123, 249-268.

Zhang, C.S., Wang, L.J., Li, G.S., Dong, S.S., Yang, J.R. and Wang, X.L., 2002. Grain size effect on multi-element concentrations in sediments from the intertidal flats of Bohai Bay, China. *Applied Geochemistry* 17, 59-68.

Zong, Y., 1997. Mid- and late-Holocene sea-level changes in Roudsea Marsh, northwest England: a diatom biostratigraphical investigation. *The Holocene* 7, 311-323.

Zong, Y. and Horton, B.P., 1999. Diatom-based tidal-level transfer functions as an aid in reconstructing Quaternary history of sea-level movements in the UK. *Journal of Quaternary Science* 14, 153-167.

Zuther, M., Brockamp, O. and Clauer, N., 2000. Composition and origin of clay minerals in Holocene sediments from the south-eastern North Sea. *Sedimentology* 47, 119-134.

Danksagung

Besonderer Dank gilt meinem Doktorvater Prof. Dr. Hans-Jürgen Brumsack, der mir in der Arbeitsgruppe Mikrobiogeochemie die Möglichkeit zur Promotion eröffnete. Er stand mir während meiner Zeit an der Universität Oldenburg und darüber hinaus stets mit fachlichem Rat zur Seite. Er war immer offen für Diskussionen und hat durch viele Anregungen wesentlichen Anteil am Erfolg dieser Arbeit.

PD Dr. Holger Freund danke ich für die fachliche Unterstützung während meiner Arbeit und die Begutachtung dieser Arbeit.

Mein spezieller Dank gilt Dr. Olaf Dellwig, der mich bei fachlichen und analytischen Fragen und Problemen fortwährend und mit viel Engagement unterstützt hat. Er gab mir in zahlreichen Diskussionen viele Denkanstöße und hat mich wenn nötig angespornt voran zu kommen.

Ebenso bin ich Dr. Bernhard Schnetger zu Dank verpflichtet, da er auf seine unverwechselbare Art meine analytische Denk- und Arbeitsweise gefordert und gefördert hat.

Großer Dank geht an Jan Barkowski für die ausgezeichnete Zusammenarbeit.

Weiterhin möchte ich Malte Groh für seine großartige Unterstützung während der Probenahmen danken.

Außerdem möchte ich meinen Dank Eleonore Gründken, Carola Lehners, Martina Wagner, Renè Ungermann und Sebastian Eckart für ihre vielseitige Unterstützung bei den Laborarbeiten aussprechen.

Maik Grunwald, Melanie Beck und Frank Schoster danke ich für viele anregende Diskussionen und die fantastische Arbeitsatmosphäre im Büro.

Den Mitarbeitern der Werkstatt des ICBM-Terramare möchte ich für den Bau meiner Probenahmesysteme und die umfangreiche und unkomplizierte bohrtechnische Unterstützung danken.

Nicht zuletzt danke ich allen nicht namentlich genannten Mitgliedern der AG Mikrobiogeochemie für die schöne Zeit in Oldenburg.

Curriculum vitae

Name: Kerstin Kolditz

Geburtsdatum: 09.09.1974

Geburtsort: Jena

1981-1990	Allgemeinbildende Polytechnische Oberschule Orlamünde
1990-1993	Sportgymnasium Jena, Abschluss: Abitur, Leistungskurse: Mathematik, Physik
09/1993-06/1996	Ausbildung bei der TEAG Thüringer Energie AG, Abschluss: Industriekauffrau
10/1996-10/2003	Studium der Geologie an der Friedrich-Schiller-Universität Jena, Institut für Geowissenschaften, Abschluss: Diplom-Geologin Thema der Diplomarbeit: Hydrogeologische und hydrogeochemische Untersuchungen am Altlastenstandort Teerverarbeitungswerk Rositz/Ostthüringen
10/2004-12/2007	wissenschaftliche Mitarbeiterin am Institut für Biologie und Chemie des Meeres der Carl von Ossietzky Universität Oldenburg, AG Mikrobiogeochemie
seit 10/2008	Laboringenieurin bei der IBU-tec advanced materials AG

Veröffentlichungen

Poster

Kolditz, K., Barkowski, J., Dellwig, O., Freund, H., Brumsack, H.-J.: Salt marshes – an iron source for pyrite formation? International Conference and 97th Annual Meeting of the Geologische Vereinigung e.V., 01.-05.10.2007, Bremen

Kolditz, K., Barkowski, J. Dellwig, O., Freund, H. Brumsack, H.-J.: Iron enrichments in salt marshes of NW Germany. Goldschmidt Conference 2007, 19.-24.08.2007, Köln

Kolditz, K., Dellwig, O., Freund, H., Brumsack, H.-J.: Deep pore water profiles of salt marsh sediments at Langeoog island (NW Germany). 14th Coastal Ecology Workshop, 21.-22.09.2006, Wilhelmshaven

Vorträge

Kolditz, K., Dellwig, O. Liebezeit, G., Freund, H., Brumsack, H.-J.: Geochemistry of deep pore water in the salt marshes at Langeoog island (NW Germany). 9th International Estuarine Biochemistry Symposium, 07.-11.05.2006, Warnemünde

Artikel

Kolditz, K., Dellwig, O., Barkowski, J., Beck, M., Freund, H., Brumsack, H.-J. 2009: Salt marsh restoration: Effects of de-embankment on pore water geochemistry. Journal of Coastal Research 25:1222-1235

Kolditz, K., Barkowski, J., Dellwig, O., Bahlo, R., Leipe, T., Freund H., Brumsack, H.-J., 2009. Geochemistry of Holocene salt marsh and tidal flat sediments on a barrier island in the southern North Sea (Langeoog, NW Germany), Sedimentology, in review

Barkowski, J., Kolditz, K., Brumsack, H.-J.; Freund, H., 2009: The impact of tidal inundation on salt marsh vegetation after de-embankment on Langeoog Island, Germany – Six years time series of permanent plots. Journal of Coastal Conservation: Planning and Managemant 13: 182-206

Barkowski, J., Kolditz, K., Brumsack, H.-J., Freund, H., (in prep.): Sediment accumulation on a salt marsh after de-embankment on Langeoog Island, Germany, Estuarine Coastal and Shelf Science

Beck, M., Dellwig, O., Kolditz, K., Freund, H., Liebezeit, G., Schnetger, B., Brumsack, H.-J., 2007: In situ pore water sampling in deep intertidal flat sediments. Limnology and Oceanography-Methods 5:136-144

Dellwig, O., Beck, M., Lemke, A. Lunau, M., Kolditz, K., Schnetger, B., Brumsack, H.-J., 2007: Non-conservative behaviour of molybdenum in coastal waters: Coupling geochemical, biological, and sedimentological processes. Geochimica et Cosmochimica Acta 71:2745-2761.

Appendix

Non-conservative behaviour of molybdenum in coastal waters: Coupling geochemical, biological, and sedimentological processes

Olaf Dellwig, Melanie Beck, Andreas Lemke, Mirko Lunau, Kerstin Kolditz, Bernhard Schnetger, Hans-Jürgen Brumsack

Abstract

Non-conservative behaviour of dissolved Mo was observed during specific time periods in the water column of the Wadden Sea of NW Germany. In July 2005 dissolved Mo declined within 36 hours from a level only slightly below seawater (82 nM) to a minimum value of 30 nM, whereas in August 2002 dissolved Mo revealed a tidal cyclicity with maximum values up to 158 nM at low tide. In contrast, cruises in August 2003 and 2004 displayed an almost conservative behaviour of Mo. The decrease in dissolved Mo during July 2005 and elevated values in August 2002 were accompanied by Mo enrichments on aggregates in the water column of the Wadden Sea. Along with Mo, dissolved Mn showed unusual concentration patterns in July 2005, with values distinctly below the common summer level (by a factor of five). A direct relation between the loss of Mo and scavenging by freshly formed MnO_x phases could not be inferred from our data because both metals revealed inverse patterns. Parallel to decreasing dissolved Mo concentrations dissolved Mn showed an increasing trend while particulate Mn decreased. Such finding is compatible with the formation of oxygen-depleted zones in aggregates, which provide suitable conditions for the rapid fixation of Mo and parallel release of Mn by chemically and/or microbially mediated processes. Our assumption is supported by biological (e.g. number of aggregate-associated bacteria) and sedimentological (e.g. aggregate abundance and size) parameters. The production of organic components (e.g. TEP) during breakdown of an algae bloom in July 2005 led to the formation of larger Mo-enriched aggregates, thus depleting the water column in dissolved Mo. After deposition on and incorporation into sandy tidal flats these aggregates are rapidly decomposed by microbial activity. Pore water profiles document that during microbial decomposition of these aggregates, substantial amounts of Mo are released and may replenish and even enrich Mo in the open water column. We postulate a conceptual

model for the observed non-conservative behaviour of Mo in coastal waters, which is based on the tight coupling of geochemical, biological, and sedimentological processes.

Introduction

Molybdenum is an essential trace metal for planktonic organisms, e.g. cyanobacteria, as it plays an important role in nitrogen metabolism. Mo forms a cofactor for various nitrogen-fixation and nitrate reductase systems (e.g. Fogg and Wolfe, 1954; Arnold, 1955; Fogg, 1962; Robson et al., 1986). Despite its biological requirement, Mo is the most abundant trace metal in ocean water (about 107 nM) and generally displays a conservative behavior unaffected by biological activity (Collier, 1985; Morris, 1975). However, Berrang and Grill (1974) found variable Mo concentrations in coastal waters of Saanich Inlet ranging from 73 to 107 nM. The authors suggested a non-biotic coupling to Mn oxidation and subsequent scavenging by freshly formed MnO_x phases. Adelson et al. (2001) also ascribed importance to Mn cycling on Mo behaviour. They proposed a model for the removal of MoO_4^{2-} from surface waters and its pre-concentration at the sediment/water interface by settling $Mn(Mo)O_x$ phases. A special feature of this model is that MoO_4^{2-} is not necessarily reduced during transfer to the sediment. Moreover, MoO_4^{2-} is released at the sediment/water interface from where it may diffuse back into the water column and/or into the sediment. Within the sediment MoO_4^{2-} can be fixed by thiol or covalent bondings to transition metals followed by reduction and final burial as sulphide, which leads to typical Mo enrichments frequently observed in TOC-rich marine sediments (e.g. Brumsack, 2006).

In contrast, Head and Burton (1970) observed decreasing Mo concentration in the estuary of Southampton Water during spring, which they attributed to its utilisation by plankton and/or complexing by organic particles. Yamazaki and Gohda (1990) also observed Mo depletion in coastal waters (Seto Inland Sea, North Pacific, minimum 69 nM), which was explained by scavenging of Mo as an organically associated species; a relationship, which was suggested earlier by Szalay and Szilagyi (1967) and Brumsack and Gieskes (1983). More recently, Tuit and Ravizza (2003) reported both, positive and negative Mo concentration anomalies in a region of nitrogen-fixation in the Eastern Equatorial Pacific (+ 5nM, -3 nM), which presumably are related to biological processes. A coupling of Mo anomalies to Mn was not observed by these authors. Recent publications by Engel et al. (2004) and Lunau et al. (2006a)

emphasise the importance of organic macromolecules produced during algae blooms on particle dynamics in the water column. These compounds are supposed to maintain aggregate formation in the water column, which possibly also influences the cycles of trace metals via scavenging by organic matter or reduction in the suboxic interior of larger particles. Evidence for the existence of oxygen-depleted zones is provided by studies of Alldrege and Cohen (1987) who demonstrated substantial oxygen depletion in marine snow. In addition, Ploug et al. 1997 measured microscale distributions of oxygen in laboratory-made aggregates and concluded that anoxic conditions can prevail for a few hours. Stable anoxic conditions, however, would require a high and continuous carbon supply.

In this contribution we present data, which show distinct non-conservative behaviour of Mo (positive and negative anomalies) in coastal waters of the Southern North Sea during time-periods associated with changes in productivity. These data were obtained during several ship cruises in the backbarrier tidal flat of Spiekeroog Island and the adjoining near-coastal German Bight between 2002 and 2005 (Figs. 1a and b). Along with Mo, we present Mn data, which also reflect a much more complex seasonal variability as assumed so far (e.g. Dellwig et al., 2007). Earlier investigations suggested a simple seasonal behaviour of Mn, with concentrations of dissolved Mn increasing from winter to summer by a factor of about 10 due to elevated release from the tidal flat sediments. In contrast, data from 2005 point towards a distinctly higher variability of Mn during summer which seems to be controlled by internal recycling processes in the Wadden Sea system. Thus, the major goal of this paper is to provide possible explanations for the observed unusual behaviour of both metals. Previous work in the study area has shown that Mn-oxidation forms a prominent process in the Wadden Sea (Dellwig et al., 2007), which can influence the patterns of other trace metals like Mo via scavenging. However, we strongly focus on the influence of microbial and sedimentological processes on the geochemistry of Mo and Mn, and postulate a tight coupling between these processes.

Geographical setting

The Wadden Sea of the Southern North Sea with its tidal flats and barrier Islands has formed about 7,500 BP as a result of the Holocene sea-level rise (Streif, 1990). Today, the morphology of the coastline, which stretches about 500 km from Den Helder in the Netherlands to Esbjerg in Denmark, is largely determined by human activities (e.g. dike building). The East-

Frisian Wadden Sea, which represents about 15% of the entire Wadden Sea, forms our major study area. It is characterised by mesotidal conditions (tidal range 2.2-2.8 m).
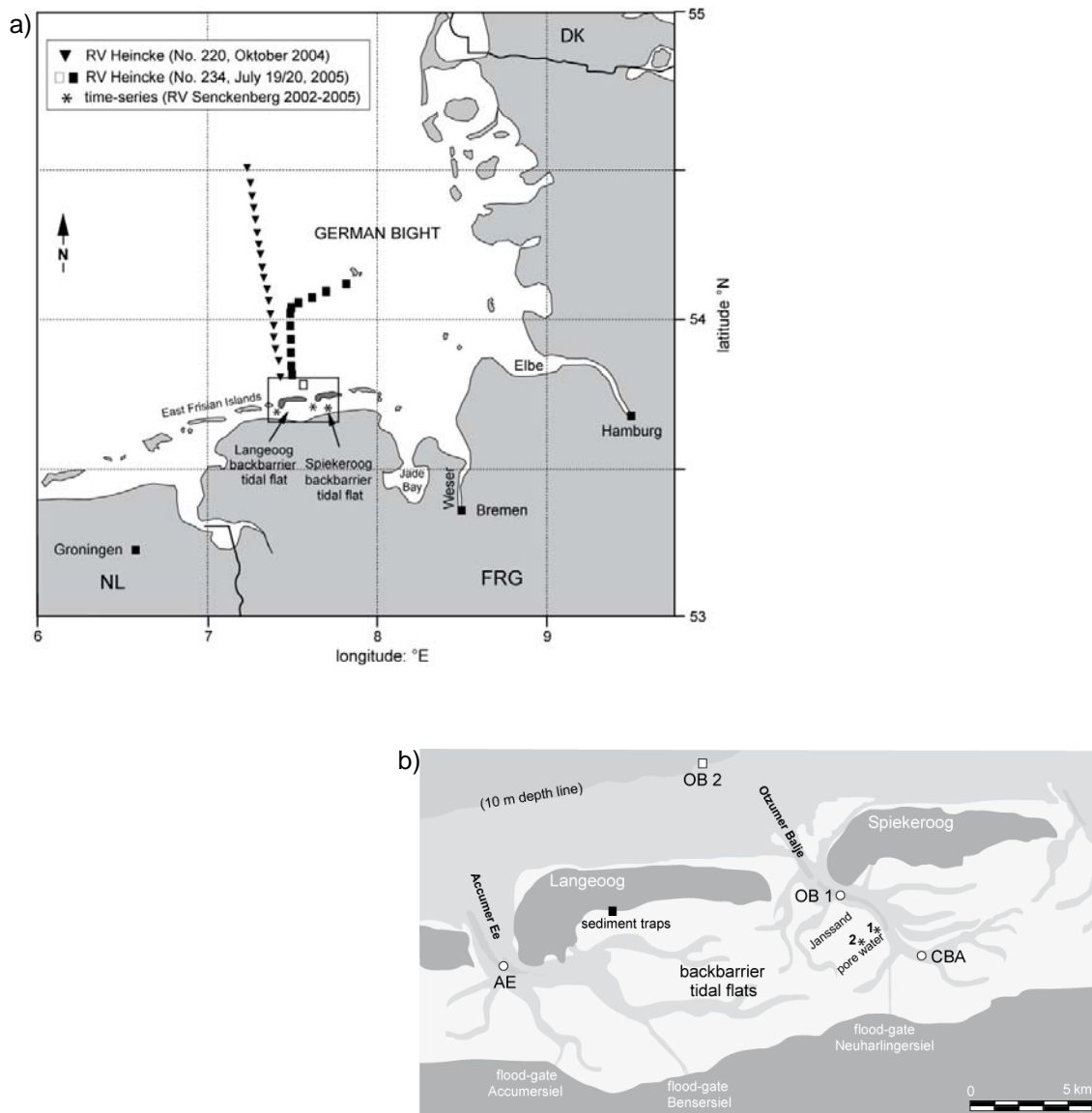
Fig. 1: a) map of the study area showing the sampling sites during several cruises in the Wadden Sea of NW Germany. The square denotes the main study area in the backbarrier tidal flats of the Islands of Spiekeroog and Langeoog. b) detailed map of the backbarrier areas of the Islands of Spiekeroog and Langeoog showing the time-series locations in the tidal inlets (Otzumer Balje, OB 1; Accumer Ee, AE), at the 10 m depth line (OB2), and in the central backbarrier area (CBA). The asterisks mark the locations of the pore water sampling sites on the Janssand tidal flat. The black square indicates the location of sediment traps at the transition zone of tidal flats and salt marshes of Langeoog Island. The light grey areas indicate tidal flats emerging at low tide.

Figure 1a shows the sampling locations during the cruises in the German Bight and the adjacent backbarrier tidal flats. This contribution is based on data from the following cruises: RV Heincke 220 (October 2004), RV Heincke 234 (July 2005), RV Senckenberg (January 2004, 2005; February 2002, 2003; April 2003, 2005; May 2002; July 2005; August 2002, 2003;

November 2002-2005). Further sampling was done on a time-series station in the tidal inlet of Spiekeroog Island in August, September, and October 2005.

Sampling was performed in intervals of 10 to 30 min during transects (RV Heincke 220: 54°29.94'N/7°19.92'E to 53°47.92'N/7°32.79'E and 234: 53°48.04'N/7°30.62'E to 54°06.09'N/745.47'E) and every 30 min during time-series in 2002-2004 (RV Senckenberg). In 2005 sampling intervals were raised to 60 min. While samples between 2002 and 2004 originate exclusively from surface waters, sampling on RV Senckenberg in 2005 was done almost simultaneously at three depth intervals.

Figure 1b shows our main study area in the backbarrier tidal flats of the Islands of Spiekeroog and Langeoog. The locations OB1 in the tidal inlet of Spiekeroog Island (Otzumer Balje; 53°44.87'N/7°40.29'E) and CBA (central backbarrier area; 53°43.43'N/7°43.32'E) mark the sampling campaigns with RV Senckenberg. OB2 (53°48.21'N/7°26.95'E) is positioned at the 10m-depth line where sampling was performed during one cruise with RV Heincke in July 2005. Additionally, a sampling campaign was carried out in the tidal inlet of Langeoog Island at position AE in July 2005 (Accumer Ee; 53°43.53'N/7°26.95'E). In the transition zone between tidal flats and salt marshes of the Island of Langeoog (53°44.77'N/7°31.46'E samples from sediment traps were taken monthly between March and November 2005.

The light grey areas in Figure 1b indicate tidal flats emerging at low tide. The Janssand is one of the flats in the backbarrier area of Spiekeroog Island. In this area sandy sediments predominate, however at depths exceeding 3 m these are intermingled with silt-clay layers. Pore water samples were taken at two locations on this flat (asterisks in Fig. 1b). Location 1 is situated very close to the main tidal channel of the backbarrier area of Spiekeroog Island (53° 44,183' N, 007° 41,904' E), whereas location 2 is positioned further towards the centre of the sand flat (53°43.96' N/7°41.28' E). Pore waters were retrieved *in situ* from the sediment using permanently installed samplers. The construction and the use of these samplers are described in more detail by Beck et al. (2007).

Material and Methods

Geochemistry

Mo, Mn, Al: Depending on SPM contents, 0.25 to 1.5 l of seawater were filtered through pre-weighed Millipore Isopore membrane filters (0.4 µm polycarbonate PC) for multi-element

analyses. Filters were rinsed with 60 ml purified water, dried at 60°C for 48 h and re-weighed for the determination of total SPM. Samples for analysis of dissolved metals in seawater and pore water were taken with pre-cleaned PE-syringes and 0.45 μm SFCA syringe filters. These samples were acidified to 1 vol. % HNO_3 (conc.) in pre-cleaned PE-bottles.

For multi-element analysis the PC filters were treated overnight with 1 ml HNO_3 and 2 ml $HClO_4$ in closed PTFE autoclaves (PDS-6; Heinrichs et al., 1986) at room temperature to oxidise organic matter. Then the filters were decomposed at 160°C. SPM residues were digested in the same PTFE vessels at 180°C after adding a mixture of 1 ml concentrated $HClO_4$ and 3 ml concentrated HF. After digestion acids were evaporated at 180°C, residues were re-dissolved and fumed off three times with 2 ml semi-concentrated HCl and diluted with 2 vol. % HNO_3 to a final dilution of 2,500 or 5,000. All acids were pre-cleaned by sub-boiling distillation, except for HF (suprapure quality). Material from sediment traps was sieved and the <63 μm fraction was digested with $HClO_4$ and HF.

Particulate Al and Mn were analysed by ICP-OES (Perkin Elmer Optima 3000XL), whereas particulate Mo as well as dissolved Mn and Mo were measured by ICP-MS (Thermo Finnigan MAT ELEMENT). Dissolved trace metals were determined directly from 25-fold diluted samples. The analytical procedure applied is similar to the method published by Rodushkin and Ruth (1997). Data presented here are based on measurements of Mo98 in low resolution and Mn55 in medium resolution with Y89 and Cs133 as internal standards, respectively. As we measured Mo98 instead of Mo95, the interference of BrO was negligible. However, Mo showed significant memory effects within the sample introducing system (e.g. tubings, nebuliser), which required sufficient wash and take up times (60-90 s). Contamination effects were excluded by measurement of filter and onboard procedural blanks. As filters for the analysis of particulate Mn and Mo were thoroughly rinsed with purified water any corrections for residual salt were unnecessary. This is also supported by measurement of particulate Na, which only reflected the normal detrital background level.

Precision (1σ) and accuracy of all measurements were checked by parallel analysis of international and in-house reference materials. GSD-4 and our in-house shale standard TW-TUC were used as a reference for particulate samples (Al: precision 2.2%, accuracy -0.6%; Mn: 1.5%, -0.9%; Mo: 9.0%, -2.1%), whereas reference seawater standards CASS-3 and CASS-4 (Canada) were used for dissolved samples (Mn: 6.1%, 6.7%; Mo: 2.6%, 1.8%). For the analysis

of Mn in pore water, a spike solution was added to these reference standards as the concentration for Mn was much higher in the Wadden Sea pore waters than in the original reference materials. The final Mn concentration in the reference standards was 3640 nM.

Particulate organic carbon (POC) and total particulate nitrogen (TPN): Subsamples of 100 mL were filtered onto precombusted and preweighed GF/F filters (Whatman, 25 mm diameter), rinsed with 2-5 ml of distilled water to remove salt and kept frozen at -20°C until further analysis. Prior to analysis the filters were exposed to the fume of concentrated hydrochloric acid for 12 h to remove carbonates. Thereafter, filters were transferred into tin capsules (IVA, Meerbusch, Germany) and analysed for POC and TPN by a FlashEA 1112 CHN-analyser (Thermo Finnigan). Analysis was done at a combustion temperature of 1000°C and a column temperature of 35°C. Concentrations were calculated by an external calibration curve with Methionin (0.1-2.5 mg).

Chlorophyll-a and Phaeopigments: Subsamples of 500 ml were filtered onto GF/F filters (Whatman, 47 mm diameter), immediately wrapped into aluminum foil and kept frozen at -20°C until further analysis in the shaded lab within one week. Filters were mechanically hackled and extracted in hot ethanol (75°C) for 1 h in the dark. Concentrations of chlorophyll-*a* and phaeopigments were determined spectrophotometrically and calculated following the procedure described by von Tümpling and Friedrich (1999). Chlorophyll$_{total}$ was calculated as the sum of chlorophyll-*a* and phaeopigments.

Dissolved organic carbon: The measurements of dissolved organic carbon (DOC) were performed on GF/F-filtrates by combustion and IR-detection with a multi N/C 3000 analyser (Analytik Jena). The filtrate was stored in brown glass bottles and acidified with semi-concentrated HCl (500 µl per 100 ml). The analysis was checked by measurements of K-hydrogenphthalate solutions containing 2 and 3 mg l^{-1} C (precision 4.6%; accuracy -0.4%).

Sedimentology

Documentation of aggregate abundance and size: Photos were taken with an *in situ* camera device. Samples were illuminated by a red light diode laser (λ=658 nm, 50 mW), and the abundance and size distribution of the aggregates were documented by digital photography using a Sony Cybershot DSC-F828. The resolution of the DSC-F828 is 15 µm per pixel. Further data processing and image analysis was done in the lab using the software package analySIS V

3.0 (Soft Imaging System, Münster, Germany). We determined abundance, size distribution, equivalent circular diameter (ECD), and surface area of the aggregates. For further details of data analysis see Lunau et al. (2004).

Suspended particulate matter (SPM): Subsamples of 500-1000 ml were filtered onto precombusted (2 h, 450°C) and preweighed GF/F filters (Whatman, 47 mm diameter). Filters were rinsed with 10-20 ml of distilled water to remove salt and kept frozen at -20°C until further analysis in the lab within one week. After drying for 12 h at 60°C, filters were adapted to room temperature for 30 min and weighed again. SPM was calculated as the difference between filter weight before and after sample filtration and normalised per liter.

Microbiology

Bacterial cell counts: Subsamples were transferred into 5 ml cryotubes (Nunc) onboard ship, preserved with 2% (final concentration) glutardialdehyde (resp. 1%/0.05% PFA/GDA mixture in April 2005) and stored at -20°C until further processing. Abundances of total and free-living bacteria (FL) were enumerated by epifluorescence microscopy after staining with SybrGreen I, applying a new detachment procedure. In brief: for the determination of the free living bacteria cells were washed with 3-5 ml of a TAE-methanol mix (1:1, pH 7.4) before the filters were transferred to a microscope slide and stained by SybrGreen I mixed into the mounting solution (1:40) containing moviol 4-88 (polyvinylalcohol 4-88). For the determination of total bacteria samples were treated with 10-30% methanol (35°C) and ultrasonicated before centrifugation. The number of aggregate-associated bacteria (AGG) was calculated as the difference of total bacteria and FL bacteria. This procedure is particularly suitable for samples with high loads of SPM and results in a very efficient detachment of AGG bacteria, yielding reliable numbers of the latter with a standard error of <15%. For further details of the method see Lunau et al. (2006b).

Stained cells were counted with a Zeiss Axiolab 2 microscope at 1,000x magnification by using a 100x Plan-Apochromat oil-immersion objective (lamp: HBO 50, filter set: Zeiss, Ex 450-490, FT 510, LP 515). The filtered sample volume yielded 60-150 stained cells in the counting grid. For each sample ten grids and a minimum of 600 cells per filter were enumerated.

CTD

CTD data were determined with a CTD probing system (Model OTS 1500, ME Meerestechnik-Elektronik, Germany) equipped with sensors for measuring pressure, conductivity and temperature. Salinity and density were calculated according to UNESCO standards (UNESCO 1981).

Results

Biological properties

The data presented in Table 1 provide an overview about several biological parameters in surface samples from the Wadden Sea cruises in 2005. These data were obtained from surface samples. Concentrations of chlorophyll-*a* increase roughly by a factor of two from January to April and July and decrease again towards November. This finding is consistent with the occurrence of spring and summer algae blooms, whereas the generally less pronounced autumn bloom is not covered by our cruises. The percentage of phaeopigments from total chlorophyll designates the quality of the algae material and provides information about the state of the bloom. The percentage shows highest values during January and November when resuspension of formerly deposited algal detritus is highest. In contrast April and July values are distinctly lower as both cruises cover algae blooms and indicate fresh algal material. However, the percentage of July is higher when compared with April, which may be indicative for a final stage of the bloom. A further difference during the algae blooms in April and July 2005 is seen in DOC data, which are higher in July due to release of organic compounds during the breakdown of the bloom (Tab. 1). The occurrence of algae blooms also leads to elevated organic matter contents of particles as seen in POC values during April and July.

Additionally, Table 1 presents the number of free-living bacteria (FL) and aggregate-associated bacteria (AGG) in surface water of the Wadden Sea for the cruises in 2005. Interestingly, the number of FL and AGG bacteria is comparable in January and April, which may be due to pronounced resuspension in January. In contrast, the number of FL and AGG bacteria is distinctly higher in July when compared with the previous cruises, which implies elevated microbial activity in the water column during summer. Unusually high numbers are seen in November, which is most likely caused by remnants of prior blooms and resuspension.

Tab. 1: Average surface values and ranges (in parentheses) of several biological, meteorological, and sedimentological parameters for the Wadden Sea of Spiekeroog Island (tidal inlet OB1 and central backbarrier area CBA).

	Wadden Sea January 2005	Wadden Sea April 2005	Wadden Sea July 2005	Wadden Sea November 2005
Chlorophyll-a [µg l^{-1}]	2.3 (1.2-3.3)	4.8 (3.2-6.4)	5.0 (3.1-6.7)	2.2 (0.6-3.2)
Phaeopigments [µg l^{-1}]	6.0 (2.9-9.6)	1.6 (0.6-2.0)	3.1 (0.3-5.12)	5.8 (1.7-8.8)
Phaeopigments / Chlorophyll$_{total}$ [%]	64	25	38	73
DOC [mM]	0.20 (0.17-0.24)	0.19 (0.15-0.24)	0.25 (0.2-0.32)	0.28 (0.22-0.44)
POC [%]	3.4 (2.5-5.0)	7.1 (2.9-16.3)	7.6 (1.1-28.7)	2.4 (0.5-4.5)
free-living bacteria (FL) [cells x10^6 ml^{-1}]	1.1 (0.6-1.4)	0.7 (0.4-1.2)	1.7 (1.0-2.3)	1.6 (1.4-1.8)
aggregate-associated bacteria (AGG) [cells x10^6 ml^{-1}]	0.7 (0.2-1.0)	0.7 (0.2-1.9)	1.3 (0.3-3.2)	1.6 (1.1-2.2)
av. wind speed [m s^{-1}]	11.2	3.7	12.5	4.6
av. wind direction [°]	230	171	265	216
SPM [mg l^{-1}]	72 (29-128)	8 (2-18)	22 (6-66)	52 (21-95)
aggregate number (AGA) [ml^{-1}]	500 (60-2400)[*]	-	280 (110-420)	-
aggregate size (ECD) [µm]	88 (64-110)[*]	-	118 (91-139)	-

[*] Data from 2003 (Lunau et al., 2006)

Sedimentological properties

Average surface values of SPM concentrations for the cruises in 2005 are given in Table 1. Generally, maximum SPM concentrations coincide with maximum current velocities, particularly in surface samples. In addition, wind speed and direction are important factors controlling the SPM load of the water column. Similar values for both parameters are seen during the cruises in January and July 2005. Highest concentrations of SPM are observed in January while in April data are considerably lower and amount to only 10 to 20% of the winter values. From July towards November SPM values increase again. Distinctive features in July 2005 are differences for the three sampling depths, which are less pronounced in January 2005 (Fig. 2). Especially the SPM concentrations of the bottom samples are remarkably high when compared with the surface values. In addition, the difference between both locations in the tidal inlet (OB1) and the central part of the tidal basin (CBA) is more pronounced in July 2005.

Furthermore aggregate properties differ between winter and summer times (Tab. 1). Even if we cannot provide data for the winter of 2005, a statistical comparison of February 2003 (Lunau et al, 2006a) with July 2005 (this study) showed significant differences in aggregate numbers (Mann-Whitney-Test, P=0.026) and size (t-Test, P=0.002). Mean aggregate abundance over a tidal cycle was almost twice as high in February compared to July (500 ml^{-1} vs. 280 ml^{-1}), while aggregate size revealed distinctly higher values during the growing season (ECD: 118µm in July vs. 88µm in February).
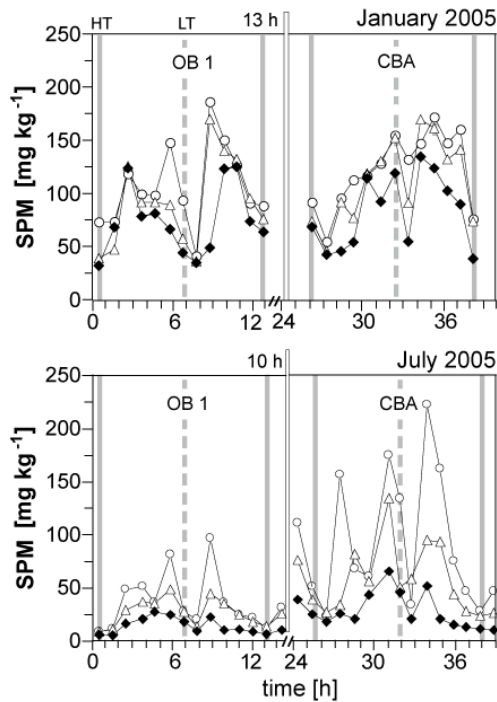
Fig. 2: Tidal patterns of suspended particulate matter (SPM) for the Wadden Sea cruises in January and July 2005 (Spiekeroog Island). The vertical grey and dashed lines denote high tide (HT) and low tide (LT). The vertical rectangle marks a time gap between the sampling campaigns. Please note that wind speed and direction are comparable during both cruises (Tab. 1).

Mo and Mn in the water column of the Wadden Sea

Molybdenum: Table 2 presents concentrations of dissolved Mo (Mo_{diss}) in the backbarrier tidal flat of Spiekeroog Island (tidal inlet Otzumer Balje OB1; central backbarrier area CBA) for the cruises in January, April, July, and November 2005. Values of Mo_{diss} normalised to a salinity of 33.7 (offshore value from October 2004) are shown as well. During the cruises in January, April, and November salinity normalised Mo_{diss} shows the expected conservative behaviour. Values are essentially identical to the offshore concentration, which was determined on samples from a cruise in October 2004 (54°30, 7°20 to 54°20, 7°23) during a period of low biological activity. Previous Wadden Sea cruises in winter, spring, and autumn 2002 to 2004 confirm this conservative behaviour (not shown) with normalised values similar or slightly above the offshore value.

Non-conservative behaviour of Mo_{diss} was observed in July 2005 with values distinctly below the seawater level. Based on almost identical salinities during that time interval (Tab. 2), a noticeable influence of fresh water via the flood-gate in Neuharlingersiel can be excluded (compare Fig. 1b). The tidal pattern of Mo_{diss} in July 2005 is visualised in Figure 3a. As salinity variations were comparatively small and close to the offshore value during these cruises, we present only absolute concentrations in Figure 3. At the beginning of the cruise in July 2005 Mo_{diss} displays a value of 82 nM and within the following 36 hours its concentration decreases

107

dramatically to a minimum value of 30 nM, which is less than one third of the seawater value. This rapid loss in Mo_{diss} is seen in the entire water column as indicated by the similar patterns of the three depth intervals investigated (surface, middle app. 7 m above seafloor, and bottom app. 1.5 m above seafloor) and seems to be independent of the tidal exchange, i.e., input of Mo-rich seawater during high tide. Furthermore, this phenomenon spans the whole tidal basin because data from both, the tidal inlet (OB1) and the central part of the backbarrier tidal flat (CBA) show the same trend of decreasing Mo_{diss} concentrations. The rate of Mo_{diss} loss is about 2 nM h^{-1} at location OB1 and 1.5 nM h^{-1} at CBA, with a more pronounced linearity of Mo loss in the tidal inlet (OB1: r=0.89; CBA: r=0.69).

Tab. 2: Average surface values and ranges (in parentheses) of water temperature, salinity as well as dissolved and particulate geochemical parameters for the Wadden Sea (tidal inlet OB1 and central backbarrier area CBA) and the German Bight. $Mo_{diss,33.7psu}$ indicates values normalized to offshore salinity.

	Wadden Sea January 2005	Wadden Sea April 2005	Wadden Sea July 2005	Wadden Sea November 2005	German Bight offshore October 2004
temperature [°C]	7.1 (6.5-7.4)	10.1 (8.8-12.2)	19.3 (18.6-20.1)	8.9 (7.4-9.8)	15.7 (15.6-15.8)
salinity [psu]	31.1 (29.7-32.0)	32.4 (32.1-32.6)	31.9 (31.5-32.1)	29.9 (29.3-30.3)	33.7 (33.6-33.8)
Mo_{diss} [nM]	95 (90-101)	99 (95-101)	57 (30-82)	91 (87-94)	103 (100-105)
$Mo_{diss, 33.7 psu}$ [nM]	103 (98-107)	102 (97-105)	60 (32-86-30)	103 (98-108)	
Mo_{part} [mg kg^{-1}]	1.3 (1.1-1.5)	2.0 (1.2-3.6)	15.3 (3.8-39.6)	3.3 (1.9-4.2)	2.0 (0.7-3.2)
Mn_{diss} [nM]	48 (20-113)	331 (121-679)	135 (51-256)	65 (36-125)	12 (9-20)
Mn_{part} [mg kg^{-1}]	714 (653-754)	461 (178-703)	1205 (803-1636)	875 (678-1045)	1020 (996-1039)
Al_{part} [%]	5.7 (5.4-6.1)	4.1 (1.8-5.8)	5.3 (4.5-5.9)	5.8 (5.0-6.4)	4.1 (3.8-4.6)

The decreases in Mo_{diss} were also observed in July 2005 during parallel sampling at position OB2 off Spiekeroog Island at the 10 m depth line and in the western backbarrier tidal flat of Langeoog Island (AE) where sampling started about 14 hours prior to the campaign at Spiekeroog Island (compare Fig. 1b). The concentration of Mo_{diss} at position OB2 and AE (not shown) decrease from 93 nM to 74 nM and from 70 to 47 nM, respectively.

Additionally, a transect from Langeoog Island towards Helgoland Island was carried out about 2 hours before sampling at location CBA in the backbarrier tidal flat of Spiekeroog (Figs. 1a [black squares] and 4a). Measurements of Mo_{diss} reveal that the non-conservative behaviour of Mo in the Wadden Sea is seen further offshore, too. Thus, the "normal" seawater concentration of Mo is only observed at a distance of more than 25 km offshore the barrier islands, reflecting that this phenomenon of drastically decreasing Mo_{diss} concentrations covers the entire Wadden Sea system and parts of the Southern German Bight.

Subsequent sampling campaigns in the tidal inlet of Spiekeroog at position OB1 show that the concentrations of Mo_{diss} are still below 66 nM in mid-August (Fig. 4b). In mid-September

a level close to the seawater value is attained, which suggests that Mo_{diss} depletion lasts at minimum of one month. During mid-October Mo_{diss} increases further and exceeds the seawater level with an average value of 112 nM and 124 nM when normalised to offshore salinity, respectively. In contrast, the sampling campaign in November 2005 again reveals a seawater-like level of 91 nM, which is identical with the German Bight value when normalised to salinity (Fig. 3d, Tab. 2).

Comparison with previous summer cruises from August 2002 to 2004 provides evidence about this variable behaviour of Mo in the Wadden Sea water column (Figs. 3 b-d). While the data from July 2005 reveal a negative anomaly of Mo_{diss}, the cruise in August 2002 is characterised by a distinct positive anomaly with maximum concentrations (158 nM) at low tide. In contrast to this, data from August 2003 and 2004 reveal an almost conservative pattern with concentrations close to the seawater value.

Regarding the values of particulate Mo (Mo_{part}) during the cruises in 2005 (Tab. 2) it becomes evident that along with decreasing concentrations of Mo_{diss} substantial enrichments of Mo are seen on aggregates in summer when compared with the other seasons. In comparison to the geogenic background (Mo/Al: 0.15; Wedepohl, 2004) aggregates are enriched on average by a factor of 20. Despite of the general enrichment, Mo/Al-ratios in July 2005 (Fig. 3e) display a variable pattern with a certain trend to higher values during high tide and more pronounced enrichments in surface samples. The comparison to other summer cruises from 2002 to 2004 (Figs. 3 f-h) reveals that Mo enrichments on aggregates are only seen during phases of Mo_{diss} anomalies, i.e. during July 2005 and August 2002.

Certain Mo enrichments are also observed in samples of sediment traps (<63 μm) from Langeoog Island between March and November 2005 (Fig. 5). The pattern of Mo/Al-ratios reveals elevated values during July 2005, which coincides with the observed increase in Mo/Al-ratios on SPM from the water column of the Spiekeroog backbarrier tidal flat during that time (Fig. 3e).
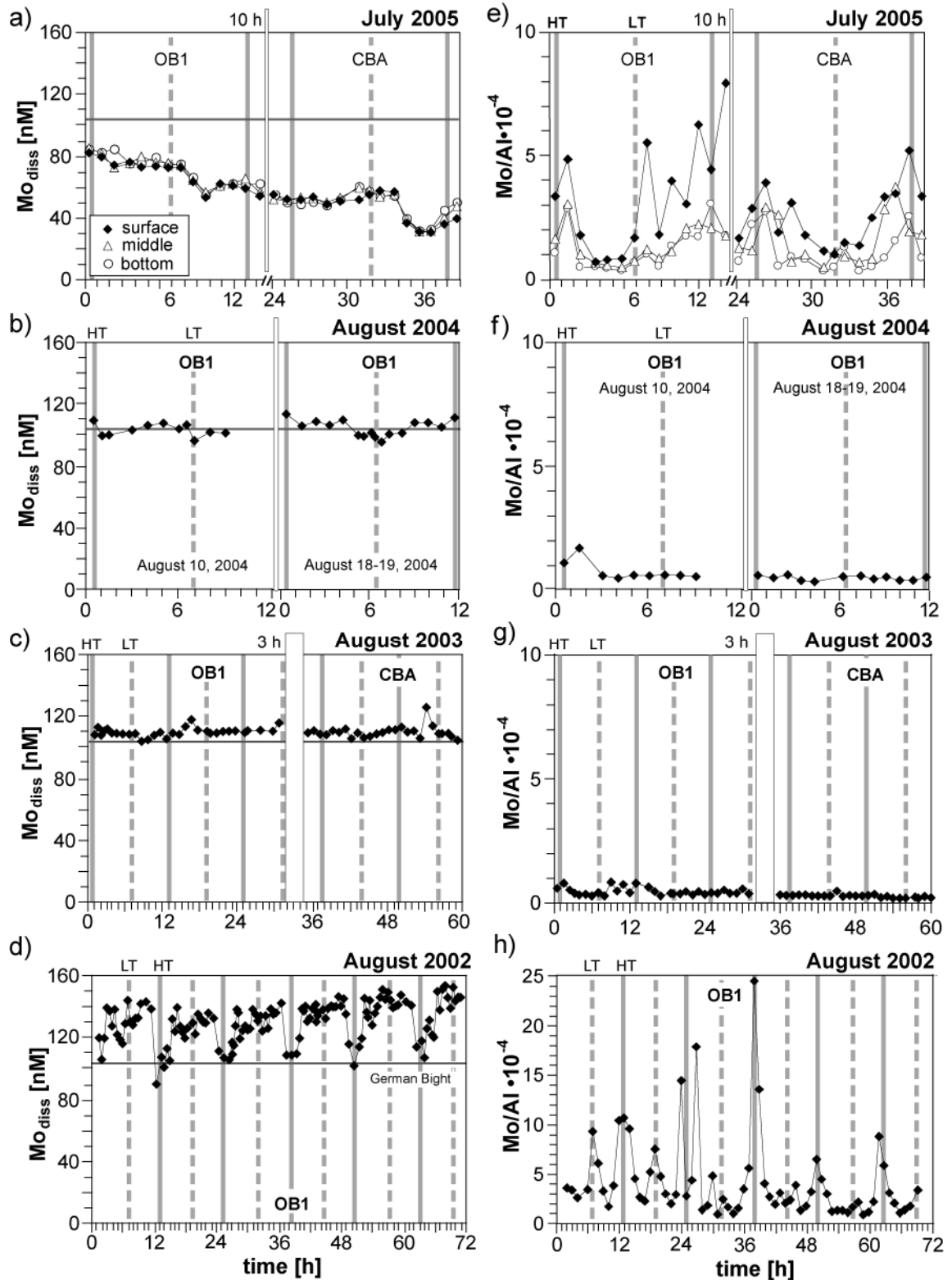
Fig. 3: Tidal patterns of dissolved Mo and Mo/Al ratios for the Wadden Sea cruises (Spiekeroog Island) from summer 2002 to 2005. The vertical grey and dashed lines denote high tide (HT) and low tide (LT). The vertical rectangle marks a time gap between both sampling campaigns. The gray line denotes the Mo level for the offshore German Bight (data from October 2004).

Manganese: The Wadden Sea cruise in July 2005 is not only special regarding Mo_{diss} but also with respect to Mn_{diss}. Earlier investigations on the behaviour of Mn in the Wadden Sea environment revealed a clear seasonal dependence with concentrations increasing by a factor of about 10 from winter towards summer (Dellwig et al., 2007) and vice versa. This behaviour was explained by elevated Mn concentrations in the pore fluids of the tidal flat sediments in summer due to more pronounced reducing conditions and therefore a higher release of Mn during ebb tide. Average concentrations of 700 nM were reported for Mn_{diss} in August 2002 and 2003 while values in winter (February 2002, 2003: 70 nM), spring (May 2002, April 2003: 300 nM), and autumn (November 2002, 2003: 80 nM) were distinctly lower. During the cruises in January and April 2005 Mn_{diss} follows this increasing trend (Figs. 6 a-d, Tab. 2). Based on the results of cruises in 2002 and 2003, Mn_{diss} should have been twice as high as the spring values in summer. However, a converse behaviour without any tidal dependence is observed in July 2005, with Mn_{diss} values distinctly lower than in spring.
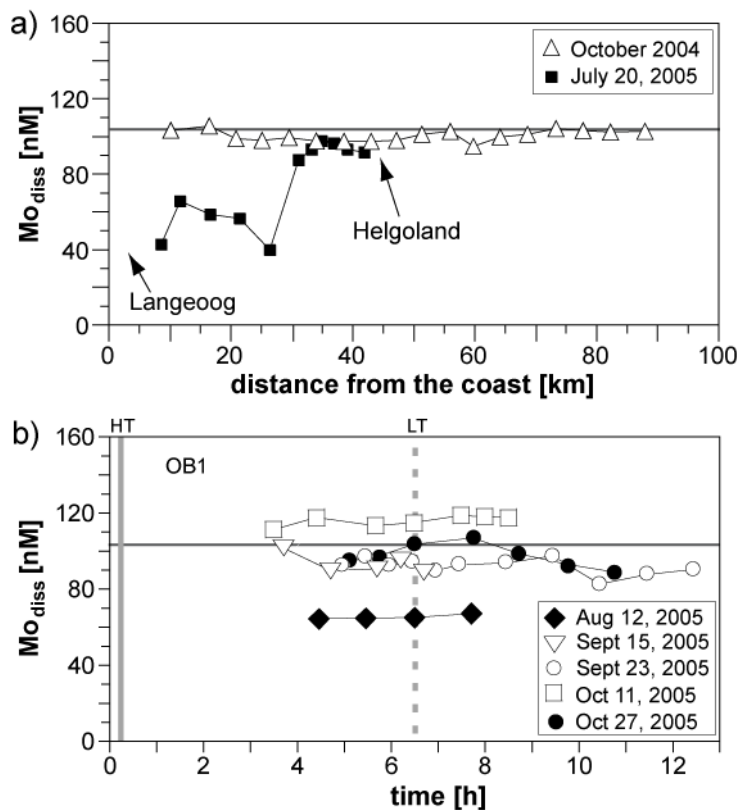
Fig. 4: Dissolved Mo of (a) transects from Langeoog Island into the German Bight, and (b) several sampling campaigns at position OB 1 in the tidal inlet of Spiekeroog Island. The grey line denotes the Mo level for the offshore German Bight (data from October 2004).

Ensuing sampling in the tidal inlet of Spiekeroog Island revealed that an increase in Mn_{diss} occurred somewhat later than it was observed for Mo_{diss} (Figs. 4b and 7). In the case of Mn_{diss} increasing values are not observed until the end of September. The average value of 300 nM on September 23 is similar to previous cruises in the Wadden Sea during September (av. 280 nM, Hinrichs, 2001). Concentrations of Mn_{diss} continue to increase until early October and reach a maximum value of 530 nM. Two weeks later, Mn_{diss} dropped to values between 140 to 278 nM, which reflects the general decrease towards the November level seen in Figure 6 d.
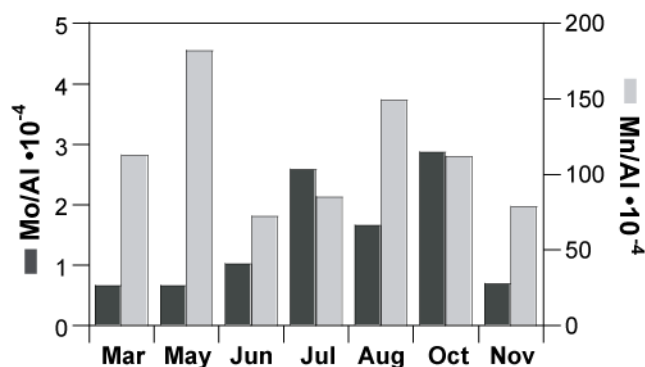
Fig. 5: Mo/Al and Mn/Al ratios of material (<63 µm) from sediment traps of the backbarrier salt marsh of Langeoog Island from March to November 2005.

In contrast, particulate Mn (Figs. 6e-h) shows the typical enrichments in summer when compared with the other seasons, as observed during earlier cruises as well (Dellwig et al., 2007). However, the pattern from July 2005 reveals a trend of decreasing Mn/Al-ratios parallel to increasing concentrations of Mn_{diss}.

Mo and Mn in the pore water of the Wadden Sea

Figure 8 shows pore water profiles of Mo_{diss} and Mn_{diss} for the sampling sites close to the low water line (location 1) and for the centre of the sand flat (location 2). At both sites (see Fig 1b), concentrations of Mo_{diss} reveal elevated levels in the uppermost portion of the sediment and a strong decline at a sediment depth of about 0.5 m. Especially at location 2 an increase in Mo_{diss} concentrations in the upper part of the sediment is observed from July to August. Maximum values reach 370 nM, which suggests pore waters as a significant Mo source during that time when compared with the concentration in the water column in August (av. 66 nM). Elevated values lasted until September, whereas in November the profile is similar to the one in July. In contrast, at location 1, which is close to the main tidal channel, Mo_{diss} shows a high variability but does not significantly exceed the seawater level.
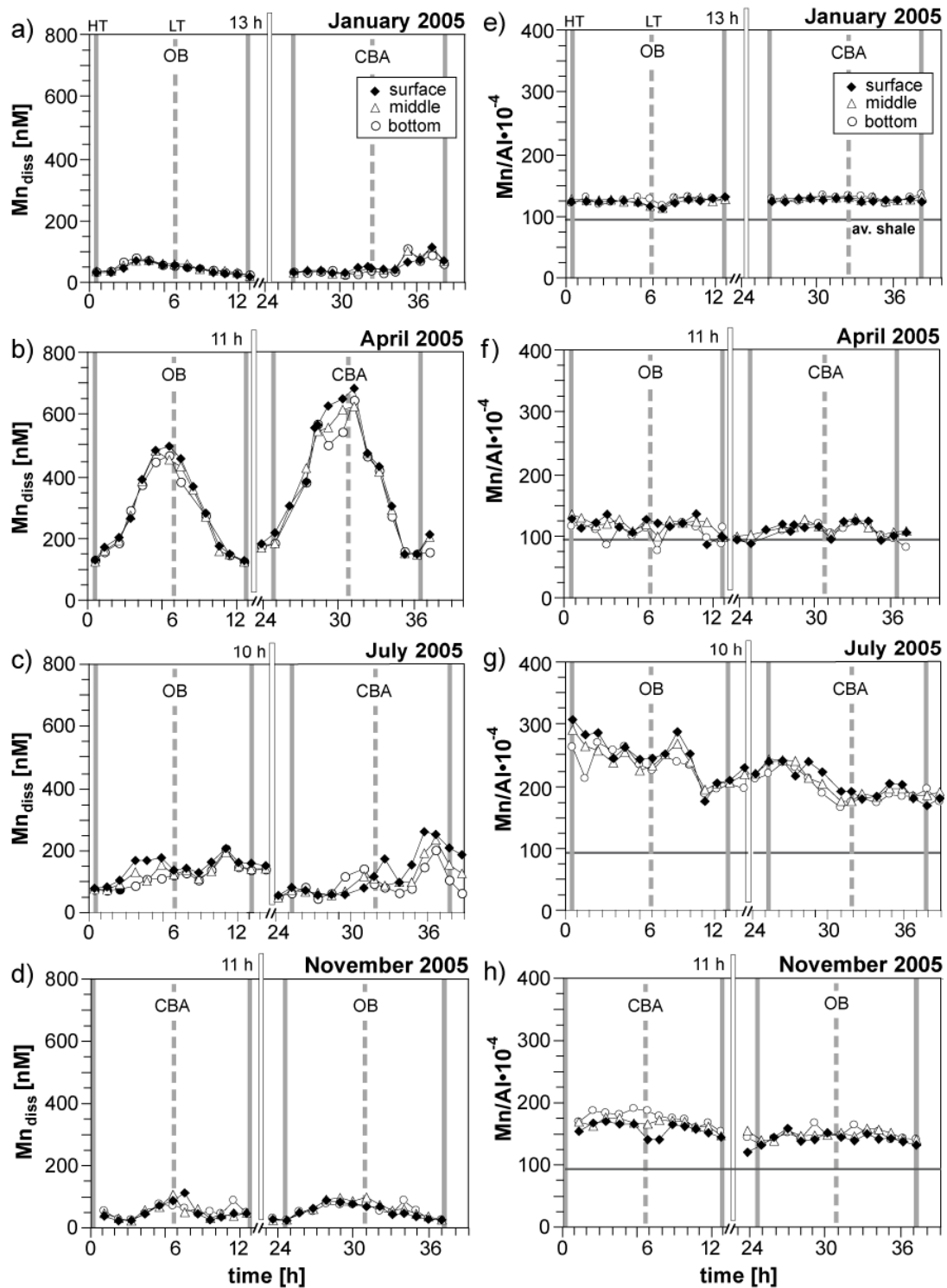
Fig. 6: Tidal patterns of dissolved Mn and Mn/Al ratios for the Wadden Sea cruises in 2005 (Spiekeroog Island). The vertical grey and dashed lines denote high tide (HT) and low tide (LT). The vertical rectangle marks a time gap between the sampling campaigns. The grey line denotes the average shale level (Wedepohl, 2004).
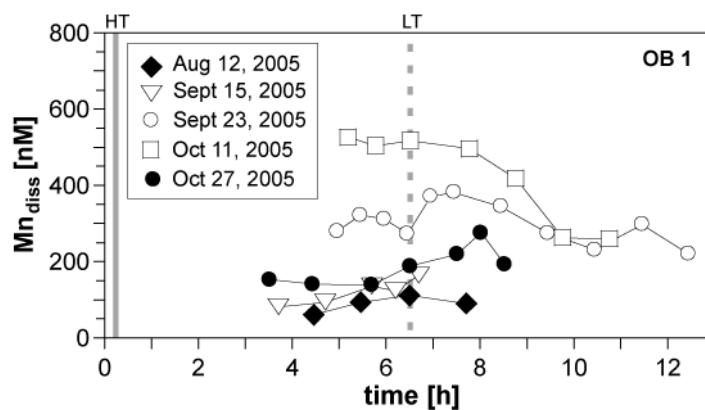
Fig. 7: Dissolved Mn from several sampling campaigns at position OB 1 in the tidal inlet of Spiekeroog Island during summer and autumn 2005. The vertical grey and dashed line denotes high tide (HT) and low tide (LT).

Pore water Mn_{diss} concentrations increase about 10-fold from 1,400 nM to a maximum concentration of 15,000 nM from July to August in the upper centimetres of the sediment at location 2. Extremely high values are also observed in September, especially at 0.3 m depth. Similar to Mo_{diss}, location 1 reveals less pronounced enrichments in Mn_{diss}. An exception forms the uppermost sample in September, when Mn_{diss} exceeds 15,000 nM. When comparing these results with the development of Mn_{diss} concentrations in the water column (Fig. 7) it seems evident that the pore waters represent a significant source for Mn_{diss} as well.

Discussion

Biological and sedimentological conditions

The results presented so far document non-conservative behaviour of Mo_{diss} in the Wadden Sea during specific time intervals in summer as reflected by both, negative but also positive concentration anomalies (Figs. 3a and d). In contrast, cruises in August 2003 and 2004 (Figs. 3b and c) displayed a more or less conservative pattern, which may reflect a transitional behaviour between extreme situations. Decreasing concentrations were also observed in the western backbarrier area of Langeoog Island (not shown) and in the adjoining near-coastal waters of the German Bight (Fig. 4a), which gives evidence that a larger area is affected by this phenomenon.
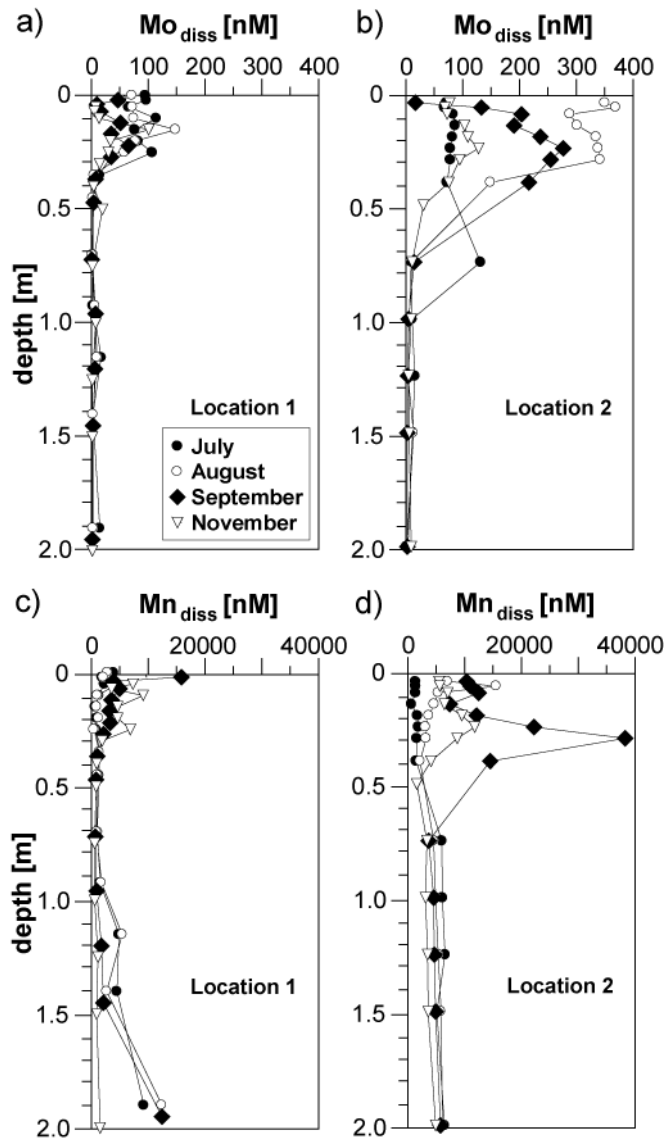
Fig. 8: Comparison of Mo and Mn pore water profiles between July and November 2005 from two locations at the Janssand tidal flat of the backbarrier area of Spiekeroog Island (compare Fig. 1 b).

Processes causing removal and at a later stage release of Mo_{diss} are necessary to explain such differing concentration signatures. For understanding the individual mechanisms causing such phenomena, it is essential to know about the distinctive characteristics of the individual summer cruises. For that reason, the first part of the discussion deals with the biological and sedimentological aspects, while in the following chapters we will discuss the processes of removal and release of Mo.

The chlorophyll-*a* concentrations (Tab. 1) point towards the occurrence of algae blooms during both cruises in April and July 2005. However, taking the percentage of phaeopigments from total chlorophyll into account, which is indicative for the quality of algae material, it becomes obvious that in July 2005 the algae bloom was in a later stage, most likely in a phase of breakdown. Consequently, the onset of lyses of algae may have led to a release of elevated

amounts of labile organic compounds. It is well known that such fresh and labile DOC is very rapidly degraded by bacteria (Coveney and Wetzel, 1989; Muenster, 1993). It also has the potential to form transparent exopolymer particles (TEP) from dissolved precursors. Thus we postulate, that the degradation of such algal material by free-living bacteria, which are twice as abundant in July as in April (Tab. 1), initiates the formation of larger aggregates in the Wadden Sea water column as recently observed by several authors (e.g. Engel et al., 2004; Chen et al., 2005; Lunau et al., 2006a; Passow and De la Rocha, 2006). A further indication of degradation and release of organic compounds is given by elevated DOC values in July when compared with the bloom in April (Tab. 1). Former cruises in August 2002 and 2003 showed lower DOC values as well (av. 0.21 mM; Dellwig et al., 2007) and shed light on the special situation during the cruise in July 2005.

Aggregation is documented by the comparison of ECD values between winter and summer (Tab. 1). Along with POC, our data suggest the occurrence of larger organic-rich aggregates in summer, whereas the winter situation is dominated by smaller inorganic particles. These larger aggregates offer favourable conditions for the formation of suboxic micro-zones, an assumption that is supported by investigations of Alldrege and Cohen (1987) and Ploug et al. (1997). The authors detected significant oxygen depletion in marine snow and laboratory-made aggregates by the use of microelectrodes. Additionally, Nielsen et al. (2005) found a distinctly higher potential for anammox inside larger aggregates when compared with smaller ones. For the formation of suboxic zones within the aggregates elevated microbial activity is necessary, a prerequisite, that is indicated by distinctly higher numbers of aggregate-associated bacteria in July 2005 (Tab. 1).

Aggregation during breakdown of algae blooms is of crucial importance for sedimentological and geochemical budgets of the Wadden Sea environment as the larger aggregates behave hydraulically different (Chang et al., 2006a and b). This change is seen in the varying SPM loads during the cruises in 2005 (Fig. 2), which are mainly attributed to three variables: (i) the tidal state, (ii) weather conditions, and (iii) hydrological properties of aggregates. The tidal influence can be regarded in a first approximation as constant as the cruises took place during similar tidal states (spring tide at the end of the campaign). The second parameter, i.e., wind speed and wind direction, is of major importance for the hydrodynamic conditions in the Wadden Sea. For that reason it is essential that weather

conditions are almost identical when comparing SPM concentrations of different cruises, which is only the case for January and July 2005 (Tab. 1). Nonetheless, surface SPM concentrations and the number of aggregates are considerably higher in January when compared with July, which has to be attributed to the different hydraulic properties of SPM in winter and summer (Tab. 1). To solve this discrepancy in SPM load between both cruises, huge amounts of larger aggregates have to be deposited on the tidal flats during summer. This assumption is in accordance with sedimentological investigations carried out in the backbarrier area of Spiekeroog Island by Chang et al. (2006a and b). The authors report that in summer, the surface sediment comprises a mud drape, whereas during winter the same tidal flats are dominated by sand. They also suggest that the finer particles deposited in summer are incorporated into larger flocs and aggregates and are therefore hydraulically similar to co-deposited sand.

Overall, from a biological and sedimentological view the distinctive feature in July is the breakdown of an algae bloom, which accelerated bacterial activity and growth. As a result organic matter is released by lyses and bacterial decomposition of algal material initiates the formation of larger aggregates. Huge amounts of these organic-rich aggregates are deposited on the tidal flats, thereby serving as a potential shuttle for the transfer of material and compounds from the open water column to the sediment layer. In contrast, earlier cruises in August 2002-2004 did not record this development at its initial stage. Thus, the question remains whether this special situation in July 2005 can be made responsible for the observed behaviour of Mo?

Removal of Mo from the water column

For the removal of Mo_{diss} from the water column several processes are conceivable, which comprise uptake by phytoplankton, fixation in reducing tidal flat sediments, scavenging by Mn-oxides, complexation by organic matter as well as processes in the suboxic interior of larger aggregates.

Although Mo forms an essential micro-nutrient for the nitrogen-metabolism of phytoplankton and bacteria (Howarth and Cole, 1985; Paerl et al., 1987), which can be enriched in marine cyanobacteria during nitrogen fixation (Tuit et al., 2004), culture experiments have shown that Mo uptake rates are too low (0.4 pM µg chl^{-1} h^{-1}; Marino et al., 2003) for explaining

the Mo_{diss} depletion rate of 2 nM h^{-1} observed in July 2005. A further possibility may be the fixation of Mo_{diss} as sulphide in reducing tidal flat sediments. Again, this possibility seems to be less plausible as such process cannot explain the observed rapid loss of more than 60% of Mo_{diss} from the water column within 36 hours. Moreover, Mo burial in sediments prevails during the entire summer when microbial activity is high and reducing conditions in the sediments are most pronounced. Even though the settling of aggregates transfers high amounts of organic matter to the sediment, which accelerates microbial activity, our pore water profiles do not proof elevated Mo fixation in July 2005 (Figs. 8 a and b).

One important mechanism may be the scavenging of Mo_{diss} by freshly formed MnO_x phases during bacterial oxidation of Mn_{diss}. Adelson et al. (2001) postulated a model for scavenging of Mo by MnO_x phases in order to explain Mo enrichments in sediments of Chesapeake Bay. Mn^{2+} refluxing from sediments is converted to particulate $Mn(Mo)O_x$ during oxidation in the upper water column. Sedimentation of these particles leads to preconcentration of Mo at the sediment-water interface. Mo is liberated during reduction of Mn-oxide phases at or close to the sediment surface from where it may diffuse downward until it is fixed by organic thiols or HS^-. Extremely low Mn_{diss} concentrations and associated enrichments in Mn_{part} in Wadden Sea samples from July 2005 (Figs. 6c and g) point towards intense oxidation of Mn^{2+}. Therefore, formation of $Mn(Mo)O_x$ phases might explain the depletion in Mo_{diss} (Fig. 3c) or vice versa the enrichment of Mo_{part} on SPM (Fig. 3e) observed in July 2005. Unfortunately, we do not know whether Mn-oxidising bacteria exhibit enhanced activity during an algae breakdown, which would be important information as Mn-oxidation forms a common process in the study area during summer (Dellwig et al., 2007). Comparing the Mn/Al-ratios of the summer aggregates (August 2002: 260; August 2003: 316; August 2004: 302; July 2005: 227) no unusual enrichments are observed for the cruises in July 2005 and August 2002. SPM from the latter cruises is even slightly depleted in Mn, which contradicts a relation between Mo_{diss} depletion and Mn oxidation. In addition, unusually low values of Mn_{diss} in July 2005 (Fig. 6c) are most likely not due to elevated bacterial Mn oxidation but rather caused by exhaustion of the sedimentary reservoir. A finding that is supported by low Mn_{diss} concentrations in pore waters especially at location 2 in July 2005 (Fig. 8d).

Moreover, the patterns of Mn_{diss} and Mn_{part} display an opposite trend in July 2005. While Mn_{diss} tends to increase, the contents of Mn_{part} decline, which points towards release of Mn from

SPM and argues against elevated Mn oxidation and associated Mo scavenging. The conversion of the contents of Mn_{part} into volume specific units reveals an average concentration of 272 nM, which is twice as high as the average concentration of Mn_{diss} (135 nM). Therefore, the gain in Mn_{diss} during the investigated time-period in July 2005 could be explained by release from SPM (Fig. 6c). However, release from the particulate phase would require suboxic zones in aggregates, which can be caused by an elevated number and activity of aggregate-associated bacteria, respectively (Tab. 1). A similar process was already postulated by Klinkhammer and McManus (2001). They explained mid-depth Mn maxima in the Columbia River estuary by reduction of Mn in the suboxic interior of aggregates. In addition, the authors point out the connection between Mn release and bacterial activity. Therefore, on the basis of our data, a relation between Mn-oxidation and Mo depletion can only hardly be deduced. Nevertheless, the possible adsorption of Mo on still existing MnO_x coatings on aggregates cannot be completely disregarded.
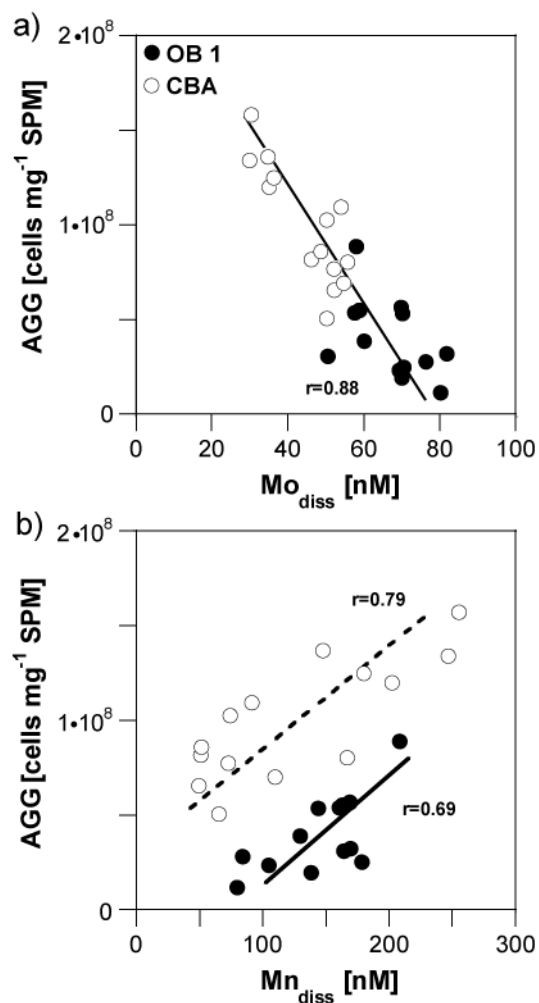
Fig. 9: Correlation diagrams of dissolved Mn and Mo versus aggregate-associated bacteria (normalized to SPM) for surface water samples from the backbarrier area of Spiekeroog Island in July 2005.

Despite the aforementioned reduction of MnO_x phases, oxygen-depleted micro-zones in aggregates may be the loci for Mo_{diss} reduction and removal from the water column as well. In view of the xy-plots shown in Figure 9 a relationship between bacterial abundance on aggregates and Mo_{diss} and Mn_{diss} concentrations becomes obvious. Thus, we postulate that increasing abundance and activity of bacteria on organic-rich aggregates produces oxygen-depleted micro-zones, which enable fixation of Mo and release of Mn from the aggregates. Unfortunately, our data do not provide information about the particular mechanism of Mo fixation. In addition to chemical processes, reduction by bacteria is also conceivable as shown by Ghani et al. (1993). The same is true for Mn, either bacteria may start to reduce Mn_{part} directly, or Mn may be reduced chemically in suboxic zones.

Besides this direct fixation of Mo in micro-zones, fresh algal organic matter and certain humic substances are also capable to capture MoO_4^{2-} from solution (Szilagyi, 1967; Bertine, 1972; Volkov and Formina, 1974; Nissenbaum and Swaine, 1976; Disnar, 1981; Brumsack and Gieskes, 1983; Alberic et al., 2000), particularly when the organic matter is sulphurised (Tribovillard et al., 2004). An increase in organic matter content of SPM is evident from POC data, which show elevated values in spring and especially during summer (max, 28.7%; Tab. 1). Additionally, Bertine (1972) report increased Mo scavenging and/or reduction of Mo by organic acids with decreasing pH. This should be the case in the suboxic interior of aggregates as shown by Alldrege and Cohen (1987) and Ploug et al. (1997).

Both processes, reduction in oxygen-depleted zones and scavenging by organic matter are strongly coupled to biological activity. The release/bacterial degradation of fresh algal organic matter especially during breakdown of blooms causes aggregation, and is therefore limited to a specific time interval. Only such processes are able to explain the abrupt decrease in Mo_{diss}, whereas the processes mentioned before are not limited to a certain time interval or event. For instance, fixation of Mo in sediments as well as scavenging of Mo by MnO_x should occur during the entire summer.

Fate of Mo on aggregates

As seen in Figures 3a and e, the rapid loss of Mo_{diss} in July 2005 corresponds with substantial enrichments of Mo_{part} on aggregates. However, it is of crucial importance whether the Mo enrichment on SPM is balanced by the loss in Mo_{diss}. This requires the direct

comparison of dissolved and particulate metal concentrations per volume unit. For that reason, we calculated excess element concentrations, which reflect the amount of Mo added to SPM in addition to the geogenic background. This excess fraction is calculated according to the following equations (average shale data from Wedepohl, 2004):

$$Mo_{background} = (Mo/Al)_{av.\ shale} \times Al_{sample}$$

$$Mo_{excess} = Mo_{sample} - Mo_{background}$$

The conversion of Mo_{excess} into volume specific Mo concentrations (Mo_{xs}) is done by multiplication with SPM concentrations. The resulting concentrations of Mo_{xs} indicate that the particulate phase, even though highly enriched in Mo, cannot explain the observed loss in Mo_{diss} in the water column. The average value of Mo_{xs} (2.5 nM) only explains 6% of the loss in Mo_{diss}. In our view, this discrepancy can only be explained by the rapid sedimentation of Mo-rich particles following particle aggregation during breakdown of an algae bloom (see Chapter 5.1.).

According to M. Beck (pers. comm.) deposited aggregates formed a widespread fluffy layer on the tidal flat sediments next to the pore water sampling site 2. Unfortunately, this fluffy material is not available for geochemical analyses. However, the geochemical composition of these aggregates is most likely reflected in sediment trap samples collected in the backbarrier salt marsh of Langeoog Island (Fig. 5). This material shows enrichments in Mo from summer to early autumn. Furthermore, the pattern of Mn is in accordance with an alternating dominance of Mn-oxidation and Mn-reduction. Mn-oxidation prevails in spring and late summer, whereas in June and July, when aggregation along with the development of suboxic micro-zones in aggregates becomes more important, decreasing values are due to intense Mn-reduction.

In our view it is rather likely that the deposition of such aggregates may explain the discrepancy in the balance between Mo_{diss} loss and the apparent lack of particulate Mo_{xs} to compensate for this loss. Thus, we propose that large amounts of Mo_{diss} are removed from the water column owing to deposition of Mo-rich and still Mn-rich aggregates during breakdown of an algae bloom in early summer. Additionally, with the transfer of Mo and Mn into the upper sediment layer by settling aggregates organic matter is added to the sediment, which favours microbial activity and therefore the decomposition of buried aggregates.

Fate of Mo in the sediments: Implications from the pore water

Aggregates formed in the open water column were deposited on the sand flat Janssand in July 2005 especially at location 2 (Fig. 1b), leading to the accumulation of a fine layer of Mo- and still Mn-rich particulate matter at the sediment surface. Although still under debate, adherence of deposited aggregates on the tidal flats may be favoured by release of extracellular polymeric substances (EPS) from benthic diatoms and cyanobacteria. As EPS compounds exhibit stickiness, they are presumably increasing the erosion threshold (Stal, 2003). This material is supposed to be subsequently incorporated into subsurface layers of the sediment. The transport of particulate matter into permeable sandy sediment by boundary flows, which interact with sea bed topography, for example sediment wave ripples, has often been described and modelled (de Beer et al., 2005; Huettel and Rusch, 2000; Rusch and Huettel, 2000; Precht and Huettel, 2003). While these aggregates are incorporated into the sediment, Mn and Mo are released once the aggregates experience reducing conditions in slightly deeper sections of the sediment (Duinker et al., 1974; Burdige, 1993). Stabilisation of Mo in the pore water is probably assured by complexation with dissolved organic matter (Brumsack and Gieskes, 1983). The microbially induced release of both metals, which is caused by decomposition of organic aggregates, explains the observed increases in Mo_{diss} and Mn_{diss} in the pore water at location 2 from July to September 2005 (Figs. 8 b and d) reasonably well.

Due to tidal dynamics, exchange processes occur between the surface sediment pore waters and the open water column (Huettel et al., 1998). This process contributes Mo_{diss} and Mn_{diss} to the water column as seen in increasing concentrations in August and September 2005 (Figs. 4b and 7). The same phenomenon of Mo_{diss} release from pore water may explain the positive anomaly in Mo_{diss} at low tide observed in August 2002 (Fig. 5a). The hypothesis of Mo release from pore water is supported by observations of Dalai et al. (2005) who explained excess concentrations of Mo at salinity >5 in the Chao Phraya Estuary by release from pore waters and changing redox conditions. Furthermore, experiments with *in situ* benthic flux chambers carried out by Morford et al. (2007) revealed substantial release of Mo from Boston Harbor sediments.

In the case of Mn, settling of Mn-rich aggregates forms an important process for the Mn budget of the Wadden Sea environment. The comparison of Mn_{diss} between July 2005 and April 2005 (Tab. 2) reveals an unusually low level during the summer cruise. In addition to intense

Mn-oxidation in the water column, this observation seems to be caused to a certain degree by exhaustion of the tidal flat sediments of reactive Mn. This assumption is in accordance with the findings of Dellwig et al. (2007) who showed that during spring and especially summer, the Mn budget of the Wadden Sea water column is almost completely controlled by release from pore waters. Therefore, deposition of aggregates and concomitant Mn reduction form a recharge mechanism explaining the increasing Mn_{diss} values observed in September and early October 2005 (Fig. 7).

Summary and concluding remarks

Non-conservative behaviour of dissolved Mo was observed in the Wadden Sea of NW Germany, i.e., negative but also positive anomalies. In the backbarrier tidal flat of Spiekeroog Island concentrations of dissolved Mo declined from a seawater-like level to a minimum value of 30 nM within 36 hours during July 2005. This phenomenon was also observed in the adjoining backbarrier tidal flat of Langeoog Island and in near-coastal water masses about 25 km offshore. Further measurements provide evidence that this depletion, which is accompanied by significant Mo enrichments on SPM, lasted for at minimum four weeks. In contrast, elevated Mo_{diss} values (maximum 158 nM) were observed in August 2002. During this period Mo_{diss} displayed a tidal cyclicity with maximum concentrations during low tide, which points towards the tidal flat sediments as the dominant source.

This non-conservative behaviour of Mo can only be explained by the tight coupling of biological, sedimentological, and geochemical processes, as summarised in the sketch shown in Figure 10. The controlling forces are algae blooms and the associated growth of bacteria. While the algae spring bloom does not influence the total number of bacteria, this does not seem to be the case for the algae bloom in summer, when bacterial activity and number increased significantly. Bacterial decomposition of algae releases organic compounds, which promote aggregation of suspended mineral particles. MoO_4^{2-} seems to be reduced in oxygen-depleted zones of larger aggregates and/or is "scavenged" by freshly formed organic matter resulting in prominent Mo_{part} enrichment. A relation between the depletion of Mo and the formation of MnO_x phases is not indicated by our data.

Mn_{diss} concentrations are unusually low during this specific time period, which is either caused by exhaustion of the tidal flat sedimentary pool in reactive Mn or Mn-oxidation in the

water column, which also diminishes the concentration in Mn_{diss} and leads to Mn enrichments on aggregates.

Huge amounts of larger aggregates and associated Mo and Mn are deposited on the tidal flats, leading to a depletion of these elements in the water column. Microbial decomposition of shallowly buried aggregates leads to release of Mo and Mn from the sediments and replenishes the trace metal pool in the water column, as seen in increasing trace metal concentrations in the pore water pool in late summer as well as subsequently in the water column.

In addition to the transfer of trace metals into the sediments via deposition of aggregates, this process also leads to a sudden deposition of huge amounts of organic matter, which enhances microbial activity in the sediments.
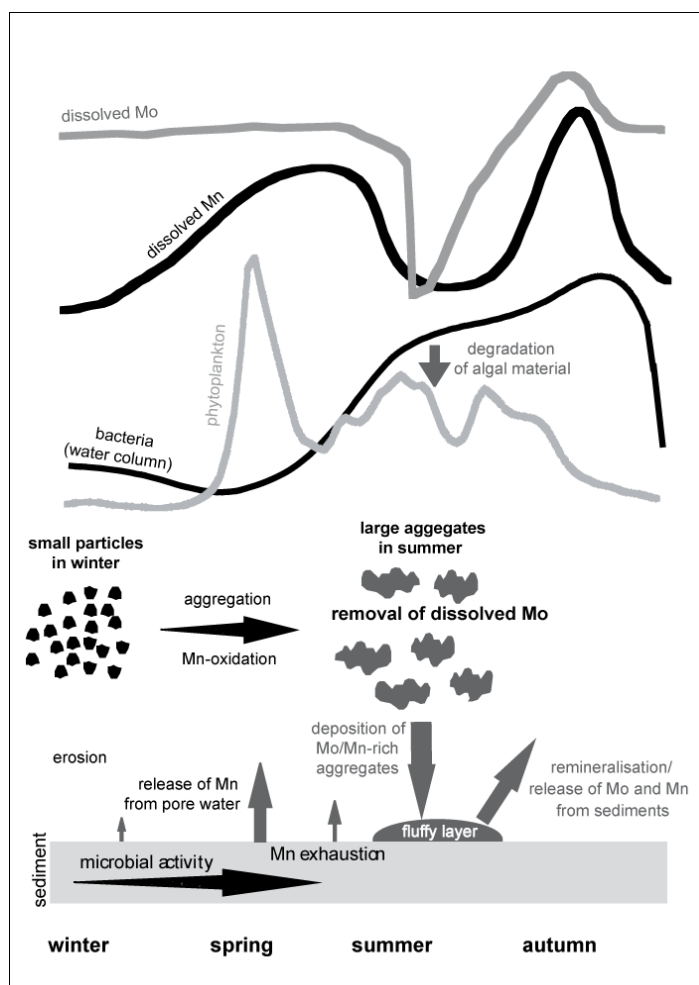
Fig. 10: Illustration of the postulated model for non-conservative be-haviour of Mo in coastal waters, which is based on the tight coupling between geochemical, biolo-gical, and sedimento-logical processes. Phytoplankton pattern bases on model results by Kohlmeier (2004).

The postulated coupling of biological, sedimentological, and geochemical processes may also be of significant relevance for Mo and possibly other trace metal enrichments in TOC-rich marine deposits. Thus, the transfer of Mo to the sediments via settling aggregates will concentrate Mo at the sediment/water interface from where it may diffuse into the deeper anoxic zone where it may finally be fixed as a sulphide.

Acknowledgements

References

Adelson, J. M., Helz, G. R., Miller, C. V., 2001. Reconstructing the rise of recent coastal anoxia; molybdenum in Chesapeake Bay sediments. *Geochim. Cosmochim. Acta* 65(2), 237-252.

Alberic, P., Viollier, E., Jezequel, D., Grosbois, C., Michard, G., 2000. Interactions between trace elements and dissolved organic matter in the stagnant anoxic deep layer of a meromictic lake. *Limnol. Oceanogr.* 45(5), 1088-1096.

Alldrege, A. L., Cohen, Y., 1987 Can microscale chemical patches persist in the sea? Microelectrode study of marine snow, Fecal pellets. *Science*, 235, 689-691.

Beck, M., Dellwig, O., Kolditz, K., M., Liebezeit, G., Brumsack, H.-J., 2007 In situ pore water sampling in deep intertidal flat sediments. *Limnol. Oceanogr.: Methods.* accepted

Berrang, P. G., Grill, E. V., 1974. The Effect of Manganese Oxide scavenging on Molybdenum in Saanich Inlet, British Columbia. *Mar. Chem.* 2, 125-148.

Bertine, K. K., 1972. The Deposition of Molybdenum in anoxic Waters. *Mar. Chem.* 1, 43-53.

Brumsack, H. J., Gieskes, J. M., 1983. Interstitial Water Trace-Metal Chemistry of Laminated Sediments from the Gulf of California, Mexico. *Mar. Chem.* 14(1), 89-106.

Brumsack, H.-J., 2006. Trace metal content of recent organic carbon-rich sediments: Implications for Cretaceous black shale formation. *Palaeogr., Palaeoclim., Palaeoecol.* 232, 344-361.

Burdige, D. J., 1993. The Biogeochemistry of Manganese and Iron Reduction in Marine-Sediments. *Earth-Science Rev.* 35(3), 249-284.

Chang, T. S., Bartholomä, A., Flemming, B. W., 2006a. Seasonal dynamics of fine-grained sediments in a back-barrier tidal basin of the German Wadden Sea (Southern North Sea). *J. Coast. Res.* 22(2), 328-338.

Chang, T. S., Jördel, O., Flemming, B. Bartholomä, A., 2006b. The role of particle aggregation/disaggregation in muddy sediment dynamics and seasonal sediment turnover in a back-barrier tidal basin, East Frisian Wadden Sea, southern North Sea. *Mar. Geol.* 235, 49-61.

Chen, M. S., Wartel, S., Temmerman, S., 2005. Seasonal variation of floc characteristics on tidal flats, the Scheldt estuary. *Hydrobiol.* 540, 181-195.

Collier, R. W., 1985. Molybdenum in the Northeast Pacific-Ocean. *Limnol. Oceanogr.* 30(6), 1351-1354.

Coveney, M. F., Wetzel, R. G., 1989. Bacterial metabolism of algal extracelluar carbon. *Hydrobiologia* 173**:** 141-149.

de Beer, D., Wenzhöfer, F., Ferdelman, T. G., Boehme, S. E., Huettel, M., van Beusekom, J. E. E., Böttcher, M. E., Musat, N., Dubilier, N., 2005. Transport and mineralization rates in North Sea sandy intertidal sediments, Sylt-Romo Basin, Wadden Sea. *Limnol. Oceanogr.* 50(1), 113-127.

Dalai, T. K., Nishimura, K., Nozaki, Y., 2005. "Geochemistry of molybdenum in the Chao Phraya River estuary, Thailand: Role of suboxic diagenesis and porewater transport." *Chemical Geology* 218(3-4): 189-202.

Delafontaine, M.T., Flemming, B.W., Thimm, M., 2004. Large-scale trends in some mass physical properties of Danish Wadden Sea sediments, and implications for organism-sediment interactions. *Danish J. Geogr.* 104, 27-36.

Dellwig, O., Hinrichs, J., Hild, A., Brumsack, H. J., 2000, Changing sedimentation in tidal flat sediments of the southern North Sea from the Holocene to the present: a geochemical approach. *J. Sea Res.* 44(3-4), 195-208.

Dellwig, O., Bosselmann, K., Kölsch, S., Hentscher, M., Hinrichs, J., Böttche,r M.E., Reuter, R., Brumsack, H.-J., 2007. Sources and fate of manganese in a tidal basin of the German Wadden Sea. *J. Sea Res.* 57, 1-18.

Disnar, J.-R., 1981. Etude expérimentale de la fixation de métaux par un matériau sédimentaire actuel d`origine algaire- II. Fixation "in vitro" de UO_3^-, Cu^{2+}, Ni^{2+}, Zn^{2+}, Pb^{2+}, Co^{2+}, Mn^{2+}, ainsi quede VO_3^-, MoO_4^{2-} et GeO_3^{3-}. *Geochim. Cosmochim. Acta* 10, 2152-2161.

Duinker, J. C., van Eck, G. T., M., Nolting, R. F., 1974. On the behaviour of copper, zinc, iron and manganese, and evidence for mobilization processes in the Dutch Wadden Sea. *Netherlands J. Sea Res.* 8(2-3), 214-239.

Engel, A., Thoms, S., Riebesell, U., Rochelle-Newall, E., Zondervan, I., 2004. Polysaccharide aggregation as a potential sink of marine dissolved organic carbon. *Nature* 428(6986), 929-932.

Flemming, B.W., Delafontaine, M.T., 2000. Mass physical properties of intertidal muddy sediments: some applications, misapplications, and non-applications. *Cont. Shelf Res.* 20, 1179-1197.

Fogg, G.E., Wolfe, M., 1954. Nitrogen metabolization of blue-green algae. *Symp. Soc. Gen. Microbiol.* 4: 99-125.

Fogg, G.E., 1962. Extracellular products. In: Baldwin, R.A. (Ed.) *Physiology and biogeochemistry of algae.* Academic Press Inc., New York, pp. 475-489.

Ghani, B., Masataka, T., Hisham, N. Z., Kishimoto, N., Ismail, A. K. M., Tano, T., Sugio, T., 1993. Isolation and characterization of a Mo6+-reducing bacterium. *App. Environ. Microbiol.* 59(4), 1176-1180.

Head, P. C., Burton, J. D., 1970. Molybdenum in some ocean and estuarine waters. *J. Mar. Biol. Assoc. U.K.* 50, 439-448.

Heinrichs, H., Brumsack, H.-J., Loftfield, N., König, N., 1986. Verbessertes Druckaufschlußsystem für biologische und anorganische Materialien. *Z. Pflanzenernährung Bodenkunde* 149, 350-353.

Hinrichs, J., 2001. Geochemical tracers in the deep-sea and the North Sea. Ph D Thesis. University of Oldenburg.

Howarth, R. W., Cole, J. J., 1985. Molybdenum Availability, Nitrogen Limitation, and Phytoplankton Growth in Natural-Waters. *Science* 229(4714), 653-655.

Huettel, M., Ziebis, W., Forster, S., Luther, G. W., III., 1998. Advective transport affecting metal and nutrient distributions and interfacial fluxes in permeable sediments. *Geochim. Cosmochim. Acta* 62(4), 613-631.

Huettel, M., Rusch, A., 2000. Transport and degradation of phytoplankton in permeable sediment. *Limnol. Oceanogr.* 45(3), 534-549.

Klinkhammer, G.P., McManus, J., 2001. Dissolved manganese in the Columbia River estuary: Production in the water column. *Geochim. Cosmochim. Acta* 65, 2835-2841.

Kohlmeier, C., 2004. Modellierung des Spiekerooger Rückseitenwatts mit einem gekoppelten Euler-Lagrange-Modell auf der Basis von ERSEM. PhD Thesis, University of Oldenburg, Germany, 224p.

Lunau, M.,Sommer, A., Lemke, A., Grossart, H.-P., Simon, M., 2004. A new sampling device for microaggregates in turbid aquatic systems. *Limnol. Oceanogr.: Methods* 2, 387-397.

Lunau, M., Lemke, A., Dellwig, O., Simon, M., 2006a. Physical and biogeochemical controls of microaggregate dynamics in a tidally affected coastal ecosystem. *Limnol. Oceanogr.* 51(2), 847-859.

Lunau, M., Lemke, A., Walther, K., Martens-Habbena, W., Simon, M., 2006b. An improved method for counting bacteria from sediments and turbid environments by epifluorescence microscopy. *Environ.l Microbiol.* 7, 961-968.

Mendel, R.R., 2005. Molybdenum: biological activity and metabolism. *Dalton Trans.* 3404-3409.

Morris, A. W., 1975. Dissolved Molybdenum and Vanadium in Northeast Atlantic Ocean. *Deep-Sea Res.* 22(1), 49-54.

Morford, J., Martin, W. R., Kalnejais, L. H., Francois, R., Bothner, M., Karle, I.-M., 2007. Insights on geochemical cycling of U, Re and Mo from seasonal sampling in Boston Habor, Massachusetts, USA. *Geochim. Cosmochim. Acta* 71, 895-917.

Muenster, U., 1993. Concentrations and fluxes of organic carbon substrates in the aquatic environment. *Antonie Van Leeuwenhoek* 63, 243-274.

Nielsen, M., Bollmann, A., Sliekers, O., Jetten, M., Schmid, M., Strous, M., Schmidt, I., Larsen, L. H., Nielsen, L. P., Revsbech, N. P., 2005. Kinetics, diffusional limitation and microscale distribution of chemistry and organisms in a CANON reactor. *Fems Microbiol. Ecol.* 51(2), 247-256.

Nissenbaum, A., Swaine, D.J., 1976. Organic matter-metal interaction in recent sediments, the role of humic substances. *Geochim. Cosmochim. Acta* 40, 809-816.

Paerl, H. W., Crocke,r K. M., Prufert, L. E., 1987. Limitation of N-2 Fixation in Coastal Marine Waters - Relative Importance of Molybdenum, Iron, Phosphorus, and Organic-Matter Availability. *Limnol. Oceanogr.* 32(3), 525-536.

Passow, U., 2002 Transparent exopolymer particles (TEP) in aquatic environments. *Progress Oceanogr.* 55(3-4), 287-333.

Passow, U., De la Rocha, C. L., 2006. Accumulation of mineral ballast on organic aggregates. *Global Biogeochem. Cycles* 20(1).

Ploug, H., Kühl, M., Buchholz-Cleven, B., Jørgensen, B. B., 1997. Anoxic aggregates – an ephemeral phenomenon in the pelagic environment? *Aquat. Microb. Ecol.* 13, 285-294.

Precht, E., Huettel, M., 2003. Advective pore-water exchange driven by surface gravity waves and its ecological implications. *Limnol. Oceanogr.* 48(4), 1674-1684.

Robson, R. L., Eady, R. R., Richardson, T. H., Miller, R. W., Hawkins, M., Postgate, J. R., 1986. The Alternative Nitrogenase of Azotobacter-Chroococcum Is a Vanadium Enzyme. *Nature* 322(6077), 388-390.

Rodushkin, I., Ruth, T., 1997. Determination of trace metals in estuarine and sea-water reference materials by high resolution inductively coupled plasma mass spectrometry. *J. Anal. Atomic Spec.* 12(10), 1181-1185.

Rusch, A., Huettel, M., 2000. Advective particle transport into permeable sediments - evidence from experiments in an intertidal sandflat. *Limnol. Oceanogr.* 45(3), 525-533.

Schoemann, V., de Baar, H. J. W., de Jong, J. T. M., Lancelot, C., 1998. Effects of phytoplankton blooms on the cycling of manganese and iron in coastal waters. *Limnol. Oceanogr.* 43(7), 1427-1441.

Stal, L. J., 2003. Microphytobenthos, their extracellular polymeric substances, and the morphogenesis of intertidal sediments. *Geomicrobiol. J.* 20(5), 463-478.

Streif, H., 1990. Das ostfriesische Küstengebiet. Gebrüder Borntaeger, Berlin.

Szalay, A., Szilagyi, M., 1967. Association of Vanadium with Humic Acids. *Geochim. Cosmochim. Acta* 31(1), 1-6.

Szilagyi, M., 1967. Sorption of molybdenum by humus preparations. *Geochem. Int.* 4, 1165-1167.

Tribovillard, N., Riboulleau, A., Lyons, T., Baudin, F. O., 2004. Enhanced trapping of molybdenum by sulfurized marine organic matter of marine origin in Mesozoic limestones and shales. *Chem. Geol.* 213(4), 385-401.

Tuit, C.B., Ravizza, G., 2003. The marine distribution of molybdenum. *Geochim. Cosmochim. Acta* 67(18): A495-A495 Suppl. 1.

UNESCO, 1981. The Practical Salinity Scale 1978 and the International Equation of State of Seawater 1980. Tenth Report on the Joint Panel on Oceanographic Tables and Standards. UNESCO Technical Paper in Marine Science 36, UNESCO, Paris.

Volkov, I.I., Formina, L.S., 1974. Influence of organic material and processes of sulphide formation on distribution of some trace elements in deep-water sediment of Black Sea. *AAPG Memoir* 20, 457-476.

von Tuempling, W., Friedrich, G., 1999. Biologische Gewässeruntersuchung. Jena; Stuttgart; Lübeck; Ulm, G. Fischer.

Wedepohl, K. H., 2004. The Composition of Earth's Upper Crust, Natural Cycles of Elements, Natural Resources. In: Merian, E., Anke, M. Ihnat, M., Stoeppler, M. (Eds.), *Elements and their Compounds in the Environment,* 2nd Edition. Wiley-VCH, pp. 3-17.

Yamazaki, H., Gohda, S., 1990. Distribution of Dissolved Molybdenum in the Seto Inland Sea, the Japan Sea, the Bering Sea and the Northwest Pacific-Ocean. *Geochem. J.* 24(4), 273-281.

In situ pore water sampling in deep intertidal flat sediments

Melanie Beck, Olaf Dellwig, Kerstin Kolditz, Holger Freund, Gerd Liebezeit, Bernhard Schnetger & Hans-Jürgen Brumsack

Abstract

In this study a multilevel in situ pore water sampler is presented which allows pore water sampling down to 5 m sediment depth. The sampler forms a crucial tool to study biogeochemical processes on different time scales in advective pore water systems. After insertion into the sediment, the sampler stays on site allowing repetitive sampling at identical locations and depth intervals. The sampler has been successfully tested for one year in sandy sediments in the backbarrier tidal flats of Spiekeroog Island at the German North Sea coast. Depth profiles of redox sensitive elements show a high depth resolution and are not affected by oxidation artefacts during extraction. Seasonal variations owing to advection and changing microbial activity are apparent for some element species even at sediment depths of 5m.

Introduction

Pore water studies are essential to understand early diagenetic exchange processes between the sediment and water column in aquatic ecosystems. In permeable systems, like tidal flats or salt-marshes, they are crucial for a better understanding of biogeochemical cycles and fluid flow. Chemical transformations in pore waters, often mediated by microbial activity and redox conditions, regulate exchange processes between the solid and dissolved phase within the sediment. For example, particulate Mn (IV) is transformed into dissolved Mn (II) under anaerobic conditions (e.g. Sundby and Silverberg 1981; Burdige 1993; Thamdrup et al. 1994), while dissolved Mo (VI) in sulphide containing solutions is converted to a series of Mo(VI) thioanions ($MoO_xS_{4-x}^{2-}$, x = 0-3) (Erickson and Helz 2000; Vorlicek et al. 2004). In solutions containing both sulphide and S(0)-donors (i.e. polysulphides), Mo is transformed into Mo(IV) or $Mo(V)_2$ polysulphide/sulphide anions, which are easily scavenged by Fe compounds and organic matter (e.g. Helz et al. 1996; Erickson and Helz 2000; Zheng et al. 2000; Vorlicek et al. 2004).

Numerous techniques have been developed to sample sediment pore water. These can be divided into ex situ and in situ methods. Ex situ methods, which are widely used at present, comprise squeezing or centrifugation of slices of sediment cores. During squeezing, pressure applied to the core forces pore water through a sampling port. In core section squeezers, sediment samples are compressed to retrieve the pore water (Reeburgh 1967; Sasseville et al. 1974; Robbins et al. 1976). In whole core squeezers, an intact sediment subcore is pressurised and pore water is expelled through a single sampling port at the top or through several sampling ports located at specific depths along the core liner (Bender et al. 1987; Jahnke 1988). For the extraction of pore water from sediments by centrifugation, special centrifuge tubes are used combining the separation of particles from pore water and the filtration of the resulting fluid (Saager et al. 1990).

A number of artefacts are inherent to ex situ methods because the sediment has to be removed from the natural environment for pore water retrieval. Differences in temperature and pressure between the natural environment and the location where the cores are processed potentially affect samples (Bischoff et al. 1970), and oxygen contamination of anaerobic sections can occur even if samples are handled under an inert atmosphere.

In contrast, in situ methods like dialysis, rhizon extraction or suction filtration possess less potential for artefacts. In dialysis samplers, a volume of originally deionised water is allowed to equilibrate with sediment pore water (Hesslein 1976). Dialysis sampling permits a high spatial and temporal resolution. For example, osmosamplers were developed to autonomously collect continuous water samples in remote locations for up to several years (Jannasch et al. 2004). Recently, a rhizon system was developed by Seeberg-Elverfeldt et al. (2005), consisting of a hydrophilic porous polymer tube which is inserted horizontally into the sediment. Pore water flows from the sediment into the space between this porous tube and a central supporting wire, from where it can be sampled via an elastic tube.

Suction filtration forms a third in situ method employed for the extraction of pore water. Several apparatus have been developed, with the simplest single level sampler consisting of a modified glass pipette (Makemson 1972). Howes et al. (1985), Berg and McGlathery (2001), and Nayar et al. (2006) developed modified, more robust versions of single level samplers. Multilevel suction filtration samplers were proposed by Sayles et al. (1973), Montgomery et al. (1981), Watson and Frickers (1990), Hursthouse et al. (1993), and Bertolin et al. (1995). In

general, these latter suction samplers consist of a tube equipped with sampling ports at different depths. They are installed in the sediment, mostly by manually driving them into the sediment, and pore water is obtained by the use of suction. For the extraction of pore water, Charette and Allen (2006) presented the application of a suction filtration system which was originally designed for soil gas sampling by AMS (AMS^{TM} Gas Vapor Probe System, USA). This system can be used to sample multiple depths down to 10 m and is recovered after sampling.

The AMS sampling system represents the only in situ method described in the open literature, which allows sampling of pore water in sediment depths exceeding 1 m. Most in situ samplers were constructed for the extraction of pore water from the upper decimetres of the sediment at high spatial resolution. Furthermore, most sampling devices were not designed for long term pore water sampling at one location or, in case of osmosamplers, long term sampling would only be possible at a few distinct depth intervals. In order to investigate processes occurring in advective deep pore water systems at depths down to 5 m throughout the year, a new suction sampler was constructed. In this contribution we describe the new in situ, multilevel pore water sampler, which is used for sampling pore waters in porous tidal flat sediments at different time scales. The construction of the sampler, its insertion into the sediment as well as the sampling procedure are shown, and examples of pore water profiles obtained are presented.

Material and Procedures

In situ pore water sampler

Sampler construction – A scheme of the new in situ pore water sampler designed for retrieval of pore water from depths down to 5 m is shown in Figure 1. Each sampler is composed of a polyethylene (PE) pipe with an outer diameter of 64 mm. Holes were drilled into the sampler walls allowing the insertion of a connector assembly into the pipe which connects the sampling port to teflon tubes with an inner diameter of 4 mm located inside the plastic pipe. The connector is screwed into disc shaped PE plates with an outer diameter of 26 mm which are glued to the outer sampler wall. The sampling ports are covered by two plies of nylon gauze of 100 and 50 μm pore size which serve as pre-filters. The gauzes are attached to the pipe by a second disc shaped PE plate with an outer diameter of 45 mm and a central opening of 9 mm. These plates are fixed to the pipe by stainless steel screws. These screws are replaced by

nylon screws in our latest design. But according to our own experience stainless steel screws had no contamination effect on trace metal analysis. The plates around the sampling ports were installed to prevent vertical flow along the sampler walls while extracting pore water from the sediment. The distribution of the sampling orifices forms a spiral along the pipe to minimize the effect of local sampling on adjacent ports via lateral and vertical flow. The teflon tubes located inside the sampler pipe link the sampling orifice to sampling devices located at the sediment surface. At the top, the sampler is sealed with a removable cap to prevent seawater from entering the teflon tubes.
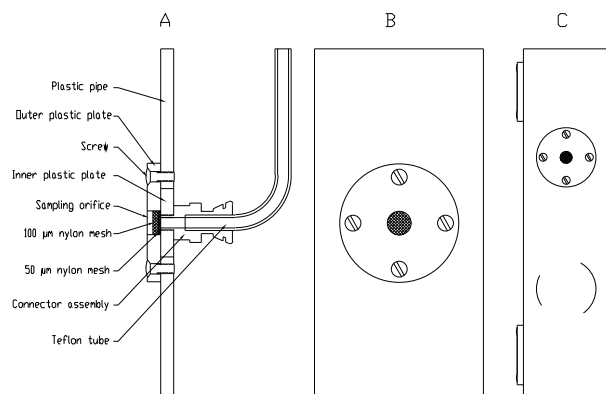
Fig. 1: In situ pore water sampler: (A) Vertical cross section of a single sampling port, (B) Close-up of one sampling port from the outside, (C) Part of the sampler showing five sampling ports with a distance of 5 cm between adjacent ports and a spirally rotation of 90° around the sampler wall.

Due to the limited space available within the plastic pipe for teflon tubes, each in situ pore water sampling system consists of two samplers. The short sampler (1 m length) has 11 sampling ports at 0.05 m, 0.07 m, 0.10 m, 0.15 m, 0.20 m, 0.25 m, 0.30 m, 0.40 m, 0.50 m, 0.75 m and 1.0 m sediment depth. The long sampler (5 m length) has 10 sampling ports located at 1.0 m, 1.25 m, 1.5 m, 2.0 m, 2.5 m, 3.0 m, 3.5 m, 4.0 m, 4.5 m, and 5.0 m sediment depth.

Insertion of the samplers – For the insertion of the pore water sampler into the sediment, an aluminium tube with an inner diameter of 76 mm was driven into the sediment by a vibro corer to a depth equivalent to the length of the sampler. The sediment inside the aluminium tube was removed by a sediment corer and the pore water sampler was inserted into the empty aluminium tube. Then the aluminium tube was drawn out of the sediment by a tripod while the pore water sampler remained in the sediment. To ensure that the sampler stayed positioned and was not slackened by the tidal currents, the inside of the sampler pipe was filled with sand.

Pore water sampling – In sandy water-saturated sediments the pore water sampler enables the extraction of pore fluids via 50 ml PE-syringes. The vacuum generated by a syringe is sufficient to retrieve pore water even from depths of 5 m. However, a transportable vacuum pump (VK2, UMS GmbH, München, Germany) was used where pore water was extracted from sediments with higher contents of clay and silt and from less water-saturated sediments in salt-marshes. The maximum negative pressure applied to the sampling system by the vacuum pump was 700 hPa. Depending on the sampling depth and on the diameter of the teflon tubes used, different volumes of pore water were discarded before taking the sample for analyses. For depths of up to 1 m, at least 20 ml of pore water were discarded, this volume increased to at least 40 ml for depths of up to 3 m, and to 60 ml for depths exceeding 2 m. The volume necessary to discard resulted from the volume of tubing from the port to the sampling device. The volume of the tubing was 4 ml, 25 ml, and 65 ml for sampling depths of 0.3 m, 2 m and 5 m, respectively. At all sampling ports, pore water samples of 100 ml were extracted for later analysis.

Sampling area

The sampling area is located in the German Wadden Sea, a large tidal flat area located between the Frisian coastline and its barrier islands in Northwest Germany. This study was conducted in the East-Frisian Wadden Sea which is characterised by mesotidal conditions (tidal range 2-4 m). Pore water samples were taken on a sand flat (Janssand) and on a mixed flat (Neuharlingersieler Nacken) of the backbarrier area of the Island of Spiekeroog (Fig. 2). The tidal flat is covered by 1 - 2 m of water during high tide, and become exposed for approximately 4 - 6 h during low tide. In the sand flat area sandy sediments predominate, however at depths exceeding 3 m the sands are intermingled with silt-clay layers. The sand flat surface is almost horizontal, except for the margin where the sediment surface slopes towards the main tidal creek. At low tide the distance between the sampling location and the water line is approximately 70 m and the difference in altitude1.5 m. As an example, results are presented (see below) from one sampling location on the sand flat which is situated near the main tidal creek (53° 44,183' N; 007° 41,904' E).

Sample analysis

The samples were analysed for trace elements (Mn, Mo, U, V), SO_4^{2-}, and dissolved organic carbon (DOC). In this study, some results for selected redox sensitive species (SO_4^{2-}, Mn, Mo, U, and V) are presented, and refer to the full set of data which will be published elsewhere.

For the analysis of dissolved metals, the samples were filtered through 0.45 µm SFCA (surfactant-free cellulose acetate) syringe filters. Subboiled HNO_3 was added to obtain a concentration of 1% (v/v) in all samples. Mn, Mo, U and V were analysed by ICP-MS (Thermo Finnigan MAT Element) in 25-fold dilution. The applied analytical procedure is similar to the method published by Rodushkin and Ruth (1997). Precision and accuracy were checked by the reference seawater standard Cass 4 (Seawater reference material for trace metals, National Research Council, Canada). A solution containing Mn was added to the reference standard to control accuracy and precision of the analyses as Mn concentrations are much higher in the Wadden Sea pore water than in the original reference material. Precision / accuracy were 4.0% / 2.2% for Mn, 5.8% / 0.8% for Mo, 4.4% / -5.0% for U, and 7.3% / 4.4% for V. Samples for sulphate analysis were filtered through 1.2 µm GF/C filters. Sulphate was analysed by ion chromatography (Dionex DX 300) in a 250-fold dilution, with standard Atlantic Seawater (Salinity 35.0 (± 0.2%); OSIL, UK) used to control the precision (3.0%) and accuracy (-5.3%) of the measurements. Samples for DOC analysis were filtered through 1.2 µm GF/C filters, and 1 ml HCl (1:1, v:v) was added to 40 ml sample. DOC was analysed by high temperature catalytic oxidation using a multi N/C 3000 analyzer (Analytik Jena).
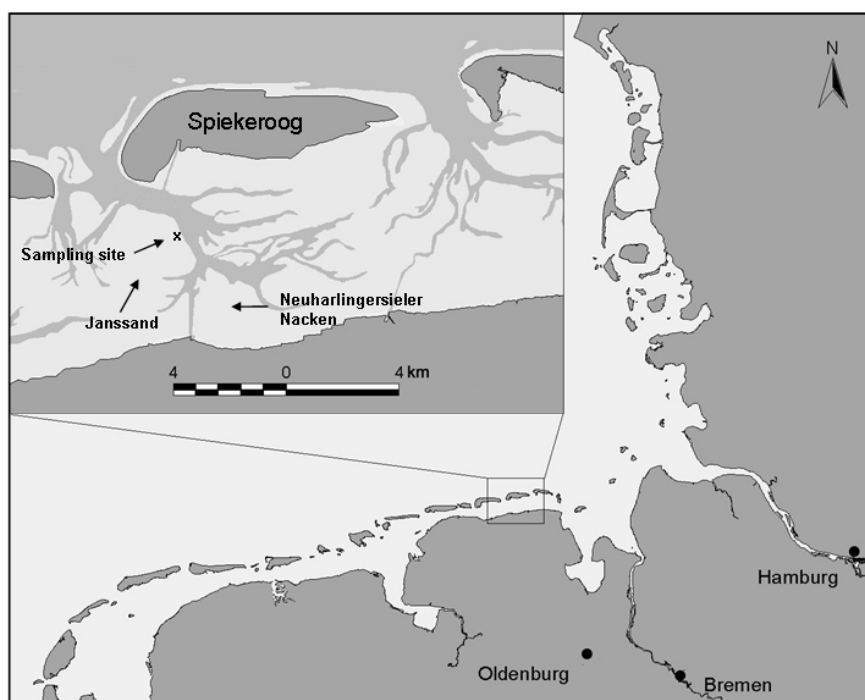
Fig. 2: Sampling area located in the tidal backbarrier area of the Island of Spiekeroog, one of the barrier islands of the NW German Wadden Sea. The cross marks the sampling location (Janssand: 53° 44.183' N, 007° 41.904' E).

Assessment

Comparison of sampling techniques

Before our newly developed samplers were installed, the in situ AMS[TM] gas vapour probe kit was used to sample pore water at a nearby location. Due to technical problems, sampling was only possible down to 2 m depth, nevertheless the general trends with depth obtained for SO_4^{2-}, Mn, Mo, and U were similar to those using the new in situ sampler (Fig. 3). Regarding Mo and U, the decrease in concentration is shifted slightly towards greater depths when the AMS system was used for sampling. This is probably not due to the different sampling techniques, but to the distance between to two sampling locations and the different sampling dates. The results for Mo and U furthermore partly differ in the upper 0.5 m of the sediment as the resolution with depth is better using our sampling technique. Both sampling techniques seem to be suitable to obtain in situ pore water samples without altering concentrations of redox sensitive elements by oxidation effects. Preferential flow along the samplers which could falsify the depth profiles would even be more likely to occur using the AMS system as it has to be redeployed in the sediment for each sampling. However, preferential vertical flow does not

seem to occur as it would have an impact on Mo and U concentrations, which decrease from sea water concentrations in the near-surface layers to much lower concentrations at depths where reducing conditions prevail. Compared to the AMS system, the new sampler stays on site after its insertion into the sediment. This offers the possibility of the sediment/pore water system to equilibrate before conducting repetitive samplings at identical locations. We regard this as an important advantage of the new sampling system.
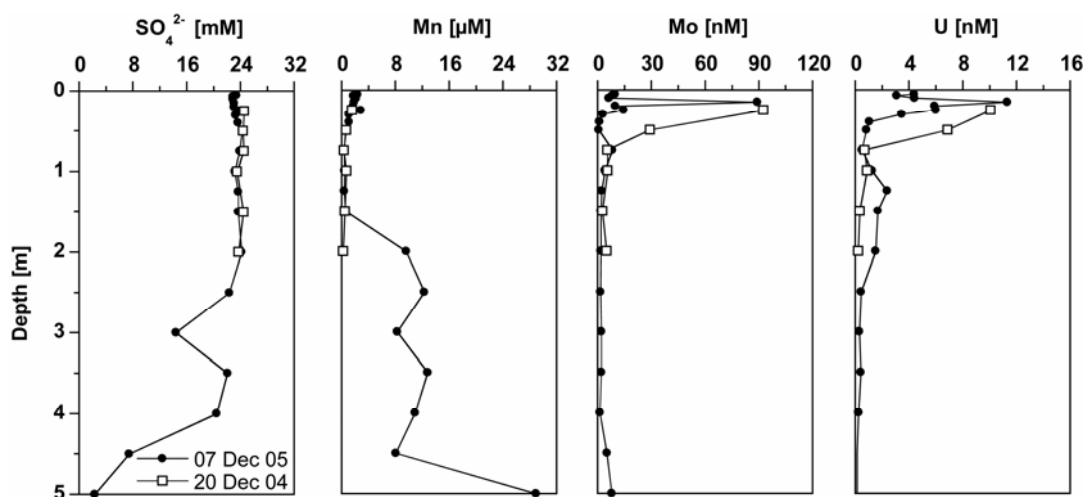
Fig. 3: Comparison of two in situ sampling techniques, our new developed sampler (filled dots) and the AMS^{TM} gas vapour probe kit (open squares). Samples taken with the AMS sampler were extracted at a location close to our permanently installed samplers.

Oxidation effects during sampling

First samples were taken two weeks (April 2005) and seven weeks (May 2005) after the insertion of the samplers into the sediment. At several sampling depths exceeding 0.5 m, Mo and U concentrations were higher in April compared to May (Fig. 4). These changes can be ascribed to oxidation effects still seen in redox sensitive elements like Mo and U even after two weeks of equilibration. The depths profiles obtained from May 2005 onwards remained essentially stable at lower concentration levels in depths exceeding 0.5 m, which supports our hypothesis that oxygen introduced into the sediment during the insertion of the sampler has caused the initially high Mo and U concentrations. We therefore regard both elements as sensitive proxies for oxygen contamination. The oxidation effect seemed less pronounced for Mn and V as the depth profiles of these elements were similar in April and May 2005. V is known to form complexes with DOC (Brumsack and Gieskes 1983, Wehrli and Stumm 1989), which are supposed to be less sensitive to oxidation. Regarding Mn, the reaction with O_2 is slow

resulting in a half life for Mn(II) disappearance of 340 days at pH ~ 8 in seawater with P_{O2} ~ 0.21 atm (Morgan 2005). The results from these first sampling sequences suggest the need of a prolonged equilibration time, which was achieved at least seven weeks after insertion. The accurate equilibration time unfortunately could not be determined as the oxidation artefacts in April 2005 were not evident before a comparison of data was possible with those obtained during later sampling campaigns.
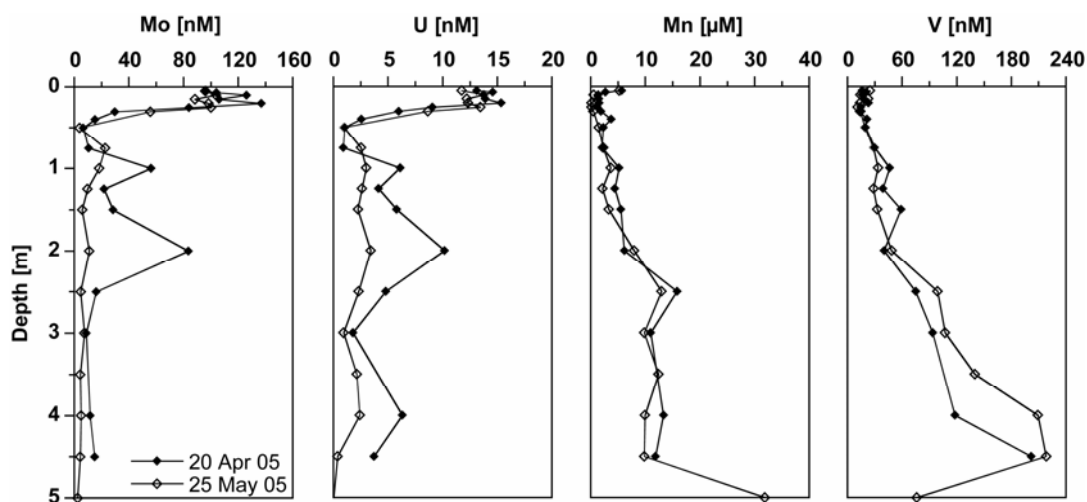
Fig. 4: Pore water depth profiles of Mn, V, Mo, and U. Samples were taken with the in situ sampler in a sandy tidal flat sediment, NW Germany, in April and May 2005. The samples in April were extracted after two weeks equilibration time, whereas the samples in May were taken seven weeks after the insertion of the samplers into the sediment.

In November 2004 pore water samples were obtained in situ by using the AMS[TM] gas vapour probe kit and ex situ by centrifugation of sediment core material during a sampling carried out on a mixed tidal flat (Neuharlingersieler Nacken). As the sediment core sampling was not performed under N_2 atmosphere, pore water results show the potential oxidation effect on concentrations of redox sensitive elements. Severe artefacts are seen when comparing the results of the two sampling techniques (Tab. 1). For example, the sample at 1 m sediment depth showed a Mo concentration of 18 nM using the in situ AMS technique compared to a concentration of 865 nM in the centrifuged sample. Concentrations of Mo exceeding the sea water level (approximately 105 nM) by more than 8-fold represent oxidation artefacts as the study site is known to be anaerobic below a few centimetres depth. U concentrations in centrifuged pore waters are as well significantly higher than in the in situ samples. An opposing

effect is seen for Mn as the oxidation of Mn during the sampling of the core led to lower concentrations in centrifuged pore water samples compared to samples taken in situ.

Tab. 1: Comparison of the in situ AMS sampling technique and the ex situ centrifugation of sediment core slices. The results of the sediment core sampling show the effect of oxygen on concentrations of redox sensitive elements. The sediment core was not treated under a nitrogen atmosphere.

Depth [m]	Mn [µM]		Mo [nM]		U [nM]	
	in situ	ex situ	in situ	ex situ	in situ	ex situ
0.5	2.2	2.2	19	331	1.1	16.5
1.0	3.4	1.6	18	866	3.6	40.3
1.8	8.8	0.1	6	528	0.3	38.1

Sample volume

The sediment volume from which pore water is extracted by the in situ sampler at each sampling port can be calculated via the assumption that this volume is of approximately half-spherical shape around the sampling port. The radius (in cm) of the hemisphere can be described via equation (1)

$$r = \sqrt[3]{\frac{3 \cdot V_{sample}}{2 \cdot \phi \cdot \pi}} \qquad (1)$$

with V_{sample} being the volume of pore water sampled (ml), and ϕ the porosity of the sediment. In this study, about 120 to 160 ml of pore water were extracted at each sampling port depending on the depth of the sampling port and the volume within the tubing necessary to be discarded. The porosity of sandy sediments in the sampling area is approximately 0.45 (B.W. Flemming, pers. comm.). Based on these parameters, a radius of 5.0 cm or 5.5 cm is derived for the resulting hemisphere extracting 120 or 160 ml pore water, respectively. This radius is larger than the smallest distance between the sampling ports in the uppermost part of the sediment. As the rotation angle from one sampling port to the other is 90°, the distance of adjacent sampling ports is 7.3 cm or 11.5 cm for a difference in depth of 5 m or 10 cm, respectively. Consequently, for a difference in depth of 5 cm the hemispheres of adjacent sampling ports may partly overlap, whereas no overlap of the hemisphere will occur for differences in depth exceeding 10 cm. The sampled hemispheres therefore may have partly interfered for ports

located at less than 0.3 m depth. To avoid mixing of pore water in the upper sections of the sediment, smaller volumes of pore water should be sampled at these depths. For a difference in depth of 5 cm between adjacent sampling ports, the maximal pore water volume sampled should be 45 ml. Since the volume of the tubing is less than 10 ml at depths less than 0.3 m, at least 35 ml of sample can be taken for analysis. The volume of pore water, which can be extracted without any overlap of the hemisphere, increases to 180 ml if the difference in distance of adjacent ports is 10 cm. At greater depths, an overlap of the hemispheres around adjacent sampling ports can generally be excluded because the distance between the ports by far exceeds the calculated radius of the hemisphere.

We are assuming that the volume of extracted pore water forms a hemisphere. The extracted volume could also be of ellipsoidal shape, especially at higher flow velocities or during extraction of pore water from sediment layers with changing permeabilities, like alternating sand/mud layers. If the ellipsoid extends perpendicular to the sampler, then the length and width of the ellipsoid would be even smaller than the radius calculated for a hemisphere. In this case the overlap of pore water volumes extracted from adjacent sampling ports would be reduced. Nevertheless, the adaptation of the volume sampled to the distance between the sampling ports remains an important aspect. As the main application of our sampling device is the sampling of pore waters from greater depths, a vertical resolution of less than 5 cm was not considered to be essential. Well adapted sampling devices do exist for high resolution applications in surface sediment. A suitable vertical spacing of the sampling ports of 10 cm is recommended if large pore water volumes of about 100 ml are required. By reducing the extracted pore water volume to 35 ml a vertical spacing of 5 cm is possible. Changing the construction of the sampler by mounting the sampling ports at an angle of 120° around the sampler tube would allow interference-free sampling of 110 ml at 5 cm depth intervals. Preferential flow along the sampler seem unlikely to occur as the concentrations of several redox-sensitive metal species sharply decrease from sea water-like values in the upper part of the sediment to significantly lower concentrations in deeper layers. For example, Mo concentrations close to the sea water level of 105 nM would have been determined at depths exceeding 0.3 m if sea water percolated along the sampler walls into the sediment.

Pore water profiles

The in situ sampler was successfully used to sample pore waters in tidal flat sediments in the coastal area of NW Germany. Examples shown here represent samples from a sandy tidal flat. They highlight both, the importance to obtain in situ pore water samples of depths exceeding 1 m as huge changes in element concentrations can be observed below this depth, but also the necessity for a high density of sampling ports in the upper 100 cm of the sediment body, as many processes occur especially in this section (Huettel et al. 1998; Huettel and Rusch 2000; Rusch and Huettel 2000).

At the study site, aerobic conditions prevailed only in the upper few cm of the sediment (Billerbeck et al. 2006b). Thus, shortly below the sediment surface, other electron acceptors like SO_4^{2-} are used for microbial organic matter degradation. Consequently, SO_4^{2-} retained sea water concentrations (26 mM at 31 psu) only in the upper 0.5 m of the profile and decreased below this depth (Fig. 5). Due to the reducing conditions in the sediment, high concentrations of dissolved Mn (II) are apparent in the pore waters (Fig. 5). Mo concentrations showed only slight deviations from sea water concentration (110 nM) in the upper part of the sediment (Fig. 5). However, concentrations sharply decreased at depths exceeding 0.3 m, suggesting that soluble MoO_4^{2-} was converted into Mo species which were subsequently scavenged by organic matter or Fe compounds (Helz et al. 1996).
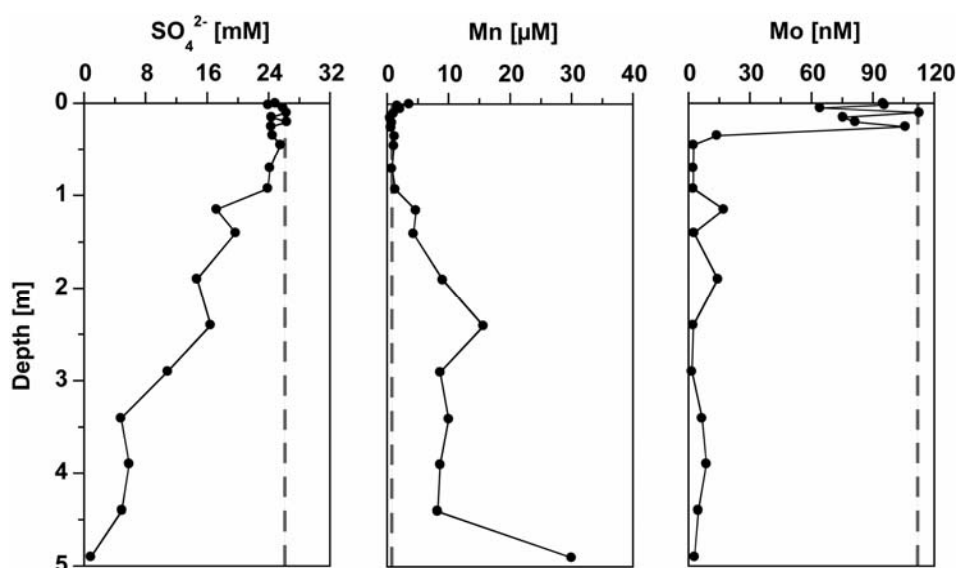
Fig. 5: Pore water depth profiles of SO_4^{2-}, Mn and Mo. Samples taken with the in situ sampler in a sandy tidal flat sediment, NW Germany, on July 19th 2005. Dashed lines mark concentrations in the open water column of the tidal flat: SO_4^{2-} calculated for 31 psu, Mn from Dellwig et al. (2007), and Mo from Dellwig, O. (unpublished data).

Seasonal variation

Depth profiles resulting from repetitive sampling at the same location for different seasons are shown for DOC and SO_4^{2-} (Fig. 6). The depth profile for May 2005 represents a characteristic profile for spring and early autumn, whereas the profile for August 2005 is shown as a typical example for the summer months June, July, and August. The depth profile for March 2006 forms a representative profile for samplings from November to April. During the summer months concentrations of SO_4^{2-} decreased more strongly with depth compared to the other seasons, whereas the concentrations of DOC increased in the same time period at depths of about 1 m to 3 m. During autumn and winter the contrary was seen in the deeper part of the sediment, i.e. increased concentrations of SO_4^{2-} and decreased concentrations of DOC. These changes in concentration seem to be caused by advection (Billerbeck et al. 2006a,b; Wilson and Gardener 2006) and by changing microbial activity due to variations in temperature (Vosjan 1974).
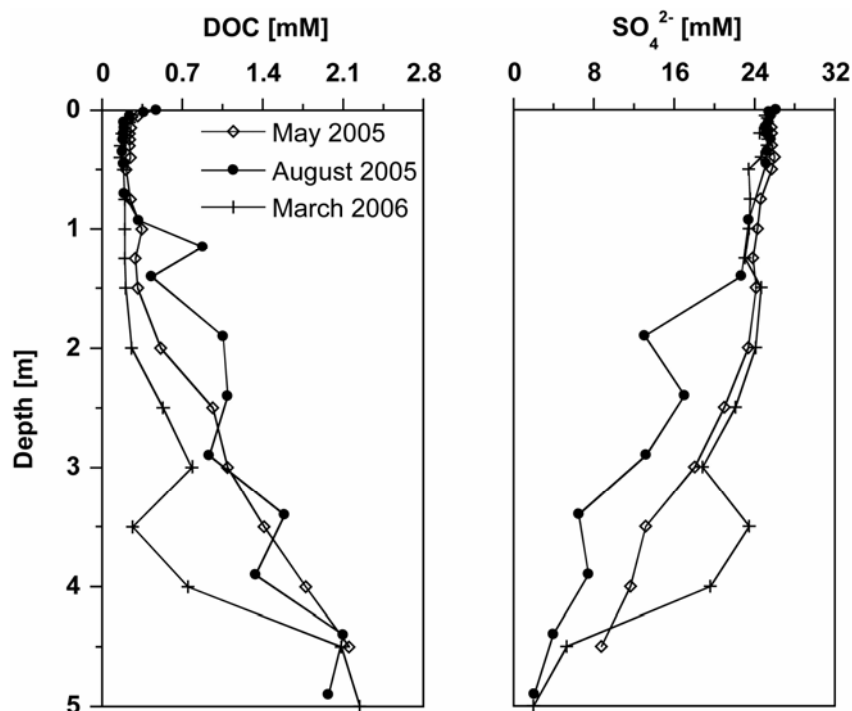
Fig. 6: Seasonal variation of the pore water depth profiles of DOC and SO_4^{2-}. Samples were taken with the in situ sampler in a sandy tidal flat sediment, NW Germany.

Discussion

Bufflap and Allen (1995) discuss possible reasons why pore water sampling methods may alter trace metal concentrations in pore waters. As potential sources of error they list oxidation of anoxic pore waters and sediments, disturbance of sediment cores leading to disruptions of sediment layers, metal contamination and temperature artefacts. In this study, pore water samples were extracted in situ and consequently temperature artefacts can be ruled out. With regard to the analysis of trace metals, the sampler was constructed avoiding metal components, and therefore the possibility of metal contamination by components of the sampler is rather unlikely. Oxidation artefacts are the source of error which are most difficult to prevent. However, the installation of the new sampling system definitely prevents any contact of the sample with oxygen.

Another potential source of error is the formation of preferential water paths along the sampler walls, hence smoothing the trends in the depth profiles. The depth profile of Mo with its sharp decrease in concentrations at about 0.3 m depth (Fig. 5), but also strong variations in the concentrations of other elements observed between adjacent sampling ports suggest that this phenomenon can be neglected. If samples are not filtered immediately after extraction, particles present in the pore water can form another source of error, as trace metals can be adsorbed to or released by such particles. Using the proposed sampler, all samples are pre-filtered during extraction. Furthermore, the samples were filtered immediately after extraction via syringe filters. In principle, it would be possible to use 0.45 µm filters at the sampling ports of the sampler to avoid an additional filtration step. However, this bears the risk of clogging sampling ports by particles.

The in situ pore water sampler described in this study offers several new possibilities to gain meaningful insights into the biogeochemical processes occurring in permeable sediments. Compared to in situ samplers currently in use, the new sampler allows the extraction of pore waters from several metres depths. For the determination of chemical transformation processes occurring in pore waters of intertidal sediments influenced by advection, sampling of pore waters down to depths of at least several metres is essential. Depth profiles of major and trace elements demonstrate that chemical transformations do not only occur at the sediment-water interface or shortly below the sediment surface, but at greater depth as well.

The new sampler is suitable for studies of seasonal pore water composition as samples can be taken at an identical location for extended periods of time. In permeable sediments influenced by advection the replacement and re-equilibration of pore water is assumed to occur within some hours allowing the determination of pore water compositions within tidal cycles. Furthermore, the permanently installed samplers allow to clearly distinguish between temporal variations and spatial heterogeneity. So far, the new samplers have been used for a period of one year and are still working properly. Even the necessary equilibration time of several weeks is not considered to be disadvantageous in the light of its long lifespan. All these aspects indicate that the new in situ sampler is a powerful tool to investigate biogeochemical cycles in tidal flat sediments, salt-marsh soils or in other temporarily inundated environments.

Comments and recommendations

The sampler proofed to be very suitable to sample pore water in permeable water saturated sandy sediments. For the extraction of pore water from muddy sediments (mixed flat Neuharlingersieler Nacken) or partly unsaturated sediments (salt-marsh sediments of Langeoog Island) the sampler is also appropriate, however the sampling is much more time consuming. A further improvement to adapt the sampler to such environments seems possible, e.g. via the enlargement of the sampling port to facilitate the extraction of pore water by extending the area through which suction directly acts on the sediment.

Further fields of application are the analysis of CH_4, N_2O or H_2S contents in the pore water. However, degassing of the sample has to be taken into account once the sample is transferred into sampling containers. In general, pore waters retrieved by this sampler seem to be as suitable for the analysis of dissolved gases as sediment cores where losses of gas are also supposed to occur. For example, a first comparison of CH_4 concentrations determined in samples taken with the in situ sampler and in samples from sediment cores showed similar results.

Acknowledgements

The authors would like to thank Helmo Nicolai and his colleagues at TERRAMARE Research Centre for assembling the pore water samplers. His experience and practical suggestions were of great help during the realisation of the project. Furthermore, we wish to

References

Bender, M., W. Martin, J. Hess, F. Sayles, L. Ball, and C. Lambert., 1987. A whole-core squeezer for interfacial pore-water sampling. Limnol. Oceanogr. 32(6): 1214-1225.

Berg, P., and K.J. McGlathery., 2001. A high-resolution pore water sampler for sandy sediments. Limnol. Oceanogr. 46(1): 203-210.

Bertolin, A., D. Rudello, and P. Ugo., 1995. A new device for in-situ pore-water sampling. Mar. Chem. 49: 233-239.

Billerbeck, M., U. Werner, K. Bosselmann, E. Walpersdorf, and M. Huettel., 2006a. Nutrient release from an exposed intertidal sand flat. Mar. Ecol. Prog. Ser. 316: 35-51.

Billerbeck, M., U. Werner, L. Polerecky, E. Walpersdorf, D. deBeer, and M. Huettel., 2006b. Surficial and deep pore water circulation governs spatial and temporal scales of nutrient recycling in intertidal sand flat sediment. Mar. Ecol. Prog. Ser. 326: 61-76.

Bischoff, J.L., R.E. Greer, and A.O. Luistro., 1970. Composition of interstitial waters of marine sediments: temperature of squeezing effect. Science 167(3922): 1245-1246.

Brumsack, H.J., and J.M. Gieskes., 1983. Interstitial water trace-metal chemistry of laminated sediments from the gulf of California, Mexico. Mar. Chem. 14(1): 89-106.

Bufflap, S.E., and H.E. Allen., 1995. Sediment pore-water collection methods for trace-metal analysis - a review. Water Res. 29(1): 165-177.

Burdige, D.J. 1993., The biogeochemistry of manganese and iron reduction in marine sediments. Earth Sci. Rev. 35(3): 249-284.

Charette, M.A., and M.C. Allen., 2006. Precision groundwater sampling in coastal aquifers using a direct-push, shielded-screen well-point system. Ground Water Monit. R. 26(2): 87-93.

Dellwig, O., K. Bosselmann, S. Kölsch, M. Hentscher, J. Hinrichs, M.E. Böttcher, R. Reuter, and H.-J. Brumsack., 2007. Sources and fate of manganese in a tidal basin of the German Wadden Sea. J. Sea Res. 57:1-18.

Erickson, B.E., and G.R. Helz., 2000. Molybdenum(VI) speciation in sulfidic waters: stability and lability of thiomolybdates. Geochim. Cosmochim. Acta 64(7): 1149-1158.

Helz, G.R., C.V. Miller, J.M. Charnock, J.F.W. Mosselmans, R.A.D. Pattrick, C.D. Garner, and D.J. Vaughan., 1996. Mechanism of molybdenum removal from the sea and its concentration in black shales: EXAFS evidence. Geochim. Cosmochim. Acta 60(19): 3631-3642.

Hesslein, R.H., 1976. An in situ sampler for close interval pore water studies. Limnol. Oceanogr. 21(6): 912-914.

Howes, B.L., J.W.H. Dacey, and S.G. Wakeham., 1985. Effects of sampling technique on measurements of porewater constituents in salt marsh sediments. Limnol. Oceanogr. 30(1): 221-227.

Huettel, M., W. Ziebis, S. Forster, and G.W. Luther III., 1998. Advective transport affecting metal and nutrient distributions and interfacial fluxes in permeable sediments. Geochim. Cosmochim. Acta 62(4): 613-631.

Huettel, M., and A. Rusch., 2000. Transport and degradation of phytoplankton in permeable sediment. Limnol. Oceanogr. 45(3): 534-549.

Hursthouse, A.S., P.P. Iqbal, and R. Denman., 1993. Sampling interstitial waters from intertidal sediments. An inexpensive device to overcome an expensive problem? Analyst 118: 1461-1462.

Jahnke, R.A., 1988. A simple, reliable, and inexpensive pore-water sampler. Limnol. Oceanogr. 33(3): 483-487.

Jannasch, H.W., C.G. Wheat, J.N. Plant, M. Kastner, and D.S. Stakes., 2004. Continuous chemical monitoring with osmotically pumped water samplers: OsmoSampler design and applications. Limnol. Oceanogr. Methods 2: 102-113.

Makemson, J.C., 1972. An interstitial water sampler for sandy beaches. Limnol. Oceanogr. 17(4): 626-628.

Montgomery, J.R., M.T. Price, J. Holt, and C. Zimmermann., 1981. A close-interval sampler for collection of sediment pore waters for nutrient analyses. Estuaries 4(1): 75-77.

Morgan, J.J., 2005. Kinetics of reaction between O_2 and Mn(II) species in aqueous solutions. Geochim. Cosmochim. Acta 69(1): 35-48.

Nayar, S., D. Miller, S. Bryars, and A.C. Cheshire., 2006. A simple, inexpensive and large volume pore water sampler for sandy and muddy substrates. Estuar. Coast. Shelf S. 66: 298-302.

Reeburgh, W.S., 1967. An improved interstitial water sampler. Limnol. Oceanogr. 12(1): 163-165.

Robbins, J.A., and J. Gustinis., 1976. A squeezer for efficient extraction of pore water from small volumes of anoxic sediment. Limnol. Oceanogr. 21(6): 905-909.

Rodushkin, I., and T. Ruth., 1997. Determination of trace metals in estuarine and sea-water reference materials by high resolution inductively coupled plasma mass spectrometry. J. Anal. Atom. Spectrom. 12: 1181-1185.

Rusch, A., and M. Huettel., 2000. Advective particle transport into permeable sediments - evidence from experiments in an intertidal sandflat. Limnol. Oceanogr. 45(3): 525-533.

Saager, P.M., J.-P. Sweerts, and H.J. Ellermejer., 1990. A simple pore-water sampler for coarse, sandy sediments of low porosity. Limnol. Oceanogr. 35(3): 747-751.

Sasseville, D.R., A.P. Takacs, and S.A. Norton., 1974. A large-volume interstitial water sediment squeezer for lake sediments. Limnol. Oceanogr. 19(6): 1001-1004.

Sayles, F.L., T.R.S. Wilson, D.N. Hume, and P.C. Mangelsdorf, Jr., 1973. In situ sampler for marine sedimentary pore waters: evidence for potassium depletion and calcium enrichment. Science 181(4095): 154-156.

Seeberg-Elverfeldt, J., M. Schlüter, T. Feseker, and M. Kölling., 2005. Rhizon sampling of porewaters near the sediment-water interface of aquatic systems. Limnol. Oceanogr.: Methods 3: 361-371.

Sundby, B., and N. Silverberg., 1981. Pathways of manganese in an open estuarine system. Geochim. Cosmochim. Acta 45(3): 293-307.

Thamdrup, B., R.N. Glud, and J.W. Hansen., 1994. Manganese oxidation and in situ manganese fluxes from a coastal sediment. Geochim. Cosmochim. Acta 58(11): 2563-2570.

Vorlicek, T.P., M.D. Kahn, Y. Kasuya, and G.R. Helz., 2004. Capture of molybdenum in pyrite-forming sediments: Role of ligand-induced reduction by polysulfides. Geochim. Cosmochim. Acta 68(3): 547-556.

Vosjan, J.H., 1974. Sulphate in water and sediment of the Dutch Wadden Sea. Neth. J. Sea Res. 8: 208-213.

Watson, P.G., and T.E. Frickers., 1990. A multilevel, in situ pore-water sampler for use in intertidal sediments and laboratory microcosms. Limnol. Oceanogr. 35(6): 1381-1389.

Wehrli, B., and W. Stumm., 1989. Vanadyl in natural waters: Adsorption and hydrolysis promote oxygenation. Geochim. Cosmochim. Acta 53(1): 69-77.

Wilson, A.M., and L.R. Gardener., 2006. Tidally driven groundwater flow and solute exchange in a marsh: Numerical simulations. Water Resour. Res. 42, W01405.

Zheng, Y., R.F. Anderson, A. van Geen, and J. Kuwabara., 2000. Authigenic molybdenum formation in marine sediments: a link to pore water sulfide in the Santa Barbara Basin. Geochim. Cosmochim. Acta 64(24): 4165-4178.

The impact of tidal inundation on salt marsh vegetation after de-embankment on Langeoog Island, Germany – Six years time series of permanent plots

Barkowski, J. W.; Kolditz, K.; Brumsack, H.-J. and Freund, H.

Abstract

Salt marsh succession after de-embankment was monitored on the East Frisian barrier island Langeoog by investigating permanent plots. Seventy years after embankment salt marsh plants were once again influenced mainly by the tidal regime. From 2002 to 2004 the former high marsh and glycophytic vegetation died out and was replaced by species of lower salt marsh zones. Nitrophytic halophytes like *Suaeda maritima, Atriplex prostrata* and *Artemisia maritima* established first because of the high nutrient content in the soil, a direct result of former vegetation decay. With decreasing nitrogen afterwards other species became more competitive. Until 2007 *Atriplex portulacoides* became more dominant in the lower marsh and *Elymus athericus* reached dominance in areas where grazing has been abandoned in the high marsh. The dynamics in the study area is much lower than in natural marshes due to the still existing drainage system. Therefore vegetation units with low species diversity are widespread.

Introduction

Climate change and sea level rise are a great concern today, especially along shallow coastlines existing in the southern part of the North Sea. Extended salt marshes are a good natural defence against the sea, because the vegetation reduces wave energy (Cooper et al. 2001; Wittig et al. 2004; Wolters et al. 2005a). However, most (over 90 %) parts of these areas are embanked or are still in anthropogenic use (Reise 2005). More than that, salt marshes along the North Sea are mostly narrow areas which in many regions of the coastal mainland eroding because of the coastal squeeze (Adam 2002; Doody 2004; Hughes 2004; Wolters et al. 2005c). In the future it might be necessary to breach more of the existing seawalls to allow development of potentially natural salt marshes. An important question is: How long will natural succession last after de-embankment of several hundred hectares of former embanked salt marshes? Wolters et al. (2005a) present an overview where mostly smaller areas were de-

embanked, but there are few studies dealing with the detailed change in salt marsh vegetation in large de-embanked areas. One example for an area including 350 ha on the Baltic Sea is described by Bernhardt & Koch (2003) in detail. Wolters et al. (2005b) postulate that the reestablishment of the potentially natural vegetation will take years because of the limited seedbank and the short distance transport of diaspores by the tides. Therefore there is an essential need for long-term monitoring (Wolters et al. 2005b). Especially permanent plots (PPs) are a very common method to document changes in vegetation succession (Bakker 1978; Bakker et al. 1996; Beeftink et al. 1978; Bernhardt & Koch 2003; Kiehl et al. 2007; Roozen & Westhoff 1985; Wolters et al. 2005a). The great advantage of analysing PPs is that a detailed overview of the changes in species coverage due to influence of apparently less important factors is obtained. Vegetation mapping is often more related to point out changes in vegetation units than to single species, so a combination of both methods is useful (Barkowski 2003; Barkowski & Freund 2006; Freund et al. 2003). This study gives answers to important questions concerning vegetation succession following de-embankment by monitoring PPs from 1 year before to 4 years after de-embankment. How do the salt marsh zones differ in their succession following tidal inundation? How do single species react? Wolters et al. (2005a) postulate an increase in species number as a measurement for restoration success, but after the former vegetation dies how long will it take? Important local factors such as the drainage system or grazing intensity have to be taken in account.

Methods

Study area

The salt marshes on Langeoog Island can be considered as three separate areas. One area is located on the west end of Langeoog Island (Fig. 1) and second in the east. Both of them are natural grown salt marshes. The study area includes the third region, a 378.5 ha area of salt marsh which was under intensive anthropogenic influence. It is completely ditched for drainage and in 1934/35 a summer dike was build to allow for grazing by cattle. A total of 218 ha were excluded of regular inundation in this so called summer polder. The dike was between 2 m NN and 2.25 m NN high (Alhorn & Kunz 2002; Harnischmacher 1949) and the salt marsh behind was only flooded 15 to 25 times a year during storm surges. Forty-six PPs were made in

1936 and monitored to document the effect of embankment in the vegetation. In 1948 they were controlled again (Harnischmacher 1949) so the data serves as a baseline study.

As a measure for nature conservation the former summer dike on Langeoog Island was partly removed in 2003/2004 (Fig. 1). Altogether 218 ha were exposed to the normal tidal regime again. The whole summer polder was grazed by cattle intensively until 1992. Grazing was abandoned in most parts of the area after 2002 before dike breaching (Barkowski 2003; Steffens 2003).
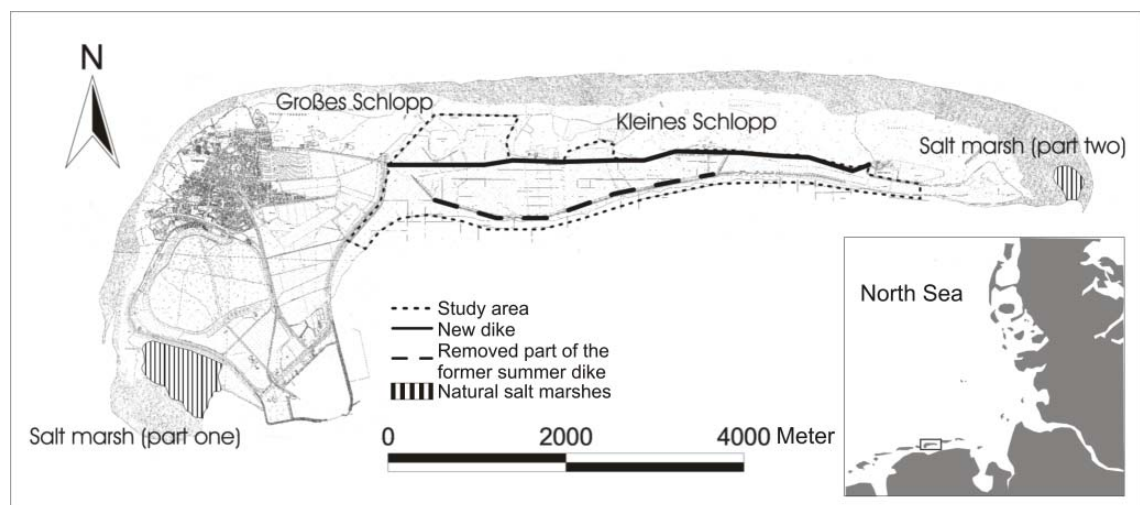
Fig. 1: Investigation area (marked by the short dashed line) and natural salt marshes in Langeoog Island. Position of the former summer dike and the new dike. Insert shows the position of Langeoog in the North Sea

In 2000 the permanent plots where reactivated and additionally new permanent plots (PP 50 to 84) were made (Fig. 2) (Freund et al. 2003). In 2002 all plots were examined in order to obtain the reference state of vegetation 1 year prior to de-embankment.

De-embankment started in 2003 by removing the sluices within the summer dike and the whole project was completed in September 2004. To protect the dunes and to allow safe travelling to the east end of Langeoog Island a new dike with a crest height of 3.2 m NN was built (Fig. 1). The construction of this dike caused the separation of the "Großes" and "Kleines Schlopp" from the rest of the salt marsh. These two areas resulted from a storm surge in 1717 which divided the island in three parts. It took until the beginning of the 20th century to close the dune ridges, followed by the development of salt marsh vegetation.

To document the daily impact of tidal inundation on the former sheltered vegetation within the summer polder from 2004 to 2007 the PPs were monitored. This research was part of a project in which geochemistry (Kolditz et al. 2009) was combined with vegetation data.

The PPs are marked on each corner with a magnet located 25 cm deep. In addition two wooden poles were set at the northern corners of each site. Each PP is approximately 4 m² and is predominately square. In 2005 five new PPs were made at locations of special interest (PP 85 to 89), for example where the former summer dike was located (Fig. 2). The top soil was removed at seven locations (PP 24b, 25b, 26b, 42b, 43b, 62b and 85b) to document how succession starts without former vegetation.
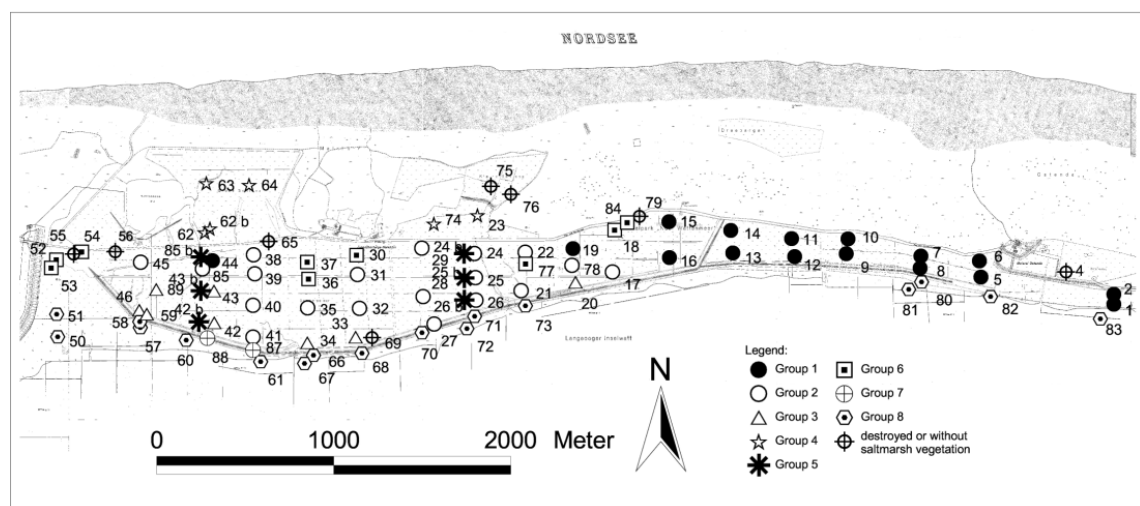
Fig. 2: Position of 83 PPs in the investigation area and their membership to the group, as well as, those PPs which were not considered in this studying

In this paper the years 2002 to 2007 are primarily considered in order to show the effects of de-embankment while the history of the vegetation of the summer polder before has already been well described in Barkowski (2003), Barkowski & Freund (2005), Freund et al. (2003), Harnischmacher (1949), Petersen (2001), Petersen (2003) and Steffens (2003).

The salt marsh was subdivided into four zones: high marsh, middle marsh, low marsh and pioneer zone. Splitting up the middle marsh from the high marsh follows partly the definition of Freund et al. (2003), Petersen (2001) and Roozen & Westhoff (1985). In this article the zones are defined as: Pioneer zone - dominated by *Salicornia stricta, Spartina anglica or Suaeda maritima* with a coverage of Puccinellion species under 15 %; low marsh – dominated by *Atriplex portulacoides, Puccinellia maritima* and mixed units of Puccinellion species; middle marsh – dominated by *Limonium vulgare, Juncus gerardii* and mixed units of Puccinellion and

Armerion species (for example *Artemisia maritima* and *Atriplex portulacoides*); high marsh - dominated by *Festuca rubra, Elymus athericus, E. repens, Ononido-Caricetum distantis, Artemisietum maritimae* and salt influenced grassland.

The vegetation inside the summer polder was mainly covered by vegetation units of the middle and high marsh in 2002 (Fig. 3). Additionally many glycophytic species had colonized the study area since 1936. The distribution of vascular plants did not follow salinity or inundation gradients but were strongly affected by other factors such as grazing intensity inside the summer polder, however outside the summer polder the opposite was true. Here the abiotic factors caused a normal salt marsh zonation which was predominant until 2002.
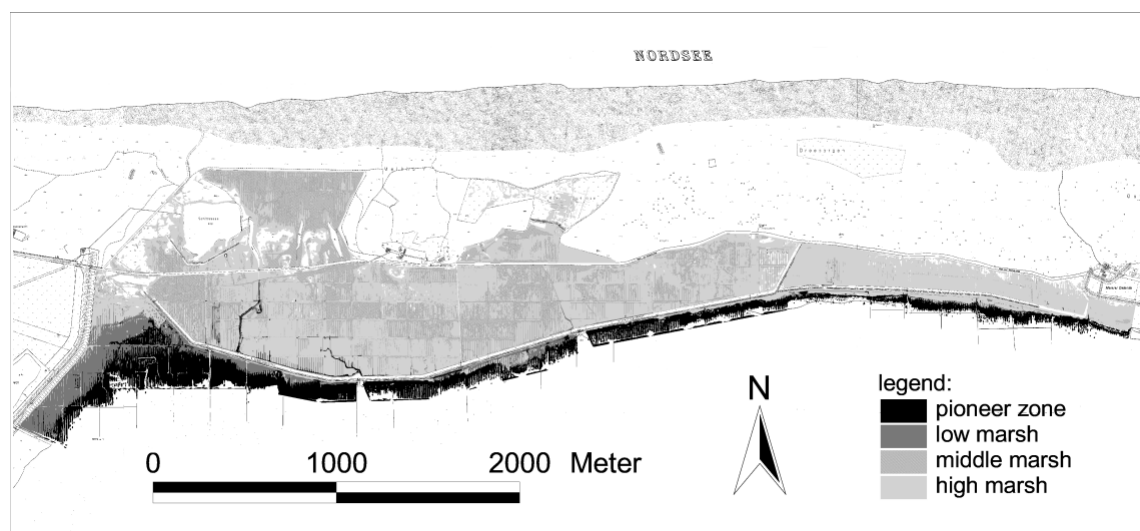
Fig. 3: Salt marsh zones in the investigation area on Langeoog Island in 2002

Sampling relevès

A total number of 83 PPs is located in the investigation area (Fig. 2). The number of examined PPs varies during the investigation period (72 PPs in 2002, 33 PPs in 2004, 82 PPs in 2005, and 83 PPs in 2006 and 2007). Additionally, since 2005 seven PPs with removed top soil were investigated. Coverage estimation was carried out by the same person at the beginning of August in each listed year using a decimal scale (Londo 1976). This procedure ensures a high comparability of the single investigations.

Key species

Thirteen species were chosen as key species. The criteria were: presence in a representative number of PPs; characteristic species for a special salt marsh zone; proof of an important process, for example the increased appearance of nutrients. The key species are: *Salicornia stricta* and *Suaeda maritima* for the pioneer zone; *Aster tripolium, Atriplex portulacoides* and *Puccinellia maritima* for the lower marsh; *Limonium vulgare* and *Juncus gerardii* for the middle marsh; *Atriplex prostrata* and *Artemisia maritima* belong to the middle and high marsh depending on their accompanying vegetation; *Festuca rubra, Elymus athericus, E. repens* and *Potentilla anserina* are key species for the high marsh.

An example of why a particular species was not considered a key species is *Spartina anglica.* It was not chosen because it only dominates in a few PPs outside the former summer polder and is barely present inside the summer polder during the time of monitoring.

The appearance of species each year is always calculated based on the total number of PPs. The year 2002 is considered as the condition before de-embankment, so every species which is present in this year is treated as established. To calculate changes in vegetation, every coverage value has been set to the maximum percent value of the scale (compare Londo 1976), for example scale 3 = 35 % coverage.

Groups of Permanent Plots

To characterize the changes in salt marsh vegetation in the different zones the PPs were divided into eight functional groups to describe succession processes easier (Tab. 1 and Fig. 2). The criteria for characterizing the groups were: a similar position in the investigation area and/or a similar succession since 2002. The presence and dominance of key species and other characteristic species were also important criteria. For each group only examples of the PPs are described in detail. The following PPs were not considered in this study (PP 4, 55, 56, 65, 69, 75, 76 and 79) because they were destroyed, located outside the investigation area or were colonized each by non salt marsh vegetation. An increasing species number is often defined as restoration success (compare Wolters et al. 2005a) so the average species number for each group was calculated for every year of monitoring (Tab. 3).

The vegetation data of the PPs was supplemented by information of the average monthly inundation from the "Wasser- und Schifffahrtsdirektion Nordwest" WSA Emden. In

addition chemical data was used to describe succession processes for some PPs on a north to south transect through all salt marsh zones. For measuring pH a WTW pH/Cond 340i device with a pH-electrode SenTix 20 was used. Conductivity was examined with a TetraCon 325 electrode.

To obtain information about elevation above NN and distances to tidal channels of the PPs, aerial pictures from the "Nationalparkverwaltung Niedersächsisches Wattenmeer" and an elevation class model were analysed using a Geographical Information System (ArcGis).

Tab. 1: Functional groups of PPs with their salt marsh zonation before and after de-embankment, characteristics and grazing intensity

Group	Salt marsh zone in 2002	Salt marsh zone after de-embankment	Supplementary characteritics	Grazing	PPs belonging to group
1	high marsh	high marsh	*Elymus athericus*	abandoned 1992 to 1994	1, 2, 5 to 16, 19, 44
2	high marsh	middle marsh	-	abandoned 2002	17, 21, 22, 24 to 29, 31, 32, 35, 38 to 41, 45, 78, 85
3	high marsh	low marsh; pioneer zone	-	abandoned 2002	20, 33, 34, 42, 43, 46, 59, 89
4	high marsh	high marsh; glycophytic vegetation	embanked by the new dike	grazed by cattle	23, 62 to 64, 62b, 74
5	not existent	pioneer zone; low marsh; middle marsh	top soil removed	no grazing	24b, 25b, 26b, 42b, 43b, 85b
6	high marsh	high marsh	constant characteristic species	partly grazed by horses	18, 30, 36, 37, 52 to 54, 77, 84
7	not existent	pioneer zone; low marsh	former summer dike	no grazing	87, 88
8	low marsh; pioneer zone	low marsh; pioneer zone	outside the former summer dike; expansion of *Atriplex portulacoides*	no grazing	50, 51, 57, 58, 60, 61, 66 to 68, 70 to 73, 80 to 83

Nutrient Analysis

Pore water samples were taken with portable capillary lances at different depths for analysis of nitrogen. Sampling always took place adjacent to PPs in order to combine nutrient data directly with the vegetation. For determining Total Dissolved Nitrogen (TDN) the analysis was carried out according to Grasshoff et al. (1999). Three replicates per sample depth were made and average values were calculated. A Dr Lange Xion 500 photometer was used for analysing TDN.

Results

Distribution of key species within the PPs

The key species and their increase or decrease after de-embankment is documented below. The species are listed in order of their appearance from the pioneer zone to the high marsh in the investigation area. Only species with a relevant validity for the whole area or an important part were chosen.

Species of the pioneer zone

In 2002 the pioneer species *Salicornia stricta* was only present in PPs outside the summer polder with exception in PP 59. Altogether *S. stricta* was found in 22.9 % of all 83 PPs. The coverage was between 1 % and 55 % (Fig. 4). It was primarily an element in vegetation units of the lower marsh at this time, however, *S. stricta* dominated in PP 73 and 81 in the pioneer zone (Fig. 2 and 3). Since 2004 *Salicornia stricta* expanded into the area of the former summer polder. It was found in 4 PPs where it was absent in 2002. Because of the low number (33) of investigated PPs in 2004 where *S. stricta* was situated, it appears that the portion of colonized PPs decreased (Tab. 2). This can be considered a sampling artefact. In 2005 *S. stricta* was present in 25 additional PPs so that the portion of all PPs where it was growing increased considerably. On 25.5 % of the PPs which were already inhabited by *S. stricta* the coverage increased as well. There were only decreases in coverage outside the former summer polder. In the two following years *Salicornia stricta* continued to spread out onto more PPs, however in 2007 the coverage decreases by 10-20 % in 47.1 % of the PPs. From 2002 to 2007 the number of PPs where this species is present increased significantly (Tab. 2).

Like *Salicornia stricta Suaeda maritima* was located in 2002 primarily in PPs in front of the summer dike (group 8 in Fig. 2). However, in none of the PPs was *Suaeda maritima* a dominant species (Fig. 5). In 2004 *S. maritima* colonized further PPs as well as increased its coverage on already inhabited PPs (Tab. 2). This upward trend continued through to 2005. In this year *S. maritima* was present in 56.6 % of the PPs. On some PPs it was clearly dominant, for example PP 40 (Fig. 5 and Tab. 2). In 2006 the expansion stagnated. On 51.1 % of the already colonized PPs the coverage decreased up to 50 %. This trend switched 2007 again and

Suaeda maritima extended onto 65 % of the PPs. Yet it did not reach the average coverage of 2005 on most sample plots, e.g. PP 40 (Fig. 5).
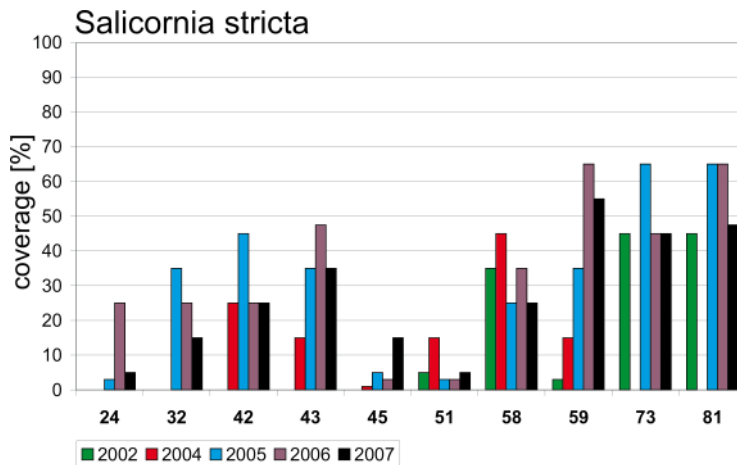
Fig. 4: Coverage of *Salicornia stricta* at selected PPs. PP 73 and 81 were not monitored in 2004

Species of the low marsh

The focus of the distribution area of *Aster tripolium, Atriplex portulacoides* and *Puccinellia maritima* in 2002 was outside the summer polder. Inside they were only present in PP 59. Some single specimens of *Aster tripolium* inhabited PP 40, 42 and 45. *Atriplex portulacoides* was also present in PP 26 (Fig 2). In 2004 after de-embankment *Aster tripolium* spread out on more PPs within the former summer polder and increased its coverage on the already colonized PPs (Tab. 2 and Fig. 6). The following year was characterized by equilibrium between new inhabited PPs and places where *Aster tripolium* disappeared (Tab. 2 and Fig. 6). Additionally coverage of *A. tripolium* decreased on many of the already occupied PPs. In 2006 this trend changed in favour of *A. tripolium*. The species spread out on new locations and increased its coverage (Tab. 2). This tendency continued until 2007 where *Aster tripolium* inhabited 55.5 % of all PPs.
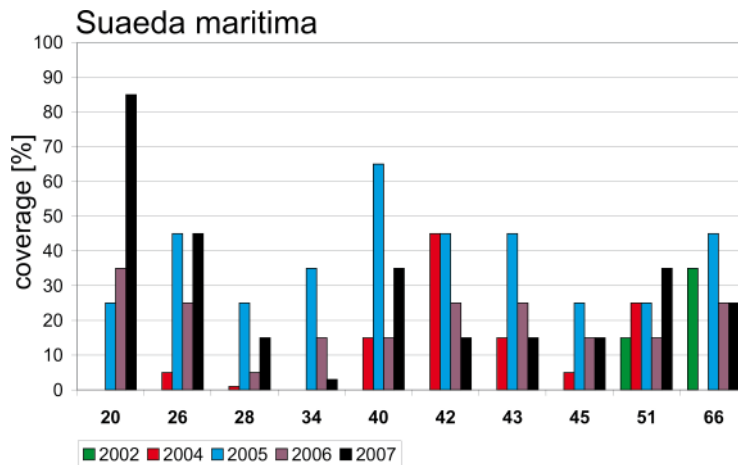
Fig. 5: Coverage of *Sueda maritima* at selected PPs. PP 34 and 66 were not monitored in 2004
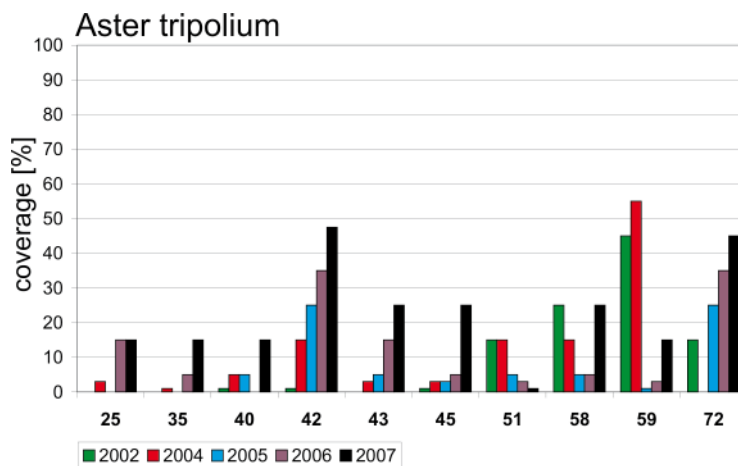
Fig. 6: Coverage of *Aster tripolium* at selected PPs. PP 72 was not monitored in 2004

As mentioned before *Atriplex portulacoides* was mainly situated outside the summer polder in 2002. The coverage of this species was quite heterogeneous. In some PPs *A. portulacoides* reached absolute dominance (Fig. 7) but in PP 70 only a single small specimen was present (coverage < 5 %). In 2004 *A. portulacoides* colonized additional PPs mostly inside the former summer polder with a low coverage (Tab. 2). In the already inhabited PPs the species increased its coverage. Until 2007 the expansion of *A. portulacoides* persisted. The portion of inhabited PPs increased continuously from 13.3 % in 2002 to 48.2 % in 2007, as well as, the species coverage (Tab. 2). On some sites *A. portulacoides* was able to establish itself after absence in 2002 and became dominant (PP 42 in Fig. 7).
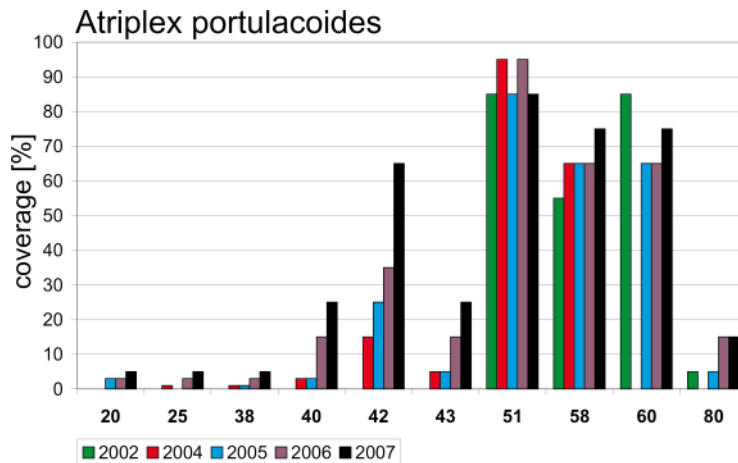
Fig. 7: Coverage of *Atriplex portulacoides* at selected PPs. PP 60 and 80 were not monitored in 2004

Puccinellia maritima only dominated PPs outside the summer polder in 2002 (PP 68 and 70) but usually it only accompanied other species. In 2004 *P. maritima* established itself in some PPs within the summer polder with low coverage (Tab. 2 and Fig. 8). On the already situated PPs coverage decreased. This tendency continued in 2005 and switched completely in 2006. *P. maritima* was found at fewer locations, but was able to increase its coverage on 33.3 % of the remaining PPs. The following year was characterized by a doubling of the situated PPs and a small increase of coverage on some of the PPs. Altogether *Puccinellia maritima* was able to expand its territory from 2002 to 2007 (Tab. 2).
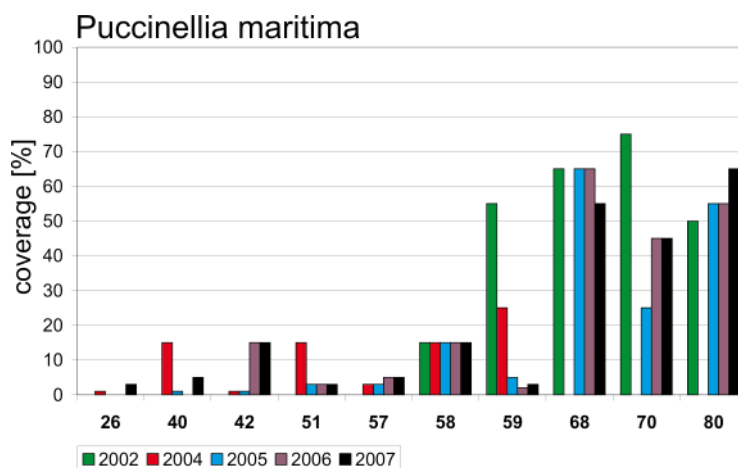
Fig. 8: Coverage of *Puccinellia maritima* at selected PPs. PP 68, 70, and 80 were not monitoted in 2004

Tab. 2: Proportion of colonized PPs, percentage of already inhabited PPs where species coverage decreased and increased

	Colonized PPs [%]	PPs where coverage decreased [%]	PPs where coverage increased [%]		Colonized PPs [%]	PPs where coverage decreased [%]	PPs where coverage increased [%]
Salicornia stricta (pioneer species)				**Suaeda maritima (pioneer species)**			
2002	22,9			2002	16.9		
2004	10.8	22.2	33.3	2004	14.5	8.3	25.0
2005	56.6	14.9	25.5	2005	56.6	4.3	27.7
2006	59.0	28.6	34.7	2006	56.6	51.1	27.7
2007	61.5	47.1	25.5	2007	65.1	20.4	40.7
Aster tripolium (low marsh species)				**Atriplex portulacoides (low marsh species)**			
2002	14.5			2002	13.3		
2004	19.3	12.5	25.0	2004	18.1	6.7	26.7
2005	25.3	38.1	14.3	2005	30.1	16.0	28.0
2006	37.4	12.9	32.3	2006	39.8	6.1	45.5
2007	55.4	10.9	34.8	2007	48.2	10.0	45.0
Puccinellia maritima (low marsh species)				**Limonium vulgare (middle marsh species)**			
2002	12.1			2002	9.6		
2004	12.1	20.0	0.0	2004	4.8	25.0	0.0
2005	21.7	33.3	5.6	2005	12.1	20.0	30.0
2006	18.1	13.3	33.3	2006	9.6	25.0	50.0
2007	36.1	6.7	16.7	2007	14.5	33.3	16.7
Juncus geradii (middles marsh species)				**Atriplex prostrata (middle and high marsh species)**			
2002	27.7			2002	34.9		
2004	21.7	44.4	27.8	2004	31.3	7.7	38.5
2005	21.7	13.0	60.9	2005	56.6	6.4	55.3
2006	30.1	32.0	24.0	2006	49.4	48.8	22.0
2007	31.3	53.9	15.4	2007	43.4	41.7	22.2
Artemisia maritima (middle and high marsh species)				**Festuca rubra (high marsh species)**			
2002	39.8			2002	61.5		
2004	20.5	11.8	52.9	2004	27.7	26.1	56.5
2005	41.0	35.3	23.5	2005	54.2	37.8	33.3
2006	44.6	18.9	46.0	2006	57.8	33.3	31.3
2007	45.8	29.0	29.0	2007	59.0	26.5	34.7
Elymus athericus (high marsh species)				**Elymus repens (high marsh species)**			
2002	19.3			2002	26.5		
2004	8.4	0.0	28.6	2004	6.0	60.0	40.0
2005	22.9	26.3	36.8	2005	21.7	38.9	27.8
2006	31.3	19.2	34.6	2006	27.7	17.4	43.5
2007	36.1	16.7	56.7	2007	24.1	70	5
Potentilla anserina (high marsh species)							
2002	57.8						
2004	25.3	81.0	0.0				
2005	34.9	58.6	13.8				
2006	32.5	37.0	40.7				
2007	24.1	30.0	45.0				

Species of the middle marsh

The two key species allocated only to the middle marsh show different succession after de-embankment. In 2002 *Limonium vulgare* was only distributed outside the summer polder except in PP 9 (Fig. 2). Until 2005 *L. vulgare* expanded its distribution a bit (Tab. 2), but it decreased in 2006. In 2007 *L. vulgare* colonized some new PPs (Tab. 2 and Fig. 9). The main

focus of the distribution area of *Limonium vulgare* was located outside the former summer polder pre and post de-embankment.
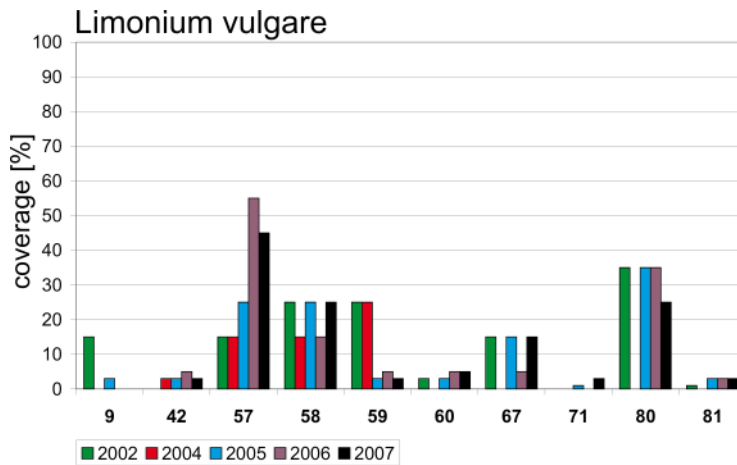
Fig. 9: Coverage of *Limonium vulgare* at selected PPs. PP 9, 60, 66, 71, 80, and 81 were not monitored in 2004

In contrast to *Limonium vulgare, Juncus gerardii* was only distributed in PPs within the summer polder in 2002 with exception of PPs 52 and 54. These PPs are situated very high about NN (Fig. 2). In fact *J. gerardii* supported by grazing (Bakker et al. 1985) expanded massively during embankment. Most of the sites were still grazed by cattle in 2002 or grazing was abandoned a short time before (compare Barkowski 2003). On many PPs *J. gerardii* dominated with coverage over 50 % (Fig. 10). In 2004 *J. gerardii* colonized further PPs and increased its coverage at 44.4 % of the already situated PPs (Tab. 2 and Fig. 10). One year later there was a sharp decrease in coverage of *J. gerardii*. The species lost ground in 60.9 % of the colonized PPs. This trend only lasted for 1 year and in 2006 *J. gerardii* again spread out onto new PPs and increased in coverage on most of the PPs (Tab. 2 and Fig. 10). In 2007 the species increased coverage in 53.9 % of the colonized PPs. Until 2007 *J. gerardii* was able to establish itself on PPs again which were colonized in 2002, as well. This process of die out after de-embankment and reestablishment after 5 years appears to be an adaptation to the new conditions. The colonization of new PPs (PP 29 in Fig. 10) was more an exceptional case.
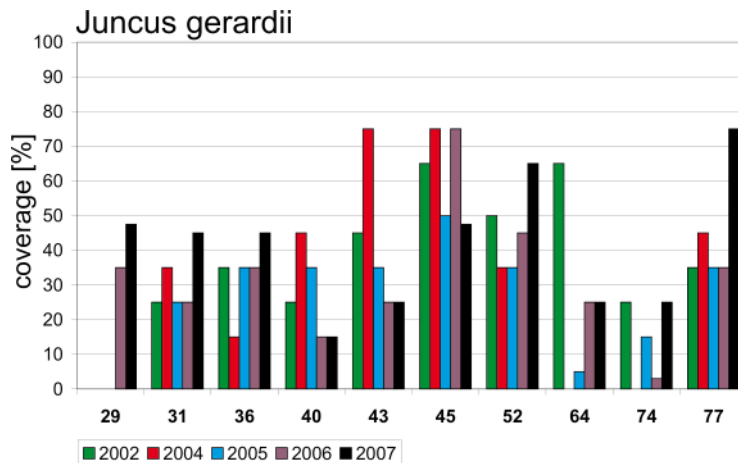
Fig. 10: Coverage of *Juncus gerardii* at selected PPs. PP 64 and 74 were not monitored in 2004

Species between middle and high marsh

Atriplex prostrata and *Artemisia maritima* are the species placed in this group. The PPs colonized by *Atriplex prostrata* in 2002 were located within the summer polder except PP 52. In most of the PPs just a few specimens were present with low coverage. Only on some places within a gull breeding colony where grazing had been abandoned it was able to expand a bit more (compare Fig. 2 and Fig. 11). In 2004 the portion of PPs where *A. prostrata* was present increased and additionally the species enlarged its coverage on the already colonized PPs (Tab. 2). The expansion of *A. prostrata* reached its maximum in 2005. In this year the species inhabited 57.9 % of the PPs and increased in coverage in most of the colonized PPs. The following years were characterized by a decrease. Until 2007 *A. prostrata* existed in only 43.3 % of the PPs and it lost much coverage, with the result that in many PPs only individual specimens were present. An exception was in the east of the investigation area (Fig. 2). Here *A. prostrata* spread out in some PPs (PP 8 and 16 in Fig. 11) dominated mostly by *Elymus* species.
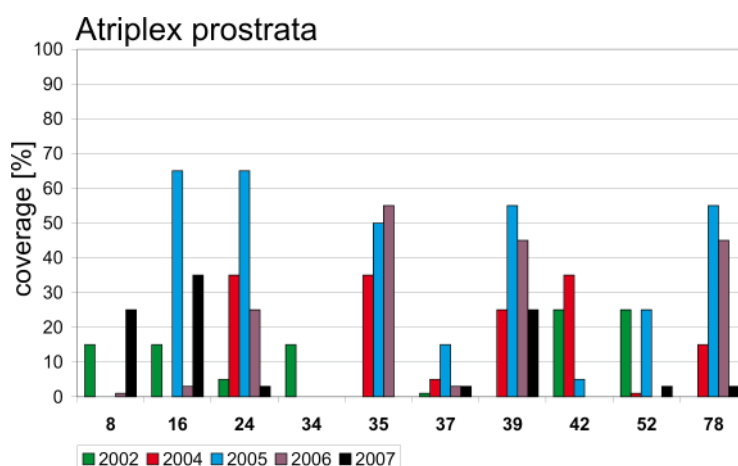
Fig. 11: Coverage of *Atriplex prostrata* at selected PPs. PP 8, 16, and 34 were not monitored in 2004

In contrast to *Atriplex prostrata, Artemisia maritima* was situated in PPs outside the summer polder, as well as, inside in 2002. These places were mostly non grazed and located in areas surrounding bird breeding colonies. The range of coverage varied between one single specimen (PP 37) and absolute dominance (PP 41). In 2004 the portion of colonized PPs remained constant but *A. maritima* increased in coverage in more than half of the PPs (Tab. 2). One year later the expansion continued in some PPs, but mostly coverage was constant or decreased (Tab. 2 and Fig. 12). Expansion of *A. maritima* stagnated in 2007 and finally it inhabited 45.8 % of the PPs.
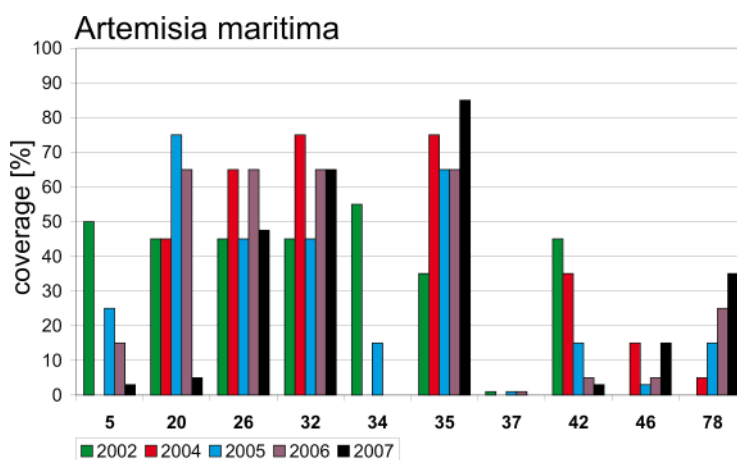
Fig. 12: Coverage of *Artemisia maritima* at selected PPs. PP 5 and 34 were not monitored in 2004

Species of the high marsh

Festuca rubra, Elymus athericus, E. repens and *Potentilla anserina* belong to this group but their succession after de-embankment differed markedly.

Elymus athericus and *E. repens* were only present in PPs within the summer polder in 2002. Their focus of distribution was located in the eastern part of the investigation area (group 1 in Fig. 2). On many sites one or both became dominant with coverage between 50 % and 100 % (Fig. 13 and 14). After de-embankment succession of the two *Elymus* species was quite different. *E. athericus* further colonized PPs in 2004 which are located more in the western part of the investigation area and it increased in coverage on the already inhabited PPs. In 2005 an equilibrium concerning the expansion and decline of *E. athericus* was reached, but a tendency was identified when the position of the PPs was considered. In the east *E. athericus* increased and it decreased in the west. The following 2 years showed a clear expansion tendency in the whole investigation area. In 2007 *E. athericus* even became absolutely dominant on the

colonized PPs in the east (PP 5, 7, 12, 15 and 19 in Fig. 2 and 13). From 2002 to 2007 *E. athericus* spread out from 19.3 % of the PPs to 36.1 %.
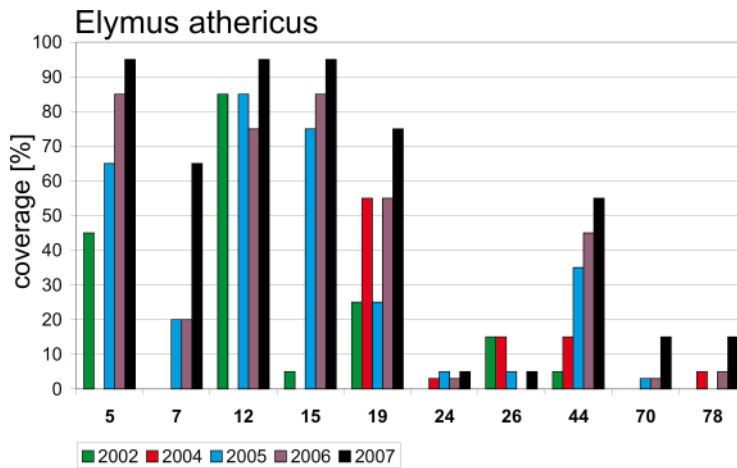
Fig. 13: Coverage of *Elymus athericus* at selected PPs. PP 5, 7, 12, 15, and 70 were not monitored in 2004

In 2004 only a few potential habits of *E. repens* were monitored, so the decrease of this species must be interpreted carefully. In 2005 however, this tendency of decline was clearly proved. Especially on the western locations *E. repens* was replaced by other species mostly by *E. athericus*. The coverage of *E. repens* decreased in 38.9 % of the inhabited PPs (Tab. 2). In the following year *E. repens* expanded on locations in the west again and increased in coverage in the PPs in the east, as well. The expansion process switched again in 2007, with the result that *E. repens* was absent in most of the former situated western PPs. In addition it lost coverage on the majority of all colonized PPs. Since 2002 the number of colonized PPs only decreased by 2.4 %, but coverage of *E. repens* within these locations decreased more clearly (Fig. 14). The decrease of *E. repens* was linked to an increase of *E. athericus* in most of the colonized PPs.

Elymus repens

Festuca rubra was present in almost all PPs inside the summer polder and on two locations outside in 2002. The average coverage was between 30 % and 50 %. In 2004 the portion of inhabited PPs decreased slightly and in addition in most of the colonized PPs the coverage decreased, as well (Tab. 2). One year later the number of PPs inhabited by *F. rubra* remained constant. There was no clear tendency in changing coverage by *Festuca rubra,* as it nearly decreased in as many PPs as it increased (Tab. 2). In 2006 and 2007 there was a small expansion on new PPs but this was accompanied with a loss of coverage. Since 2002 the number of PPs inhabited by *F. rubra* stayed relatively constant but within the majority of these PPs the species lost its dominance (Fig. 15).
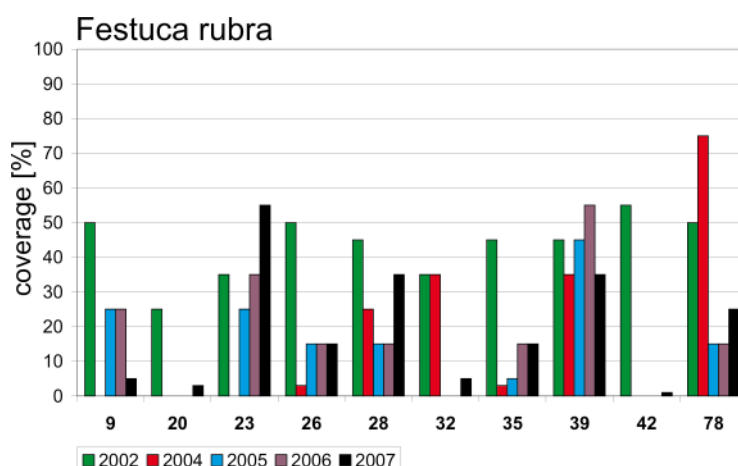
Festuca rubra

Fig. 15: Coverage of *Festuca rubra* at selected PPs. PP 9 and 23 were not monitored in 2004

Like the other three mentioned high marsh species, before de-embankment *Potentilla anserinas* distribution was focused inside the summer polder. There it was found in almost all PPs in 2002, but it inhabited only one PP outside. A total of 57.8 % of the PPs were colonized by *Potentilla anserina*. On most of these locations *P. anserina* covered more than 50 % and some PPs were completely dominated by this species (PP 20, 21, 28, 32, 39 and 78 in Fig. 16). In 2004 the portion of PPs inhabited decreased slightly (Tab. 2) but *P. anserina* decreased significantly in coverage on 81 % of these PPs. The loss of coverage reached up to 70 % (PP 32). In the following year *P. anserina* died off in most of the eastern PPs (compare Fig. 2 and Fig. 16) and it decreased again in coverage on 58.6 % of the still colonized PP. Both 2006 and 2007 were characterized by the further loss in presence of *P. anserina* (Tab. 2). Additionally, coverage decreased on the remaining locations in the south and east within the investigation area. However, *P. anserina* was able to spread out a little on northern PPs close to the new dike (Fig. 2) and especially on locations behind it. Until 2007 *Potentilla anserina* had disappeared from 58.3 % of the PPs inhabited in 2002.
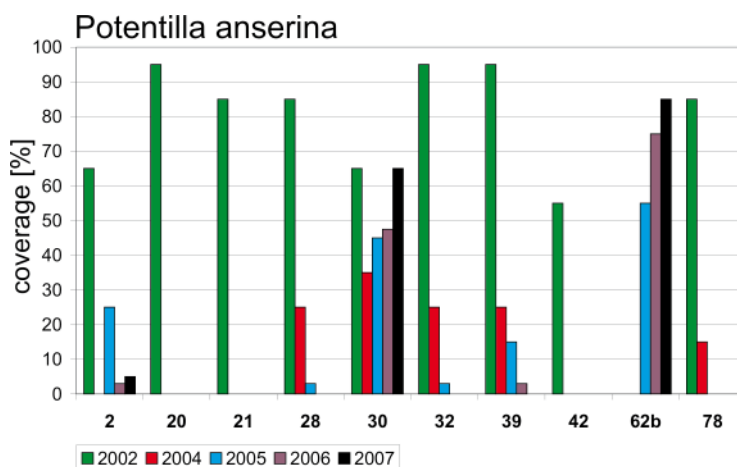
Fig. 16: Coverage of *Potentilla anserine* at selected PPs. PP 2 and 21 were not monitored in 2004. PP 62b was not monitored in 2002 and 2004

Vegetation succession of the Permanent Plots from 2002 to 2007

Wolters (2005a) defined success of salt marsh restoration as the increase and presence of characteristic species. One important problem is to determine how long it takes after de-embankment until it is possible to assess this situation. In the following sections the vegetation succession of the functional groups of PPs (Tab. 1) is described dealing with this question.

Group 1: High marsh; Elymus sp. (non grazed since 1992 or 1994)

All PPs in this group are located in the eastern part of the investigation area, except PP 44, which is placed on dune remnants situated within the summer polder (Fig. 2 and Tab. 1). The height above NN of these PPs is between 1.9 m and 2.6 m. Grazing by cattle was stopped on these locations in 1994 or in 2002 at PP 19 (compare Barkowski 2003, Steffens 2003). The vegetation of these PPs was mainly characterized by *Elymus athericus* and *E. repens.* Some of the higher located PPs in this group showed an increasing portion of *Phragmites australis* (PP 10 and 14 in Fig. 2). Due to the composition of species all PPs are classified as high marsh from 2002 to 2007 (Fig. 17).

Fig. 17: Vegetation zonation of functional PP groups from 2002 to 2007: sg (*salt influenced grassland*); hm (*high marsh*); mm (*middle marsh*); lm (*low marsh*); pz (*pioneer zone*)
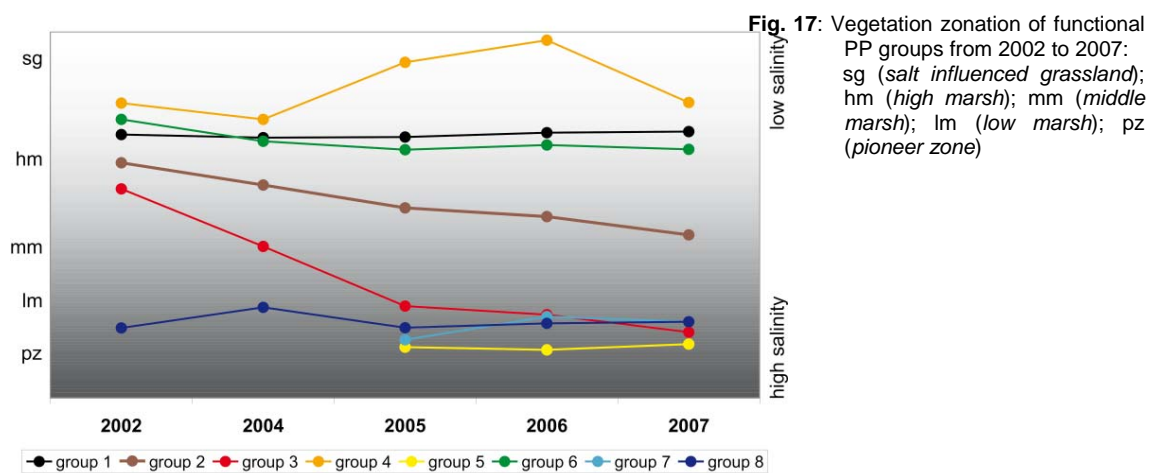
PP 12 is described as an example for this group (Fig. 18). Since 2002 especially *Elymus athericus* dominated the vegetation in this PP and was able to increase its coverage until 2007. Species like *Artemisia maritima, Agrostis stolonifera* and *Potentilla anserina* disappeared in 2005. The coverage of *Festuca rubra* clearly decreased after de–embankment, as well. *Elymus repens* and *Atriplex prostrata* were also present in this PP and varied in coverage from year to year. In 2006 *E. repens* increased in coverage, but in 2007 a decrease in coverage followed (Tab. 2 and Fig. 14). The average number of species situated in a PP in this group decreased continuously from 8.3 in 2002 to 5.9 in 2007 (Tab. 3).

Group 2: high marsh to middle marsh; unspecific (grazed extensive until 2002)

This group includes PPs which composition of species from 2002 to 2007 showed a clear tendency from higher marsh to middle marsh (Fig. 17). All sites are located 1.5 m to 2.2 m above NN and belong to the western part of the summer polder (Fig. 2 and Tab. 1). The PPs of this group are situated 0.5 m below the average altitude of PPs of group 1. Predominantly vegetation units dominated by *Festuca rubra, Juncus gerardii, Carex distans* and *Ononis spinosa* represented the state of 2002. Until 2007 the former dominant species disappeared or decreased in coverage. Since 2004 species like *Artemisia maritima, Atriplex prostrata, Atriplex portulacoides* and *Suaeda maritima* started to invade the PPs in this group and partly became dominant.

As an example for this group the succession of PP 78 will be presented in detail (Fig. 18). In 2002 the vegetation was characterized by a high coverage of *Potentilla anserina* (85 %), *Festuca rubra* (50 %) and *Agrostis stolonifera* (45 %). In addition species of the upper Armerion (*Carex distans, Trifolium fragiferum*) and glycophytic species like *Lolium perenne, Trifolium repens, T. pratense, Cirsium arvense* and *Poa pratensis* were present. Only *Juncus gerardii* was present as an element of the lower Armerion. In the year 2004 a clear decrease of all glycophytes was evident and until 2005 they had disappeared like the upper Armerion species with the exception of *Festuca rubra*. Instead of these plants *Artemisia maritima* and *Atriplex prostrata* started to expand. Until 2006 the two pioneer species *Salicornia stricta* and *Suaeda maritima* were increasing in coverage, as well. In 2007 *Salicornia stricta* further increased its coverage whereas *Suaeda maritima* decreased. Additionally *Festuca rubra* and *Juncus gerardii* recovered and expanded a little (Fig. 18). *Elymus athericus* was able to establish itself as an element of the high marsh. The composition of the vegetation in 2007 was a mixture of species from all salt marsh zones. The number of species in this group decreased until 2005 as a result of the decline of more glycophytic related species. In the following 2 years the number of species rose again and mostly salt marsh species of the middle and low marsh replaced former vegetation.

Tab. 3 Average number of species for the PP groups from 2002 to 2007. The values from group 1 and 8 in 2004 (bold) have to be carefully interpreted due to monitoring only a small number of PPs belonging to these groups. In 2002 PPs of group 5 and 7 have not been monitored, as well as, the PPs of groups 4, 5 and 7 in 2004

	2002	2004	2005	2006	2007
group 1	8.3	**8.0**	6.2	6.3	5.9
group 2	10.1	9.1	8.3	9.2	9.4
group 3	8.6	7.6	6.1	6.0	5.8
group 4	12.6	-	12.6	14.5	12.6
group 5	-	-	1.3	3.8	5.0
group 6	15.2	13.0	12.7	14.4	10.9
group 7	-	-	2.5	5.5	9.0
group 8	5.2	**6.3**	5.8	5.8	6.4

Group 3: high marsh to low marsh or pioneer zone; unspecific (non grazed until 1994)

The PPs in this group are 1.3 m and 1.6 m above NN so they are clearly located lower the PPs in group 1 and 2. All sites of group 3 were situated directly behind the former summer dike or completely located in the west of the polder (Fig. 2 and Tab. 1). In 2002 these PPs were characterized by vegetation of the high marsh especially by *Festuca rubra, Juncus gerardii* and *Artemisia maritima*. Until 2007 the succession in group 3 led to vegetation units of the lower marsh and the pioneer zone (Fig. 17). Species like *Salicornia stricta, Atriplex portulacoides* and *Suaeda maritima* dominated these PPs 4 years after de-embankment. Although PP 89 was made in 2005 it was assigned to this group because its state of vegetation in 2002 could be reconstructed using vegetation mapping from that year (Barkowski 2003). In 2002 *Juncus gerardii* dominated this PP and in 2007 it was *Salicornia stricta*.

PP 46 was taken as an example for the detailed description of this group (Fig. 18). In 2002 there were only species of the upper Armerion (for example *Festuca rubra, Elymus repens*) and glycophytic species (*Trifolium repens, Potentilla anserina* and *Poa pratensis*) present in this PP. Two years later these species had disappeared or were only represented by a few specimens. *Atriplex prostrata* was dominating this PP in 2004 with coverage of 65 %.
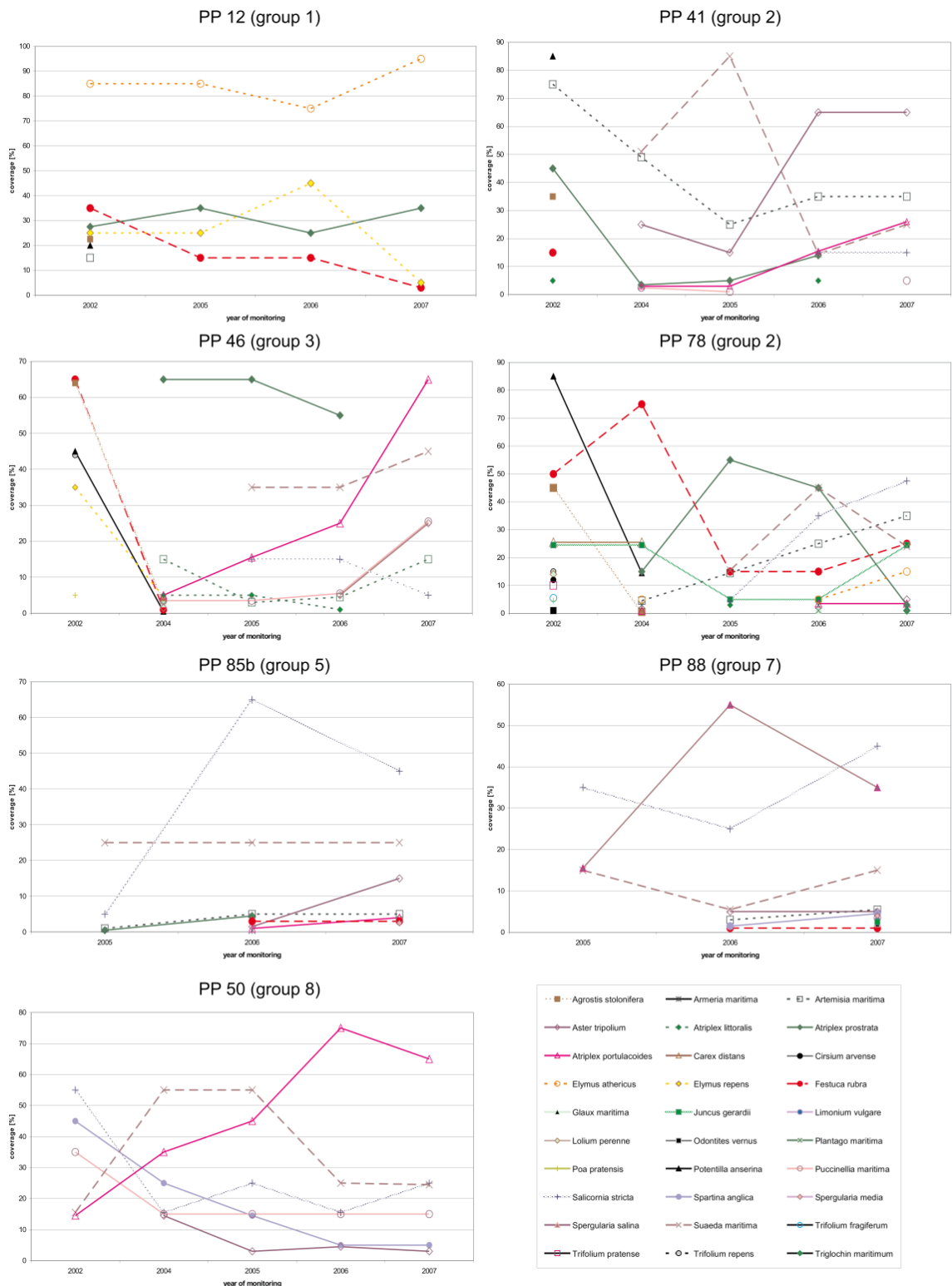
Fig. 18: Vegetation succession of PP 12, 41, 46, 50, 78, 85b, and 88 from 2002 to 2007

Species having a lower degree of coverage were among others *Artemisia maritima, Atriplex portulacoides* and *Puccinellia maritima* in PP 46 (Fig. 18). In 2005 the pioneer species *Salicornia stricta* and *Suaeda maritima* colonized PP 46. The glycophytes and the upper

Armerion species completely disappeared, whereas *Atriplex prostrata* still dominated this PP. Until 2007 *A. prostrata* disappeared but *Atriplex portulacoides* increased its coverage and became dominant. The only Armerion species in this PP was *Artemisia maritima* with coverage of 15 %. *Suaeda maritima, Puccinellia maritima, Aster tripolium* and *Salicornia stricta* were growing in this PP as companions (Fig. 18). This succession from vegetation related to the high marsh over a state of middle marsh vegetation to the low marsh was representative for group 3. During the investigation period the number of species decreased continually from 8.6 in 2002 to 5.8 in 2007. Additionally the composition of species changed dramatically.

Group 4: high marsh; glycophytes (still grazed and embanked)

This group contains PPs located within the so called Großes and Kleines Schlopp (Fig. 1 and 2, Tab. 1). These areas were separated from the rest of the investigation area by the new dike. Because of its crest height (3.2 m above NN) the PPs of this group were inundated less often than during the time of the former summer dike (crest height 2-2.25 m above NN). A further difference to the other groups is the continuous grazing of this area. The PPs located in the Großes Schlopp (PP 62, 63 and 64 in Fig. 2) were characterized by a decrease of *Juncus gerardii* since 2002 (PP 64 in Fig. 10) and an increase of glycophytic species. A change in succession was recognizable in 2007 after controlled and natural flooding after storm surges in this area. Salt marsh species like *J. gerardii* were able to expand a little but more important was the decrease of fresh grassland species (compare Fig. 17). PP 62b is different than the other PPs within the Großes Schlopp because the top soil was removed in February 2005. This was done to obtain information about species which were able to establish themselves first on blank soil. Since 2005 this PP has been dominated by *Potentilla anserina* (PP 62b in Fig. 16). In the first year of monitoring *Trifolium repens* was also present with 55 % coverage but it decreased especially in 2007 when the PP was inundated several times. *Festuca rubra* and *Agrostis stolonifera* increased their coverage from 2002 to 2007. Most of the other species present in this PP were represented by only a few specimens. There was no great difference between PP 62b and the three other sites within the Großes Schlopp (PP 62, 63, 64).

The two PPs located in the Kleines Schlopp (PP 23 and 74) were characterized in 2002 by *Carex distans, Ononis spinosa* and *Juncus gerardii*. Following completion of the new dike salt marsh species decreased and glycophytic species like *Lolium perenne* and *Trifolium repens*

expanded. Both species were present in 2002 as companions. In 2007 after the area had been inundated like the Großes Schlopp the glycophytes decreased slightly and the salt marsh species *Juncus gerardii* and *Festuca rubra* were able to claim more coverage (PP 74 in Fig. 10; PP 23 in Fig. 15). The number of species stayed constant at 12.6 from 2002 to 2005. In 2006 it increased up to 14.5 because of the establishment of glycophytes. One year later the average number of species declined again to 12.6 (Tab. 3).

Group 5: top soil removed; unspecific

In this group PPs are summarized where the top soil (approximately 10 cm) had been removed in February 2005. The PPs were arranged in two "north to south" transects and each of them was placed next to a PP where the topsoil had not been removed (Fig. 2, Tab. 1). They are located between 1.5 m and 1.8 m above NN. After removing the top soil the species number was zero in this group in spring 2005. As expected it rose continuously in the first years after de-embankment (Tab. 3). The PPs of the eastern transect (24b, 25b, 26b) were not colonized by vascular plants except some *Suaeda maritima* specimens in 26b. In 2006 the pioneer species *Salicornia stricta* and *Suaeda maritima* were dominating these three PPs. However, in 25b and 26b there were already species of the middle and high marsh present (*Atriplex prostrata* and *Elymus athericus*). In the following year species like *Artemisia maritima, Atriplex portulacoides, Aster tripolium* and *Puccinellia maritima* colonized one or more of the PPs but *Salicornia stricta* and *Suaeda maritima* remained dominant.

There was a similar succession of the vegetation of the western transect (PP 42b, 43b and 85b). In 2005 *Salicornia stricta* and *Suaeda maritima* were the dominating species in all three PPs. In addition in PP 85b *Artemisia maritima* and *Atriplex prostrata* were also present. Until 2007 species like *Atriplex portulacoides, Aster tripolium* or *Puccinellia maritima* inhabited the PPs. In this year PP 85b was already colonized by eight species from all salt marsh zones (Fig. 18).

Group 6: high marsh; unspecific (very heterogeneous group, but constant characteristic species for each PP)

Group 6 is a more heterogeneous group which contains PPs with vegetation of the high marsh (Fig. 2, Tab. 1). They all stayed quite constant in their composition of species and salt marsh zonation (Fig. 17). This group is composed of PPs located outside the summer polder (52, 53 and 54) as well as PPs embanked in 2002 (18, 30, 36, 37, 77 and 84). They are situated on an altitude level (1.9 m and 2.6 m above NN) similar to group 1. In contrast to group 1 these PPs were not dominated by *Elymus* species. Most of the sites inside the summer polder were grazed until 2002 and PP 30 and 37 are still grazed by horses very restrictively. In PP 30 and 77 *Elymus athericus* was present since 2006 respectively 2007 with a few specimens and in PP 18 both *Elymus* species were present since 2002 but were still not dominant. Otherwise the PPs were characterized by changing coverage of *Juncus gerardii, Festuca rubra, Potentilla anserina* and *Agrostis stolonifera*. Additionally in PP 30 and 84 *Carex distans* and *Ononis spinosa* were an important element of the vegetation.

Outside the summer polder the PPs of group 6 were characterized by completely different types of vegetation. PP 53 was dominated by *Bolboschoenus maritimus* and *Cotula coronopifolia* from 2002 to 2007. Only the composition of the accompanying species changed from year to year. In PP 52 characterizing species (*Juncus gerardii, Glaux maritima, Plantago maritima* and *Odontites vernus*) showed a great constancy from 2002 to 2007 whereas the composition of companions changed.

The PP 54 exhibited a vegetation type similar to the *Centaurio – Saginetum nodosae* (Diemont, Sissingh et Westhoff 1940) from 2002 to 2006. In 2007 the vegetation changed to a *Festuca rubra* dominated type, after a ditch has been dug adjacent to the PP.

The number of species was quite different in this group for each PP, but there was a tendency of a decreasing number of species from 2002 to 2007. A temporary increase was only documented in 2006 (Tab. 3).

Group 7: unspecific (situated where the former summer dike was located)

Only two PPs (87 and 88) belong to this group. They have to be separated from the other PPs because of their unique position at the location of the former summer dike (Fig. 2,

Tab. 1). In contrast to the PPs of group 5 which also showed no vegetation in February 2005, PP 87 and 88 were covered in August 2005 with vegetation up to 40 % (Fig. 18). The dominating species were *Salicornia stricta* and *Suaeda maritima*, but in PP 88 *Spergularia salina* was present in 2005 with coverage of over 10 %. In the following 2 years the number of species rose rapidly. Especially in PP 88 12 species were present in 2007. These plants represented all salt marsh zones (Fig. 18). Like group 5 the number of species increased continually from zero in 2004 to nine in 2007.

Group 8: Low marsh and pioneer zone; Atriplex portulacoides and unspecific (outside summer polder)

In this group all PPs were selected which were located outside the former summer polder (Fig. 2, Tab. 1) except the PPs of group 6 (52, 53, 54). The sites were never embanked and are between 1.3 m and 1.8 m above NN. They were characterized by vegetation of the low marsh or the pioneer zone (Fig. 17). A tendency which most of these PPs had in common was the expansion of *Atriplex portulacoides*. There were however in some PPs great differences in coverage (compare Fig. 7). The locations 51, 58, 60 and 72 were dominated by *A. portulacoides* from 2002 to 2007. In PP 50 this species was able to replace *Salicornia stricta* and *Spartina anglica* which were the dominant species in 2002 (Fig. 18). Additionally *A. portulacoides* increased in coverage in PP 57, 61, 71 and 80.

PP 82 was dominated constantly by *Spartina anglica*. In PP 57, 61, 66, 67, 71, 73, 81 and 83 *Spartina anglica, Salicornia stricta* and *Suaeda maritime* were able to compete against other species and had various coverage. Among others *Limonium vulgare* and *Puccinellia maritima* were frequent companions. *P. maritima* reached dominance in PP 68, 70 and 80. These PPs were situated on the highest places in group 8 and contained the greatest number of species. Even middle and high marsh species like *Artemisia maritima* and *Elymus athericus* were able to establish themselves here.

In this group the average number of species rose from 5.2 in 2002 to 6.4 in 2007. The year 2004 is excluded because only four of 17 PPs of this group had been monitored.

Discussion

In this chapter the results already presented separately as key species and functional groups are now combined to draw an overall picture of salt marsh succession after de-embankment on Langeoog Island.

Until 2002 vegetation expanded in the entire area within the Langeooger summer polder composed primarily of high marsh species and even glycophytes. Species distribution was caused by factors like nutrient availability, grazing intensity and soil properties (Barkowski 2003; Petersen 2003; Steffens 2003) and it was not dependent on the inundation frequency as is the case normally in common salt marshes. After the summer dike was removed the impact of the regular inundations caused an intensive die out of the former vegetation and led to new vegetation succession. Therefore flooding by seawater became the primary cause of species establishment (compare Roozen & Westhoff 1985). Now the zonation of the salt marsh is dependent on salinity. Kolditz et al. (2009) showed this on one transect (PP 60, 42, 85, 62) on Langeoog Island (Fig. 2). In Figure 19 the salinity for PP 42 is presented as an example for low marsh and in Figure 20 PP 85 as an example for high marsh. PP 62 situated in the Großes Schlopp showed very low salinity (0 to 8 ‰) and served as an example for the previous embanked situation before 2003. The pH results do not show much spatial variation or great amplitudes (Kolditz et al. 2009) (Fig. 21 and 22). Therefore pH is not considered to have a major influence on vegetation. The die out of the eminently fresh water related species turns out to be a direct effect of the flooding with seawater.
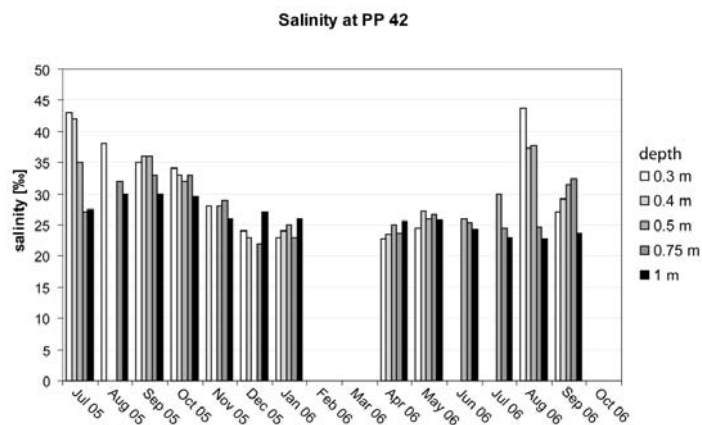
Fig. 19: Salinity at PP 42 from July 2005 to September 2006 at different depths

Dependent on the number of inundations glycophytic and high marsh species disappeared in the very low parts of the summer polder. The key species *Potentilla anserina* died out in a large part of the investigation area especially in the areas below Mean High Tide Level, because of increasing salinity after de-embankment. The same processes led to a die out of *Festuca rubra, Agrostis stolonifera* and *Juncus gerardii* in areas close to the former summer dike. The huge amount of biomass resulting from the decay of former vegetation (especially PPs of group 2 and 3) led to an increase of nutrients in the first years after de-embankment.
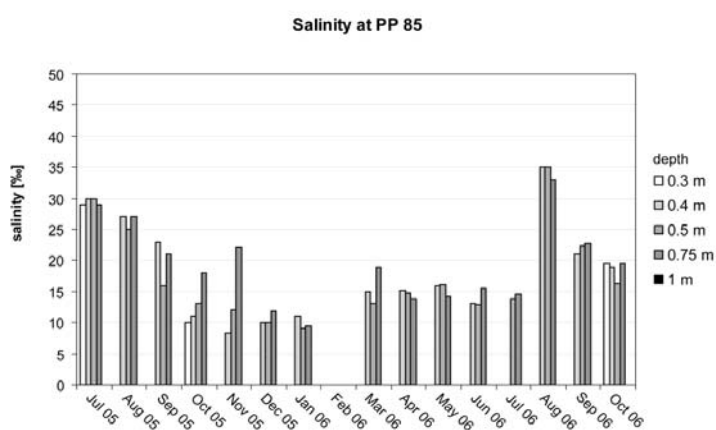
Fig. 20: Salinity at PP 85 from July 2005 to September 2006 at different depths
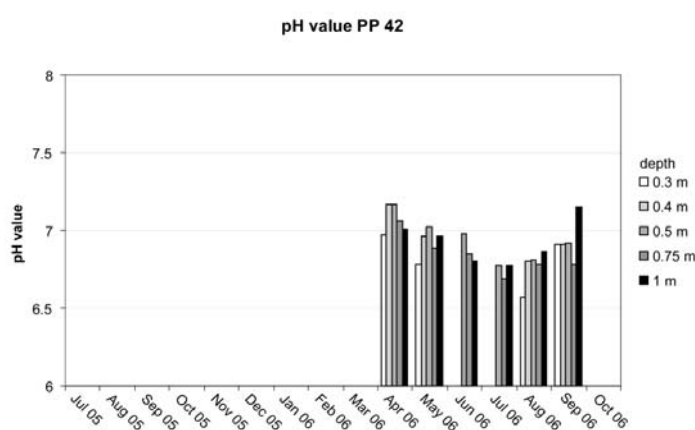
Fig. 21: pH at PP 42 from April 2006 to September 2006 at different depths

Principally the release of nitrogen after 2002 all over the former summer polder influenced the composition of species intensely. Nitrogen is the limiting nutrient for salt marsh plants (Adam 2002; Bakker & Piersma 2005; Cartaxana & Catarino 1997; van Wijnen & Bakker

1997; van Wijnen & Bakker 1999) so it primarily influences salt marsh succession. Data of pore water analyses from PP 42 (Fig. 23) documented a peak of TDN in spring 2005 which might be the major result of the de-embankment and additionally an effect of increased winter storm surges in 2004/05. Storm surges usually deliver a lot of biomass which serves as a nitrogen source (compare Leendertse et al. 1997). In spring 2006 TDN was at an extremely lower concentration level. Both results are supported by distribution of more nitrophytic plants in 2005 than in 2006.

pH value PP 85
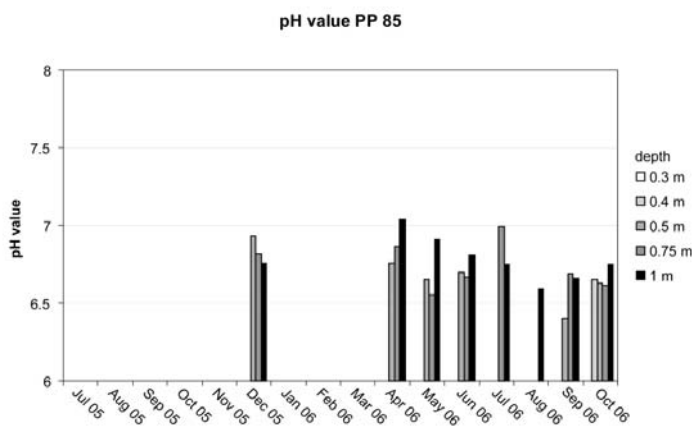
Fig. 22: pH at PP 85 from December 2005 to October 2006 at different depths

The expansion of three nitrophytic key species (*Suaeda maritima, Atriplex prostrata* and *Artemisia maritima*) started in 2004 after de-embankment and increased in 2005. This does not appear to be an adaptation to special salt marsh zones by the species but rather seems to be due to nutrient availability which apparently at this time is much more important as the key distribution factor than elevation (compare Roozen & Westhoff 1985). *S. maritima* had its focus of distribution in the lower and the other two species in the higher parts of the salt marsh. However, specimens of *S. maritima* were found in the high marsh in large numbers too (PP 40 in Fig. 5). Therefore nitrogen gave those three species an advantage in competition (compare Beeftink et al. 1978). Another reason was the high number of seeds these species can produce (Chang et al. 2007) and the easy dispersal by the tides of their seeds (Tessier et al. 2002). Additionally it was important that species were located in the direct surrounding of the summer polder in order to be able to colonize the investigation area this fast (Wolters et al. 2005a; Wolters et al. 2005b). Before de-embankment small numbers of specimens of *S. maritima, Artemisia maritima* and *Atriplex prostrata* were already present. These nitrophytic species established especially in breeding colonies of gulls with high nutrient content in the soil (Barkowski 2003) (PP 40 in Fig. 5 and PP 34 in Fig. 11 and 12).
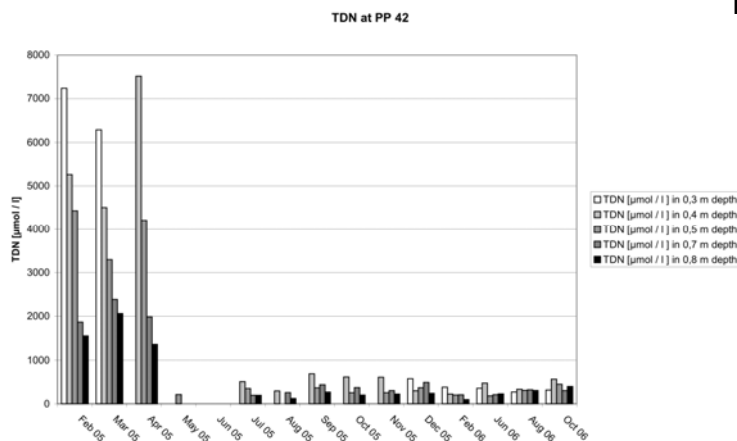
Fig. 23: Total dissolved nitrogen in pore water at PP 42 from February 2005 to October 2006 at different depths

In 2006 the huge amount of nitrogen had disappeared (Fig. 23) because of absorption by plants, washing out by pore water and additionally a result of fewer storm surges in the previous winter 2005/2006. The reduction in TDN levels increased the competitiveness and enhanced expansion of other salt marsh plants such as *Salicornia stricta, Atriplex portulacoides* or *Aster tripolium*. One reason for the much slower establishment of the key species *A. portulacoides* was its almost complete absence inside the summer polder until 2002. This species focus in 2002 was in the western part of the investigation area outside the summer polder. A still existing part of the summer dike in the west (Fig. 1) prevented direct transport of seeds to the polder by the tides. This result coincided with the definition of species pools and their influence on salt marsh succession as postulated by Wolters et al. (2005 a). In 2007 *A. portulacoides* had inhabited most of the potentially available habitat in the low marsh and increased its coverage significantly. This succession is described by Wolters et al. (2005 a) and Beeftink et al. (1978) as well. They predicted *A. portulacoides* as the dominant species in the low marsh and *Elymus athericus* in the high marsh. This was supported by the still existing anthropogenic ditch system, which prevents hydrodynamic activity common in a dendritic creek system. On Langeoog Island on many parts of the salt marsh this situation is given. Taking the low marsh in the west of the investigation area and the succession from 2002 to 2007 as an example (group 8) for the future (PP 51 in Fig. 7 and PP 50 in Fig. 18) then *Atriplex portulacoides* will become the absolute dominant species in the low marsh. Species such as *Aster tripolium, Puccinellia maritima* and *Suaeda maritima* are only competitive in areas where *Atriplex portulacoides* communities are disturbed (Beeftink et al. 1978). Especially *Puccinellia maritima* needed a longer time to establish itself in the former summer polder. Additionally *A.*

portulacoides was supported by the transport of fresh sediment into the investigation area after de-embankment. The accretion allowed a good aeration of the soil which resulted in an increase of *A. portulacoides* (Roozen & Westhoff 1985).

East of the former summer polder where grazing had been abandoned more than 15 years before, especially *Elymus athericus* and partly *E. repens* were able to expand and obtained absolute dominance (PPs of group 1). Other species were mostly replaced and suppressed. The effects of de-embankment were demonstrated by a decrease of *E. repens* in favour of *E. athericus* because *E. athericus* is able to tolerate a higher inundation frequency than *E. repens* (compare Esselink et al. 2002). In addition *E. athericus* reacts positively to increasing nitrogen availability (Leendertse et al. 1997; van Wijnen & Bakker 1997; van Wijnen & Bakker 2000). The highest parts of the eastern salt marsh are under the influence of fresh water coming from adjacent dunes. Under these brackish conditions *Phragmites australis* became competitive and expanded extensively (compare Bakker et al. 2003). On locations with high nitrogen availability *Cirsium arvense* expanded in the east, too. After abandoning grazing in most of the western parts of the former summer polder *Elymus athericus* established itself in more PPs in the west. Especially the PPs of group 2 were suitable. Thus, the situation of an almost complete monoculture in a large part of the summer polder is quite realistic (van Wijnen & Bakker 1999; Wolters et al. 2005a). On many parts of the mainland salt marshes this problem is found, too. To prevent this kind of succession some measures such as controlled grazing (Bakker et al. 2003; Kleyer et al. 2003) or the establishment of a more natural dendritic ditch system would help (Reise 2005). Group 6 was not so much influenced by the drainage system. The PPs in this group are as high above NN as the PPs in group 1 but they are characterised by individual factors like water logging (PP 53) or by a small mosaic of little hollows and hillocks. A greater dynamic is the result of these factors which prevents dominance by any one single species.

Another important reason for preventing monocultures is the role of salt marshes as important nature conservation areas. Especially for invertebrates and breeding birds it is necessary to provide a variety of different habitats to accommodate a larger number of species.

Comparing the investigation area with the two other salt marshes of Langeoog Island (Fig. 1) the differences between natural or anthropogenic influenced salt marshes become apparent.

Both of the potentially natural areas are quite small but show a higher species diversity. For example *Atriplex pedunculata, Carex extensa* and *Oenanthe lachenalii* are found there, yet are missing completely in the investigation area. *Juncus maritimus* covers large areas in the east and the west of Langeoog, but there are still only single specimens inside the former summer polder. A reason for this kind of species distribution could be a lack of hydrodynamics caused by the old anthropogenic persistent drainage system. Additionally the transport of seeds from the east and west to the former summer polder by the tides is more by chance. As Wolters et al. (2005a) and Dausse et al. (2008) mentioned species which belong to the regional species pool will take a long time to establish in new areas. Even *Limonium vulgare,* which is present in the investigation area, could not establish itself on many locations inside the former summer polder. Group 5 and group 7 documented a succession with salt marsh species only present in the direct surrounding after removing the former vegetation and top soil completely. Due to these facts, judging the success of a salt marsh restoration program by monitoring individual species or evaluating the number of present species has to be done carefully. The period of time after de-embankment or the location of the salt marsh with its surrounding areas must be considered as well. If species richness is the most important factor for a potential natural salt marsh, then seeds of key species must be specifically sown within the restoration area to obtain the desired results.

The opposite situation of the de-embanked summer polder is found in the Großes and Kleines Schlopp. These areas have been separated from the rest of the investigation area by a dike higher than the old summer dike, so natural flooding has become nearly impossible. The salt marsh species were replaced progressively by glycophytes (PPs of group 4). Grazing by cattle prevented the dominance of grass species like *Elymus* spec., *Phragmites australis* or *Dactylis glomerata*. Some natural and controlled inundations in winter 2006/2007 showed that salt marsh species could expand again. Therefore with little effort the Großes and Kleines Schlopp could remain salt influenced areas. The grazing activities make clear that species diversity in ditched salt marshes is increased and mono cultures are prevented.

Inundation frequency and its effect on vegetation

Before de-embankment the summer polder was flooded mostly by storm surges in winter. The average inundation rate was approximately 16 times per year. In all functional

groups of PPs located in the former summer polder the inundation frequency increased after de-embankment. Group 8 is located outside the summer polder so inundation frequency remained constant. Within group 4 the inundation rate decreased dramatically because the PPs in this group are located behind the new dike. Now there is only one natural inundation per year. This explains expansion of glycophytes in this group.

The inundation frequency of group 1 rose marginally to 21 times a year. This might explain the advantage of *Elymus athericus* against *Elymus repens*. The average frequency of group 6 was nearly the same (25 times per year) but *Elymus athericus* did not establish itself within this group. Therefore other abiotic factors such as those previously mentioned must have a great influence on the extent of expansion of *E. athericus*.

There were 97 inundations per year in group 2. The increasing influence of seawater led to the die out of glycophytes like *Potentilla anserina* and benefited halophytes like *Artemisia maritima, Atriplex prostrata, Atriplex portulacoides* and *Suaeda maritima*. After adapting to the new conditions, *Juncus gerardii* and *Festuca rubra* were able to expand in this group again. The abandonment of grazing also enabled *E. athericus* to colonize PPs within group 2. The vegetation of group 3 changed more intensively than in the other groups. Inundation frequency increased up to 261 times per year. This was comparable to group 8 (276 times per year). After die out of the former vegetation of 2002 the new composition of species of group 3 was also comparable to group 8 (compare PP 46 and 50 in Fig. 18). Reestablishment of natural salt marsh zonation occurs faster if the former vegetation vanished completely and there is a more or less natural salt marsh nearby.

Group 5 and 7 showed intermediate inundation frequencies from 150 to 200 times per year. In both groups the succession started on bare soil. Therefore first pioneer annual species with high seed productivity like *Salicornia stricta* and *Suaeda maritima* were able to spread out (Wolters et al. 2005b) but until 2007 more competitive species of other salt marsh zones also were able to establish (PP 88 in Fig. 18).

Salt marshes as coastal defence

Salt marshes as a part of coastal defence became more important, thus many restoration projects all around the North Sea are being realized (Wolters et al. 2005a). The main tasks of salt marshes are to decrease wave energy and prevent eroding through is vegetation

density and structure. Salt marsh vegetation is also responsible for retaining sediment from the water. This increase of salt marsh elevation accompanied by expected sea level rise is likewise an important argument for restoration projects. Wittig et al. (2004) documented that natural vegetation is more effective in coastal protection than anthropogenic influenced vegetation. Therefore it is important to start to consider the establishment of specific species early. It is necessary to break up the old drainage structure and accelerate the development of a dendritic creek system (compare Dausse et al. 2008). An anthropogenic drainage system with parallel ditches which reduces hydrodynamic processes can remain for centuries (Freund & Streif 1999). A dendritic ditch system like in natural salt marshes should be established to promote sedimentation (Reed et al. 1999). Fresh sediment allows good aeration in the soil which is important for many salt marsh species (Roozen & Westhoff 1985). On Langeoog Island natural erosion of the drainage system and creation of meandering creeks only takes place at some sites close to three big tidal channels.

Conclusion

Salt marsh restoration is a long time process. The results of this research show that only a few years after de-embankment the zonation of salt marsh is re-established but it takes mush longer for the species richness and composition of a natural salt marsh to be obtained. De-embankment is indeed in important factor for restoration however it should not be the only human measure made in the restoration process. The construction of a dendritic ditch system could accelerate succession.

Even grazing activities should not be abandoned completely to prevent mono cultures. On Langeoog Island the most successful species after de-embankment were *Atriplex portulacoides* in the low marsh and *Elymus athericus* in the high marsh. Especially in areas with low dynamics they became dominant. Due to a high nutrient availability after decay of the former vegetation temporary communities of nitrophytic plants like *Suaeda maritima, Atriplex prostrata* and *Artemisia maritima* expanded massively. After the decline of nitrogen availability other salt marsh species became more competitive. Species richness decreased after de-embankment and has not reached the level of 2002 until 2007. Monitoring vegetation succession on Langeoog Island should be continued to complete the picture.

Acknowledgments

References

Adam, P. (2002) Salt marshes in a time of change. Environ. Conserv. 29 (1): 39–61

Ahlhorn, F. & Kunz, H. (2002) The future of historically developed summer dikes and polders: a salt marsh use conflict. *Littoral*: 365–374

Bakker, J. P. (1978) Changes in a salt-marsh vegetation as a result of grazing and mowing – a five year study of permanent plots. Vegetatio 38 (2): 77–87.

Bakker, J. P., Bos, D. & de Vries, Y. (2003) To graze or not to graze: That is the question. In: Wolff, W. J., Essink, K., Kellermann, A., van Leeuwen, M. A. (ed) Challenges to the Wadden Sea, Proceedings of the 10th International Scientific Wadden Sea Symposium, Groningen, pp 67–88

Bakker, J. P., Dijkstra, M. & Russchen P. T. (1985) Dispersal, Germination and early establishment of halophytes and glycophytes on a grazed and abandoned salt-marsh gradient. New Phytol. 101: 291–308

Bakker, J. P., Olff, H., Willems, J. H. & Zobel, M. (1996) Why do we need permanent plots in the study of long-term vegetation dynamics? J. of Veg. Sci. 7: 147–156

Bakker, J. P. & Piersma, T. (2005) Restoration of intertidal flats and tidal salt marshes. In: Van Andel, J. & Aronson, J (ed), Restoration Ecology: The new frontier, 1st edn. Blackwell Publ., Groningen, pp 174–192

Barkowski, J. (2003) Vegetationskundliche und paläoökologische Untersuchungen auf dem Langeooger Sommerpolder – Westteil. Unpubl. Thesis, Universität Hannover, Institut für Geobotanik, 111 p.

Barkowski, J. & Freund, H. (2005) 70 Jahre Vegetationsveränderungen im Langeooger Sommerpolder – Ergebnisse von Vegetationskartierungen, Monitoring und paläoökologischen Untersuchungen. Schr. des Arbeitskreises Landes- und Volkskd. 4: 96–111

Barkowski, J. & Freund, H. (2006) Die Renaturierung des Langeooger Sommerpolders – Eine zweite Chance für die Salzwiese? Oldenbg. Jahrb. 106: 257–278

Beeftink, W. G., Daane, M. C., de Munck, W. & Nieuwenhuize, J. (1978) Aspects of population dynamics in Halimione portulacoides communities. Vegetatio 36: 31–43

Bernhardt, K.-G. & Koch, M. (2003) Restoration of a salt marsh system: temporal change of plant species diversity and composition. Basic and Appl. Ecol. 4: 441–451

Cartaxana, P. & Catarino F. (1997) Allocation of nitrogen and carbon in an estuarine salt marsh in Portugal. J. of Coast. Conserv. 3: 27–34

Chang, E. R., Veeneklaas, R. M. & Bakker J. P. (2007) Seed dynamics linked to variability in movement of tidal water. J. of Veg. Sci. 18 (2): 253–262

Cooper, N. J., Cooper T. & Burd, F. (2001) 25 years of salt marsh erosion in Essex: Implications for coastal defence and nature conservation. J. of coast. Conserv. 7: 31–40

Doody, J. P. (2004) „Coastal squeeze" – an historical perspective. J. of Coast. Conserv. 10: 129–138

Dausse, A., Bonis, A., Bouzillé, J.-B. & Lefeuvre J. C. (2008) Seed dispersal in a polder after partial tidal restoration: Implications for salt-marsh restoration. Appl. Veg. Sci. 11: 3-12

Esselink, P., Fresco, L. F. M. & Dijkema, K. S. (2002) Vegetation change in a man-made salt marsh affected by a reduction in both grazing and drainage. Appl. Veg. Sci. 5: 17–32

Freund, H. & Streif, H. (1999) Natürliche Pegelmarken für Meeresspiegelschwankungen der letzten 2000 Jahre im Bereich der Insel Juist. PGM 143: 34-45

Freund, H., Petersen, J. & Pott, R. (2003) Investigations on recent and subfossil salt-marsh vegetation of the East Frisian barrier islands in the southern North Sea (Germany). Phytocoen. 33 (2-3): 349–375

Grasshoff, K., Kremling, K. & Ehrhardt, M. (1999) Methods of Seawater Analysis. Wiley-VCH, New York, 632 pp.

Harnischmacher, R. (1949) Gutachten über die Entwicklung der domänenfiskalischen Hellerwiesen auf der Nordseeinsel Langeoog nach Ausführung der Sommerbedeichung in den Jahren 1935/36 bis zum Jahre 1948. Unpubl. expert report

Hughes, R. G. (2004). Climate change and loss of saltmarshes: consequences for birds. Ibis 146 (1): 21–28

Kiehl, K. , Schröder H. & Stock M. (2007) Long – term vegetation dynamics after land – use change in Wadden Sea salt marshes. Coastl. Rep. 7: 17–24

Kleyer, M., Feddersen, H. & Bockholt, R. (2003) Secondary succession on a high salt marsh at different grazing intensities. J. of Coast. Conserv. 9: 123–134

Kolditz, K., Dellwig, O., Barkowski, J., Beck, M., Freund, H. & Brumsack H. (2008) Salt marsh restoration: Effects of de – embankment on pore water geochemistry. J. of Coast. Res. (in review)

Leendertse, P. C., Rozema, J. & Andrea, A. (1997) Effects of nitrogen addition on the growth of the salt marsh grass *Elymus athericus.* J. of Coast. Conserv. 3: 35–40

Londo, G. (1976) The decimal scale for relevés of permanent quadrats. Vegetatio 33 (1): 61-64

Petersen, J. (2001) Die Vegetation der Wattenmeer-Inseln im raum-zeitlichen Wandel – ein Beispiel für den Einsatz moderner vegetationsanalytischer Methoden. Ber. d. Reinh.-Tüxen-Ges. 13: 139-155

Petersen, J. (2003) Ersatzmaßnahme zur Europipe I und II auf der Insel Langeoog – Erfassung der 2000 angelegten Dauerbeobachtungsflächen im Bereich des Sommerpolders. Bericht: Auftraggeber Land Niedersachsen, NLWKN – Betriebsstelle Norden. 186 p.

Reed, D. J., Spencer, T., Murray, A. L., French, J. R. & Leonard, L. (1999) Marsh surface sediment deposition and the role of tidal creeks: Implications for created and managed coastal marshes. J. of Coast. Conserv. 5: 81–90

Reise, K. (2005) Coast of change: Habitat loss and transformations in the Wadden Sea. Helgol Mar Res 59: 9–21

Roozen, A. J. M. & Westhoff, V. (1985) A study on long-term salt-marsh succession using permanent plots. Vegetatio 61: 23-32

Steffens, M. (2003) Vegetationskundliche und paläoökologische Untersuchungen auf dem Langeooger Sommerpolder – Ostteil. Unpubl. thesis, Universität Hannover, Institut für Geobotanik. 122 p.

Tessier, M., Gloaguen, J.-C. & Bouchard, V. (2002) The role of spatio-temporal hererogeneity in the establishment and maintenance of *Suaeda maritima* in salt marshes. J. of Veg. Sci. 13: 115–122

van Wijnen, H. J. & Bakker, J. P. (1997) Nitrogen accumulation and plant species replacement in three salt marsh systems in the Wadden Sea. J. of Coast. Conserv. 3: 19–26

van Wijnen, H. J. & Bakker, J. P. (1999) Nitrogen and phosphorus limitation in a coastal barrier salt marsh: the Implications for vegetation succession. J. of Ecol. 87: 265–272

van Wijnen, H. J. & Bakker, J. P. (2000) Annual nitrogen budget of a temperate coastal barrier salt-marsh system along a productivity gradient at low and high marsh elevation. Perspect. in Plant Ecol. and Syst. (3/2): 128–141

Wisskirchen, R. & Haeupler, H. (2000) Standardliste der Farn- und Blütenpflanzen Deutschlands. Ulmer, Stuttgart, DE, 760 p.

Wittig, S., Kraft, D., Meyerdirks, J. & Schirmer, M. (2004) Risikobewertung ökologischer Systeme an der deutschen Nordseeküste im Klimawandel. Coastl. Rep. 1: 127–135

Wolters, M., Garbutt, A. & Bakker, J. P. (2005a) Salt-marsh restoration: Evaluating the success of de-embankments in north-west Europe. Biol. Conserv. 123: 249-268

Wolters, M., Garbutt, A. & Bakker J. P. (2005b) Plant colonization after managed realignment – the relative importance of diaspore dispersal. J. of Appl. Ecol. 42: 770–777

Wolters, M., Bakker, J. P., Bertness, M. D., Jefferies, R. L., Möller, I. (2005c) Salt marsh erosion and restoration in south-east England: Squeezing the evidence requires realignment. J. of Appl. Ecol. 42: 844–851

Bulk parameters and XRF-data [%]

site LT3 – saline influenced grassland

Depth [m]	TS	TC	TIC	TOC	SiO_2	TiO_2	Al_2O_3	Fe_2O_3	MgO	CaO	Na_2O	K_2O	P_2O_5
0.09	0.02	0.69	0.00	0.69	92.39	0.21	2.00	0.52	0.17	0.24	0.53	0.72	0.00
0.15	0.02	0.68	0.00	0.68	92.51	0.18	1.67	0.43	0.12	0.23	0.47	0.63	0.00
0.22	0.01	0.18	0.00	0.18	93.51	0.36	1.85	0.54	0.13	0.25	0.47	0.69	0.00
0.30	0.01	0.04	n.d.	n.d.	92.97	0.27	1.55	0.38	0.09	0.24	0.39	0.57	0.00
0.40	0.00	0.03	n.d.	n.d.	92.27	0.69	1.77	0.84	0.12	0.33	0.48	0.66	0.00
0.51	0.01	0.08	n.d.	n.d.	93.86	0.44	1.79	0.63	0.14	0.27	0.39	0.55	0.00
0.59	0.02	0.04	n.d.	n.d.	86.08	2.40	2.93	2.75	0.29	0.85	0.44	0.56	0.04
0.94	0.01	0.05	n.d.	n.d.	92.71	0.96	2.02	1.20	0.17	0.44	0.41	0.56	0.01
1.03	0.01	0.08	n.d.	n.d.	91.93	0.74	1.96	0.99	0.16	0.38	0.43	0.61	0.00
1.12	0.01	0.07	n.d.	n.d.	92.92	0.81	2.01	1.08	0.17	0.43	0.43	0.55	0.00
1.22	0.01	0.06	n.d.	n.d.	88.89	1.46	2.40	1.81	0.22	0.59	0.43	0.56	0.01
1.32	0.01	0.04	n.d.	n.d.	92.66	0.55	1.82	0.76	0.14	0.36	0.40	0.58	0.00
1.43	0.01	0.05	n.d.	n.d.	94.25	0.33	1.54	0.51	0.12	0.27	0.38	0.57	0.00
1.54	0.07	0.14	0.00	0.14	93.36	0.22	1.80	0.51	0.14	0.27	0.40	0.64	0.00
1.62	0.11	0.22	0.04	0.18	92.02	0.37	1.76	0.73	0.17	0.48	0.46	0.63	0.00
1.72	0.10	0.42	0.16	0.26	90.91	0.34	1.81	0.68	0.17	1.09	0.49	0.69	0.00
1.80	0.48	1.93	0.97	0.96	77.12	0.33	3.72	1.69	0.54	5.21	0.43	0.94	0.02
1.92	0.06	0.12	0.00	0.12	92.13	0.25	1.61	0.49	0.13	0.42	0.41	0.64	0.00
2.01	0.06	0.27	0.10	0.17	93.67	0.21	1.65	0.48	0.14	0.71	0.43	0.63	0.00
2.94	0.07	0.37	0.17	0.20	91.44	0.25	1.70	0.54	0.14	1.11	0.39	0.60	0.00
3.02	0.05	0.08	n.d.	n.d.	95.24	0.11	1.53	0.30	0.09	0.31	0.47	0.71	0.00
3.12	0.06	0.10	n.d.	n.d.	94.35	0.11	1.74	0.30	0.11	0.45	0.50	0.75	0.00
3.22	0.04	0.13	0.06	0.06	92.81	0.19	1.65	0.37	0.11	0.55	0.41	0.67	0.00
3.31	0.04	0.04	0.01	0.03	94.92	0.16	1.32	0.29	0.07	0.25	0.42	0.59	0.00
3.42	0.06	0.07	0.04	0.04	93.44	0.27	1.75	0.47	0.13	0.46	0.46	0.66	0.00
3.52	0.05	0.05	n.d.	n.d.	93.99	0.12	1.60	0.33	0.10	0.30	0.45	0.67	0.00
3.61	0.05	0.09	n.d.	n.d.	92.53	0.21	1.79	0.44	0.14	0.42	0.52	0.73	0.00
3.71	0.05	0.12	0.07	0.05	92.28	0.29	1.99	0.52	0.17	0.59	0.58	0.77	0.00
3.80	0.05	0.12	0.06	0.06	92.38	0.28	2.03	0.53	0.17	0.60	0.57	0.75	0.00
3.91	0.18	0.58	0.22	0.36	88.58	0.35	3.02	0.99	0.35	1.43	0.61	0.99	0.01
3.97	0.45	1.43	0.61	0.82	78.15	0.39	5.25	1.85	0.80	3.21	0.80	1.40	0.04

n.d. = not determined

Contiunation XRF-data [mg/kg]

site LT3 – saline influenced grassland

Depth [m]	As	Ba	Co	Cr	Mn	Mo	Ni	Pb	Rb	Sr	U	V	Y	Zn	Zr
0.09	2	147	2	6	39	0	0	9	25	31	0	12	7	12	250
0.15	3	157	1	3	39	0	0	4	22	30	1	11	7	8	252
0.22	2	146	1	18	101	0	0	8	23	30	1	9	10	9	676
0.30	1	154	1	9	70	0	0	5	19	28	0	10	9	4	430
0.40	3	149	1	46	240	0	0	6	21	30	0	10	18	10	1539
0.51	2	142	1	25	155	0	0	6	20	27	1	8	12	11	888
0.59	9	137	7	197	1069	0	7	10	20	53	4	30	48	43	4907
0.94	4	132	3	74	395	0	1	7	19	35	1	14	21	15	2124
1.03	3	153	2	50	302	0	0	6	22	33	1	17	17	22	1615
1.12	4	138	2	61	349	2	0	5	20	34	2	17	18	15	1628
1.22	6	157	5	122	658	1	1	7	20	41	3	23	29	25	3018
1.32	2	156	0	33	217	0	0	5	20	33	0	10	13	9	993
1.43	2	141	0	20	101	1	0	3	21	27	3	9	10	5	623
1.54	3	151	2	7	54	0	0	3	23	28	1	11	7	5	279
1.62	4	142	2	19	124	0	0	4	22	31	1	12	9	7	752
1.72	2	153	2	18	132	1	0	6	25	52	2	17	9	8	669
1.80	10	165	5	26	170	2	8	7	41	170	2	36	12	22	326
1.92	2	152	1	6	77	0	0	5	22	31	1	8	8	5	340
2.01	3	147	3	8	70	0	0	3	21	37	0	9	8	6	343
2.94	2	155	0	8	77	0	0	5	21	50	1	9	8	5	402
3.02	2	164	0	0	0	0	0	2	23	29	0	8	4	2	129
3.12	2	168	1	0	0	0	0	3	24	34	0	8	6	2	139
3.22	1	160	0	5	31	0	0	5	23	36	1	10	7	3	312
3.31	1	148	1	2	15	1	0	3	19	23	1	2	6	1	275
3.42	2	163	2	11	70	0	0	3	23	35	2	8	9	4	426
3.52	2	165	0	1	8	1	0	3	23	28	1	6	5	2	124
3.61	1	164	1	3	54	0	0	5	23	36	0	5	9	6	262
3.71	2	177	1	14	77	0	0	4	24	41	1	8	10	5	399
3.80	3	175	0	15	77	0	0	4	24	39	1	9	10	4	480
3.91	5	189	4	26	116	0	3	6	35	64	1	21	14	12	590
3.97	7	249	6	34	155	1	6	10	55	111	1	37	16	25	402

Bulk parameters and XRF-data [%]

site LT4 – high salt marsh

Depth [m]	TS	TC	TIC	TOC	SiO$_2$	TiO$_2$	Al$_2$O$_3$	Fe$_2$O$_3$	MgO	CaO	Na$_2$O	K$_2$O	P$_2$O$_5$
0.08	0.20	8.26	0.00	8.26	61.27	0.56	8.16	3.23	1.26	0.64	1.34	1.67	0.17
0.16	0.01	0.45	n.d.	n.d.	94.05	0.29	1.59	0.47	0.12	0.26	0.42	0.55	0.00
0.30	0.01	0.11	n.d.	n.d.	93.69	0.16	1.76	0.54	0.13	0.24	0.53	0.72	0.00
0.39	0.01	0.06	n.d.	n.d.	91.30	0.92	2.09	1.40	0.17	0.50	0.54	0.63	0.01
0.51	0.01	0.06	n.d.	n.d.	91.23	0.97	2.46	1.25	0.21	0.46	0.59	0.73	0.01
0.61	0.05	0.04	n.d.	n.d.	93.22	0.45	1.94	0.67	0.16	0.39	0.54	0.63	0.00
0.73	0.01	0.11	n.d.	n.d.	92.70	0.46	1.88	0.81	0.16	0.34	0.56	0.62	0.00
0.81	0.02	0.09	n.d.	n.d.	90.82	1.07	2.21	1.40	0.20	0.49	0.56	0.65	0.01
0.90	0.01	0.09	n.d.	n.d.	92.30	0.67	2.04	1.00	0.18	0.37	0.56	0.64	0.00
1.00	0.02	0.38	0.00	0.38	91.19	0.46	2.38	0.95	0.23	0.34	0.53	0.71	0.00
1.12	0.01	0.04	n.d.	n.d.	94.39	0.38	1.68	0.58	0.13	0.31	0.48	0.57	0.00
1.22	0.02	0.04	n.d.	n.d.	94.30	0.30	1.46	0.91	0.13	0.32	0.49	0.48	0.00
1.31	0.02	0.06	n.d.	n.d.	93.53	0.28	1.54	0.47	0.13	0.26	0.49	0.54	0.00
1.40	0.03	0.08	n.d.	n.d.	93.46	0.22	1.53	0.41	0.14	0.25	0.51	0.53	0.00
1.52	0.04	0.11	n.d.	n.d.	93.66	0.32	1.63	0.53	0.15	0.46	0.61	0.65	0.00
1.62	0.24	0.53	0.20	0.33	88.85	0.33	2.62	0.95	0.33	1.23	0.60	0.79	0.00
1.71	0.13	0.35	n.d.	n.d.	91.48	0.38	2.13	0.75	0.22	1.08	0.63	0.69	0.00
1.82	0.15	0.52	0.23	0.29	89.00	0.24	2.13	0.71	0.25	1.31	0.55	0.69	0.00
1.90	0.07	0.19	n.d.	n.d.	93.32	0.22	1.69	0.52	0.17	0.63	0.50	0.60	0.00
2.00	0.08	0.33	n.d.	n.d.	91.89	0.18	1.72	0.45	0.15	0.89	0.49	0.65	0.00
2.07	0.06	0.16	n.d.	n.d.	95.03	0.09	1.26	0.25	0.11	0.52	0.47	0.55	0.00
2.73	0.07	0.36	n.d.	n.d.	91.99	0.23	1.66	0.47	0.16	1.18	0.57	0.61	0.00
2.84	0.05	0.14	n.d.	n.d.	94.82	0.13	1.29	0.28	0.10	0.53	0.49	0.56	0.00
2.92	0.04	0.08	n.d.	n.d.	94.97	0.15	1.54	0.32	0.12	0.35	0.49	0.57	0.00
3.00	0.07	0.15	n.d.	n.d.	94.02	0.12	1.51	0.32	0.14	0.46	0.56	0.62	0.00
3.11	0.14	0.45	0.17	0.27	91.29	0.19	2.05	0.57	0.24	1.02	0.60	0.71	0.00
3.22	0.08	0.23	0.00	0.00	93.50	0.17	1.78	0.42	0.17	0.63	0.56	0.66	0.00
3.32	0.05	0.11	0.00	0.00	95.13	0.10	1.16	0.23	0.09	0.34	0.39	0.50	0.00
3.42	0.05	0.08	0.00	0.00	94.12	0.11	1.66	0.29	0.11	0.41	0.61	0.79	0.00
3.50	0.05	0.09	0.00	0.00	93.57	0.12	1.71	0.29	0.13	0.48	0.58	0.70	0.00
3.62	0.05	0.05	0.00	0.00	94.62	0.18	1.38	0.34	0.09	0.32	0.45	0.56	0.00
3.72	0.05	0.04	0.00	0.00	94.38	0.23	1.30	0.37	0.10	0.32	0.45	0.51	0.00
3.82	0.04	0.04	0.00	0.00	94.76	0.19	1.51	0.35	0.10	0.45	0.48	0.58	0.00
3.92	0.05	0.05	0.00	0.00	93.90	0.21	1.60	0.37	0.11	0.35	0.52	0.63	0.00
4.00	0.05	0.11	0.00	0.00	93.28	0.24	1.93	0.43	0.16	0.57	0.60	0.70	0.00
4.12	0.53	1.44	0.68	0.77	78.53	0.33	4.80	1.80	0.80	3.24	0.89	1.19	0.03
4.21	0.29	0.79	0.49	0.30	83.93	0.32	3.65	1.13	0.52	2.36	0.80	1.09	0.02

n.d. = not determined

Contiunation XRF-data [mg/kg]

site LT4 – high salt marsh

Depth [m]	As	Ba	Co	Cr	Mn	Mo	Ni	Pb	Rb	Sr	U	V	Y	Zn	Zr
0.08	17	230	9	78	163	0	21	72	80	81	3	83	20	131	370
0.16	1	147	2	13	70	0	0	11	20	30	1	8	8	7	504
0.30	3	177	2	10	23	0	0	6	26	37	2	12	6	8	192
0.39	5	150	1	85	356	0	0	7	23	39	2	18	24	20	2685
0.51	5	158	2	68	372	0	0	6	25	40	2	14	22	17	1931
0.61	2	147	2	34	155	0	0	5	25	41	2	13	11	9	881
0.73	2	143	1	38	170	0	0	7	24	37	2	10	11	12	891
0.81	4	152	3	108	449	0	0	7	26	43	4	24	24	16	2559
0.90	4	148	2	56	263	0	0	5	25	40	2	15	15	12	1502
1.00	4	159	1	39	155	0	0	9	29	40	2	21	12	16	969
1.12	2	137	3	21	147	0	0	3	20	30	1	6	11	7	721
1.22	1	111	1	23	108	0	0	5	19	33	1	12	8	20	488
1.31	1	143	2	12	85	0	0	4	20	27	0	7	9	7	426
1.40	1	134	2	7	70	0	0	5	19	26	1	9	7	4	348
1.52	1	146	0	30	108	0	0	7	24	39	2	10	9	7	624
1.62	4	143	3	26	108	0	0	7	33	57	2	20	10	11	500
1.71	4	159	2	26	124	2	0	4	25	52	2	13	9	8	581
1.82	5	143	2	8	77	0	0	2	26	57	2	14	8	9	381
1.90	2	148	2	13	70	0	0	4	24	42	1	8	7	4	347
2.00	2	151	4	4	46	0	0	6	23	43	2	10	8	5	268
2.07	2	147	1	0	0	0	0	2	19	30	0	5	6	2	116
2.73	1	156	2	17	54	0	0	5	23	59	1	13	7	6	349
2.84	1	143	1	0	8	0	0	4	19	34	1	7	5	2	197
2.92	2	151	0	1	15	0	0	4	20	29	1	8	6	0	226
3.00	1	146	1	4	46	0	0	5	23	36	1	10	6	3	157
3.11	3	161	1	9	31	0	0	3	27	50	0	15	9	7	246
3.22	2	158	1	6	23	0	0	5	23	37	1	9	8	4	248
3.32	1	141	0	0	0	0	0	3	18	25	0	6	5	1	155
3.42	1	166	0	0	0	0	0	4	25	33	0	2	6	1	127
3.50	2	175	1	0	0	0	0	4	24	36	0	10	5	3	140
3.62	1	141	2	2	31	0	0	4	19	26	0	4	7	1	269
3.72	2	147	1	14	62	0	0	4	20	33	1	12	8	2	409
3.82	2	153	1	2	54	0	0	4	20	34	1	6	6	3	260
3.92	3	159	0	6	46	0	0	2	21	31	0	8	8	2	299
4.00	2	162	2	7	62	0	0	3	23	41	0	8	7	4	346
4.12	8	203	5	25	170	0	7	10	50	114	2	38	14	25	262
4.21	5	212	4	22	116	0	0	6	40	88	0	23	14	14	452

Bulk parameters and XRF-data [%]

site L5 – transition zone low salt marsh/pioneer zone

Depth [m]	TS	TC	TIC	TOC	SiO_2	TiO_2	Al_2O_3	Fe_2O_3	MgO	CaO	Na_2O	K_2O	P_2O_5
0.09	0.32	7.41	0.35	7.06	52.49	0.68	11.14	5.17	1.97	1.88	1.63	2.23	0.27
0.22	0.11	2.59	0.15	2.45	72.64	0.70	7.59	3.52	1.23	0.90	1.08	1.58	0.13
0.31	0.02	0.25	n.d.	n.d.	89.68	0.81	2.73	1.31	0.34	0.54	0.57	0.71	0.01
0.39	0.02	0.06	n.d.	n.d.	90.23	1.17	2.13	1.51	0.23	0.50	0.58	0.56	0.01
0.51	0.02	0.06	n.d.	n.d.	93.09	0.49	1.89	0.72	0.19	0.43	0.64	0.64	0.00
0.90	0.03	0.31	n.d.	n.d.	89.98	0.64	2.46	1.19	0.29	0.54	0.62	0.70	0.01
1.02	0.03	0.09	n.d.	n.d.	92.51	0.50	1.83	0.75	0.18	0.44	0.57	0.57	0.00
1.17	0.03	0.06	n.d.	n.d.	92.61	0.46	1.79	0.69	0.17	0.48	0.56	0.56	0.00
1.29	0.04	0.07	n.d.	n.d.	93.90	0.25	1.53	0.48	0.14	0.41	0.57	0.56	0.00
1.41	0.04	0.04	n.d.	n.d.	94.51	0.17	1.24	0.32	0.12	0.28	0.54	0.49	0.00
1.52	0.06	0.05	n.d.	n.d.	96.15	0.14	1.34	0.32	0.13	0.40	0.53	0.51	0.00
1.62	0.10	0.06	n.d.	n.d.	94.56	0.10	1.19	0.24	0.11	0.25	0.65	0.55	0.00
1.76	0.07	0.14	n.d.	n.d.	93.71	0.11	1.35	0.29	0.13	0.33	0.61	0.56	0.00
1.92	0.09	0.15	n.d.	n.d.	93.61	0.15	1.46	0.40	0.17	0.47	0.54	0.54	0.00
2.04	0.19	0.55	n.d.	n.d.	89.05	0.26	2.46	0.77	0.30	1.18	0.77	0.85	0.00
2.17	0.07	0.13	n.d.	n.d.	92.13	0.23	2.22	0.45	0.20	0.61	0.77	0.83	0.00
2.27	0.14	0.44	0.13	0.31	91.32	0.24	2.16	0.56	0.24	0.91	0.62	0.74	0.00
2.39	0.39	2.37	0.35	2.02	84.85	0.18	2.03	0.67	0.33	1.82	0.91	0.75	0.00
2.52	0.20	0.49	0.12	0.37	91.39	0.20	1.97	0.65	0.25	0.76	0.64	0.68	0.00
2.70	0.07	0.32	n.d.	n.d.	92.97	0.16	1.59	0.38	0.18	0.56	0.62	0.64	0.00
2.92	0.12	0.31	0.10	0.21	90.90	0.22	2.23	0.51	0.23	0.70	0.76	0.78	0.00
3.01	0.20	0.59	0.12	0.48	91.52	0.18	1.85	0.61	0.23	0.76	0.60	0.65	0.00
3.12	0.05	0.17	n.d.	n.d.	93.98	0.13	1.38	0.27	0.13	0.49	0.53	0.56	0.00
3.22	0.05	0.18	n.d.	n.d.	94.26	0.16	1.32	0.32	0.14	0.35	0.57	0.55	0.00
3.35	0.29	0.73	0.25	0.47	86.84	0.20	3.01	0.89	0.40	1.59	0.81	0.97	0.00
3.52	0.33	0.84	0.39	0.46	85.53	0.26	3.35	1.03	0.47	1.98	0.97	1.08	0.01
3.62	0.08	0.09	n.d.	n.d.	93.82	0.14	1.42	0.32	0.13	0.39	0.66	0.60	0.00
3.71	0.07	0.08	n.d.	n.d.	94.53	0.27	1.25	0.41	0.13	0.39	0.54	0.50	0.00
3.83	0.12	0.36	n.d.	n.d.	89.34	0.22	2.53	0.53	0.27	1.25	0.88	0.95	0.00
3.92	0.14	0.48	n.d.	n.d.	87.25	0.34	3.31	0.77	0.38	1.78	0.89	1.06	0.01
4.06	0.61	1.41	0.64	0.77	76.24	0.44	5.25	1.91	0.84	3.37	1.23	1.37	0.04
4.19	0.25	0.65	n.d.	n.d.	86.10	0.30	3.28	0.93	0.43	1.81	0.86	1.05	0.01
4.32	0.30	0.69	n.d.	n.d.	85.57	0.33	3.33	1.08	0.46	1.83	0.84	0.98	0.01
4.42	0.07	0.12	n.d.	n.d.	92.95	0.18	1.81	0.36	0.17	0.56	0.65	0.66	0.00

n.d. = not determined

Contiunation XRF-data [mg/kg]

site L5 – transition zone low salt marsh/pioneer zone

Depth [m]	As	Ba	Co	Cr	Mn	Mo	Ni	Pb	Rb	Sr	U	V	Y	Zn	Zr
0.09	18	287	13	107	635	0	33	86	113	122	3	122	26	201	216
0.22	16	225	11	81	496	0	12	53	77	77	3	79	21	125	770
0.31	4	145	2	71	333	0	0	13	30	42	3	28	19	22	1839
0.39	5	133	2	105	534	0	0	7	23	40	4	27	27	18	2908
0.51	1	147	1	32	178	0	0	7	25	39	1	12	10	7	637
0.90	4	150	2	56	294	0	0	10	29	45	1	24	16	19	1120
1.02	3	134	1	33	201	0	0	5	22	38	2	20	10	9	745
1.17	1	136	2	33	217	0	0	7	22	43	1	14	10	6	594
1.29	2	152	1	13	116	0	0	4	21	37	2	11	7	4	313
1.41	1	116	0	9	39	0	0	4	19	28	2	6	6	2	233
1.52	2	121	1	4	23	0	0	4	21	34	1	7	5	2	168
1.62	0	136	1	2	0	0	0	4	21	30	1	2	5	1	108
1.76	1	147	1	9	8	0	0	4	23	31	1	9	4	3	117
1.92	2	137	2	8	23	0	0	4	23	33	0	9	6	3	208
2.04	3	175	3	21	85	0	0	7	32	63	1	17	9	8	317
2.17	2	195	1	17	46	0	0	4	31	47	1	11	7	2	323
2.27	2	172	1	12	132	0	0	6	29	53	2	10	8	7	316
2.39	4	162	1	15	46	2	0	6	30	81	3	19	8	8	247
2.52	3	159	3	12	46	0	0	6	27	45	2	16	9	6	281
2.70	2	156	3	14	23	0	0	4	24	39	1	9	6	3	269
2.92	3	176	1	12	46	0	0	5	30	51	1	14	9	5	320
3.01	3	150	1	13	39	0	0	6	27	43	2	14	6	7	247
3.12	0	140	1	11	15	0	0	5	23	35	2	7	6	3	269
3.22	1	138	1	6	31	0	0	3	22	30	1	10	6	3	278
3.35	4	189	2	17	62	0	0	6	38	74	1	19	9	10	179
3.52	4	207	3	22	93	0	0	7	41	87	0	26	12	12	293
3.62	1	134	2	5	15	0	0	4	22	35	1	6	5	1	188
3.71	2	135	0	13	70	0	0	3	20	32	1	10	7	1	387
3.83	2	206	0	17	54	0	0	5	34	65	2	10	9	6	270
3.92	2	231	1	27	240	0	0	8	37	86	1	18	13	9	567
4.06	8	239	5	46	201	0	4	12	54	128	2	41	18	26	493
4.19	3	206	3	24	108	0	0	8	39	82	2	22	9	10	428
4.32	5	193	2	30	124	0	0	8	39	81	0	23	11	12	461
4.42	1	149	0	11	31	0	0	6	25	41	1	8	7	4	259

Bulk parameters and XRF-data [%]

site L6 – low salt marsh

Depth [m]	TS	TC	TIC	TOC	SiO$_2$	TiO$_2$	Al$_2$O$_3$	Fe$_2$O$_3$	MgO	CaO	Na$_2$O	K$_2$O	P$_2$O$_5$
0.04	0.17	2.81	0.00	2.81	68.52	0.73	8.53	4.05	1.41	1.65	1.27	1.74	0.19
0.13	0.07	1.50	0.06	1.43	78.93	0.55	5.90	2.72	0.88	0.61	0.90	1.28	0.12
0.21	0.03	0.52	0.00	0.52	87.45	0.48	2.77	1.23	0.35	0.65	1.01	1.23	0.04
0.29	0.02	0.31	n.d.	n.d.	90.33	0.43	2.84	1.11	0.32	0.42	0.64	0.80	0.02
0.40	0.02	0.13	0.00	0.13	88.82	0.87	2.49	1.32	0.27	0.47	0.59	0.69	0.01
0.50	0.02	0.07	n.d.	n.d.	90.42	0.82	2.28	1.17	0.23	0.48	0.65	0.68	0.01
0.60	0.01	0.05	n.d.	n.d.	92.41	0.57	2.16	0.86	0.20	0.43	0.60	0.68	0.00
0.68	0.01	0.04	n.d.	n.d.	93.86	0.44	1.77	0.61	0.15	0.34	0.57	0.59	0.00
0.78	0.02	0.00	n.d.	n.d.	93.46	0.34	1.65	0.52	0.13	0.30	0.62	0.70	0.00
0.90	0.01	0.08	n.d.	n.d.	92.42	0.65	2.17	0.97	0.21	0.45	0.66	0.65	0.00
1.01	0.01	0.17	0.00	0.17	89.31	0.79	2.49	1.26	0.26	0.52	0.74	0.71	0.02
1.10	0.01	0.10	n.d.	n.d.	92.08	0.76	2.27	1.12	0.24	0.49	0.59	0.68	0.01
1.21	0.02	0.16	n.d.	n.d.	92.97	0.43	2.13	0.82	0.20	0.42	0.57	0.68	0.00
1.30	0.01	0.03	n.d.	n.d.	95.98	0.25	1.56	0.45	0.13	0.28	0.55	0.58	0.00
1.40	0.01	0.02	n.d.	n.d.	93.79	0.30	1.60	0.49	0.14	0.30	0.59	0.58	0.00
1.50	0.02	0.03	n.d.	n.d.	94.96	0.20	1.56	0.38	0.13	0.32	0.52	0.57	0.00
1.62	0.04	0.02	n.d.	n.d.	95.01	0.16	1.18	0.31	0.11	0.21	0.53	0.47	0.00
1.75	0.04	0.02	n.d.	n.d.	95.21	0.11	1.20	0.24	0.11	0.18	0.52	0.48	0.00
1.91	0.06	0.03	n.d.	n.d.	94.94	0.10	1.19	0.24	0.10	0.20	0.72	0.57	0.00
2.02	0.05	0.05	n.d.	n.d.	95.71	0.07	1.19	0.21	0.10	0.17	0.57	0.51	0.00
2.14	0.09	0.10	n.d.	n.d.	95.1	0.11	1.32	0.34	0.13	0.33	0.53	0.54	0.00
2.25	0.13	0.27	0.13	0.15	91.82	0.19	1.92	0.56	0.23	0.80	0.69	0.68	0.00
2.41	0.16	0.83	0.28	0.55	88.77	0.22	2.29	0.63	0.27	1.50	0.80	0.83	0.00
2.50	0.16	0.62	0.12	0.50	90.54	0.22	2.18	0.54	0.25	0.87	0.76	0.82	0.00
2.65	0.18	2.35	1.65	0.70	77.83	0.16	1.71	0.50	0.27	7.60	0.72	0.62	0.00
2.75	0.09	0.30	n.d.	n.d.	92.79	0.16	1.56	0.40	0.18	0.53	0.63	0.62	0.00
3.11	0.15	0.68	0.40	0.29	88.23	0.24	2.21	0.60	0.25	1.56	0.81	0.84	0.00
3.29	0.05	0.16	n.d.	n.d.	94.19	0.21	1.27	0.34	0.15	0.36	0.63	0.54	0.00
3.40	0.08	0.48	0.03	0.45	92.93	0.09	1.39	0.26	0.15	0.57	0.59	0.58	0.00
3.51	0.13	0.32	0.12	0.20	91.4	0.18	2.08	0.51	0.23	0.80	0.74	0.81	0.00
3.63	0.07	0.07	n.d.	n.d.	93.46	0.15	1.55	0.33	0.14	0.42	0.62	0.63	0.00
3.80	0.07	0.07	n.d.	n.d.	95.07	0.10	1.33	0.28	0.11	0.35	0.59	0.58	0.00
3.92	0.06	0.25	n.d.	n.d.	92.69	0.16	1.89	0.39	0.18	0.67	0.67	0.74	0.00
4.09	0.06	0.07	n.d.	n.d.	93.8	0.17	1.45	0.34	0.13	0.40	0.58	0.59	0.00
4.20	0.06	0.06	n.d.	n.d.	94.23	0.15	1.40	0.31	0.12	0.36	0.56	0.56	0.00
4.30	0.16	0.45	0.29	0.16	87.66	0.28	2.92	0.73	0.34	1.59	0.99	1.06	0.01

n.d. = not determined

Contiunation XRF-data [mg/kg]

site L6 – low salt marsh

Depth [m]	As	Ba	Co	Cr	Mn	Mo	Ni	Pb	Rb	Sr	U	V	Y	Zn	Zr
0.04	19	263	10	86	875	0	20	58	83	89	1	90	25	117	721
0.13	18	208	8	58	658	0	14	45	58	58	2	60	17	87	557
0.21	6	147	2	34	256	0	0	15	32	54	1	26	13	31	680
0.29	5	177	3	24	232	1	1	15	31	41	0	22	11	26	438
0.40	3	152	2	60	372	1	0	12	25	38	2	16	19	20	1434
0.50	4	139	3	49	349	1	0	6	24	40	2	14	17	16	1204
0.60	3	160	1	34	240	0	0	6	23	39	1	9	14	13	838
0.68	2	154	1	19	155	0	0	5	21	34	1	13	8	5	478
0.78	2	149	1	15	108	0	0	4	23	29	1	6	8	5	444
0.90	3	165	2	41	271	0	0	6	23	39	1	10	14	11	1001
1.01	6	154	1	55	364	0	0	8	25	43	0	14	17	19	1234
1.10	5	141	4	53	333	0	0	5	23	37	1	14	18	16	1285
1.21	4	163	1	22	201	0	0	6	25	37	1	11	10	12	638
1.30	3	154	0	9	77	0	0	4	21	29	0	5	6	5	285
1.40	3	144	1	10	108	0	0	3	20	30	1	7	8	7	405
1.50	1	157	1	7	62	0	0	5	20	28	2	7	8	4	245
1.62	1	126	2	5	31	0	0	3	19	26	1	9	6	3	161
1.75	1	119	2	4	0	0	0	4	20	27	1	8	5	7	97
1.91	2	135	3	0	0	0	0	2	19	26	0	6	4	0	121
2.02	1	143	1	0	0	0	0	6	19	22	1	5	5	0	91
2.14	2	131	1	0	0	0	0	3	20	23	0	4	5	4	137
2.25	3	160	3	9	31	0	0	4	26	46	1	10	6	6	248
2.41	4	172	3	6	62	1	0	3	28	67	2	12	8	8	332
2.50	3	185	2	9	46	1	0	4	27	49	3	16	5	6	329
2.65	2	136	1	4	31	3	0	5	24	229	2	9	7	7	225
2.75	3	148	1	1	15	0	0	2	22	31	0	10	8	7	229
3.11	3	165	1	10	70	0	0	4	29	65	1	12	8	7	365
3.29	1	130	0	5	39	2	0	4	18	25	1	7	7	3	397
3.40	2	145	1	0	0	0	0	2	21	35	2	10	5	2	123
3.51	3	163	1	6	31	3	0	3	28	46	1	7	8	5	217
3.63	1	135	2	5	23	0	0	5	24	37	0	3	6	1	170
3.80	2	142	1	0	0	0	0	2	19	28	1	2	6	2	114
3.92	1	165	1	6	23	0	0	5	28	45	0	6	5	3	215
4.09	2	146	1	5	23	0	0	2	19	30	1	6	6	2	255
4.20	1	149	1	0	23	0	0	4	19	30	1	4	7	3	195
4.30	4	212	1	18	77	1	0	4	34	72	2	12	11	8	449

Bulk parameters and ICP-OES data of the SST [%]

site	date	TS	TC	TIC	TOC	Ti	Al	Fe	Mg	Ca	K	P
LT6	07.03.2006	2.11	4.79	1.15	3.64	0.30	5.34	3.18	1.84	5.11	1.72	0.12
LT6	02.05.2006	0.52	5.79	1.23	4.56	0.30	6.99	3.49	1.54	4.44	1.66	0.26
LT6	06.06.2006	2.07	5.65	1.23	4.42	0.29	6.19	3.15	2.01	5.69	1.46	0.43
LT6	04.07.2006	7.01	5.47	0.60	4.87	0.13	4.31	1.34	2.52	13.53	0.68	0.46
LT6	01.08.2006	4.72	8.67	0.55	8.12	0.19	4.93	1.90	1.94	7.87	0.96	0.56
LT6	05.09.2006	3.42	6.66	1.01	5.58	0.27	4.99	2.65	1.74	8.16	1.22	0.29
LT6	10.10.2006	1.69	4.54	1.06	3.48	0.23	3.91	2.33	2.46	4.43	1.27	0.17
LT6	15.11.2006	0.93	5.57	0.94	4.63	0.23	3.65	2.26	1.66	3.38	1.50	0.15
LT6	12.12.2006	1.26	4.50	1.24	3.26	0.29	4.78	2.89	1.51	4.39	1.75	0.11
LT6	09.01.2007	1.06	3.78	1.07	2.71	0.24	3.90	2.37	1.83	3.91	1.62	0.10
LT5	07.02.2006	2.45	4.79	1.01	3.78	0.33	5.78	3.47	1.57	6.63	1.67	0.31
LT5	11.04.2006	2.66	4.54	1.02	3.52	0.31	5.29	3.00	1.53	6.90	1.50	0.29
LT5	02.05.2006	1.42	5.76	1.46	4.30	0.34	5.74	3.23	1.41	6.22	1.68	0.35
LT5	06.06.2006	0.70	6.28	1.47	4.81	0.33	5.44	3.42	2.28	5.28	1.63	0.40
LT5	04.07.2006	3.90	5.89	0.38	5.51	0.29	5.46	2.98	1.72	6.24	1.29	0.59
LT5	10.10.2006	2.28	5.87	1.08	4.79	0.28	5.07	3.11	2.00	4.29	1.57	0.20
LT5	14.11.2006	1.03	5.67	1.01	4.66	0.26	4.10	2.60	1.71	3.70	1.50	0.16
LT5	12.12.2006	1.16	5.21	1.45	3.76	0.31	5.59	3.44	1.87	5.06	1.66	0.17
LT5	09.01.2007	n.d.	n.d.	n.d.	n.d.	0.25	4.26	2.63	1.79	3.89	1.64	0.11
LT5	13.02.2007	1.02	4.60	1.40	3.20	0.28	4.43	2.75	1.61	4.93	1.52	0.12
LT4	07.03.2006	0.44	5.34	1.32	4.02	0.30	5.56	3.26	1.27	4.57	1.61	0.18
LT4	01.04.2006	0.44	14.20	3.78	10.42	0.12	2.80	1.49	4.84	13.02	0.73	0.79
LT4	02.05.2006	0.51	12.11	4.44	7.67	0.12	2.28	1.27	7.29	13.37	0.56	0.85
LT4	06.06.2006	0.32	3.67	1.07	2.60	0.02	0.25	0.13	3.67	2.81	0.68	0.28
LT4	01.08.2006	0.34	4.59	1.40	2.70	0.01	0.11	0.06	2.70	3.99	0.67	0.33
LT4	10.10.2006	0.43	11.98	1.92	10.06	0.06	1.37	0.73	3.44	7.12	0.44	0.77

Continuation ICP-OES data of the SST [mg/kg]

site	date	As	Ba	Co	Cr	Mn	Mo	Ni	Pb	Sr	V	Y	Zn	Zr
LT6	07.03.2006	20	192	11	94	423	1,9	36	53	267	96	18	160	133
LT6	02.05.2006	27	212	11	112	353	1,1	43	56	213	113	20	250	137
LT6	06.06.2006	20	184	10	91	349	4,8	37	61	392	99	17	271	116
LT6	04.07.2006	22	84	5	63	383	5,2	29	36	924	53	8	264	59
LT6	01.08.2006	22	119	8	74	582	7,4	32	53	672	71	11	278	74
LT6	05.09.2006	19	158	9	88	389	4,4	36	63	552	81	15	213	101
LT6	10.10.2006	11	143	7	71	305	3,7	25	38	330	73	13	112	104
LT6	15.11.2006	14	137	7	64	366	2,1	23	34	226	69	13	113	100
LT6	12.12.2006	19	183	10	81	409	1,4	30	45	206	90	18	126	127
LT6	09.01.2007	17	147	8	68	411	1,3	25	39	205	75	14	107	103
LT5	07.02.2006	22	200	11	103	435	2,0	41	95	441	113	18	191	112
LT5	11.04.2006	22	195	10	92	273	1,1	35	65	463	102	18	293	119
LT5	02.05.2006	19	211	12	105	377	4,0	42	67	333	109	19	188	140
LT5	06.06.2006	13	196	12	101	363	4,8	37	53	332	107	18	217	122
LT5	04.07.2006	25	180	11	99	650	4,7	44	55	539	100	17	351	107
LT5	10.10.2006	14	180	10	92	372	5,4	35	51	299	96	18	156	117
LT5	14.11.2006	16	157	8	72	444	2,0	26	38	222	78	15	117	124
LT5	12.12.2006	20	203	11	95	574	1,3	36	50	240	110	19	154	130
LT5	09.01.2007	16	152	9	73	461	1,3	27	41	203	85	15	117	98
LT5	13.02.2007	19	170	9	79	527	0,9	28	43	237	85	17	121	125
LT4	07.03.2006	16	220	9.	95	463	1.8	32	100	264	115	24	177	401
LT4	01.04.2006	7	146	5	64	228	5.8	31	42	1505	49	10	351	37
LT4	02.05.2006	6	113	4	42	223	6.2	20	56	892	34	7	358	16
LT4	06.06.2006	2	17	0	6	46	2.2	4	11	609	4	1	108	6
LT4	01.08.2006	2	13	0	5	57	1.7	3	4	797	2	0	97	3
LT4	10.10.2006	5	81	3	27	119	7.0	12	28	1240	23	5	346	26

Grain size distribution of the SST [%]

site	date	coarse sand >600 µm	medium sand 200-600 µm	sine sand 63-200 µm	coarse silt 20-63 µm	medium silt 6.3-20 µm	fine silt 2-6.3 µm	clay <2 µm
LT6	07.03.2006	0.00	0.00	1.12	39.54	30.26	18.43	10.65
LT6	11.04.2006	0.00	0.00	0.22	43.40	32.63	16.31	7.44
LT6	02.05.2006	0.00	0.00	0.70	33.58	31.46	22.49	11.77
LT6	06.06.2006	0.00	0.00	0.96	39.36	30.40	18.38	10.90
LT6	04.07.2006	0.05	0.24	1.14	24.85	33.52	24.35	15.85
LT6	01.08.2006	0.00	0.00	1.15	33.60	31.95	20.10	13.20
LT6	05.09.2006	0.00	0.00	0.74	37.13	33.07	18.39	10.67
LT6	10.10.2006	0.00	0.00	0.10	37.36	31.89	19.36	11.29
LT6	15.11.2006	0.00	0.00	1.63	44.18	29.65	16.69	7.85
LT6	12.12.2006	0.00	0.00	2.15	42.38	30.62	17.20	7.65
LT6	09.01.2007	0.00	0.00	0.21	35.51	35.45	20.27	8.56

Continuation of grain size distribution of the SST [%]

site	date	coarse sand	medium sand	sine sand	coarse silt	medium silt	fine silt	clay
		>600 µm	200-600 µm	63-200 µm	20-63 µm	6.3-20 µm	2-6.3 µm	<2 µm
LT5	07.02.2006	0.00	0.00	0.52	36.67	31.38	19.68	11.75
LT5	11.04.2006	0.00	0.00	0.57	38.73	30.74	18.52	11.44
LT5	02.05.2006	0.00	0.00	0.12	34.78	34.05	19.64	11.41
LT5	06.06.2006	0.00	0.00	0.05	26.06	42.15	20.64	11.10
LT5	04.07.2006	0.00	0.00	0.58	35.48	32.05	19.06	12.83
LT5	05.09.2006	0.00	0.00	0.14	41.04	35.68	16.29	6.85
LT5	10.10.2006	0.00	0.00	0.46	38.10	32.70	18.32	10.42
LT5	14.11.2006	0.00	0.00	1.35	44.50	30.71	16.27	7.17
LT5	12.12.2006	0.00	0.00	0.68	38.33	30.81	19.48	10.70
LT5	09.01.2007	0.00	0.00	0.03	29.02	38.22	23.09	9.64
LT5	13.02.2007	0.00	0.00	1.30	43.64	30.22	16.89	7.95
LT4	07.03.2006	0.01	0.01	1.89	32.46	30.37	22.98	12.01
LT4	01.04.2006	0.01	0.00	0.05	16.90	39.95	27.54	15.55
LT4	02.05.2006	0.01	0.00	0.32	25.84	36.25	23.58	14.00
LT4	06.06.2006	0.01	0.02	0.34	29.01	35.66	21.39	13.57
LT4	01.08.2006	0.02	0.04	0.72	26.77	34.22	22.63	15.60
LT4	10.10.2006	0.02	0.02	0.33	24.53	38.71	22.76	13.63
LT4	15.11.2006	0.00	0.00	0.10	31.60	37.70	20.65	9.95
LT4	12.12.2006	0.00	0.00	0.59	43.14	33.27	16.12	6.88
LT4	09.01.2007	0.00	0.00	1.20	41.56	31.09	17.89	8.26
LT4	13.02.2007	0.00	0.00	1.13	42.94	30.87	17.06	8.00

Sediment amount of the SST [kg/m²/mounth]

site	date	LT6	LT5	LT4
	10.01.2006	2.08	2.11	2.24
	07.02.2006	0.26	0.22	0.13
	07.03.2006	0.89	0.96	0.22
	11.04.2006	0.22	0.29	0.43
	02.05.2006	0.10	0.17	0.32
	06.06.2006	0.29	0.37	1.64
	04.07.2006	0.28	0.25	0.56
	01.08.2006	0.24	0.16	1.29
	05.09.2006	0.85	0.19	0.63
	10.10.2006	0.93	0.59	0.65
	15.11.2006	3.43	3.28	1.84
	12.12.2006	1.06	2.07	0.27
	09.01.2007	1.40	1.12	0.44
	13.02.2007	2.22	1.86	1.13

Diatoms of LT1 and LT2

Depth [mNN]	TDV	Σ poly-halo-bous	Σ oligo-halo-bous	Σ meso-halo-bous	% ploy-halo-bous of TDV	% oligo-halo-bous of TDV	% meso-halo-bous of TDV	Σ diatom fragments	Σ diatom fragments Centrales	Σ diatom fragmemts Pennales
1.87	349	78	1	270	22.3	0.3	77.4	261	88	173
1.85	337	250	5	82	74.2	1.5	24.3	485	173	312
1.81	3	0	0	0	0.1	0.0	0.2	800	267	533
1.66	3	0	0	0	0.0	0.0	0.2	267	67	200
1.61	11	0	0	0	0.6	0.0	0.0	1209	291	918
1.56	0	0	0	0	0.0	0.0	0.0	1	1	0
1.53	0	0	0	0	0.0	0.0	0.0	18	3	15
1.49	35	33	0	2	94.3	0.0	5.7	1197	434	763
1.45	0	0	0	0	0.0	0.0	0.0	1	0	1
1.41	34	32	0	2	94.1	0.0	5.9	726	268	459
1.34	36	29	0	6	80.6	0.0	16.7	1011	372	639
1.29	12	0	0	0	0.6	0.1	0.1	1183	333	850
1.15	1	0	0	0	0.0	0.0	0.1	300	300	0
1.05	15	0	0	0	0.6	0.0	0.2	1993	640	1353
0.94	1	0	0	0	1.0	0.0	0.0	1500	300	1200
0.79	4	0	0	0	0.1	0.0	0.2	400	0	400
0.64	1	0	0	0	0.1	0.0	0.0	1000	200	800
0.54	0	0	0	0	0.0	0.0	0.0	4	1	3
0.49	11	0	0	0	0.4	0.0	0.2	1418	400	1018
0.29	11	4	0	7	36.4	0.0	63.6	1045	109	936
0.09	86	84	0	2	97.7	0.0	2.3	843	247	597
0.01	56	55	0	1	98.2	0.0	1.8	977	302	675
-0.04	6	0	0	0	0.4	0.0	0.0	3333	817	2517
-0.16	39	36	0	3	92.3	0.0	7.7	370	110	260
-0.37	291	269	5	17	92.4	1.7	5.8	1460	508	952
-0.53	70	64	0	6	91.4	0.0	8.6	348	102	246
-0.71	2	2	0	0	100.0	0.0	0.0	90	19	71
-0.78	344	315	4	25	91.6	1.2	7.3	1296	431	865
-0.9	0	0	0	0	0.0	0.0	0.0	3	0	3
-1.06	0	0	0	0	0.0	0.0	0.0	33	1	32
-1.2	6	5	0	1	83.3	0.0	16.7	54	9	45
-1.32	27	20	0	7	74.1	0.0	25.9	310	44	266
-1.42	331	297	2	32	89.7	0.6	9.7	1046	300	746
-1.47	329	311	2	16	94.5	0.6	4.9	844	217	627
-1.6	483	472	3	8	97.7	0.6	1.7	1035	402	633
-1.74	37	7	0	30	18.9	0.0	81.1	87	2	85
-1.77	348	325	0	23	93.4	0.0	6.6	633	166	467
-1.81	370	309	3	58	83.5	0.8	15.7	546	192	354
-1.86	337	309	1	27	91.7	0.3	8.0	547	229	318
-1.91	370	338	7	25	91.4	1.9	6.8	482	164	318
-1.96	338	306	4	28	90.5	1.2	8.3	454	155	299
-2.01	377	345	4	28	91.5	1.1	7.4	569	174	395
-2.06	362	350	3	9	96.7	0.8	2.5	511	157	354
-2.11	323	298	1	24	92.3	0.3	7.4	828	237	591
-2.16	273	246	7	20	90.1	2.6	7.3	590	178	412
-2.21	239	220	5	14	92.1	2.1	5.9	353	103	250

TDV = total number of diatom valves

Pore water salinity [psu] from January 2006 to February 2007

Depth [m]	Jan 06	Mar 06	Apr 06	May 06	Jun 06	Jul 06	Aug 06	Sep 06	Oct 06	Nov 06	Dec 06	Jan 07	Feb 07
site sGL													
0.0	11.0	9.0	8.1	4.9	10.7	12.8		5.8	9.0	13.2	14.9		8.7
0.05										11.6			
0.07													
0.1													
0.15													
0.2										12.0			
0.25													
0.3											6.3		4.1
0.4		13.0						3.0	3.2		8.9		4.7
0.5			8.4	4.4							10.3		4.6
0.75	0.0	11.0	8.4	2.2	2.4	1.1		2.5	1.7	12.6	7.6		4.2
1.0	0.0				1.8	0.7		1.1	0.7	15.1	4.2		4.8
1.25	1.0	6.0	2.2		1.0				0.7	17.4	3.3		6.3
1.5					0.9			1.3	0.9	3.0	2.3		7.2
2.0	3.0	10.0	8.7	8.6	7.5	7.4		6.4	6.4	20.1	7.2		10.4
2.5	5.0	6.0	6.0	6.1	5.5	5.4		5.1	4.8	6.2	4.8		3.1
3.0													
3.5	6.0	7.0	7.3	7.4	7.3	7.4		6.8	7.1	6.9	7.3		6.5
4.0	7.0	8.0	8.4	8.3	8.4	8.3		7.9	8.2	7.9	8.4		8.3
site hiSM													
0.0		13.0	17.2	13.4	14.7	21.4	17.8	18.4	16.5	16.6	17.1		13.5
0.05										16.5			
0.07										17.5			
0.1										20.2	17.6		
0.15													
0.2													
0.25													
0.3													
0.4									19.5	19.7	16.8		
0.5	11.0	15.0	15.1	15.9	13.1		35.0	21.0	18.9	19.7	16.6		12.9
0.75	9.0	13.0	14.7	16.1	12.9	13.8	35.0	22.4	16.3	20.2	19.1		14.3
1.0	9.5	19.0	13.8	14.2	15.5	14.6	33.0	22.7	19.45	20.9	18.2		17.9
1.25	17.0	14.0	13.6	13.5	15.2	14.8	17.2	23.2	20.3	20.8	19.6		19.2
1.5					15.9		15.6	16.6	18.5	21.2	20.1		19.6
2.0		25.0	21.8	20.8	20.5	20.4	21.0	18.1	18.5	21.4	21.3		24.3
2.5		21.0	16.2	15.5	15.4	17.8	20.0	17.9	19.3	21.6	22.4		23.3
3.0		20.0	18.7	19.3	17.3	21.3	21.0	17.3	16.8	21.0	24.6		22.7
3.5		22.0		19.0	17.5	18.2	22.0	19.3	18.0	20.2	21.4		19.9
4.0		17.0	15.9	15.7	17.1	16.6	19.0	17.7	16.6	17.6	19.8		18.6
4.5		17.0	17.4	15.9	17.3	17.1	17.0	17.5	16.0	18.8	22.7		15.7
5.0				11.8	12.7	12.8	17.3	15.5	15.9	18.2	25.1		15.1

Continuation of pore water salinity [psu]

Depth [m]	Jan 06	Mar 06	Apr 06	May 06	Jun 06	Jul 06	Aug 06	Sep 06	Oct 06	Nov 06	Dec 06	Jan 07	Feb 07
site TZ/loSM													
0.0	22.0		25.9	20.6			25.6	26.1		23.7	25.3		7.8
0.05											24.9		
0.07													
0.1	21.0										25.4		
0.15	22.0									26.1	24.9		
0.2	24.0		22.7	24.8			45.1			27.2			23.2
0.25	25.0		22.2	24.3				27.3		27.5			
0.3	23.0		22.7	24.4			43.8	27.1		27.3	25.3		
0.4	24.0		23.5	27.3			37.4	29.1		29.0	26.4		22.5
0.5	25.0		25.0	26.0	26.0	30.0	37.6	31.5		31.2	28.4		24.1
0.75	23.0		23.6	26.7	25.3	24.4	24.7	32.4		25.6	24.2		24.5
1.0	26.0		25.6	25.7	24.2	22.9	22.7	23.7		24.4	25.0		25.0
1.25	25.0		25.6			23.5	22.8	27.1		24.9	25.5		24.9
1.5													
2.0													
2.5													
3.0													
3.5													
4.0													
4.5				25.5	25.1								
5.0	26.0		25.9			25.3	23.9	23.9		26.7	25.9		25.3
site loSM													
0.0	27.0	18.0	23.6	16.5	24.5	28.2	24.9	23.0	22.6	20.1	23.8		13.1
0.05													
0.07													
0.1													
0.15											24.1		
0.2							16.5	21.9		25.0	23.8		20.5
0.25										25.1	24.2		
0.3													
0.4	30.0						17.8			24.8			24.8
0.5	30.0	30.0	22.5	14.5	28.9	32.3	22.7	20.3	27.1	25.0	23.5		24.3
0.75	27.0	31.0	25.0	24.4	24.6	24.8	30.9	29.3	28.7	27.6	24.8		24.4
1.0	29.0	29.0	25.3	25.1	24.5	25.4	29.0	31.7	30.2	29.8	29.7		25.1
1.25													
1.5		32.0	28.5	27.1	26.3	25.7	26.9	31.3	31.9	30.9	30.8		29.4
2.0	32.0	33.0	30.6	29.2	28.0	27.1	26.4	29.9	33.7	33.2	31.7		31.4
2.5	32.0	32.0	29.9		25.2	26.0	28.2	27.7	28.7	32.5	33.5		27.5
3.0	33.0	33.0	30.8	29.8	30.7	30.7	30.0	29.0	27.8		33.1		32.9
3.5	31.0	32.0	29.6	28.8	29.3	29.3	28.6	28.1	29.0	32.1	31.6		29.6
4.0	31.0	32.0	29.6	29.0	28.9	29.5	29.4	29.1	29.7	30.8	30.3		30.4
4.5		32.0	29.8	29.0	29.3	29.1	28.4	28.1	27.7	30.0	30.4		30.9
5.0	32.0	32.0	30.1	29.1	29.1	29.3	28.3	28.4	27.5	29.6	29.9		30.3

Pore water pH-values from April 2006 to December 2006

Depth [m]	Apr 06	May 06	Jun 06	Jul 06	Aug 06	Sep 06	Oct 06	Nov 06	Dec 06
site sGL									
0.0	8.6	8.3	8.3	8.2		8.4	8.6	7.4	7.9
0.05								6.8	
0.07									
0.1									
0.15									
0.2								6.7	
0.25									
0.3									6.2
0.4						6.6	6.3		6.1
0.5	5.2	6.8							5.9
0.75	6.1	6.2	6.6	6.4		6.3	6.7	6.8	6.3
1.0			7.0	7.1		7.1	7.3	6.8	6.9
1.25	7.4		7.4				7.5	6.7	6.8
1.5			7.7			7.7	7.6	7.1	7.3
2.0	7.3	7.2	7.2	7.2		7.1	7.2	6.9	7.2
2.5	7.4	7.4	7.4	7.3		7.2	7.3	7.4	7.2
3.0									
3.5	7.8	7.5	7.4	7.4		7.4	7.4	7.4	7.5
4.0	7.6	7.5	7.4	7.4		7.3	7.3	7.4	7.4
site hiSM									
0.0	7.9	8.4	8.4	8.4	8.3	7.5	8.0	7.4	7.6
0.05								7.2	
0.07								7.2	
0.1								7.2	7.4
0.15									
0.2									
0.25									
0.3									
0.4							6.7	6.7	6.8
0.5	6.8	6.7	6.7			6.4	6.6	6.7	6.8
0.75	6.9	6.6	6.7	7.0		6.7	6.6	6.5	6.6
1.0	7.1	6.9	6.8	6.8	6.6	6.7	6.8	6.8	6.8
1.25	7.1	6.9	6.9	6.8	6.9	6.5	6.7	6.6	6.8
1.5			7.0		7.0	6.9	6.7	6.8	7.0
2.0	7.2	7.1	7.5	7.1		7.1	7.3	7.2	7.3
2.5	7.3	7.2	7.0	7.1		7.2	7.2	7.3	7.3
3.0	7.3	7.1	7.1	7.2		7.1	7.2	7.2	7.3
3.5		7.1	7.2	7.2		7.1	7.2	7.3	7.4
4.0	7.5	7.1	7.1	7.2		7.2	7.1	7.3	7.3
4.5	7.4	7.1	7.1	6.9		6.9	7.2	7.2	7.2
5.0		7.3	7.5	7.3	7.4	7.1	7.2	7.2	7.2

Continuation of pore water ph-values

Depth [m]	Apr 06	May 06	Jun 06	Jul 06	Aug 06	Sep 06	Oct 06	Nov 06	Dec 06
site TZ/loSM									
0.0	8.5	8.6			8.1	8.6		7.6	7.4
0.05									7.0
0.07									
0.1									7.0
0.15								6.8	6.9
0.2	7.1	6.8			6.4			6.8	
0.25	7.0	7.1				6.7		6.8	
0.3	7.0	6.8			6.6	6.9		6.9	6.9
0.4	7.2	7.0			6.8	6.9		6.9	7.0
0.5	7.2	7.0	7.0	6.8	6.8	6.9		6.9	7.0
0.75	7.1	6.9	6.9	6.7	6.8	6.8		6.8	6.9
1.0	7.0	7.0	6.8	6.8	6.9	7.2		6.9	6.8
1.25	7.1			6.8	7.0	6.9		6.9	6.9
1.5									
2.0									
2.5									
3.0									
3.5									
4.0									
4.5		7.0	6.9						
5.0				7.2	7.5	7.1		7.1	7.2
site loSM									
0.0	8.1	7.7	7.9	7.9	7.7	7.7	7.5	7.6	7.7
0.05									
0.07									
0.1									
0.15									7.0
0.2					7.3	7.1		7.1	7.1
0.25								7.1	7.0
0.3									
0.4					6.9			7.0	
0.5	7.2	7.3	7.5	7.5	6.7	6.8	6.9	7.0	7.1
0.75	7.0	6.9	6.7	6.7	6.6	6.6	6.6	6.8	7.0
1.0	6.7	6.7	6.7	6.7	6.6	6.6	6.6	6.6	6.6
1.25									
1.5	6.9	6.8	6.8	6.8	6.8	6.6	6.6	6.7	6.7
2.0	7.0	6.8	6.9	6.9	7.0	6.9	6.9	6.8	6.9
2.5	7.3		7.4	7.4	7.0	6.9	7.0	7.0	7.0
3.0	7.2	6.9	7.0	7.0	7.1	6.8	7.0		7.0
3.5	7.1	6.9	7.0	7.0	7.1	7.0	7.1	7.1	7.2
4.0	7.2	7.0	7.0	7.0	7.0	7.0	7.1	7.1	7.1
4.5	7.3	7.1	7.6	7.6	7.4	7.2	7.4	7.1	7.1
5.0	7.2	7.6	7.0	7.0	7.0	7.0	7.1	7.0	7.1

Pore water DOC [mM] from January 2006 to November 2006

Depth [m]	Jan 06	Feb 06	Mar 06	Apr 06	May 06	Jun 06	Jul 06	Aug 06	Sep 06	Oct 06	Nov 06
site sGL											
0.0		2.01	2.61	3.15	3.04	2.36	2.50		4.27	2.21	2.03
0.05											5.52
0.07											
0.1											
0.15											
0.2											5.06
0.25											
0.3					0.94						
0.4			0.49		0.86	0.58			5.82	1.36	
0.5				0.50	0.96	0.36					
0.75		5.38	1.25	0.86	1.29	3.02	3.25		4.10	5.93	4.77
1.0				1.10		8.88	15.44		11.56	10.84	4.35
1.25		15.24	4.57	11.34		20.19				16.62	3.65
1.5				21.97		22.48			20.88	20.18	7.72
2.0		2.70	3.29	3.83	3.50	3.91	3.57		4.08	3.49	5.11
2.5		2.83	2.88	2.71	2.72	3.20	3.36		3.60	3.58	4.09
3.0											
3.5		2.48	2.39	2.38	2.38	2.44	2.47		2.57	2.78	2.96
4.0		2.52	2.52	2.78	2.88	2.71	2.52		2.51	2.31	3.22
site hiSM											
0.0			1.76	1.64	1.79	1.69	1.59	1.59	1.62	1.40	1.59
0.05											0.59
0.07											0.48
0.1											0.58
0.15											
0.2											
0.25											
0.3											
0.4										2.35	1.58
0.5	1.72	0.98	1.16	1.06	1.21	1.54		2.03	2.32	2.56	1.78
0.75	1.67	1.26	1.23	1.09	1.05	1.47	1.45	1.65	1.80	2.34	1.34
1.0	1.54	1.32	0.98	0.99	1.07	0.98	1.22	1.67	1.90	1.94	1.43
1.25	1.22	1.36	1.47	1.26	1.38	1.01	1.09	1.41	1.65	1.66	1.89
1.5						1.57	1.45	1.34	1.29	1.53	1.68
2.0	1.83		1.18	1.18	1.10	1.05	1.09	1.25	1.33	1.37	1.40
2.5	1.62		1.58	2.02	2.19	2.20	1.99	1.73	1.58	1.36	1.43
3.0	1.62		1.75	1.84	1.63	1.98	1.23	1.50	1.83	1.89	1.58
3.5	1.60		1.64	1.74	1.80	1.88	1.79	1.45	1.55	1.63	1.52
4.0	1.74		1.82	1.88	1.91	1.89	1.87	1.81	1.78	1.93	1.72
4.5	1.66		1.80	1.79	1.96	1.85	1.83	1.82	1.87	1.91	1.70
5.0					1.61	1.69	1.63	1.77	1.77	1.85	1.63

Continuation of pore water DOC [mM]

Depth [m]	Jan 06	Feb 06	Mar 06	Apr 06	May 06	Jun 06	Jul 06	Aug 06	Sep 06	Oct 06	Nov 06
site TZ/IoSM											
0.0	0.48	1.03		0.92	1.45			1.55	1.26		1.43
0.05	0.85										
0.07											
0.1	0.91	1.09									
0.15		1.03									0.90
0.2		1.51		0.95	1.05			1.76			1.12
0.25	1.06	1.46		0.94	1.09				1.63		1.10
0.3	0.99	1.14		0.90	0.93			1.59	1.60		0.91
0.4	1.14	0.94		0.82	0.77			1.53	1.53		1.21
0.5		0.90		0.75	0.78	0.92	1.27	1.48	1.58		1.35
0.75	0.96	1.02		0.75	0.73	0.79	1.75	1.76	1.71		1.25
1.0	1.30	1.30		0.82	0.77	1.72	1.99	2.04	2.03		1.65
1.25	1.28	1.49		1.24			2.03	2.09	2.06		1.46
1.5											
2.0											
2.5											
3.0											
3.5											
4.0		1.25									
4.5					1.09	0.97					
5.0	1.26			1.21			0.94	1.16	1.35		1.73
site IoSM											
0.0	1.69	0.59	1.60	0.61	1.59	0.94	1.10	1.02	1.03	1.07	1.17
0.05											
0.07											
0.1											
0.15											
0.2								1.13	0.48	0.48	0.30
0.25											0.28
0.3											
0.4		0.23	0.43					0.77			0.27
0.5	0.23	0.22	0.22	0.29	0.31	0.33	0.42	0.58	0.34	0.35	0.26
0.75	0.27	0.22	0.21	0.26	0.26	0.30	0.52	0.53	0.43	0.35	
1.0	0.55	0.45	0.43	0.41	0.38	0.42	0.45	0.50	0.52	0.50	0.47
1.25	0.52										
1.5				0.60	0.53	0.44	0.42	0.46	0.48	0.53	0.52
2.0	0.56	0.48	0.57	0.56	0.52	0.53		0.51	0.49	0.54	0.55
2.5	0.55	0.50	0.53	0.51		0.42		0.56	0.53	0.52	0.49
3.0	0.52	0.49	0.48	0.50	0.61	0.48	0.50	0.55	0.54	0.55	0.50
3.5	0.50	0.51	0.50	0.51	0.55	0.47	0.49	0.54	0.49	0.51	0.52
4.0	0.48	0.46	0.48	0.48	0.58	0.50	0.49	0.44	0.47	0.49	0.51
4.5	0.51		0.53	0.54	0.63	0.58	0.57	0.58	0.60	0.72	0.58
5.0	0.68	0.64	0.67	0.64	0.80	0.53	0.57	0.57	0.58	0.72	0.56

Pore water sulphate [mM] from January 2006 to October 2006

Depth [m]	Jan 06	Feb 06	Mar 06	Apr 06	May 06	Jun 06	Jul 06	Aug 06	Sep 06	Oct 06
site sGL										
0.0		10.09	8.55	7.50	3.86	8.82	9.88		4.86	
0.05										
0.07										
0.1										
0.15										
0.2										
0.25										
0.3					5.31					
0.4			11.50		4.80	4.96			2.24	
0.5				7.81	3.59	4.90				
0.75		2.38	10.43	9.30	2.09	2.51	1.00		2.65	
1.0		2.89		7.73		3.33	0.55		0.89	
1.25		2.94	7.03	1.77						
1.5				1.34					0.30	
2.0		4.22	9.90	8.31	7.28	6.02	5.91		5.15	
2.5		5.73	5.12	6.03	5.13	4.53	4.54		11.61	
3.0										
3.5		6.54	7.01	6.97	6.70	6.14	5.93		5.68	
4.0		7.07	7.82	7.92	6.81	6.91	6.58		6.30	
site hiSM										
0.0			12.07	15.18	11.36	12.86	16.60	14.60	15.16	13.68
0.05										
0.07										
0.1										
0.15										
0.2										
0.25										
0.3										
0.4										16.91
0.5	9.28	10.50	12.31	12.86	13.30	11.93		26.92	17.45	15.80
0.75	9.12	8.77	11.56	12.74	13.14	11.04	11.21	27.62	18.47	14.43
1.0	11.34	9.56	15.74	12.43	12.08	13.42	12.33	23.19	18.91	16.41
1.25	16.53	15.01	12.01	11.94	10.85	12.62	12.22	15.70	20.49	17.23
1.5						13.40	12.38	12.42	13.58	14.65
2.0	19.75		20.91	18.74	16.22	16.89	15.97	15.68	14.93	14.95
2.5	17.61		17.17	13.65	12.20	12.42	13.28	14.84	14.59	15.95
3.0	17.93		16.51	15.99	15.89	13.97	17.09	16.23	14.15	13.51
3.5	17.03		18.53	17.20	15.55	14.96	14.44	16.84	16.04	14.93
4.0	14.23		13.95	13.74	12.96	14.23	12.91	14.35	14.80	13.66
4.5	15.27		14.69	15.30	13.55	14.16	13.80		14.58	13.02
5.0					9.41	10.95	10.47	14.11	12.69	12.94

Continuation pore water sulphate [mM]

Depth [m]	Jan 06	Feb 06	Mar 06	Apr 06	May 06	Jun 06	Jul 06	Aug 06	Sep 06	Oct 06
site TZ/loSM										
0.0	22.24	18.30		22.30	16.10			20.28	21.12	
0.05	15.35									
0.07										
0.1	16.73	17.39								
0.15		17.57								
0.2		19.67		20.36	22.05			39.29		
0.25	18.36	19.75		20.40	22.08				23.40	
0.3	18.94	18.14		20.39	21.80			38.72	22.64	
0.4	18.31	19.30		21.99	23.75			18.92	24.63	
0.5		19.04		22.19	22.95	23.63	24.46	33.36	26.57	
0.75	18.03	17.49		20.75	23.90	23.71	19.52	21.60	28.08	
1.0	21.22	20.37		22.16	21.89	19.28	17.33	18.16	18.17	
1.25	21.69	19.57		21.90			17.97	17.65	21.90	
1.5										
2.0										
2.5										
3.0										
3.5	20.43									
4.0										
4.5					21.06	21.58				
5.0	20.67	20.19		22.44			20.34	18.92	18.50	
site loSM										
0.0	12.97	20.53	14.78	22.46	13.62	20.10	22.63	19.97	19.10	18.56
0.05										
0.07										
0.1										
0.15										
0.2								13.36	17.94	23.17
0.25										
0.3										
0.4		22.55						13.97		
0.5	18.23	23.14	23.94	19.72	10.86	24.87	25.91	20.81	16.69	21.52
0.75	21.82	19.76	24.91	22.28	20.56	20.27	19.68	24.33	23.77	23.31
1.0	23.82	21.91	23.29	21.76	21.29	20.68	21.27	23.71	25.09	23.82
1.25	23.23									
1.5			25.85	24.41	22.01	22.11	20.37	21.92	24.78	24.97
2.0	24.35	25.44	27.58	27.66	24.61	23.22	21.60	21.07	25.01	26.92
2.5	18.32	24.70	26.66	26.36		20.40	19.75	23.54	23.21	23.48
3.0	23.92	24.86	27.51	27.33	25.64	25.72	24.69	24.77	24.32	23.01
3.5	23.69	22.41	25.66	25.98	24.78	25.25	24.09	23.17	23.35	23.66
4.0	24.15	23.86	25.67	26.31	24.41	23.85	24.08	24.04	24.77	24.78
4.5	23.94		25.58	25.03	24.37	23.44	22.43	23.11	22.97	22.36
5.0	23.85	23.79	26.42	26.16	24.34	23.61	23.22	23.29	24.13	23.23

Pore water chloride [mM] from January 2006 to October 2006

Depth [m]	Jan 06	Feb 06	Mar 06	Apr 06	May 06	Jun 06	Jul 06	Aug 06	Sep 06	Oct 06
site sGL										
0.0		199.00	141.39	123.54	70.34	171.17	204.11		91.32	
0.05										
0.07										
0.1										
0.15										
0.2										
0.25										
0.3					98.09					
0.4		198.46			87.13	91.71			45.45	
0.5				138.47	71.27	95.61				
0.75		12.39	170.99	161.25	38.42	43.15	18.42		43.75	
1.0		21.39		129.81		50.33	10.77		5.92	
1.25		25.24	109.98	29.71						
1.5				19.55					11.79	
2.0		51.83	166.63	135.04	138.08	111.51	113.29		99.72	
2.5		95.75	95.44	95.77	97.37	87.65	86.31		230.91	
3.0										
3.5		111.37	110.70	114.06	114.24	115.87	116.02		108.26	
4.0		122.33	128.03	131.40	127.49	130.24	130.10		123.42	
site hiSM										
0.0			207.59	277.53	213.87	243.76	344.44	284.23	305.76	273.67
0.05										
0.07										
0.1										
0.15										
0.2										
0.25										
0.3										
0.4										347.35
0.5	171.16	201.51	226.53	239.54	256.27	218.01		546.58	349.95	316.76
0.75	171.64	167.18	204.29	233.76	259.15	202.30	213.13	537.57	376.65	279.86
1.0	213.63	182.19	283.35	220.07	232.00	255.83	233.97	455.17	379.38	325.49
1.25	326.37	300.56	217.26	213.92	212.54	246.11	233.47	283.19	403.13	337.21
1.5						264.27	251.18	245.33	271.98	302.55
2.0	402.99		389.41	343.34	328.18	331.15	319.18	319.66	295.14	303.83
2.5	360.20		321.70	254.28	246.18	249.20	281.14	312.70	295.94	321.31
3.0	379.19		323.50	301.10	311.74	272.93	343.96	332.52	288.82	280.26
3.5	346.08		344.43	327.45	304.51	290.60	289.90	353.32	316.79	298.35
4.0	276.46		260.01	254.55	253.12	278.26	259.61	297.54	295.96	275.30
4.5	299.73		273.69	280.26	254.25	279.47	271.15		292.19	267.93
5.0					186.68	199.48	200.42	283.40	251.99	264.58

Continuation pore water chloride [mM]

Depth [m]	Jan 06	Feb 06	Mar 06	Apr 06	May 06	Jun 06	Jul 06	Aug 06	Sep 06	Oct 06
site TZ/loSM										
0.0	443.78	372.31		415.16	334.98			418.14	434.53	
0.05	313.48									
0.07										
0.1	343.94	357.03								
0.15		360.05								
0.2		385.52		365.98	404.94			771.27		
0.25	365.82	385.68		361.93	405.03				452.58	
0.3	381.38	368.81		363.83	405.13			751.56	448.06	
0.4	378.14	389.20		388.32	456.23			365.79	482.84	
0.5		393.57		398.07	427.07	424.44	481.26	636.89	518.31	
0.75	364.02	357.27		372.48	447.78	434.70	409.11	450.58	544.31	
1.0	428.40	426.38		408.39	423.64	397.91	372.70	381.74	396.30	
1.25	429.56	406.03		407.24			384.14	379.71	447.99	
1.5										
2.0										
2.5										
3.0										
3.5	410.27									
4.0										
4.5					422.38	415.13				
5.0	413.57	411.39		420.39			414.92	398.61	390.76	
site loSM										
0.0	255.79	421.71	296.00	417.07	268.45	406.21	455.82	416.09	383.91	375.31
0.05										
0.07										
0.1										
0.15										
0.2								260.80	370.77	473.26
0.25										
0.3										
0.4		469.60						287.39		
0.5	363.62	477.72	504.63	371.94	209.81	483.64	524.00	426.23	344.58	438.21
0.75	436.24	416.13	504.22	412.91	396.06	408.18	394.44	518.17	494.06	477.40
1.0	479.39	448.69	477.54	406.05	410.40	409.61	423.02	487.65	536.01	495.21
1.25	461.86									
1.5			527.00	455.10	436.52	443.06	414.44	453.78	531.13	531.36
2.0	495.28	502.92	559.37	506.53	475.61	451.62	428.35	433.03	496.45	543.06
2.5	373.08	493.50	528.07	484.12		404.82	404.95	470.14	461.83	483.49
3.0	476.00	496.80	553.68	496.78	496.11	503.03	496.35	499.53	486.82	454.76
3.5	472.92	459.40	527.58	475.16	482.75	481.57	476.36	470.09	469.78	475.74
4.0	476.17	487.83	519.10	500.14	482.37	477.55	477.65	488.83	489.35	490.26
4.5	476.98		525.05	474.00	486.83	473.46	458.26	478.09	472.52	459.57
5.0	479.01	483.61	532.75	481.17	471.50	453.28	465.15	480.11	488.77	470.88

Pore water iron [µM] from January 2006 to January 2007

Depth [m]	Jan 06	Feb 06	Mar 06	Apr 06	May 06	Jun 06	Jul 06	Aug 06	Sep 06	Oct 06	Nov 06	Dec 06	Jan 07
site sGL													
0.0		10.13	15.31	20.36	18.98	3.13	2.06		37.43	4.66	18.80	15.40	21.67
0.05											87.02		
0.07													
0.1													
0.15													
0.2											344.15		
0.25													
0.3				0.83	2.51				100.05			141.82	
0.4				30.57	2.24	4.88			27.10	2.69		266.98	130.36
0.5			84.33	305.09	1.81	61.67				2.51		354.00	
0.75		38.38	228.66	34.44	18.94	277.22	70.91		161.76	98.30	198.22	286.68	217.74
1.0		18.25		20.95	9.42	50.05	92.23		72.34	60.61	234.48	147.19	125.07
1.25		91.67	126.04	74.82		80.82	63.46		76.75	75.21	583.38	211.65	74.67
1.5					94.41	94.06			113.03	98.48	132.68	107.44	96.16
2.0		76.38	76.73	35.33	32.87	38.26	41.61		58.82	66.07	73.77	10.74	4.66
2.5		78.46	63.74	59.90	62.27	73.47	62.06		93.81	68.04	22.20	66.79	46.20
3.0													
3.5		62.13	68.14	73.52	76.38	78.26	72.11		72.69	80.40	61.60	55.69	61.06
4.0		74.12	71.36	80.94	81.29	78.39	70.90		81.92	102.42	71.98	81.47	87.74
site hiSM													
0.0			13.45	8.95	9.00	2.39	1.49	2.50	9.38	4.66	16.65	22.38	
0.05											4.66	0.72	0.59
0.07											0.59	0.66	
0.1											5.73	0.72	0.82
0.15													
0.2													
0.25													
0.3													
0.4									3.06	3.40	0.98	0.84	0.90
0.5	12.77	6.97	4.72	7.17	6.42	11.72	12.25	5.38	31.72	1.68	0.90	0.82	0.70
0.75	1.63	0.93	0.94	0.66		1.22	1.75	1.20	1.47	0.54	0.75	0.84	0.97
1.0	1.52	1.38	1.07	0.98	1.11	1.20	5.33	25.52	24.89	73.76	36.71	28.65	29.37
1.25	63.18	49.10	36.68	36.97	35.00	47.68	43.10	68.91	60.63	59.45	58.19	43.15	41.36
1.5					27.24	59.71	9.42	74.93	43.12	91.32	100.99	111.55	96.33
2.0	187.92		139.33	125.78	102.50	112.07	105.81	98.88	91.81	86.49	99.74	95.98	90.60
2.5	143.74		129.32	212.21	232.68	246.79	242.85	178.52	100.66	94.90	97.77	89.89	86.49
3.0	144.27		156.22	170.16	164.53	168.98	139.44	162.95	93.38	90.60	134.12	179.06	112.09
3.5	148.94		164.85	176.47	182.59	197.09	192.90	224.68	192.20	179.42	176.37	177.45	261.97
4.0	224.83		205.00	169.00	217.04	204.05	155.25	177.36	199.32	218.45	195.89	256.77	206.64
4.5	262.21		241.19	256.94	261.39	271.42	201.15	220.14	230.60	287.57	241.19	280.59	226.15
5.0					92.27	42.42	16.75	240.50	216.21	225.80	249.97	340.22	299.57

Continuation of pore water iron [µM]

Depth [m]	Jan 06	Feb 06	Mar 06	Apr 06	May 06	Jun 06	Jul 06	Aug 06	Sep 06	Oct 06	Nov 06	Dec 06	Jan 07
site TZ/loSM													
0.0	5.63	1.55		0.79				2.04	1.71		2.15	28.47	
0.05	0.94											5.19	
0.07													
0.1	0.96											0.56	
0.15	1.10											0.61	
0.2				0.20				2.14			4.66	3.04	
0.25	1.07			1.50	1.38				125.56		20.59	16.47	
0.3	7.74	1.73		4.01	9.24			50.22	74.26		5.91	10.56	
0.4	224.29	152.92		89.63	122.20			232.88	282.41		262.14	216.31	
0.5	226.93	213.02		98.33	108.80	130.40	174.41	217.45	270.75		372.98	354.90	
0.75	4.45			0.33		0.67	25.69	10.54	256.26		31.34	75.38	
1.0	134.12	46.98		35.80	61.06	25.35	29.49	99.29	113.43		77.53	71.27	
1.25	89.59	112.81		96.22			28.93	23.16	179.41		61.06	51.93	
1.5				15.04				11.59	74.21		13.79	62.85	
2.0		17.44			9.26								
2.5													
3.0													
3.5	63.12	31.65											
4.0		76.61			48.55								
4.5					78.68	56.74							
5.0	243.25	187.72		91.27			11.35	28.55	81.35		194.46	233.14	
site loSM													
0.0	9.34	1.12	12.40	1.01	10.38	0.94	1.19	5.80	2.32	0.29	9.67	3.22	1.15
0.05													
0.07											0.00		
0.1													
0.15												0.48	0.50
0.2		0.00	0.00					54.48	0.48	0.73	5.37	0.68	0.54
0.25											0.00	0.38	
0.3													
0.4		0.00	0.00					16.05	2.52		0.00	0.66	0.54
0.5	0.00	0.00	0.00	0.28	0.00	0.56	0.19	1.01	0.57	0.21	0.00	0.59	0.64
0.75	0.00	0.00	0.00	0.41	0.00	0.00	0.16	1.11	1.01	0.00	0.00	0.66	0.39
1.0	0.34	0.00	0.00	0.02	0.00	0.00	0.00	1.13	0.09	0.39	0.00	71.62	0.61
1.25	251.86	221.07			84.31			86.20				5.01	
1.5		44.03	51.65	40.88	33.61	33.52	30.95	42.07	44.69	41.00	31.87	29.90	45.66
2.0	43.70	40.23	41.04	39.72	32.76	33.01	33.73	33.02	38.26	47.81	49.60	45.48	43.51
2.5	89.92	67.07	48.15	56.13	14.75	16.65	2.14	48.75	70.31	67.33	56.23	49.60	42.62
3.0	38.92	42.21	38.69	45.20	41.82	44.51	37.55	40.70	42.09	38.68	38.14	46.02	44.05
3.5	59.73	63.70	63.24	53.82	57.94	54.04	56.02	55.97	58.10	68.76	61.42	51.75	48.88
4.0	36.03	35.36	34.68	36.74	36.26	36.39	37.21	36.13	41.35	40.47	39.93	37.78	39.39
4.5	37.83	21.42	30.09	35.13	37.26	30.37	27.31	25.20	34.64	37.24	40.83	40.65	41.00
5.0	268.75	233.00	264.79	244.44	208.34	164.34	155.77	142.32	146.09	137.70	143.43	120.69	126.42

Pore water manganese [µM] from January 2006 to January 2007

Depth [m]	Jan 06	Feb 06	Mar 06	Apr 06	May 06	Jun 06	Jul 06	Aug 06	Sep 06	Oct 06	Nov 06	Dec 06	Jan 07
site sGL													
0.0		2.99	3.01	3.40	2.34	0.58	1.02		4.15	0.00	13.52	2.67	8.83
0.05											41.16		
0.07													
0.1													
0.15													
0.2											40.36		
0.25													
0.3				9.18	2.13				0.62			9.04	9.27
0.4			26.00	10.89	1.91	2.28			0.32	2.28		16.21	7.45
0.5			30.80	13.72	2.52	17.25				10.03		24.56	
0.75			28.34	10.50	1.63	7.19	3.05		6.42	7.04	40.38	20.81	11.96
1.0				3.59		3.82	3.61		4.05	2.89	46.09	15.94	9.35
1.25		1.16			3.17								
1.5		4.18	15.63	4.84		3.34	3.54		3.16	2.39	50.83	13.92	3.11
2.0						7.33	7.65		8.65	8.18	16.26	10.23	10.34
2.5		6.59	16.61	14.25	13.62	12.31	12.39		10.35	10.01	63.24	20.40	17.56
3.0		5.37	5.86	6.39	6.08	5.29	5.62		4.87	4.84	12.73	4.51	4.47
3.5		2.82	2.82	3.11	3.13	3.20	3.73		3.12	3.48	2.48	4.54	3.55
4.0		3.60	3.51	3.93	4.01	4.37	4.84		5.10	6.41	4.35	4.86	5.17
site hiSM													
0.0			6.85	8.66	6.43	3.38	5.57	5.33	10.67	5.03		3.91	
0.05											0.35	0.00	0.00
0.07											0.00	0.00	
0.1											1.66	0.00	0.00
0.15													
0.2													
0.25													
0.3													
0.4									2.99	0.00	3.55	0.00	0.00
0.5	0.73			0.30		0.55	0.89	0.23	3.41	0.00	2.88	0.00	0.00
0.75	0.00			0.05		0.09	0.32	0.22	0.28		0.00	3.78	0.00
1.0	2.50	2.28	1.43	1.82	1.84	1.23	3.46	3.64	1.14	2.48	1.06	1.06	1.57
1.25	13.88	9.65	5.16	4.72	3.78	5.19	5.17	5.27	1.71	1.99	1.77	0.99	2.12
1.5					7.05	8.47	9.07	9.81	4.67	5.16	3.65	2.41	1.71
2.0	31.28		20.16	18.33	14.64	13.87	15.11	13.01	11.01	8.67	9.75	9.22	7.85
2.5	24.43		12.54	12.56	13.36	12.00	14.49	12.67	7.39	8.09	10.32	10.47	9.43
3.0	14.31		10.22	9.31	10.81	10.65	8.83	10.86	7.46	8.15	11.87	16.12	6.28
3.5	16.89		19.14	19.21	18.22	18.20	20.70	15.45	8.56	8.27	10.08	12.75	15.98
4.0	18.22		14.76	15.83	18.18	17.58	16.91	16.48	12.60	11.10	11.28	16.77	15.53
4.5	19.32		16.59	15.08	14.26	13.89	15.32	13.61	13.73	14.76	13.89	20.30	15.99
5.0					13.51	15.71	15.20	17.80	15.43	13.83	14.82	22.27	19.57

Continuation of pore water manganese [µM]

Depth [m]	Jan 06	Feb 06	Mar 06	Apr 06	May 06	Jun 06	Jul 06	Aug 06	Sep 06	Oct 06	Nov 06	Dec 06	Jan 07
site TZ/loSM													
0.0	10.70	52.26		9.21	31.01			30.23	6.02		57.09	44.48	
0.05	0.63											11.98	
0.07													
0.1	0.81											7.82	
0.15	1.71										18.04		
0.2		12.00		2.10				5.51			42.43	28.36	
0.25	2.47	12.70		11.22	7.28				80.40		42.33	27.82	
0.3	12.26	2.16		5.18	2.27			16.57	62.83		9.46	9.42	
0.4	74.68	25.94		5.50	4.65			7.52	22.36		29.87	40.36	
0.5	68.00	39.67		8.96	5.82	8.60	12.57	16.79	20.90		34.79	45.97	
0.75	33.46			2.18		17.28	79.62	36.02	33.98		24.53	30.56	
1.0	74.17	74.84		15.35	54.24	77.99	90.90	46.23	46.19		57.67	72.89	
1.25	86.80	79.18		66.53			70.92	71.19	63.55		56.02	63.12	
1.5				69.59				79.84	65.12		70.80	58.94	
2.0		94.79			62.49								
2.5													
3.0													
3.5	87.80	67.50											
4.0		78.44			65.58								
4.5					65.54	40.06							
5.0	82.48	68.36		63.31			41.02	30.43	38.75		47.29	60.02	
site loSM													
0.0	9.93	10.98	10.00	5.40	10.68	9.71	13.96	15.16	9.35	13.35	8.66	4.62	1.67
0.05													
0.07											0.96		
0.1													
0.15												0.00	0.00
0.2		0.00	0.00					12.99	0.11	0.00	10.00	0.00	0.00
0.25											2.65	0.00	
0.3													
0.4		0.00	0.00					9.76	5.55		3.49	0.40	0.00
0.5	0.00	0.00	0.00	0.00	0.00	0.03	0.48	6.40	0.09	0.00	1.09	0.00	0.00
0.75	0.00	0.00	0.00	0.00	0.00	0.32	0.05	0.38	0.93	2.57	0.29	0.42	0.00
1.0	1.76	2.23	0.00	1.08	0.00	0.05	0.09	0.25	2.53	3.79	1.42	2.34	0.67
1.25	7.73	8.05			6.96			5.06					
1.5		10.88	11.73	6.09	4.60	5.83	4.71	3.94	1.30	1.58	2.10	3.65	3.25
2.0	12.14	11.75	11.70	10.18	7.47	6.78	6.57	6.54	6.56	3.01	2.68	3.44	4.19
2.5	6.81	7.11	8.42	7.65	5.49	4.11	4.21	6.83	6.85		7.70	7.57	6.43
3.0	6.43	6.50	6.39	7.02	6.12	7.00	6.88	6.82	7.04	6.20	6.29	7.97	8.26
3.5	13.69	13.63	12.74	14.95	13.00	18.93	19.83	15.97	17.15	13.71	15.21	14.67	12.24
4.0	6.15	5.92	5.85	6.83	6.06	6.81	9.27	9.72	10.34	10.31	10.51	9.51	10.32
4.5	9.63	9.41	8.70	9.86	9.00	9.59	10.34	9.55	11.46	11.91	12.45	12.24	12.2
5.0	8.38	7.71	8.61	9.36	8.81	8.07	9.55	9.60	10.14	8.68	8.87	9.05	8.79

Pore water ammonia [µM] from January 2006 to January 2007

Depth [m]	Jan 06	Feb 06	Mar 06	Apr 06	May 06	Jun 06	Jul 06	Aug 06	Sep 06	Oct 06	Nov 06	Dec 06	Jan 07
site sGL													
0.0											0.027		
0.05											0.235		
0.07													
0.1													
0.15													
0.2											0.312		
0.25													
0.3												0.193	
0.4						0.002						0.215	
0.5						0.003						0.112	
0.75			0.207			0.043	0.035				0.293	0.249	0.005
1.0				0.04		0.028					0.351	0.162	0.113
1.25			0.18			0.036					0.294	0.063	
1.5						0.039					0.068	0.021	
2.0			0.302	0.189	0.102	0.094	0.071		0.343		0.295	0.299	0.276
2.5					0.019	0.062	0.029				0.137	0.013	
3.0													
3.5						0.025					0.041	0.034	
4.0						0.049					0.039	0.023	

Pore water phosphate [µM] from January 2006 to January 2007

Depth [m]	Jan 06	Feb 06	Mar 06	Apr 06	May 06	Jun 06	Jul 06	Aug 06	Sep 06	Oct 06	Nov 06	Dec 06	Jan 07
site sGL													
0.0		7.85	9.52	10.27	9.14	9.77	18.95		17.47	17.09	6.72	6.03	6.28
0.05											107.95		
0.07													
0.1													
0.15													
0.2											132.15		
0.25													
0.3					4.77							5.28	4.10
0.4			0.28		3.02	0.00			19.47	2.57		16.52	3.44
0.5				0.00	3.83	0.00						15.33	
0.75		19.30	25.97	9.45	10.38	34.62	28.05		19.52	23.68	121.85	18.51	2.53
1.0		5.71		3.55		25.61	12.10		36.34	34.94	49.74	44.75	32.86
1.25			22.22	0.00		0.00			60.80	29.74	14.08	38.46	
1.5				0.00	54.72	0.00			45.92	49.95	31.72	22.83	22.69
2.0		25.13	25.59	15.99	14.69	17.24	16.50		23.29	28.67	82.75	90.95	78.50
2.5		11.82	10.17	7.22	11.05	14.47	13.53		30.41	15.42			16.79
3.0													
3.5		10.29	7.79	7.17	8.69	7.31	7.35		8.93	16.61	10.47	15.46	4.73
4.0		7.91	5.90	7.18	7.73	7.74	6.11		15.1	7.50	13.15	8.80	6.21

Erklärung

Hiermit versichere ich, dass ich die vorliegende Arbeit selbstständig angefertigt und keine anderen als die angegebenen Quellen und Hilfsmittel verwendet habe. Zusätzlich erkläre ich, dass diese Dissertation weder in ihrer Gesamtheit noch in Teilen einer anderen wissenschaftlichen Hochschule zur Begutachtung in einem Promotionsverfahren vorliegt oder vorgelegen hat.

Weimar, im Juni 2007   Kerstin Kolditz